Université de Montréal

Identification de facteurs nucléaires modifiant l'activité des cellules souches hématopoïétiques

Par

Sonia Cellot

Programme de Biologie Moléculaire

Faculté de médecine

Thèse présentée à la Faculté de médecine
en vue de l'obtention du grade de Docteur
en biologie moléculaire

mai 2012

Université de Montréal

Faculté de médecine

Cette thèse intitulée :

Identification de facteurs nucléaires modifiant l'activité des cellules souches hématopoïétiques

présentée par :

Sonia Cellot

a été évaluée par un jury composé des personnes suivantes :

Alain Verreault, Président-rapporteur

Guy Sauvageau, Directeur de recherche

Eric Milot, Membre du jury

Stéphane Richard, Examinateur externe

Richard Momparler, Représentant du doyen

RÉSUMÉ

Les cellules souches hématopoïétiques (CSH) sont rares, mais indispensables pour soutenir la production des cellules matures du sang, un tissu en constant renouvellement. Deux caractéristiques principales les définissent; la propriété d'auto-renouvellement (AR), ou la capacité de préserver leur identité cellulaire suivant une division, et la multipotence, ce potentiel de différentiation leur permettant de générer toutes les lignée hématopoïétiques. De par leurs attributs, les CSH sont utilisée en thérapie cellulaire dans le domaine de la transplantation. Une organisation tissulaire hiérarchique est aussi préservée dans la leucémie, ou cancer du sang, une masse tumorale hétérogène devant être maintenue par une fraction de cellules au potentiel prolifératif illimité, les cellules souches leucémiques (CSL). Les travaux présentés dans ce manuscrit visent à explorer les bases moléculaires de l'AR, encore mal définies.

Certains membres de la famille des facteurs de transcription à homéodomaine HOX sont impliqués dans la régulation de l'hématopoïèse normale, et leur dérégulation peut contribuer à la transformation leucémique. En particulier, la surexpression du gène *Hoxb4* dans les CSH influence leur destin cellulaire, favorisant des divisions d'auto-renouvellement et leur expansion en culture et *in vivo*. En général, les CSH s'épuisent rapidement lorsque maintenue hors de leur niche *ex vivo*. Différents facteurs interagissent avec les HOX et modulent leur liaison à l'ADN, dont la famille des protéines TALE (Three Amino acid Loop Extension), comme MEIS1 et PBX1. En utilisant une stratégie de surexpression combinée de *Hoxb4* et d'un anti-sens de *Pbx1* dans les CSH, générant ainsi des cellules Hoxb4^{hi}Pbx1^{lo}, il est possible de majorer encore d'avantage leur potentiel d'AR et leur expansion *in vitro*. Les CSH Hoxb4^{hi}Pbx1^{lo} demeurent fonctionnellement intactes malgré une modulation extrême de leur destin cellulaire en culture. Les niveaux d'expressions de facteurs nucléaires, seules ou en combinaison, peuvent donc s'avérer des déterminants majeurs du destin des CSH.

Afin d'identifier d'autres facteurs nucléaires potentiellement impliqués dans le processus d'AR des CSH, une stratégie permettant d'évaluer simultanément plusieurs gènes candidats a été élaborée. Les progrès réalisés en termes de purification des CSH et de leur culture en micro-puits ont facilité la mise au point d'un crible en RNAi (interférence de l'ARN), mesurant l'impact fonctionnel d'une diminution des niveaux de transcrits d'un gène cible sur l'activité des CSH. Les candidats sélectionnés pour cette étude font partie du grand groupe des modificateurs de la chromatine, plus précisément la famille des histones déméthylases (HDM) contenant un domaine catalytique Jumonji. Ce choix repose sur la fonction régulatrice de plusieurs membres de complexes méthyl-transférases sur l'AR des CSH, dont l'histone méthyl-transférases MLL (Mixed Lineage Leukemia).

Cette stratégie a aussi été utilisée dans le laboratoire pour étudier le rôle de facteurs d'asymétrie sur le destin des CSH, en collaboration. Ces études ont permis d'identifier à la fois des régulateurs positifs et négatifs de l'activité des CSH. Entre autre, une diminution de l'expression du gène codant pour JARID1B, une HDM de la lysine 4 de l'histone H3 (H3K4), augmente l'activité des CSH et s'accompagne d'une activation des gènes *Hox*.

En conclusion, divers déterminants nucléaires, dont les facteurs de transcription et les modificateurs de la chromatine peuvent influencer le destin des CSH. Les mécanismes sous-jacents et l'identification d'autres modulateurs de l'AR demeurent des voies à explorer, pouvant contribuer éventuellement aux stratégies d'expansion des CSH *ex vivo*, et à l'identification de cibles thérapeutiques contre les CSL.

Mots-clés : cellules souches hématopoïétiques, Hoxb4, Pbx1, auto-renouvellement, histone déméthylases, RNAi

ABSTRACT

Hematopoietic stem cells (HSC) are rare, but essential to sustain the constant production of all mature blood cells, a constantly renewing tissue. They are defined by two main characteristics; namely self-renewal (SR), or the capacity to preserve cell identity following division, and multipotency, the differentiation potential that allows them to generate all hematopoietic lineages. Given their attributes, HSC are used for cellular therapy in the transplantation field. A hierarchy in tissue organisation is also preserved in leukemia, or blood cancer, a heterogeneous tumor mass that is sustained by a subset of cells with unlimited SR potential, the leukemia stem cells (LSC). Studies presented in this manuscript aim to explore the molecular basis underlying SR, which are still poorly defined.

Certain members of the HOX family of homeodomain transcription factors are involved in the regulation of normal hematopoiesis, and their deregulation can contribute to leukemia development. In particular, *Hoxb4* overexpression in HSC influences their fate, favouring SR divisions and their subsequent expansion in culture and *in vivo*. In general, HSC exhaust rapidly when maintained *ex vivo*, outside of their niche. Several factors interact with HOX and modulate their binding to DNA, including members of the TALE (Three Amino acid Loop Extension) protein family, such as MEIS1 and PBX1. Using a strategy of combined overexpression of *Hoxb4* and an anti-sense to *Pbx1*in HSC, generating Hoxb4^{hi}Pbx1^{lo} cells, it is possible to further impact on their SR potential and expansion *in vitro*. These Hoxb4^{hi}Pbx1^{lo} cells remain functionally intact despite extreme modulation of their cell fate in culture. Levels of expression of nuclear factors, alone or in combination, can thus impact significantly on HSC fate.

In order to identify other nuclear factors potentially involved in the process of HSC self-renewal, a strategy enabling simultaneous assessment of several gene candidates was elaborated. To this end, progress made in terms of HSC purification and their culture in micro-wells facilitated the setup of an RNAi (RNA interference) screen, measuring the functional impact of lowering gene candidate transcript levels on HSC activity. Gene candidates selected for this study belong to the greater group of chromatin modifiers, more specifically the family of histone demethylases (HDM) containing a Jumonji catalytic domain. This choice stems from the regulatory function of several members of histone methyl-transferase complexes on HSC self-renewal, including the histone methyl-transferase MLL (Mixed Lineage Leukemia). This strategy was also used in the laboratory to study the role of asymmetry factors on HSC fate, as a collaboration. These studies enabled identification of both positive and negative regulators of HSC activity. Among these, reduced expression of the gene coding for JARID1B, a histone 3 lysine 4 (H3K4) HDM, increased HSC activity was associated with *Hox* genes activation.

In conclusion, several nuclear determinants, including transcription factors and chromatin modifiers, can influence HSC fate. Underlying mechanisms and identification of additional modulators of SR remain areas to explore, which could eventually contribute to HSC expansion strategies *ex vivo*, and identification of therapeutic targets against LSC.

Keywords: hematopoietic stem cells, Hoxb4, Pbx1, self-renewal, histone demethylases, RNAi

Table des matières

Liste des figures

Liste des tableaux

Liste des abréviations

5hmC	5-hydroxymethylcytosine
5mC	5-méthylcytosine
AbdA	Abdominal-A
AbdB	Abdominal B
ADN	Acide désoxyribonucléique
AGM	Aorta-Gonad-Mesonephros
AR	Auto-renouvellement
AR-A	Auto-renouvellement asymétrique
ARN	Acide ribonucléique
AR-S	Auto-renouvellement symétrique
BCR	Breakpoint cluster region
CBP	CREB binding protein
CpG	Ilots dinucléotides cytosine-guanine
CRU	Unite de repopulation competitive
CSE	cellules souches embryonnaires
CSH	Cellules souches hématopoïétiques
CSH-CT	Cellules souches hématopoïétiques a court terme
CSH-LT	Cellules souches hématopoïétiques a long terme
CSL	Cellules souches leucémiques
CXCR4	CXC chemokine receptor 4
D-2-HG	D-2-hydroxyglutarate
DNMT	ADN méthyl-transférases
FAD	Flavin Adenine Dinucleotide 1
Gfi1	Growth factor independence 1
H3	Histone H3
HDAC	Histone déacétylase
HDM	Histones déméthylase
HMTase	Histone méthyltransferase
HOX	Homeobox

IDH	Isocitrate dehydrogenases
JmjC	Jumonji C
K	Lysine
K27	Lysine 27
K4	Lysine 4
K9	Lysine 9
KLS	Population hématopoiétique (c-kit+ Lin- sca-1+)
LDA	Essai a dilution limite
Lin	Lignage specifique
LMA	Leucémie myéloïde aigue
LMC	Leucémie myéloide chronique
LSD1	Lysine Specific Demethylase
miRNA	microRNA
MLL	Mixed lineage leukemia Mixed lineage leukemia
MOZ	MOnocytic leukemia Zinc finger protein
NA10hd	Nup98 fusionné à l'homéodomaine de Hoxa10
ncRNA	ARN non-codant
NPM1	Nucléophosmine
P	Progéniteurs
PcG	Protéine du groupe des polycomb
PHD	Plant Homeodomain
PRC1/2	Complexe polycomb repressif 1/2
R	Arginine
REST	RE1 silencing transcription factor/neuralrestrictive silencing factor
RNAi	RNA interference
SDF-1	Stromal cell Derived Factor-1
SET	Su(var)3-9, Enhancer of zeste, Trithorax
SMD	Syndromes myélodysplasiques
TPR	domaine tetratricopeptide
Trx	Trithorax

Ubx	Ultrabithorax
UTR	Région non transcrite
UTX	Ubiquitously Transcribed tetratricopeptide repeat, X chromosome

À mon très cher papa, Giuseppe Cellot (1942-2003)

Remerciements

J’aimerais exprimer toute ma reconnaissance à mon directeur de thèse Guy Sauvageau, notamment pour la très grande liberté accordée. Merci à tous les précieux collègues du laboratoire, une combinaison d’intelligence et de générosité que l’on a rarement la chance de rencontrer. J’espère que la vie me laissera assez de sagesse pour toujours garder en mémoire votre attitude envers la science et votre souci du respect d’autrui. Je ne veux pas nommer personne, de peur d’en oublier une. Merci aux collaborateurs plus étroits qui ont participé aux travaux présentés dans cette thèse; Jalila Chagraoui, Jana Krosl, Kristin Hope et Éric Deneault. Un mot de reconnaissance pour Nadine Mayotte, Tara MacRae, Simon Girard et Mélanie Fréchette pour leur grande disponibilité, leur expertise, et leur support, tout le long de ses années. Je remercie aussi pour leur soutien et leur très grande gentillesse Danièle Gagné (cytométrie de flux) et Christian Charnonneau (microscopie et graphisme), ainsi que Raphaëlle Lambert et Pierre Chagnon de la plateforme de génomique. Merci également aux précieux collègues pour m’avoir soutenue en clinique ces dernières années, en particulier Josée Hébert et Georges-Étienne Rivard, pour leur mentorat aussi.

Je tiens à souligner le support exceptionnel de Jalila Chagraoui, pour sa présence depuis le début, qui rend tout possible. Je lui dois beaucoup.

Merci à ma famille, en particulier Emilia ma maman, et à mes amis, pour leur soutien et leur très grande compréhension.

Merci aux patients…

1. INTRODUCTION

1.1 Cellules souches hématopoïétiques (CSH)

1.1.1. Définitions

Les cellules souches hématopoïétiques, représentant une infime fraction des cellules de la moelle osseuse où elles se nichent (1/10 000 cellules chez la souris), soutiennent la réplétion constante des éléments matures du sang tout au long de la vie. Elles se trouvent au sommet d'une hiérarchie où se déclinent toutes les cellules hématopoïétiques, restreignant progressivement leur potentiel de différentiation à chaque étape (Fig1.1), pour former le contingent myéloïde et lymphoïde. Deux grandes caractéristiques définissent les CSH; premièrement, elles sont capables d'auto-renouvellement (AR), un type de division cellulaire dans laquelle au moins une des cellules filles préserve l'identité de la mère, et deuxièmement elles sont pluripotentes, donnant naissance à toutes les cellules du sang. Ce type de division peut être symétrique (AR-S) (Fig1.2), augmentant le nombre de CSH comme c'est le cas lors du développement embryonnaire dans le foie fétal, ou asymétrique (AR-A), préservant leur nombre comme c'est le cas dans la vie adulte (voir aussi Cellot et al en annexe 1). Contrairement aux cellules matures dont la demi-vie est courte, variant de quelques jours à quelques mois, les CSH doivent donc maintenir une masse critique pour soutenir l'hématopoïèse toute la vie durant. Des anomalies du mode de division peuvent aussi servir de modèles pour expliquer quelques situations pathologiques. En effet, ce processus est dérégulé dans les leucémies aigues, où des rondes effrénées de division d'AR-S s'enchaînent, menant à une accumulation de blastes leucémiques dans la moelle, avec attrition secondaire du compartiment mature (Fig1.2a). Inversement, dans les anémies aplasiques, des divisions symétriques de différentiation résultent en une déplétion progressive des cellules hématopoïétiques (Fig1.2c). Les CSH s'épuisent également rapidement lorsque mises en culture *ex vivo*, hors de leur niche.

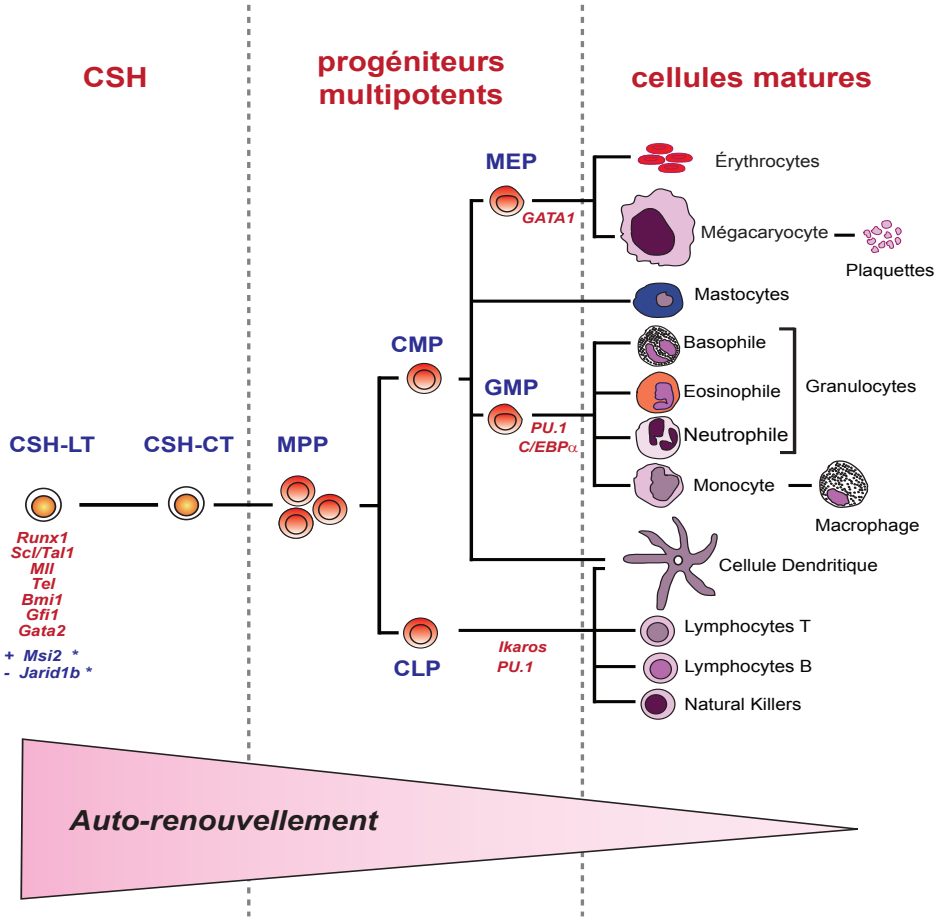

Figure 1.1 Hiérarchie du système hématopoïétique. Différentiation le long de l'axe gauche-droite. En rouge, quelques facteurs de transcription en relation avec le stade de différentiation où ils sont impliqués. CSH : cellule souche hématopoïétique. CSH-LT : cellule souche hématopoïétique-long-terme. CSH-CT : cellule souche hématopoïétique-court-terme. MPP : Progéniteur multipotent. CMP : précurseur myéloïde commun CLP : précurseur lymphoïde commun MEP : précurseur mégakario-érythrocytaire GMP : précurseur granulo-monocytaire. *Régulateurs de l'activité des CSH identifiés dans cet ouvrage. +, régulateur positif. -, régulateur négatif.

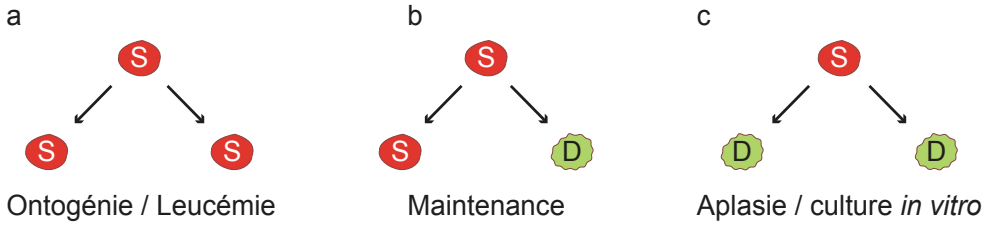

Figure 1.2 Type de divisions d'auto-renouvellement des CSH. a. Division symétrique d'expansion. b. Division asymétrique de maintien c. Division symétrique de différentiation.

1.1.2. Auto-renouvellement et destin cellulaire

Pour compléter une division d'AR préservant la nature multipotente de la CSH, une série de conditions doivent être rencontrées [1], schématisées à la (Fig1.3) (voir aussi revue en annexe 2, Cellot S et al). Le contexte doit être permissif à l'entrée en cycle cellulaire de la CSH, laquelle se trouve la majorité du temps en phase de quiescence, ou G_0, dans la vie adulte. La fréquence de division de la CSH, par des études d'incorporation de BrdU, est d'ailleurs estimée à 30-50 jours pour la souris [2, 3], alors que les CSH humaines se diviseraient tous les 175–350 jours selon de récentes estimations [4, 5]. Suivant la complétion de la division, la cellule doit bien entendu pouvoir réintégrer son état de veille, en G_0. En entamant le processus de division, la cellule doit cependant s'abstenir de se commettre à des programmes de destinées alternes, ce qui changerait son identité, comme la différentiation, la sénescence ou l'apoptose (Fig1.3). D'ailleurs, les réseaux transcriptionnels requis pour le maintien de l'état souche doivent être réprimés pour permettre, par exemple, une amorce différentiation. Dans une leucémie, au contraire, s'associe un bloc de la différentiation combiné à un potentiel accru d'AR, lié à une accumulation incessante de blastes leucémiques. La majorité des agents de chimiothérapie interfèrent avec le cycle cellulaire, mais certains, comme l'acide rétinoïque, visent à forcer les cellules malignes à emprunter une voie de différentiation, et modifier ainsi leur destin [6]. Il est intéressant de noter aussi que le long du processus de différentiation, chaque étape arbore une architecture du noyau, ou de la chromatine, spécifique à l'identité cellulaire (Fig1.4).

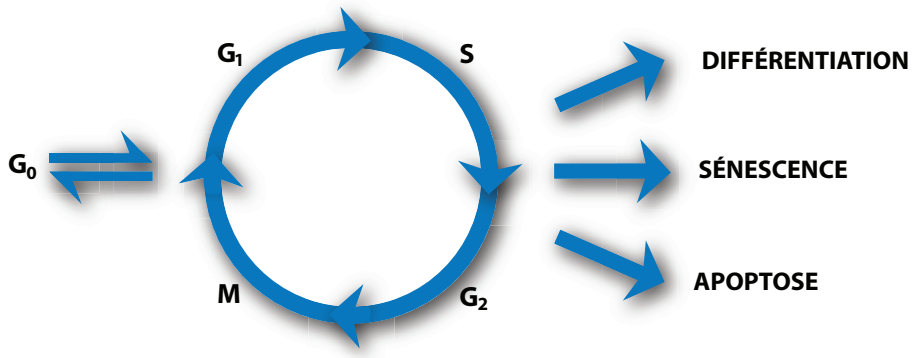

Figure 1.3 CSH et options de destin cellulaire. G0,G1,S,G2,M : phases du cycle cellulaire.

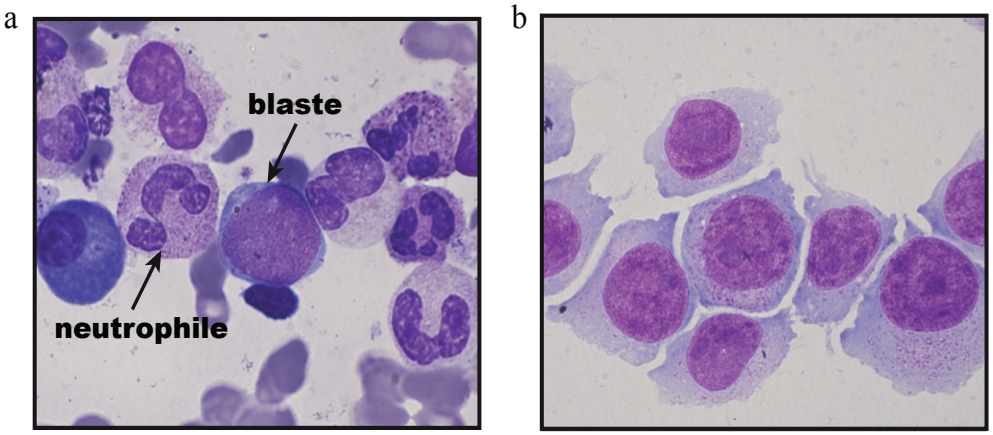

Figure 1.4 Morphologie de cellules hématopoïétiques. a. moelle normale humaine. b. Lignée cellulaire myéloïde MONO-MAC-1, avec réarrangement MLL-AF9. Coloration au Giemsa. Magnification 100x.

1.1.3. Ontogénie des CSH

Au cours du développement, plusieurs sites anatomiques successifs contribuent à l'ontogénie des CSH [7] (Fig1.5, voir aussi Cellot et al en annexe 3). Elles sont d'abord spécifiées au niveau de l'AGM (région Aorta-Gonad-Mesonephros), une structure embryonnaire comprenant l'aorte dorsale, le mésenchyme adjacent et le sillon uro-génital. Suivant leur migration vers le foie fétal, elles subissent une phase d'expansion, augmentant significativement le réservoir de CSH, au jour E15.5 chez la souris, ou autour du 70ème jour de gestation chez l'humain [8]. Les CSH vont par la suite se loger dans la moelle osseuse, pour une vague finale de modeste expansion. Après la 4ème semaine de vie de la souris, s'amorce une phase essentiellement de maintien du nombre des CSH, grâce à leur potentiel d'auto-renouvellement [9]. Le destin des CSH est donc en partie tributaire de la niche dans laquelle elles résident [10, 11]. Le microenvironnement prodigue des instructions (facteurs extrinsèques) aux cellules souches, comme la liaison entre le récepteur de chémokines (CXCR4) et son ligand CXCL12 (SDF-1; Stromal cell Derived Factor-1), favorisant la maintenance du réservoir de CSH et leur rétention dans la niche [12, 13]. Des facteurs intrinsèques à la CSH dictent aussi son comportement, dont divers facteurs nucléaires, tel que discutés plus loin, comme les facteurs de transcription ou des effecteurs épigénétiques modifiant la structure de la chromatine. Les facteurs de transcription à homéodomaine de la famille HOX [14], ainsi que l'histone-méthyltransférase MLL [15] sont des exemples de facteurs nucléaires modulant l'AR des CSH. L'élaboration de stratégies visant à identifier de nouveaux facteurs nucléaires modulant l'activité des CSH est à la base des travaux présentés dans cette thèse.

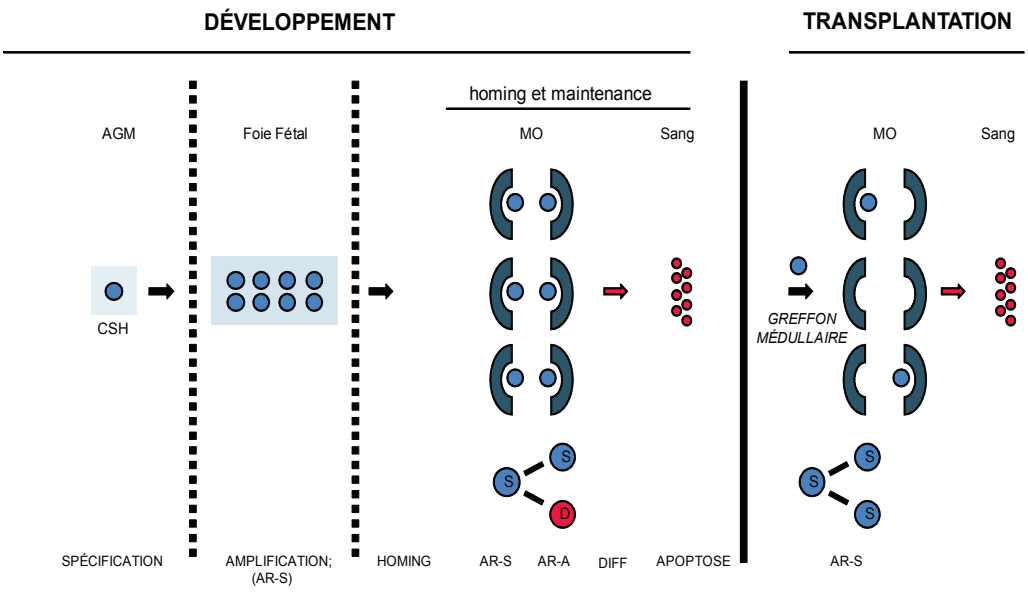

Figure 1.5 Ontogénie de la CSH. Panneau de gauche : développement de la CSH selon les diverses niches rencontrées depuis sa spécification dans l'embryon jusqu'à la moelle adulte. Panneau de droite : développement de la CSH dans le contexte d'une transplantation chez un receveur suivant un conditionnement myéloablatif. À noter que le réservoir de CSH est diminué post-transplantation, malgré une brève phase d'expansion des CSH dans les jours suivant la transplantation. CSH : cellule souche hématopoïétique AGM : aorta-gonad-mesonephros. AR-S/AR-A : auto-renouvellement-symétrique/asymétrique MO : moelle osseuse. DIFF : différentiation.

1.1.4. Purification des CSH

L'isolation des CSH demeure un défi de taille en raison de leur faible fréquence dans la moelle osseuse, et surtout en l'absence d'un marqueur de surface spécifique. Différentes populations de cellules primitives sont cependant décrites, selon leur immunophénotype et leur capacité fonctionnelle à soutenir l'hématopoïèse chez un receveur létalement irradié. On distingue au moins deux populations de cellules souches, selon leur capacité à générer toutes les lignées du sang de façon transitoire, à court-terme (CSH-CT, 4 à 6 semaines), ou à long-terme (CSH-LT) (Fig 1.6), défini pour la souris à plus de 16-20 semaines. On retrouve aussi les cellules progénitrices (P, Fig1.6), capables de soutenir l'hématopoïèse à très court-terme, dans les premières semaines suivant une transplantation. La majorité des CSH-LT de la moelle sont typiquement $CD150^{+}CD48^{-}$Ly-6A/$E^{+}CD117^{+}CD34^{-}$, et n'expriment pas de marqueurs associés à la différentiation (Lin^{-}) [16-19]. Tel que mentionné, la majorité des CSH-LT sont quiescentes *in vivo*, mais s'engage dans le cycle cellulaire après exposition à des cytokines *in vitro* [20, 21].

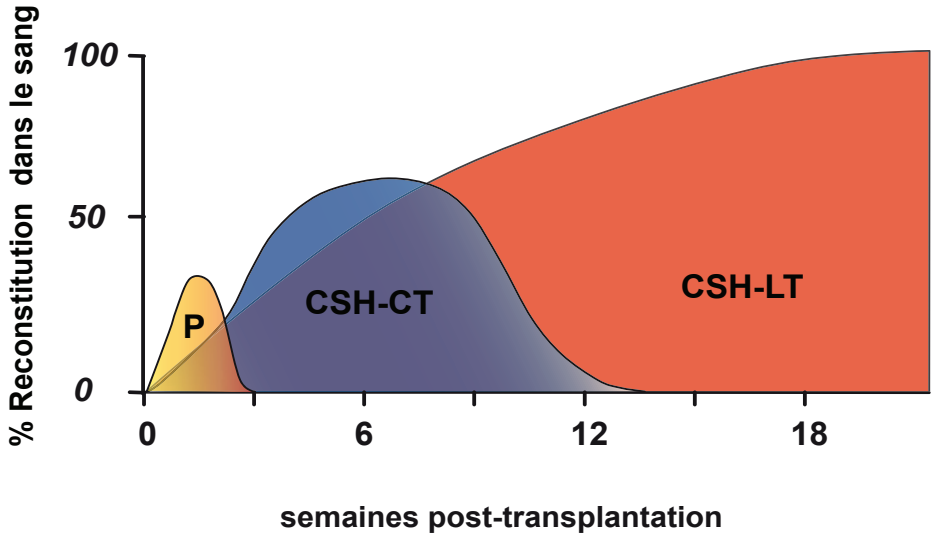

Figure 1.6 Durée de la reconstitution hématologique post transplantation selon le type cellulaire. Ordonnée : contribution à la reconstitution sanguine en %. Abscisse : nombre de semaines post-transplantation. P : Progéniteur multipotent. CSH-LT : cellule souche hématopoïétique-long-terme. CSH-CT : cellule souche hématopoïétique-court-terme.

1.1.5. Évaluation fonctionnelle des CSH

En l'absence de marqueur distinctif, la définition d'une CSH repose encore sur des bases fonctionnelles. L'essai de transplantation à dilution limite (LDA; Limit Dilution Assay) est fondé sur le principe qu'une cellule souche peut donner naissance à tous les types de leucocytes du sang, et demeure encore l'analyse de référence pour quantifier le nombre de CSH *in vivo*, ou en culture [22-24] (Fig1.7). Dans ces essais, des doses décroissantes de cellules hématopoïétiques (à l'étude) sont injectées dans divers groupes de souris létalement irradiées, simultanément à une petite dose de cellules de moelle (compétitrices), assurant ainsi la survie de l'animal à court-terme. Les leucocytes dérivés des CSH à l'étude ou des cellules compétitrices sont identifiées par des marqueurs congéniques les distinguant, soit CD45.1 (Ly5.1) et CD45.2 (Ly5.2). La reconstitution sanguine des receveurs est évaluée par cytométrie de flux après 16 semaines, et la proportion de cellules myéloïdes et lymphoïdes provenant des cellules à l'étude est quantifiée. Le seuil de reconstitution pour affirmer qu'une CSH-LT a contribué à l'hématopoïèse du receveur est établi à 1% des leucocytes du sang. La fréquence de CSH-LT (ou unité de repopulation compétitive/CRU) de la population cellulaire à l'étude est déterminée en utilisant la méthode statistique de Poisson, se basant sur la proportion d'animaux non-reconstitués pour une même dilution cellulaire reçue.

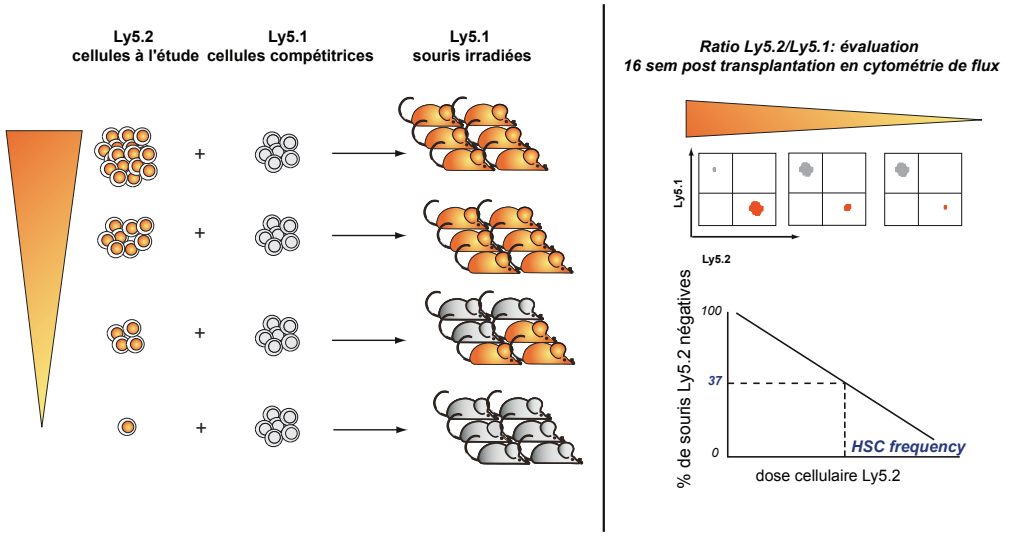

Figure 1.7 Quantification des CSH par essai de transplantation à dilution limite (LDA). Panneau de gauche : Population de cellules à l'étude transplantées chez des receveurs congéniques létalement irradiés à dilutions (doses) décroissantes, avec une dose de cellules compétitrices. Panneau de droite : haut ; analyse du ratio CD45.1 (Ly5.1)/CD45.2 (Ly5.2) par cytométrie de flux 16 semaines post transplantation, bas ; calcul de la fréquence des CSH basé sur la proportion de receveurs non reconstitués par les cellules à l'étude pour chaque groupe de souris. Voir aussi section 1.1.5 de l'introduction.

L'essai LDA est fréquemment utilisé pour mesurer l'impact d'un gène sur le processus d'AR des CSH. Dans ce contexte, un gène candidat peut être surexprimé dans une population cellulaire enrichie en CSH, en utilisant un vecteur rétroviral, et les cellules transduites sont fonctionnellement évaluées, après un période de culture plus ou moins longue [23]. Le contenu en CSH d'une population à l'étude peut ainsi être comparé à une population contrôle (cellules transduites avec un vecteur contrôle), et l'effet d'un gène candidat sur l'AR évalué. Le niveau d'expression d'un gène peut aussi être modulé en utilisant la technique d'interférence de l'ARN, ou RNAi, mesurant alors l'impact d'une diminution du transcrit d'un gène donné sur l'AR [25], tel que présenté au chapitre 3. Cette stratégie permet d'identifier à la fois des régulateurs positifs et négatifs du destin des CSH, diminuant ou augmentant respectivement le potentiel d'AR dans un essai par RNAi.

Classiquement, une population de cellules hématopoïétiques est enrichie en CSH en exposant les souris avant leur sacrifice à un agent de chimiothérapie, le 5-fluorouracile (5-FU), forçant l'entrée en cycle des cellules primitives, et favorisant subséquemment leur infection par un rétrovirus [26]. Cette approche entraîne aussi la mort cellulaire du compartiment plus différentié, concentrant ainsi les CSH (fréquence de 1 :10 000 dans la moelle normale), et diminuant le nombre total de cellules mises en culture, en général

à une concentration d'environ 1x 10^6 cellules/mL. L'avancement des connaissances en termes de purification et de culture des CSH, ont permis de concentrer davantage cette population (fréquence 1 :25 à 1 :2), et d'initier des cultures avec de petits nombres de cellules [27] (~1x 10^3 cellules/mL). Cette stratégie a rendu possible la culture en micro-puits, et l'évaluation de plusieurs gènes candidats de façon simultanée, tel que décrit au chapitre 3 et 4, et en annexe 4 (voir Deneault É, Cellot S et al).

1.1.6. Cellules souches leucémiques (CSL)

À la lumière de leurs propriétés et de leur survie à long-terme dans un organisme, par opposition aux cellules différentiées, les cellules souches sont des cibles vulnérables pour cumuler des dommages pouvant conduire à une transformation maligne. Même si la leucémie représente une forme de dérégulation de l'AR, la majorité des blastes sont limitées dans leur capacité de proliférer. Les blastes leucémiques doivent constamment être régénérés par des cellules dotées d'un puissant potentiel d'AR, les cellules souches leucémiques (CSL) [28, 29] (Fig1.8). Celles-ci retiennent ou acquièrent quelques aspects des programmes développementaux régulant le comportement normal des CSH, suggérant des similarités dans les bases moléculaires de l'AR entre les CSH et les CSL. Seules les CSL peuvent initier et soutenir le développement d'une leucémie lorsque transplantées dans un receveur secondaire. Contrairement aux CSH normales, les CSL représentent phénotypiquement des populations cellulaires hautement hétérogènes, et leur identification repose sur des essais fonctionnels de transplantation. Au final, l'élucidation des bases moléculaires sous-tendant l'AR normal pourrait aussi contribuer à l'identification de cibles thérapeutiques spécifiques pour les CSL.

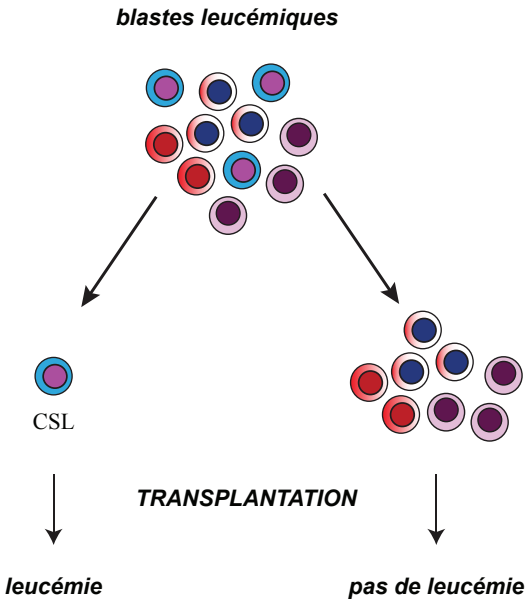

Figure 1.8 Concept de cellule souche leucémique (CSL). Panneau du haut : une leucémie est constituée d'une population cellulaire hétérogène. Panneau du bas : seule la fraction des CSL, dotées d'un potentiel d'auto-renouvellement, peuvent régénérer une leucémie chez des receveurs en transplantation secondaire.

1.1.7. Auto-renouvellement et applications thérapeutiques

La rare cellule souche est aussi responsable d'assurer la reprise de l'hématopoïèse suivant un conditionnement myéloablatif chez les receveurs d'une greffe de CSH. Pour une série de conditions malignes (eg, leucémies) ou bénignes (eg, hémoglobinopathies, déficits immunitaires), la greffe de CSH représente parfois la seule option à visée curative. Le succès de cette thérapie est tributaire du nombre absolu de CSH d'un greffon, un critère freinant l'utilisation du sang de cordon pour cette application, arborant une trop faible dose de CSH pour la majorité des patients de taille adulte. Toutefois, le sang de cordon est une source de CSH plus facilement accessible que la moelle osseuse, et permet aussi l'utilisation de greffons d'un moindre niveau d'histocompatibilité. Des stratégies permettant une modeste expansion en culture des CSH offriraient donc d'intéressantes options pour la thérapie cellulaire, incluant éventuellement la possibilité de corriger des défauts géniques *ex vivo* [30]. On estime à ~50 000 le nombre de transplantations de CSH effectuées annuellement dans le monde [31].

1.2 Facteurs nucléaires et régulation des CSH

1.2.1. Facteurs de transcription Hox

1.2.1.1. Réseau des gènes Hox

Le réseau des gènes HOX régule des processus clés du développement des mammifères, tels l'embryogénèse et l'hématopoïèse, et leur dérégulation est associée au développement de tumeurs. Hautement conservées dans l'évolution, les membres de la famille des Hox codent pour des facteurs de transcription à homéodomaine (gènes homeobox de classe 1) liant l'ADN et responsables de dicter l'identité spatio-temporelle des segments du corps le long d'un axe antéro-postérieur [32]. Chez les mammifères, on dénote 39 gènes *Hox* regroupés sur quatres régions chromosomiques distinctes, formant les complexes A, B, C et D (humain : 7p14-15,17q21-22, 12q12-13 et 2q31-37 respectivement; souris : 6C2, 11B4,15F2 and 2C3), voir Fig1.9. Chaque complexe (ou cluster) se voit sous-divisé en 13 groupements paralogues, selon le niveau d'homologie de l'homéodomaine, avec au plus 11 paralogues par secteur chromosomique. Les gènes *Hox* sont exprimés selon un principe de colinéarité spatiale selon lequel les gènes situés en 3' du complexe sont exprimés dans les structures antérieures de l'animal, et ceux en 5' dans les structures postérieures ou plus caudales. Leurs expression suit aussi un principe de colinéarité temporelle selon l'ordre de leur position dans le complexe, de 3' et en aval vers 5'. On rapporte le concept de prévalence postérieure, les gènes en 5' ayant un phénotype prédominant sur les gènes situés plus en 3'. Il existe aussi la classe 2 (*non-Hox*) des gènes homeobox, plus disparates structurellement et non regroupés physiquement en complexe sur un territoire. Environ 160 de ces gènes *non-Hox* sont répertoriés et dispersés dans le génome humain. L'élément commun qui définit principalement ces deux classes de gènes est la préservation de

la séquence codant pour l'homéodaine, permettant leur liaison à l'ADN (Fig1.10).

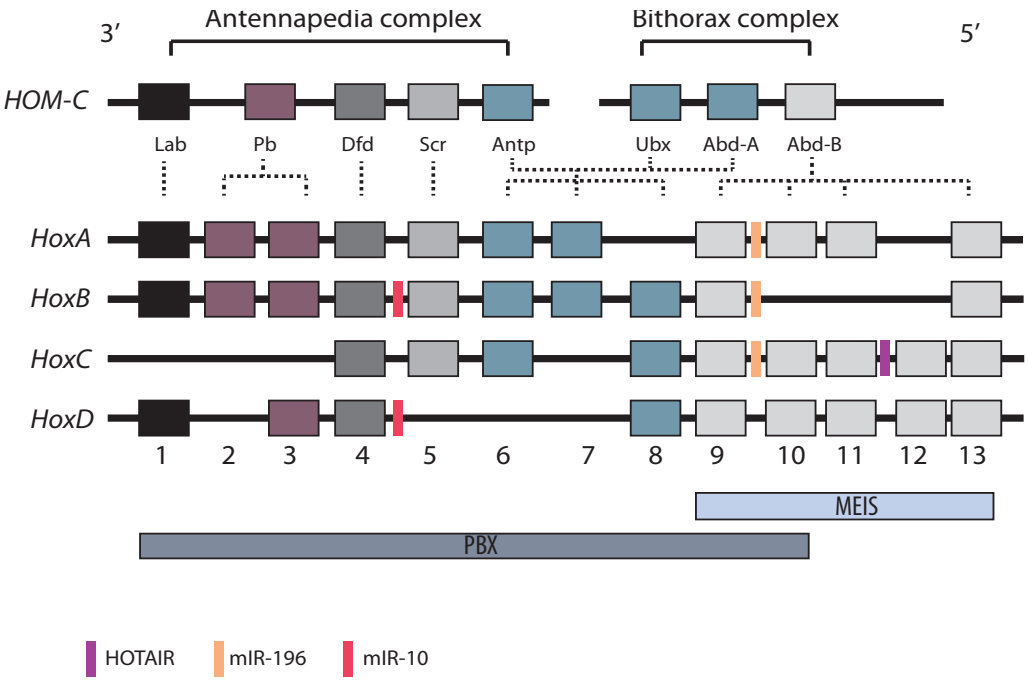

Figure 1.9 Complexes des gènes Hox. Schématisation des complexes A, B, C, et D des gènes Hox des mammifères, regroupés sur 4 chromosomes distincts, organisés en groupes paralogues 1à 13, de 3' en 5' sur le locus, selon le niveau d'homologie de l'homéodomaine. Les orthologues respectifs du complexe HOM-C (Homeotic Selector Complex) de la drosophile sont présentés en-haut du diagramme. La position des familles de microRNA mIR-10 (rouge) et mIR-196 (orange) et de l'ARN non-codant HOTAIR (violet) au sein des complexes est indiquée. La liaison préférentielle aux cofacteurs PBX1 et MEIS est indiquée au bas du diagramme. Voir section 1.2.1.1 de l'introduction. Lab: Labial; Pb: Proboscipedia; Dfd: Deformed; Scr: Sex combs reduced; Antp: Antennapedia; Ubx: Ultrabithorax; AbdA: Abdominal-A; AbdB: Abdominal B.

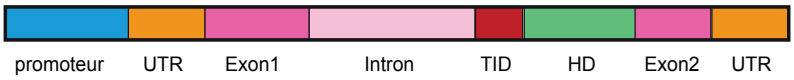

Figure 1.10 Structure des gènes Hox. Diagramme représentant les différentes portions d'un gène Hox. UTR : untranslated region ; TID; TALE interacting domain; HD : homéodomaine. Voir section 1.2.1.1 de l'introduction.

1.2.1.2. Rôle des gènes *Hox* dans le développement

Ces gènes « homéotiques » portent un nom désormais centenaire en lien avec leur découverte par les généticiens de la drosophile, et leur propension à changer un segment du

corps pour un autre lorsque mutés. La régulation segmentaire du corps de la drosophile par les complexes Bithorax (régions moyennes et postérieures) et Antennapedia (structures antérieures) sont des découvertes séminales dans le domaine [33]. En effet, une mutation de type gain-de-fonction de *Antennapedia (Antp)* résulte en une permutation de l'antenne pour des pattes [34]. La composition du complexe Bithorax (Bx-C) fut par la suite identifiée, regroupant 3 gènes, soit *Ultrabithorax (Ubx)*, *Abdominal-A (AbdA)* et *Abdominal B (AbdB)*. Une mutation de type perte-de-fonction de *Ubx* résulte d'ailleurs en une transformation de l'haltère (appendice du 3ème segment thoracique) pour une aile. Le complexe Antennapedia (Ant-C) de son côté réunit 5 gènes, soit *Labial (Lab)*, *Proboscipedia (Pb)*, *Deformed (Dfd)*,*Sex combs reduced (Scr)*, et *Antennapedia (Antp)* [35]. La sommation des deux complexe Ant-C et Bx-C résulte en l'entité HOM-C (Homeotic Selector Complex), représentant l'orchestrateur de l'identité segmentaire chez la drosophile et la structure ancestrale de l'évolution des gènes *Hox*. Les paralogues des groupes 1-8 sont plutôt reliés au complexe Ant-C, alors que les paralogues des groupes 9-13 plus similaires au gène Abd-B du complexe Bx-C, d'où la nomination classe Abd-B des gènes Hox. En 1995, E.B. Lewis a reçu le prix Nobel de physiologie pour l'ensemble de ses travaux en lien avec les gènes Hox. Une découverte séminale, dans un domaine demeurant en exploration, surtout quant au rôle des gènes Hox au niveau des cellules souches primaires normales et cancéreuses, de leur régulation, leur association en complexes, et de leurs cibles spécifiques.

1.2.1.3. Structure et collaborateurs

Le prototype architectural du gène *Hox* se compose de deux exons et un intron (Fig1.10), la séquence de 180 paires de bases codant pour l'homéodomaine se trouvant au sein deuxième exon, précédée du domaine permettant l'interaction avec les protéines de la famille TALE (Three Amino acid Loop Extension). Les facteurs de transcription HOX lient l'ADN via leur homédomaine, une structure hélice-coude-hélice de 60 acides aminés, mais de façon relativement faible *in vitro* [36-38]. L'interaction avec ses différents collaborateurs module l'affinité et la spécificité d'un facteur HOX pour une séquence d'ADN donnée, ainsi que ses propriétés trans-activatrices. Les principaux facteurs coopérant avec les gènes Hox pour la liaison à la d'ADN sont les protéines de la famille TALE, membres de la classe II des protéines à homéodomaines (non-HOX). L'interaction TALE-HOX est favorisée par la courte séquence peptidique de reconnaissance précédent l'homéodomaine, et codée par l'exon 2 des gènes *Hox* (Fig1.10). Classiquement, PBX1 et MEIS1 (et leur homologues Extradenticle/Exd et Homothorax/Hth chez la drosophile) sont les cofacteurs les plus extensivement étudiés et fonctionnellement impliquées dans la biologie des protéines HOX. De façon générale, PBX1 interagit préférentiellement avec les membres situés en 3' du locus des *Hox*, et MEIS1 avec les facteurs plus postérieurs en 5' (Fig1.9). De façon intéressante, PBX1 et MEIS1 arborent individuellement d'importantes fonctions développementales. En effet, une absence de *Pbx1* chez la souris

(*Pbx1*-/-) résulte en un phénotype embryonnaire létal entre E15.5 et E17.5, avec entre autre des anomalies du squelette axial et des CSH du foie, avec un défaut de maintenance de l'hématopoïèse [39, 40]. Une délétion homozygote de *Meis1* s'accompagne d'anomalies hématopoïétiques, ophtalmiques et angiogéniques, avec un décès à E14.5 [41, 42]. La fine modulation de l'impact transcriptionnel des HOX pourrait aussi impliquer d'autres cofacteurs, dont des protéines à doigt de zinc, tel que rapporté par certains groupes [43].

1.2.1.4. Gènes *Hox* et hématopoïèse

Un impact des gènes *Hox* sur le destin cellulaire des CSH ou des progéniteurs hématopoïétiques a été suspecté suivant les premières études décrivant leur profil d'expression dans ce tissu, au cours des années 1990. À la fois chez l'humain et la souris, le contingent hématopoïétique primitif exprime préférentiellement les gènes *Hox* des complexes A-C, excluant le complexe D [44-48]. Les approches quantitatives d'expression révèlent un enrichissement particulier pour les transcrits de *Hoxa4-7*, *Hoxa9* et *Hoxa11* dans les cellules du foie fétal, période de l'ontogénie associée à l'expansion du nombre des CSH [49]. Le niveau des transcrits des gènes *Hox* déclinent progressivement une fois le processus de différentiation amorcé [50]. L'impact fonctionnel de la modulation des niveaux des gènes *Hox* dans les cellules hématopoïétiques a fait l'objet de plusieurs études de surexpression, et de délétions, simples ou combinées, mentionnées ci-bas. De par leur organisation en complexes et leur déclinaison en groupes paralogues, certaines fonctions peuvent être redondantes parmi les facteurs, ajoutant un niveau de complexité à la l'analyse de modèles transgéniques, ainsi qu'à l'identification de gènes cibles. La sensibilité des cellules au dosage des gènes *Hox* est aussi un élément caratéristique de cette famille.

Un impact des gènes *Hox* sur l'auto-renouvellement des CSH est établi avec les études de surexpression de *Hoxb4* chez la souris, tel que discuté aussi dans le chapitre 2. Une élévation des niveaux de *Hoxb4* induit une expansion des CSH/progéniteurs *in vitro*, en présence de cytokines et de facteurs de croissance, et *in vivo* suivant la transplantation de cellules génétiquement modifiées. Ces cellules préservent un potentiel de différentiation lympho-myéloide au long-terme chez le receveur, en l'absence de transformation leucémique. Cet effet engendré par *Hoxb4* est aussi observé avec les CSH humaines et de singe [51]. L'exposition des cellules hématopoïétiques à la protéine recombinante fusionnée au domaine de transduction TAT, soit TAT-HOXB4, entraîne aussi une expansion du contingent primitif, plus modeste que la sur-expression [52]. Le comportement des cellules transduites avec *Hoxb4* a été extensivement caractérisé, mais la modulation d'autres gènes *Hox* influence la différentiation et prolifération cellulaire [14]. Par exemple, une sur-expression de *Hoxa9* permet aussi de soutenir des divisions d'auto-renouvellement des CSH en culture et *in vivo*, mais s'accompagne de transformation leucémique avec un temps de latence relativement prolongé, suggérant l'acquisition de mutations com-

plémentaires. De plus, une modulation des niveaux *Hoxa10*, *Hoxb3* ou *Hoxb6* entraîne un bloc de maturation des lignées lymphoïdes B et T, un défaut d'érythropoïèse et d'une prolifération maligne de la lignée myéloïde.

La délétion individuelle des gènes décrits ci-haut n'a que peu de répercussions développementales chez les souris homozygotes nulles dans les modèles transgéniques conventionnels. Notamment, une ablation du gène *Hoxb4* n'affecte pas l'hématopoïèse dans un modèle de souris knockout, tout au plus s'accompagnant d'une légère diminution du nombre et de la compétitivité des cellules primitives. La délétion simultanée de *Hoxb4* et *Hoxb3* entraîne un défaut similaire quoique plus prononcé. De façon intéressante, par une autre approche, une délétion substantielle du locus *Hoxb*, de *Hoxb1* à *Hoxb9*, génère des CSH fonctionnellement intactes [49]. Les cellules hématopoïétiques semblent en fait le plus sensible au dosage de *Hoxa9*, dont le transcrit est fortement enrichi dans les cellules primitives. L'ablation isolée de ce gène résulte en un phénotype plus marqué, avec un défaut de maturation des diverses lignées sanguines. De plus, les CSH *Hoxa9* nulles démontrent un défaut de reconstitution du système hématopoïétique lorsque transplantées dans le contexte d'essais de repopulation compétitive. À ce jour cependant, le phénotype le plus sévère est associé à l'ablation complète du locus des gènes *Hoxa*. Dans un contexte hétérozygote, les CSH adultes de la moelle des souris $Hoxa^{+/-}$ ont une capacité de reconstitution hématopoïétique réduite du tiers en comparaison à des cellules sauvages $Hoxa^{+/+,}$ dans des essais de reconstitution compétitive [53]. En revanche, les souris mutantes homozygotes $Hoxa^{-/-}$ succombent en période néonatale suite à une constellation d'anomalies hématologiques, cardiaques, respiratoires et de croissance [54].

1.2.1.5. Expansion des CSH et gènes *Hox*

L'exploitation des divisions d'auto-renouvellement des CSH revêt une importance particulière, tel que mentionné plus tôt, dans un contexte de thérapie cellulaire où des CSH doivent être préservées *in vitro* pour fin de manipulations génétiques, ou dans une visée d'amplification pré-transplantation. Compte tenu des limites imposées par les stratégies de purification des CSH, des outils d'expansion deviennent aussi critiques pour atteindre une masse cellulaire totale rendant permissibles les diverses analyses biochimiques. Dans cette perspective, tel que présenté au chapitre 2, l'étude de variantes des gènes *Hox* s'est avérée utile. La surexpression simple de *Hoxb4* a permis d'atteindre une augmentation du nombre de CSH de 40-fois en culture, et de 3 log *in vivo* dans les mois suivant la transplantation [55]. Des analyses biochimiques ont révélé que la liaison à l'ADN était essentielle à la fonction d'expansion de HOXB4, mais que son interaction avec PBX1 était dispensable [56]. Ensuite, les travaux du laboratoire associant une répression de *Pbx1* à une surexpression de *Hoxb4* ($Hoxb4^{hi}Pbx1^{lo}$) dans les CSH ont mené à un niveau d'expansion inégalé et supra-physiologique de l'ordre de 5 log [26] (détaillé au chapitre

2) en culture. De façon concomitante, un groupe de collaborateurs a obtenu des expansions de magnitude similaire en fusionnant divers segments de gènes homéotiques à la portion N-terminale du gène de la nucléoporine *Nup98* [57]. Cette portion de NUP98 conserverait les éléments répétitifs FG (Phénylalanine/Glycine) et les propriétés activatrices de la transcription. Parmi les gènes de fusion ainsi générées, une surexpression de *Nup98-Hoxb4* et de *Nup98* fusionné à l'homéodomaine de *Hoxa10* (NA10hd) dans les CSH ont conduit à des expansions inégalées *in vitro* de 300-fois et 2000-fois, respectivement. Suivant ces niveaux soutenus d'auto-renouvellement, les cellules primitives préservaient leurs propriétés de différentiation une fois réintroduites *in vivo*. Dans l'ensemble ces constructions devraient faciliter l'exploration des bases moléculaires de l'auto-renouvellement des CSH.

1.2.1.6. Gènes *Hox* et hémopathies malignes

En plus de leur rôle dans l'hématopoïèse normale, les gènes *Hox* sont fréquemment dérégulés dans les leucémies, par des mutations les impliquant directement ou perturbant leur expression. Tel que mentionné, une surexpression de *Hoxa9* conduit progressivement à une transformation leucémique, suivant l'acquisition d'aberrations génomiques additionnelles. MEIS1 est un collaborateur reconnu et bien caractérisé de HOXA9 dans la pathogénèse des leucémies [58]. Une surexpression conjointe de ces deux gènes dans des cellules hématopoïétiques primitives induit des leucémies myéloïdes aigues agressives, avec un temps de latence raccourci du tiers (154,1 ± 9,8 vs 55,0 ± 2,8 jours) [59]. Un bloc de différentiation conféré par HOX, associé à une force prolifération de MEIS1, pourraient expliquer cette coopération HOX/MEIS1 dans l'induction des leucémies. Une proportion fort significative des leucémies aigues, de type myéloïde ou lymphoïde, s'accompagne d'une augmentation de l'expression des gènes *Hox*, notamment *Hoxa9*, et de *Meis1*[60].

Plusieurs mutations et réarrangements chromosomiques impliqués dans les leucémies perturbent le profil d'expression des *Hox*. Notamment, une mutation dans le gène de la nucléophosmine (NPM1), bien décrite dans les LMA, est associée à une activation des gènes *Hox* et de *Meis1* [61, 62]. Certaines oncoprotéines de fusion, générée par la juxtaposition de deux régions chromosomiques dans les translocations leucémiques interfère aussi avec l'expression normale des gènes *Hox*. Les exemples abondent en ce sens, mais certainement les plus classiques sont les réarrangements impliquant l'histone méthyl-transférase MLL, ou l'histone acétyl-transférase MOZ, tel que décrits plus loin dans l'introduction (voir section 1.3). Ces modificateurs de la chromatine sont d'ailleurs bien documentés comme étant des régulateurs de l'expression des *Hox*. Un cas pédiatrique de LMA caractérisé par un réarrangement comprenant comme partenaires de fusion la nucléoporine NUP98 associée au domaine C-terminale de l'histone déméthylase JARID1A est nouvellement décrit [63]. La surexpression de cette translocation *Nup98-Jarid1a* dans

des cellules hématopoïétiques de souris en révèle le puissant potentiel oncogénique, donnant lieu à des LMA de très courte latence [64]. Dans les blastes leucémiques, le néo-oncogène engendre une augmentation de l'expression de gènes clés de l'hématopoïèse, soit *Hoxa5,7,9,10, Gata3, Meis1, Eya1* et *Pbx1*, ainsi qu'une activation épigénétique directe du locus des gènes *Hoxa*.

Non seulement la modulation de leur expression, mais des mutations impliquant directement les gènes *Hox* sont décrites dans les hémopathies malignes. Une fusion impliquant le récepteur β des cellules T et des facteurs HOXA (TCRβ-HOXA) est répertoriée dans les leucémies T, en association avec une dérégulation de l'activation des gènes du locus *Hoxa* [65, 66]. De façon notable, au moins 7 gènes *Hox* de type *Abd-B (Hoxa9, a11, a13, c11, c13, d11, d13)* se trouvent au sein de réarrangements joignant la portion N-terminale de la nucléoporine NUP98 à la portion C-terminale du gène homéotique, incluant l'homéodomaine [67]. Chez la souris, la surexpression de certaines de ces oncoprotéines à l'aide de vecteurs rétroviraux dans le compartiment hématopoïétique engendre des syndromes myéloprolifératifs évoluant vers des leucémies. Ceci est particulièrement bien décrit pour *Nup98-Hoxa9* et *Nup98-Hoxd13* [68, 69], et confirmé dans des modèles de souris transgéniques sur-exprimant de façon constitutive ces réarrangements (souris knockin) [70, 71]. De plus, ces fusions démontrent aussi une coopération avec *Meis1* et son rôle d'accélérateur de la leucémogénèse, comme les facteurs *Hox* natifs en surexpression [68, 69, 72].

1.2.1.7. Régulation des gènes Hox

Tel que discuté dans la prochaine section, les membres de la famille des Trithorax (Trx) et des Polycomb (PcG) sont d'importants orchestrateurs de la transcription des *Hox*, et classiquement de façon antagoniste. Outre ces modificateurs de la chromatine, un niveau de régulation transcriptionelle des *Hox* inclue vraisemblablement les microRNA (miRNA). Les miRNA sont de courtes séquences nucléotidiques (~22 nt) ciblant une séquence complémentaire d'ARN messager (ARNm), promouvant ainsi sa dégradation et interférant avec le processus translationnel [73, 74]. Certaines séquences codant pour des miRNA sont d'ailleurs incorporées au sein des complexes des *Hox* chez les vertébrés, dont la famille des miRNA miR-10 et miR-196 [75], (Fig1.9). Au sein des complexes des *Hox*, trois loci codent pour des membres de la famille miR-196 (Fig1.9.), lesquels arborent un haut niveau de complémentarité avec la portion 3'UTR du ARNm de *Hoxb8*, et conduisent à la fragmentation enzymatique de ce dernier [76, 77]. Ces miRNA notamment pourraient cibler d'autres transcrits des *Hox*, comme *Hoxb8*, *Hoxc8* et *Hoxa7*. Une relation inverse entre l'expression de miR-10a et *Hoxb4* est également décrite, néanmoins sans région d'homologie entre les deux séquences [76].

La découverte de longs ARN non-codant (ncARN), de taille variant entre 300 nt et 10 kb, ajoute un niveau de complexité à la régulation épigénétique des gènes *Hox*. Plus de 200 séquences de ces ncARN ont été répertoriées dans les régions génomiques contenant le réseau des *Hox* [78]. Cette étude séminale explore le réseau des *Hox* dans des fibroblastes humains, dérivés de divers sites anatomiques, correspondant à un point précis de l'axe développemental spatio-temporel. L'expression des ncARN semble aussi colinéaire, et démarque nettement des zones contigues d'activation et de répression transcriptionnelle, fidèle au tissu embryonnaire d'origine. La majorité des ncARN démontre un sens inverse de transcription par rapport aux gènes *Hox*. Les auteurs ont caractérisé un nouvel ncARN de 2.2 kb, dénommé HOTAIR (Hox Antisense Intergenic RNA), encrypté au sein du locus *Hoxc* (entre *Hoxc11* et *Hoxc12*), et régulant en trans l'activation du cluster des Hoxd. Une fonction plus répandue de ces longs ncARN serait notamment de moduler l'ancrage de modificateurs de la chromatine à l'ADN. HOTAIR favoriserait le recrutement d'un complexe PcG, soit le PRC2 (Polycomb Repressive Complex 2), et la déposition subséquente d'une marque répressive de la transcription (H3K27me3), empêchant ainsi localement l'expression génique.

1.2.1.8. Facteurs de transcription *non-Hox* et hématopoïèse

Bien que les facteurs *Hox* soient des déterminants majeurs de l'identité cellulaire des CSH, d'autres protéines nucléaires influencent le développement du système hématopoïétique. Un même facteur peut jouer un rôle à des stades de différentiation distincts, et contribué au développement normal du système sanguin ainsi qu'à la pathogénèse des leucémies lorsque dérégulé [79, 80] (Fig1.1). Plusieurs facteurs jouent ce rôle, et les membres de la famille GATA (1-3) sont énumérés à titre d'exemples. Ces protéines partagent des domaines doigt de zinc et de liaison à l'ADN. GATA 2 est essentiel au maintien des CSH et des progéniteurs [81], puis requis pour la différentiation terminale des mastocytes [82]. De plus, sa répression est nécessaire pour la permettre la différentiation le long de l'axe érythroïde [83]. De façon très intéressante, une mutation de ce facteur prédispose au développement de syndromes myélodysplasiques (SMD) et de leucémies, notamment à une entité nouvellement décrite, le syndrome MonoMac, une forme de SMD associé à un déficit immunitaire [84] par un défaut de maturation d'un précurseur lymphoïde mixte. Les familles étudiées avec ce syndrome arborent principalement des mutations faux-sens au niveau des domaines doigts de zinc, altérant possiblement les interactions protéine-protéine ou protéine-ADN.

Dans cette perspective, une base de données regroupant divers facteurs nucléaires a été générée au laboratoire (Faubert A.), et des scores de priorité attribués quant à leur probabilité d'influencer le destin des CSH. En sélectionnant les 150 candidats se trouvant au sommet de la liste, un crible de surexpression de ces gènes dans des CSH de souris a été

effectué dans notre équipe, et l'impact fonctionnel de cette modulation mesuré *in vivo* post transplantation (voir en annexe 4 Deneault É., Cellot S et al, Cell 2009). Cette étude a permis d'identifier 18 nouveaux facteurs nucléaires dont les niveaux d'expression ont un impact sur l'activité des CSH [27] (*Cnbp*, *Erdr1*, *Fos*, *Hdac1*, *Hmgb1*, *Hnrpdl*, *Klf10*, *Pml*, *Prdm16*, *Sfpi1* (*Pu.1*), *Ski*, *Smarcc1 (Baf155)*, *Sox4*, *Tcfec*, *Trim27*, *Vps72*, *Xbp1*, and *Zfp472*). De façon intéressante, certains de ces facteurs agissent de façon directe dans la CSH (cellule-autonome), ou via la production d'un facteur de croissance par un autre type cellulaire (non-cellule-autonome), tels *Fos*, *Tcfec*, *Hmgb1* et *Sfpi1*. Globalement, cette portion de travail a permis d'évaluer fonctionnellement et de façon simultanée plusieurs gènes, et d'élargir le spectre de candidats influençant le devenir des CSH.

1.2.2. Modificateurs de la chromatine

1.2.2.1 Introduction

Outre les facteurs de transcription, d'autres médiateurs nucléaires peuvent influencer le profil d'expression génique et moduler le destin cellulaire des CSH, et parmi ceux-ci, on retrouve les modificateurs de la chromatine. Ce niveau de régulation de la transcription n'altère pas la séquence de l'ADN, mais se trouve à un palier supérieur au code génétique proprement dit, nommé épigénétique. Ainsi, certaines portions du noyau cellulaire seront ouvertes et accessibles à la machinerie transcriptionnelle (euchromatine) ou fortement compactées et inatteignables (hétérochromatine). L'unité de condensation nucléaire étant composée d'un entrelacement d'ADN et de protéines (histones et non-histones), à la fois les acides nucléiques et les acides aminés peuvent faire l'objet de modifications post-translationnelles. Les ADN méthyl-transférases (DNMT), par exemple, apposent un groupement méthyl au carbone-5 des bases cytosines au sein des ilots dinucléotides cytosine-guanine (CpG) souvent situés à proximité ou à l'intérieur des régions promotrices [85]. La méthylation de l'ADN s'associe de façon générale à une répression de la transcription. Les processus de neutralisation de la méthylation de l'ADN sont encore méconnus, mais pourrait impliqués la famille des enzymes TET [86, 87], convertissant le 5-méthylcytosine (5mC) en 5-hydroxymethylcytosine (5hmC). Concernant la position terminale des histones, elles peuvent subir plusieurs modifications post-translationnelles, incluant la méthylation et l'acétylation, mais aussi la phosphorylation, l'ubiquitination, la sumoylation et l'ADP-ribosylation [88]. Dans l'ensemble, ces marques épigénétiques influencent la topographie locale de la chromatine, conférant une spécificité d'ancrage aux divers facteurs nucléaires, résultant en un patron d'expression finement orchestré qui évoluera en fonction du stade de développement et du contexte cellulaire.

1.2.2.2 Méthylation de l'ADN

Plusieurs de ces effecteurs épigénétiques jouent un rôle déterminant dans l'hématopoïèse

normale et leucémique, dont les enzymes impliquées dans la méthylation de l'ADN [89]. Il existe au moins trois types de DNMT, soit DNMT3A et DNMT3B pour la méthylation de novo, et DNMT1 pour la maintenance la méthylation [90]. Cette méthylation constitutive de l'ADN médiée par DNMT1 est essentielle pour l'auto-renouvellement des CSH, ainsi que pour leur différentiation [91, 92]. En effet, un niveau atténué de DNMT1 dans les cellules hématopoïétiques primitives entraîne une activation aberrante des gènes liés au compartiment myéloïde et nuit au développement des lignées lymphoïdes B et T. De façon intéressante, la fonction de DNMT1 est aussi nécessaire à l'activité des cellules souches leucémiques (CSL) [91], et pourrait constituer une cible thérapeutique, de par une sensibilité différentielle au dosage de l'enzyme entre les cellules normales et leucémiques [93]. La mise en évidence de mutations impliquant *Dnmt3a* dans les leucémies myéloïdes humaines [94] et les syndromes myélodysplasiques [95] soutient le concept que cette famille de protéines contribue au processus décisionnel quant au choix du destin cellulaire. DNMT3A semble dispensable pour l'activité des CSH normales [96], mais une étude récente suggèrerait une augmentation de l'auto-renouvellement, dans un contexte de transplantations sériées, en l'absence de DNMT3A [12]. Des mutations d'enzymes liées à la déméthylation de l'ADN par hydroxylation, dont TET2, sont aussi rapportées dans les cancers d'origine hématopoïétiques [97]. Le dosage et la distribution des marques épigénétiques de l'ADN semble donc influencer les programmes transcriptionnels spécifiant l'identité cellulaire.

1.2.2.3 Méthylation des histones

Non seulement l'ADN, mais aussi la composante protéique de la chromatine peut subir des modifications épigénétiques, principalement au niveau de la queue des histones. En ce sens, l'histone méthyl-transférase MLL (Mixed Lineage Leukemia) illustre de façon classique le rôle primordial d'un régulateur épigénétique dans le développement du tissu hématopoïétique normal, ou des leucémies lorsque muté. MLL est le membre fondateur du groupe du complexe de protéines Trithorax (Trx) régulant certains gènes clés du développement, dont le locus des gènes *Hox*, et ce de façon antagoniste aux protéines du groupe des Polycomb (PcG) [98]. En général, les complexes PRC2 et PRC1 des protéines PcG sont liés à la répression des gènes, et les complexes Trx (MLL ou COMPASS) à leur activation. L'activité histone méthyl-transférase (HMT) d'EZH2 (Enhancer of Zeste Homolog 2) du PRC2 catalyse la tri-méthylation de la lysine 27 de l'histone H3 (H3K27me3). Cette modification covalente sert de point d'ancrage au PRC1 qui mono-ubiquitine la lysine 119 de l'histone H2A (H2AK119Ub), résultant en une inhibition de l'expression génique. Inversement, les complexes protéiques contenant l'histone méthyl-transferase MLL (MLL1-5) opposent ces marques épigénétiques en apposant une marque de tri-méthylation à la lysine 4 de l'histone H3 (H3K4me3) aux sites d'initiation de la transcription. Cette modification est liée à la transcription génique et au recrutement des histones déméthylases UTX et JMJD3 pouvant effacer la marque répressive de H3K27me3. Les

protéines Trx induisent d'autres modifications telles l'acétylation de H3K27 (H3K27Ac) et la di-méthylation de H3K36 (H3K36me2) favorisant une configuration d'activation transcriptionnelle, et renforçant ainsi l'antagonisme envers les marques répressives des PcG. Au niveau des cellules souches embryonnaires, ces marques activatrices et répressives peuvent coexister sur un même locus, dotant ainsi les gènes régulateurs du développement d'un double potentiel d'expression, soit « ON » (H3K4me3) ou « OFF » (H3K27me3), selon le contexte cellulaire (Fig 1.11).

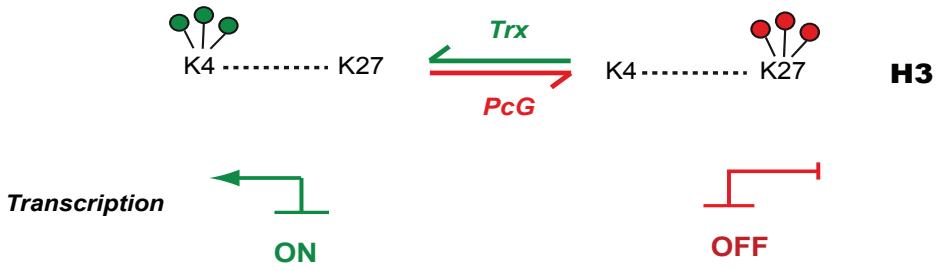

Figure 1.11 Effet des complexes Trithorax (Trx) et Polycomb (PcG) sur la transcription génique. Gauche (vert): l'action du complexe Trx favorise la tri-méthylation de la lysine 4 de l'histone H3 (H3K4) et l'activation de la transcription. Droite (rouge): l'action du complexe PcG favorise la tri-méthylation de la lysine 27 de l'histone H3 (H3K27) et la répression de la transcription.

1.2.2.4 L'histone méthyl-transférase MLL et développement normal

En tant que modificateur de la chromatine, MLL1occupe effectivement un rôle central dans la régulation de l'hématopoïèse normale et leucémique. L'étude de translocations leucémiques récurrentes impliquant la région chromosomique 11q23 a permis l'identification du gène Mll1 chez l'humain en 1991 [99]. De taille considérable, le gène Mll1 humain (~89 kb) contient 37 exons codant pour une protéine de 3969 acides aminés, ou 500kD. Deux sous-unités liées de façon non-covalente composent la protéine mature ($MLL^{N320/C180}$), résultant d'un clivage par l'action de la taspase 1 au niveau de sites de reconnaissance enzymatique (cleavage site 1 and 2; CS1, CS2, Fig1.12) [15]. Cette protéine est constituée de plusieurs domaines, dont certains conservés depuis l'orthologue Trx de la drosophile. La topographie de MLL1 est schématisée à la Fig1.12, incluant quelques domaines clés définis pour cette protéine. En bref, on retrouve depuis la portion N-terminale et en aval, trois domaines AT-hook (ATH1-3) pouvant lier l'ADN, deux signaux de localisation nucléaire (SNL1,2), et un domaine de répression transcriptionelle (TRD) contenant entre autre un motif doigt de zinc (CxxC), homologue à DNMT1. On retrouve ensuite des domaines PHD (plant homology domain, PHD1-3), pouvant médier des intéractions protéine-chromatine ou protéine-protéine, un domaine d'activation transcriptionnelle (TA) et la portion SET (Su(var)3-9, enhancer of zeste, trithorax) en C-terminale, contenant l'activité H3K4me3 méthyl-transférase de MLL1. Les protéines SET, initiale-

ment caractérisées chez la drosophile et la levure, arborent plusieurs attributs, dont celui d'évoluer au sein d'un complexe dont la composition finale dictera la résultante transcriptionnelle. On retrouve chez les cellules de mammifères au moins six H3K4 méthyl-transférases, SET1A, SET1B, MLL1-4, oeuvrant au sein de complexes COMPASS.

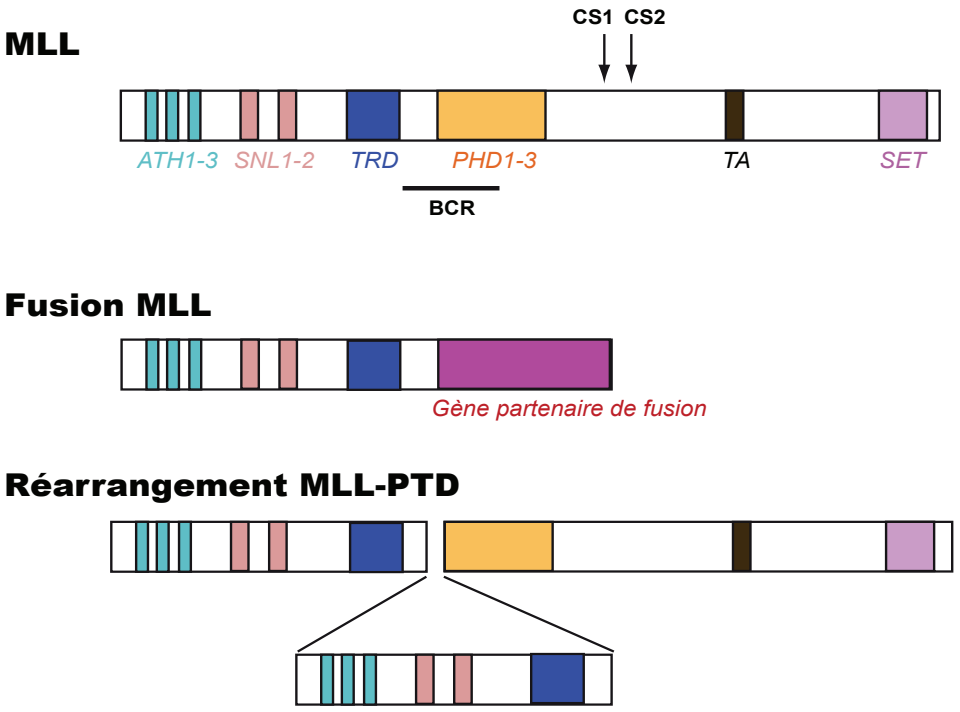

Figure 1.12 Structure du gène Mll (Mixed Lineage Leukemia) et des translocations dérivées. Panneau du haut : domaines du gène Mll. Depuis la portion N-terminale, à gauche : domaines AT-hook (ATH1-3) de liaison à l'ADN; signaux de localisation nucléaire (SNL1,2); domaine de répression de la transcription (TRD); domaines PHD 1-3 (Plant HomeoDomain); sites de clivage de la taspase 1 (CS1, CS2 : cleavage site 1 et 2); domaine de transactivation (TA); et le domaine catalytique SET (Su(var)3-9, enhancer of zeste, trithorax) en C-terminale. Le point de cassure (BCR : breakpoint cluster region) des réarrangements chromosomiques impliquant Mll est indiqué en noir. Panneau du centre : modèle de translocation chromosomique fusionnant la portion N-terminale de Mll à plus de 60 gènes partenaires différents. Panneau du bas : schéma du réarrangement chromosomique de type duplication en tandem (PTD : Partial Tandem Duplication).

Concernant Mll1, une étude de souris mutantes a permis de cerner l'importance fonctionnelle de ce gène, quelques années suivant son identification. On y rapporte notamment un retard de croissance, des cytopénies, une altération de l'expression des gènes *Hox* (dont *Hoxa7* et *Hoxc9*) et des anomalies homéotiques du squelette, anomalies décelées dans un contexte hétérozygote [100]. Une abolition homozygote de *Mll1* résulte en une létalité embryonnaire entre le jour E9.0 et E12.5, et une absence d'expression des gènes *Hox*.

Plus récemment, des modèles inductibles de délétion de *Mll1*ont permis de mettre en évidence un rôle essentiel de MLL1 dans l'auto-renouvellement des CSH. La perte de *Mll1* entraîne une aplasie médulllaire dans les 3 semaines suivant l'excision des allèles par l'enzyme Mx1-cre, par déplétion du contingent hématopoïétique primitif, les CSH étant recrutées hors de la phase de quiescence du cycle cellulaire et rapidement épuisées [101]. On note aussi une diminution de l'expression des gènes *Hoxa7*, *Hoxa9* et *Hoxa10* dans une population KLS, enrichie en CSH. Dans ce contexte, les cellules progénitrices quant à elles perdent leur potentiel prolifératif. MLL1 semble donc essentiel à la survie des cellules souches/progénitrices et à l'homéostasie du tissu hématopoïétique adulte. Différents modèles de disruption génique ont permis d'obtenir des embryons *Mll*$^{-/-}$ survivant au-delà du jour E14.5 (E12.5-E16.5) et de démontrer de façon similaire le rôle crucial de ce gène dans l'hématopoïèse fétale [102, 103]. De façon intéressante, l'abolition isolée la portion codant pour le domaine SET du gène de *Mll1* ne résulte pas en une létalité chez les souris mutantes homozygotes, mais en un phénotype léger, incluant des transformations homéotiques et une réduction de l'expression des gènes *Hox* [104].

L'activité de MLL1 se déploie donc à l'intérieur d'un complexe pouvant moduler la configuration de la chromatine par la méthylation (H3K4me3), l'acétylation (H3K27Ac) ainsi qu'une propriété de remodelage. WDR5 et ASH2L appartiennent à ce complexe, interagissant avec la portion C-terminale du domaine SET, et contribuant à l'activité méthyl-transférase de MLL1 [105, 106]. MENIN par ailleurs lie la portion N-terminale de MLL1 et assure un pont avec la machinerie transcriptionnelle [107]. L'association de MLL1 avec plusieurs régions promotrices du génome, ainsi que sa co-localisation avec la RNA polymérase II et la marque épigénitique activatrice H3K4me3, lui suggère une influence globale sur la transcription [108, 109]. Cependant, une régulation spécifique d'un sous-groupe de gènes cibles, comme les gènes *Hox*, est aussi attribuée à MLL1 [110]. Un pattern de liaison des régions promotrices beaucoup plus étendu de MLL1 sur le territoire 5' des gènes *Hoxa* est d'ailleurs décrit, de *Hoxa7* à *Hoxa13*, et sur *Hoxa1*, dans des cellules monocytaires U937 [108]. Ces mêmes régions liées pas MLL1 sont denses en tri-méthylation de la H3K4, suggérant une configuration active de la chromatine pour ce domaine de gènes cibles. MLL1 s'associe aussi à des régions génomiques codant pour des miRNA, comme le locus de mIR-17-92, impliqué dans l'hématopoïèse normale et leucémique [108, 111, 112]. Plus récemment, outre la transcription, on attribue à MLL1 des fonctions régulatrices en lien avec le cycle cellulaire, la sénescence, le dommage à l'ADN et même la signalisation (voir revue [98]).

1.2.2.5 Implication de MLL dans les leucémies

MLL1 (Mixed Lineage Leukemia; chromosome 11q23) se démarque également par son implication dans la pathogénèse des leucémies humaines. Un réarrangement chromoso-

mique associant la portion N-terminale du gène Mll1 (breakpoint cluster region BCR, Fig1.12, pour visualiser le point de cassure, s'étendant sur 8.3 kb entre les exons 8 et 13) à plus de soixante différents partenaires génère un puissant oncogène de fusion. À noter que le domaine SET, conférant l'activité méthyl-transférase du complexe MLL, est exclu de la protéine de fusion. Cette mutation est en cause dans plus de 70% des leucémies du nourrisson, générant des leucémies aigues de type myéloïde ou lymphoïde souvent mises en évidence dans les premiers mois de vie [113]. Ce même réarrangement chromosomique est aussi fréquemment responsable des leucémies secondaires, c'est-à-dire induites par des agents de chimiothérapie, en particulier les inhibiteurs de topoisomérase II [114]. Le pronostic de survie pour ces maladies, avec les modalités de traitement actuellement disponibles, demeure réservé. Selon des données récentes, la réponse au traitement semble modulée par la nature de la lésion génétique, avec un taux de survie de ~10% en présence d'une translocation t(6;11) [115], mais de l'ordre de 80% pour une t(1;11), reflétant l'hétérogénéité de cette maladie. Les partenaires de fusion de MLL peuvent se regrouper en 4 catégories fonctionnelles distinctes; les protéines nucléaires (AF4, AF9, M AF10, ENL, ELL), qui sont les plus communes, les protéines cytoplasmiques (eg, AF6), la famille des septines contrôlant divers processus cytoplasmiques dont le trafic vésiculaire, et les histones acétyl-transférases (CBP, p300) [15].

D'un point de vue mécanistique, la surexpression d'une oncoprotéine de fusion MLL, notamment t(9;11), via des constructions rétrovirales dans des progéniteurs myéloïdes induit des leucémies agressives chez la souris [116]. Ce processus entraînerait une réactivation du programme d'auto-renouvellement dans ce contingent cellulaire relativement immature et doté d'un fort potentiel prolifératif. La portion N-terminale l'oncoprotéine de fusion guiderait son ancrage vers des régions cibles du génome, en grande partie redondantes avec celles de MLL sauvage [117], alors que le partenaire de fusion remplirait une fonction de transactivation. La transformation leucémique induite par les fusions MLL repose entre autre sur l'activation des gènes *Hoxa9*, *Meis1*, mais aussi *Hoxa5*, *Hoxa10* et *Mef2c* [118-120]. Dépourvues du domaine SET de la protéine sauvage, les fusions MLL peuvent activer la transcription génique en interagissant avec l'histone méthyl-transférase DOT1L, modifiant le résidu H3K79 [121-123]. D'ailleurs DOT1L est rapporté comme essentiel pour le maintien des leucémies dérivées d'une mutation de MLL. L'interaction du tumeur suppresseur MENIN avec la fusion MLL, et leur liaison à la région promotrice du gène *Hoxa9*, semblent aussi essentiels au processus de transformation leucémique [124, 125]. Chez l'humain, ~5% des patients avec leucémies myéloïdes aigues arborent une duplication en tandem des exons 5-11 de Mll1, en l'absence de translocation [126]. Un modèle expérimental étudiant cette mutation chez la souris par méthode de « knock-kin » révèle aussi une dérégulation de l'expression de la portion 5' du locus des gènes *Hoxa* (*Hoxa7,9,10*) dans les cellules hématopoïétiques [127]. Globalement, ces études soulignent à nouveau le lien entre régulation de la chromatine, de l'expression des gènes

Hox, et du destin cellulaire.

1.2.2.6 L'histone acétyl-transférase MOZ et hématopoïèse normale

Un parallèle peut être établi en MLL1 et autre modificateur épigénétique, soit MOZ (MOnocytic leukemia Zinc finger protein), impliqué non pas dans la méthylation, mais bien dans l'acétylation des histones, une autre marque d'importance dans la régulation post-translationnelle de la chromatine. En effet, *Moz* tout comme *Mll1*, est essentiel au développement du tissu hématopoïétique. L'ablation de ce gène chez la souris résulte en un décès *in utero* (E14.5) ou à la naissance, selon le modèle transgénique utilisé, avec un défaut de maintenance des cellules souches hématopoïétiques et une dérégulation de l'expression de certains gènes, dont les gènes *Hox*, *c-Mpl* et *c-Kit* [128, 129]. Les cellules du foie fétal des souris mutantes $Moz^{-/-}$ ne peuvent pas reconstituer le système hématopoïétique d'un receveur létalement irradié. Une absence de *Moz* entraîne aussi une diminution du nombre de progéniteurs, mais préserve leur capacité de différentiation vers les lignées matures du sang. L'histone acétyl-transférase MOZ, ou MYST3, appose une marque d'acétylation au niveau des histones H2A, H3K14, H4K5, K8, K12 et K16 [130]. Elle fait partie de la famille des histones acétyl-transférases comprenant le domaine catalytique MYST (MOZ, Ybf2(Sas3), Sas2 et Tip60), avec une fonction de co-activateur de la transcription. Comme MLL, c'est une protéine de haut poids moléculaire, composée de plusieurs sous-unités (Fig1.13). De façon intéressante, l'expression du gène *Hoxa9* requiert l'acétylation de H4K16 par l'HAT MOF(ou MYST1), elle-même dépendante de la méthylation de H3K4 par MLL [105].

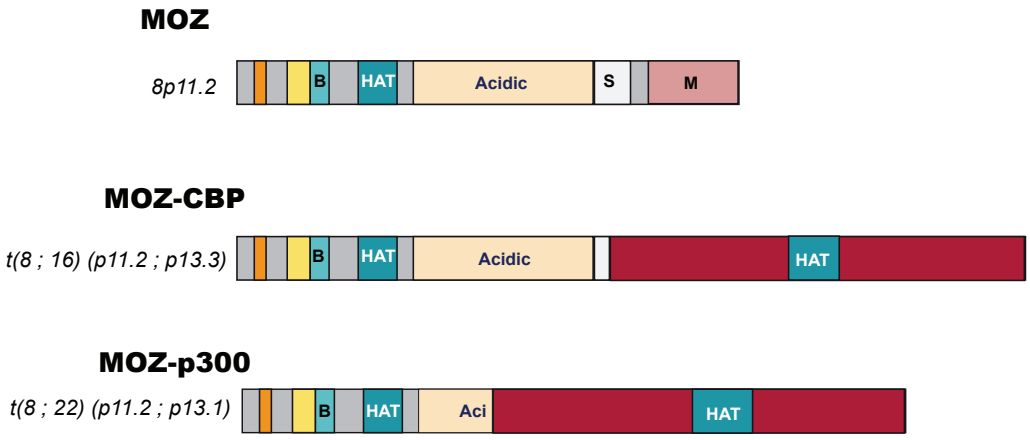

Figure 1.13 Structure du gène *Moz* et des translocations dérivées. Panneau du haut : domaines du gène Moz. Depuis la portion N-terminale à gauche : un domaine d'analogie aux histones (orange); domaine PHD (jaune), domaine basique (B); un domaine histone acétyl-transférase (HAT); un domaine riche en sérine (S); et un domaine riche en méthionine (M). Panneaux du bas : modèle de translocation chromosomique fusionnant la portion N-terminale de Moz à différents partenaires de fusion, dont CBP et p300 (rouge), contenant aussi un domaine HAT. Moz : MOnocytic leukemia Zinc finger protein; CBP : CREB binding protein.

1.2.2.7 Implication de MOZ dans les leucémies

Certaines translocations leucémiques impliquent le gène *Moz*, juxtaposant la portion N-terminale de *Moz* (8p11) (incluant le domaine Myst) à la portion C-terminale d'un un autre gène candidat, dont Cbp (CREB Binding Protein) (16p13) [131], p300(22q13) [132] et Tif2(8q13) [133]. Ceci génère une puissante oncoprotéine de fusion, capable d'induire des leucémies lorsque surexprimée dans des populations de précurseurs granulo-macrophagiqes (GM), tel que démontré chez la souris pour la fusion MOZ-TIF2, inv(8)(p11;q13) [134]. Par opposition, la t(9;22)(q34;q11) codant pour l'oncoprotéine de fusion BCR-ABL (ou chromosome de Philadelphie) et retrouvée dans la leucémie myéloide chronique (LMC) [135], ne peut induire une transformation leucémique lorsque sur-exprimée dans cette même population de progéniteurs. Ceci suggère que MOZ-TIF2 confère la capacité de réactiver un programme d'auto-revouvellement à des cellules hématopoïétiques ayant amorcé un programme de différentiation. Ces mutations résultent en une dérégulation de la transcription, dont une sur-expression des gènes *Hoxa9*, *Hoxa10* et *Meis1*, dans les leucémies humaines induites par la translocation MOZ-CBP t(8;16)(p11p13) [136]. D'abord identifiée comme une anomalie récurrente chez des patients atteints de LMA en 1996, MOZ-CBP est présente dans ~0.7% des cas, dont une grande proportion est pédiatrique [137]. Des réarrangements chromosomiques impliquant le gène Moz sont d'ailleurs rapportés dans des cas de syndrome myélodysplasique de l'enfant[138]. De plus, une trisomie 8 partielle en mosaïcisme, restreinte à la région 8p11.21-q11.21, comprenant une trentaine de gènes dont Moz, semble prédisposer au développement de leucémies myéloides [139].

1.3 Histone déméthylases et destin cellulaire

1.3.1 Réversibilité de la méthylation des histones

Tel que mentionné dans les sections précédentes, la modification post-translationnelle des histones par méthylation, tout comme par acétylation, influence les programmes transcriptionnels et contribue à la mémoire épigénétique de l'identité cellulaire. Entre autre, une topographie précise de méthylation des lysines 4 et 27 de l'histone H3 (H3K4/H3K27) doit être maintenue pour arrimer l'architecture de la chromatine au destin cellulaire [140]. Ce sont essentiellement les acides aminés en N-terminale, faisant protrusion de l'octamère d'histones du nucléosome ([H2A, H2B, H3, H4] x2), ou unité de compaction de base de la chromatine, qui sont la cible de modifications post-translationnelles. La méthylation des histones intéresse les résidus lysines (K), avec un apposition maximale de trois groupements méthyl, générant 4 statuts distincts (Kme3,2,1,0), et les résidus arginines (R), recevant tout au plus une di-méthylation (Rme2,1,0) (voir revue [141]). Ce lien N-CH3, de propriété thermodynamique hautement stable, était d'abord considéré comme perma-

nent. Seul le remplacement d'histones pas éviction, ou par dilution lors de la réplication, semblait pouvoir altérer le contenu de cette modification. Or, la découverte des histones déméthylase (HDM) a permis de démonter la réversibilité de ce lien, laissant présager la méthylation des histones comme un processus dynamique et finement régulé.

1.3.2 Enzymes et réactions

L'effacement du groupement méthyl des lysines peut s'effectuer par une réaction d'oxydation ou d'hydroxylation selon la famille d'enzymes impliquée (Fig1.14). La première HDM rapportée est l'amine oxydase LSD1 (Lysine Specific Demethylase 1), ou KDM1A, avec une affinité restreinte pour les substrats de deux groupements méthyl ou moins (Kme2,1) [142]. Cette limite est imposée par l'intermédiaire imine généré dans cette réaction, nécessitant par ailleurs le cofacteur FAD (Flavin Adenine Dinucleotide). Le concept de réversibilité de la méthylation des histones s'est d'autant plus fortifié avec la découverte des HDM arborant un domaine catalytique Jumonji C (JmjC), médiant une réaction d'hydroxylation dépendante du fer et de l' α-kétoglutarate [141]. Ces enzymes peuvent s'attaquer aux stades de tri-méthylation des lysines, et certains membres semble-raient avoir une affinité pour des substrats arginines, comme JMJD6 [143]. La neutralisation de la méthylation des arginines par déimination ou citrullination, convertissant un résidu chargé positivement en une entité neutre, est aussi un domaine d'active investigation. La famille d'enzyme PADI (Peptidyl Arginine Deiminase) est notamment étudiée en ce sens. Il devient impératif de noter que ces enzymes peuvent tout aussi bien cibler des protéines non-histones, et que seule une fraction des substrats est connue. À titre d'exemple, LSD1 démontre en plus une affinité pour la lysine 370 (K370me2/1) du suppresseur de tumeur p53, modulant ainsi son activité [144].

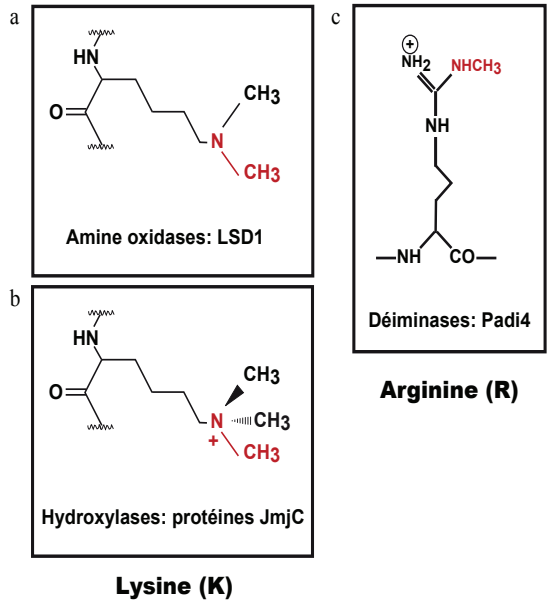

Figure 1.14 Classe d'enzymes de déméthylation. a. Les lysines amines oxydases, comme LSD1 (Lysine Specific Deaminase-1), dont le substrat peut contenir au maximum 2 groupements méthyl, nécessitant le cofacteur FAD (Flavin Adenine Dinucleotide). b. Les hydroxylases, comme la famille des protéines contenant le domaine catalytique Jumonji (JmjC), pouvant aussi cibler les substrats tri-méthylés, et dépendantes du Fer et de l'α-kétoglutarate. c. Les arginines déiminases, comme Padi4 (Peptidyl Arginine Deiminase 4), neutralisant la méthylation des résidus arginines.

1.3.3 Les protéines Jumonji

La famille de protéines JmjC regroupe à ce jour 30 membres, et leur nomenclature est récemment révisée [145]. Ceux-ci partagent un niveau d'homologie pour le domaine catalytique, mais présente une combinaison variable de modules interagissant avec la chromatine ou d'autres protéines, incluant le domaine PHD (Plant Homeodomain) (voir revue, [146]) (Fig1.15). Phylogénétiquement, il est possible de la classer en sous-familles structurellement similaires, ce qui pourrait pour certains sous-groupes (KDM4, KDM5) conférer un degré de redondance fonctionnelle, notamment dans l'analyse de souris transgéniques. Seule une portion des substrats enzymatiques spécifiques est définie, et certains domaines JmjC n'arborent pas d'activité catalytique, comme c'est le cas pour JARID2, HAIRLESS ou UTY. Comme les membres des familles Trx et PcG, ces enzymes semblent agir au sein de complexes protéiques avec d'autres facteurs nucléaires, chaque membre modulant l'activité transcriptionnelle de l'holoenzyme. D'ailleurs, une même protéine JmjC peut agir en tant qu'activateur ou répresseur de l'activité génique, selon la composition du complexe auquel elle est associée, tel que décrit pour LSD1. En effet, LSD1 peut s'associer au complexe répresseur CoREST (corepressor to REST [RE1 silencing transcription factor/neural restrictive silencing factor]) et médier la déméthylation de H3K4me2/1 [142, 147], ou avec un récepteur androgénique et agir comme co-activateur en ciblant la neutralisation d'une marque répressive (H3K9me2/1) [148]. Les JmjC peuvent interagir avec différents facteurs, incluant les facteurs de transcription, les récepteurs nucléaires, les régulateurs du cycle cellulaires, et les effecteurs épigénétiques, comme les Trx (MLL 2,3,4) [149-152], les PcG (EZH2) [153-156], ou les HDAC [157]. Concernant le complexe MLL, une coopération entre la méthylation de H3K4 et la déméthylation de H3K27 par UTX [152] ou JMJD3 [150] est décrite, renforçant ainsi globalement une marque d'activation (H3K4me3/H3K27me0), notamment au site des gènes *Hox*.

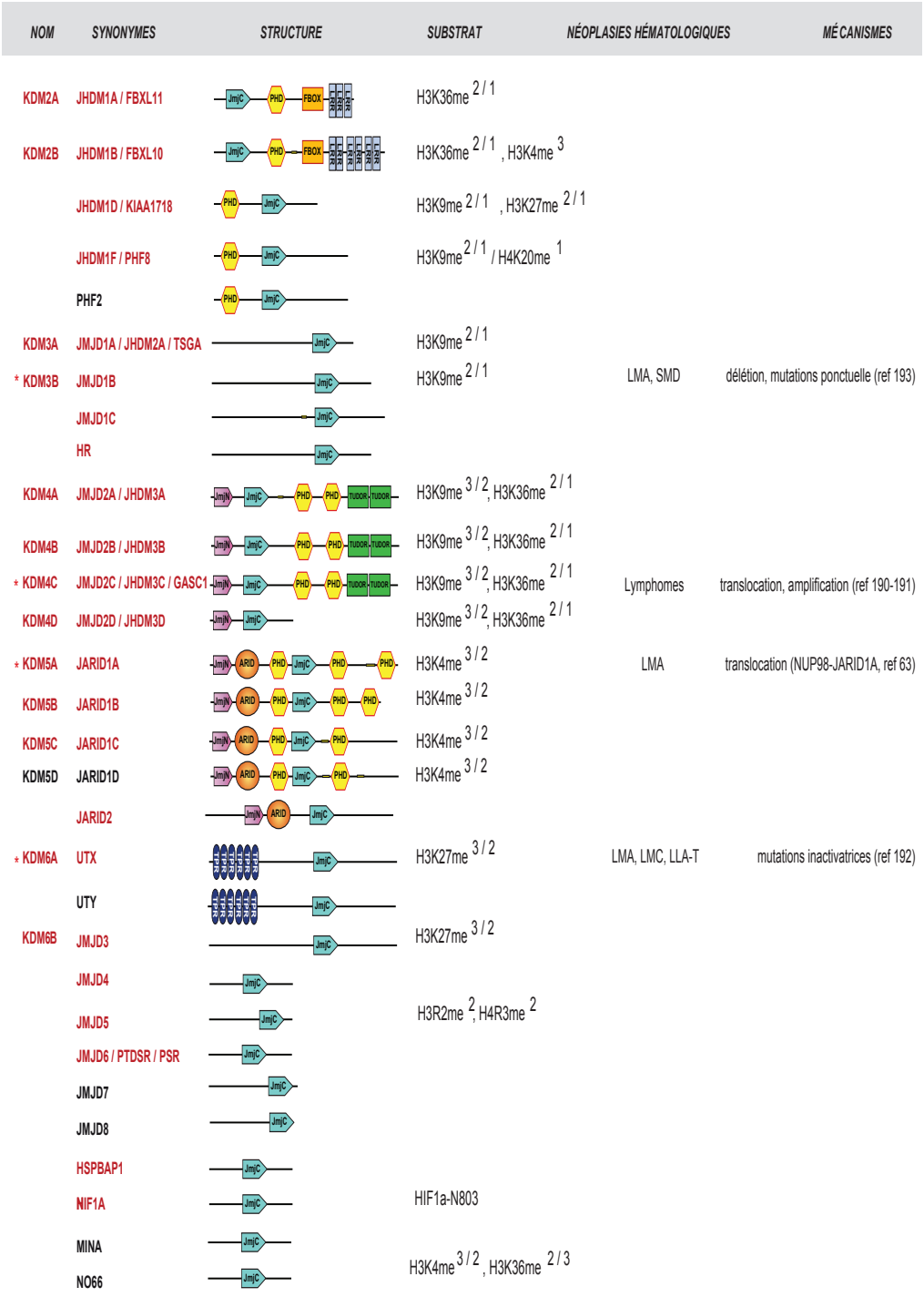

Figure 1.15 Protéines de la famille Jumonji et leurs domaines. Les différents domaines sont indiqués en couleurs. Les candidats étudiés dans le crible en RNAi présenté au chapitre 4 sont indiqués en rouge. JmjC/N: domaine jumonji en N et C-terminale; PHD: Plant HomeoDomain; LRR: Leucine Rich Repeat; ARID: AT-Rich Interaction Domain; LMA: leucémie myéloïde aigue ; LLA: leucémie lymphoïde aigue; SMD: syndrome myélodysplasique. *association aux néoplasies hématologiques.

1.3.4 Famille Jumonji et destin cellulaire

L'émergence de cette famille de protéines JmjC, et leurs rôles en tant que modulateurs épigénétiques, ont conduit à l'élaboration d'un crible en RNAi évaluant une possible fonction de ces enzymes dans la régulation du destin des CSH de la souris (voir chapitre 4). D'ailleurs, au cours de la dernière décennie, leur implication dans les processus développementaux se précise. Le membre fondateur de la famille JmjC est la protéine JARID2, dont le gène a été mis en évidence dans le contexte d'une expérience de mutagénèse de type *gene trap*, en 1995 [158]. L'inactivation de ce gène chez la souris engendre des malformations cardiaques et un développement anormal du tube neural, prenant la forme d'une croix, jumonji signifiant cruciforme en japonais. L'abolition de *Jmjd6* entraîne également de lourdes conséquences développementales, perturbant l'organogénèse de plusieurs structures, dont les reins, le tractus intestinal, le foie et les poumons, et une mortalité péri-natale [159, 160]. L'activité déméthylase propre au domaine catalytique est quant à elle décrite en 2006, en lien avec FBXL11 (JHDM1A; KDM2A) et l'identification de son substrat (H3K36me2/1) [161]. Tel que discuté au chapitre 4, les membres de la famille JmjC semblent contribuer à différents processus biologiques liés à l'identité cellulaire, dont l'auto-renouvellement [162], la sénescence[163], la prolifération [164], la différentiation [165-168], et la transformation maligne [169-171].

1.3.5 La sous-famille JARID1 (KDM5) et le destin des cellules souches embryonnaires (CSE)

Les CSE sont des cellules pluripotentes, arborant un potentiel de différentiation permissif au développement de tous les types cellulaires d'un organisme donné. De plus, leur capacité d'auto-renouvellement *in vitro* est illimitée. Ces deux propriétés correspondent aussi à une configuration de la chromatine pouvant soutenir cette identité cellulaire. Parmi les enzymes JmjC, deux candidats se sont vus attribuer un rôle dans la fine régulation de la balance entre auto-renouvellement et différentiation des SCE, soit JMJD1A (KDM3A; H3K9me2/1) et JMJD2C (KDM4C; H3K9me3/ 2, H3K36me3/2) [162]. Comme pour la tri-méthylation de H3K27, H3K9me3 est généralement associée à une répression de la transcription. Or, dans les CSE de souris, une réduction de l'expression de ces candidats par RNAi induit une activation de gènes associés à la différentiation, et une répression des déterminants de la pluripotence. L'expression de ces deux gènes semble du moins en partie régulée par OCT4, un facteur de transcription et orchestrateur majeur du destin cellulaire des CSE [172]. JMJD1A régule épigénétiquement le locus des gènes *Tcl1*, *Tcfcp2l1*, and *Zfp57*, neutralisant la di-méthylation de H3K9, favorisant ainsi l'expression de ces facteurs et le maintien d'un état cellulaire indifférencié. De plus, JMJD2C régule positivement l'expression du gène codant pour le facteur de transcription NANOG, joueur clé de l'identité cellulaire des CSE. Cette étude illustre le potentiel de deux HDM, pouvant effacer une marque répressive de la transcription (H3K9me3/2/1), de contribuer

à l'identité des cellules souches.

Certains membres de la sous-famille JARID1 (ou KDM5) participe aussi à la régulation du processus de différentiation des CSE. Dans les premières études caractérisant l'activité catalytique de ces enzymes et leur cible spécifique (H3K4me3), un lien est établi entre JARID1A (KDM5A, RPB2) et le choix du destin cellulaire [173-175]. JARID1A est identifié par la technique du double hybride chez la levure comme une protéine liant le suppresseur de tumeur RB-1 (Retinoblastoma Protein-1), et l'association entre ces deux protéines requise pour un déroulement approprié du processus de différentiation [173]. Dans les CSE, JARID1A est identifié comme un régulateur épigénétique des *Hox*, modulant localement les niveaux de tri-méthylation de H3K4. JARID1A démontre une affinité pour plusieurs loci des *Hox*, dont *Hoxa1*, *Hoxa5* et *Hoxa7* [174]. En réponse à une stimulation par l'acide rétinoïque, la transcription des gènes *Hox* est induite, corrélant avec un déplacement de JARID1A du locus, une augmentation locale de la marque activatrice H3K4me3, et la différentiation des CSE. Contrairement aux CSH, une activation des *Hox* est liée à un programme de différentiation dans les cellules embryonnaires. Parallèlement à la fonction de JARID1A, la protéine de haute homologie JARID1B (PLU-1, KDM5B) spécifie la différentiation des CSE le long de la lignée neuronale [176]. Sa présence est requise afin d'assurer la répression des gènes associés notamment à la pluripotence, et assurer ainsi une fidélité de lignée pour le tissu neuronal. Inversement, une surexpression de Jarid1b dans les CSE de souris interfère avec la différentiation neuronale [177].

Bien que la famille des JARID1 (KDM5) des mammifères regroupe 4 membres (A-D), la drosophile ne compte qu'un seul orthologue, LID (Little Imaginal Discs), une déméthylase de H3K4, conférant un phénotype embryonnaire léthal lorsque muté. Incidemment, LID a été décrit dans un crible visant à identifier d'autres membres de la famille Trx, et une activité méthyl-transférase était d'abord suspectée pour le produit de ce gène [178]. Pourtant, une activité enzymatique de déméthylation s'est bien avérée pour LID [179], et une mutation de ce gène résulte en un accroissement global de la marque activatrice H3K4me3. Deux hypothèses sont avancées pour tenter de réconcilier ces résultats. Une possibilité serait qu'une mutation de *Lid* puisse interférer avec l'ancrage du complexe Trx à la chromatine suite à la perturbation du patron de déposition de H3K4me3, ou par une altération secondaire de la stochiométrie du complexe. Alternativement, LID est rapporté comme régulant positivement la fonction de dMYC dans un crible fonctionnel chez la drosophile [180]. Le facteur de transcription dMYC lie le domaine JmjC de LID, séquestrant ainsi son activité répressive (déméthylation de H3K4), et permettant l'expression des cibles de dMYC. L'activité de dMYC dépendrait donc de la présence de LID et une perturbation de cette interaction pourrait nuire à la fonction de dMYC. Une mutation de *Lid* pourrait donc se solder par un phénotype similaire à celui d'un mutant Trx.

1.3.6 Protéines Jumonji et hématopoïèse

En descendant la hiérarchie hématopoïétique, le potentiel de différentiation devient graduellement restreint à une seule lignée cellulaire, nécessitant l'activation de gènes spécifiques et la répression des voies de développement alterne. Au sein du système hématopoïétique, l'engagement envers une voie de différentiation spécifique semble impliquer les HDM. Une étude concernant l'amine oxidase LSD1 (H3H4me2/1 HDM) a guidé la réflexion en ce sens. En effet, LSD1 a été isolé en complexe avec les répresseurs de la transcription GFI1, acteurs de l'hématopoïèse normale et leucémique (Fig1.1), en association avec le co-répresseur CoREST et les déactylases HDAC1/HDAC2 [181]. La liaison avec LSD1 est médiée par le domaine SNAG des protéines GFI1. Selon un contexte cellulaire spécifique, le complexe répresseur est recruté *in vivo* sur la majorité des cibles de LSD1, comme *c-myb*, orchestrant la différentiation le long de la lignée érythrocytaire, mégakaryocytaire et granulocytaire. Une réduction de LSD1 augmente localement, au site des promoteurs des gènes cibles, une augmentation de la marque activatrice H3K4me3, nuisant à leur répression et au déroulement du processus de différentiation.

Plus récemment, dans une étude de surexpression, la déméthylase JmjC FBXL10 (JHDM1B,KDM2B) semble contribuer au maintien du potentiel d'auto-renouvellement des cellules hématopoïétiques primitives [182]. Le gène *Fbxl10* code pour une HDM constituée d'un domaine JmjC, mais aussi d'un domaine F-box, d'une double répétition de motifs riches en leucines (LRR/Leucine Rich Repeats), d'un domaine PHD et d'un doigt de zinc CXXC. Son activité catalytique cible les marques activatrices H3K36me2/1 et H3K4me3 [183]. Ce groupe rapporte une localisation nucléaire pour cette protéine et une implication dans la répression des gènes de l'ARN ribosomal. D'autres attribuent un rôle à FBXL0 dans la régulation de la prolifération et de la sénescence via le contrôle épigénétique du locus *p15/Ink4b* [184]. Or, le compartiment primitif hématopoïétique exprime *Fbxl10* de façon préférentielle [182] (voir aussi chapitre 4). À l'aide d'une construction rétroviral, l'expression forcée de ce gène dans des populations enrichies en CSH augmente le nombre de progéniteurs multipotents *in vitro*, et confère un avantage compétitif aux CSH dans des essais de transplantations sériées. Les auteurs expliquent ce phénotype par un maintien de la répression des loci *Ink4a-c*, par délétion de la marque activatrice H3k36me2, inhibant ainsi la voie de sénescence. En parallèle, les travaux d'une autre équipe suggèrent une contribution de FBXL10 dans l'initiation et le maintien des leucémies chez la souris, toujours en évoquant un rôle de répression de la sénescence [169].

La régulation de l'hématopoïèse semble aussi impliquer UTX (Ubiquitously Transcri-

bed tetratricopeptide repeat, X chromosome, ou KDM6A), une H3K27me3 déméthylase, comprenant le domaine catalytique JmjC et le domaine tetratricopeptide (TPR). De façon générale donc, UTX efface une marque associée à une répression de la transcription. Tel que mentionné, UTX est aussi un membre des complexes MLL2/3 qui promeuvent la tri-méthylation de H3K4 et l'activation génique ([152, 185]. La délétion d'*Utx* chez la souris s'avère embryonnaire létale chez les femelles, les mâles succombant en période néonatale, et s'accompagne de sévères anomalies de développement du cœur et du tube neural [186, 187]. UTX influencerait aussi le profil d'expression des et le développement embryonnaire du poisson zèbre [188]. Dans une étude récente, une répression de Utx par RNAi au sein du contingent hématopoïétique de la souris diminue le potentiel clonogénique des progéniteurs in vitro, nuisant à leur prolifération [189]. Une baisse du transcrit d'*Utx*, qui par ailleurs est bien exprimé dans la fraction primitive des cellules hématopoïétique, interfère aussi avec la prolifération de plusieurs lignées leucémiques. Les auteurs attribuent le phénotype à une répression de l'activité génique aux loci des gènes *Mll1*, *Runx1*, et *Scl*, des régulateurs connus de l'hématopoïèse. De façon concomitante, une réduction des niveaux se H3K27me3 est décrite aux même sites génomiques. Globalement, UTX contribuerait donc au potentiel prolifératif des cellules du sang.

1.3.7 Protéines Jumonji et hémopathies malignes

Les HDM JmjC participent à la spécification cellulaire dans le contexte de l'hématopoïèse, et leur dérégulation peut ultimement mener à une transformation maligne. Des mutations impliquant directement ces gènes sont d'ailleurs rapportées (Fig1.15). Tel que mentionné, la translocation cryptique t(11;21;12)(p15;p13;p13), codant pour l'oncoprotéine de fusion NUP98-JARID1A (Fig1.16), est décrite dans un cas LMA pédiatrique, de type M7 ou mégakaryoblastique [63]. Ce réarrangement chromosomique associe la portion N-terminale de Nup98 contenant les répétitions FG transactivatrices (exons 1-13), au domaine C-terminal de Jarid1a (exons 28-31) incorporant le domaine PHD, permettant entre autre une liaison à la chromatine via la marque H3K4me3. En plus de l'activation épigénétique du locus de gènes *Hoxa*, un modèle murin de leucémie impliquant cette translocation démontre aussi que l'intégrité du domaine PHD est essentielle au processus de transformation. Possiblement, l'ancrage de NUP98-JARID1A aux loci génomiques codant pour des déterminants de l'auto-renouvellement, bloquerait l'accès à la chromatine à des complexes répresseurs de la transcription. De plus, dans les dans les lymphomes, une amplification de la région génomique 9p24, incorporant le gène de la tyrosine kinase Jak2 et Jmjd2c (KDM4C; H3K9me3/ 2, H3K36me3/2; voir section CSE plus haut) est décrite [190], ainsi qu'une translocation impliquant directement Jmjd2c [191]. Une analyse de séquençage à large échelle par un consortium de l'Institut Sanger [192] (http://www.sanger.ac.uk/genetics/CGP/Studies/) a aussi permis l'identification de mutations inactivatrices de UTX dans plusieurs spécimen tumoraux, dont des hémopathies malignes,

principalement le myélome multiple. Ceci laisserait présager a priori un rôle de tumeur suppresseur pour UTX, et ce concept fera certainement l'objet d'études ultérieures. Finalement, les délétions 5q31 sont fréquemment retrouvées dans les LMA, et cette région arbore la région codant pour l'HDM JMJD1B (KDM3B; H3K9me2) [193].

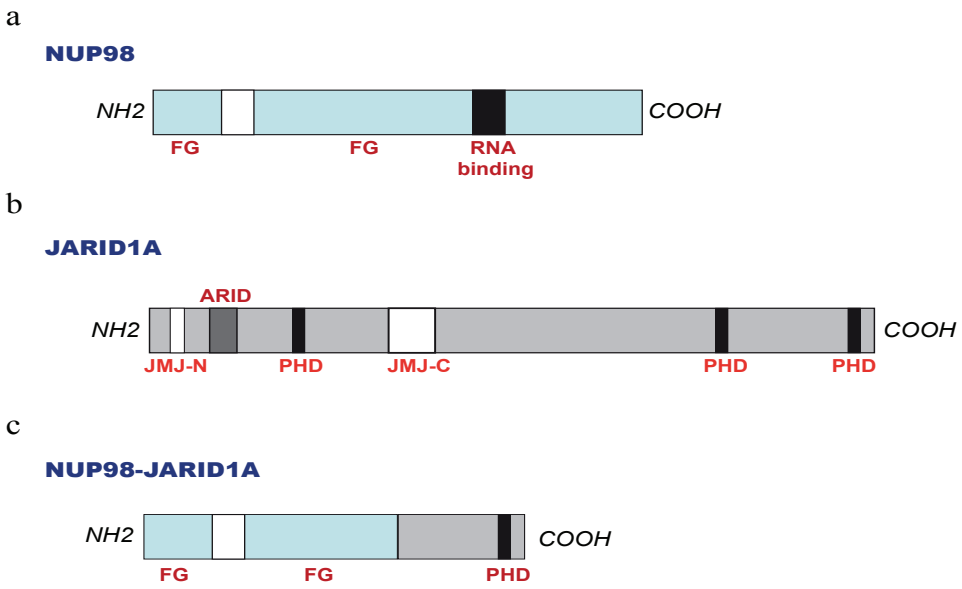

Figure 1.16 Réarrangement chromosomique entre Nup98 et Jarid1a. a. Gène codant pour la nucléoporine NUP98. b. Gène codant pour l'histone déméthylase JARID1A. c. Réarrangement chromosomique impliquant la portion N-terminale de Nup98 et la portion C-terminale de Jarid1a. F : phénylalanine ; G : glycine ; JmjN/C : domaine jumonji en N et C-terminale ; domaine PHD : Plant HomeoDomain.

Une nouvelle perspective liant les HDM JmjC au cancer implique possiblement la voie métabolique de l'α-kétoglutarate (αKG), cofacteur essentiel à l'activité de ces enzymes [194, 195]. L'isocitrate est converti en αKG par la famille d'enzyme IDH (isocitrate dehydrogenases). Or, des mutations d'Idh1 et Idh2 sont fréquentes dans les tumeurs cérébrales (~70% des gliomes de bas grade [196]) et les leucémies (16% des LMA [197]), codant pour une néo-enzyme dont l'activité est altérée (IDH1/2Δ). Par rapport à l'enzyme sauvage, IDH1/2Δ abaisse les niveaux d' αKG en diminuant la conversion de l'isocitrate, et en métabolisant l'αKG résiduel en D-2-hydroxyglutarate (D-2-HG). Les enzymes dépendantes de l'KG, comme les protéines JmjC et la famille des hydroxylases TET mentionnées plus tôt, se voient donc privées de leur cofacteur naturel, et de plus inhibées dans leur fonction par le néo-métabolite D-2-HG [194, 198]. Au total, IDH1/2Δ engendrent des répercussions épigénétiques et des anomalies métaboliques de la voie du citrate pouvant compromettre le destin cellulaire et mener à une transformation maligne.

En conclusion, la famille des protéines Jumonji participe à la régulation des processus développementaux, à divers stades de l'ontogénie et dans différents tissus, dont le système hématopoïétique. Leur implication dans l'oncogénèse se précise graduellement. L'ensemble des données émergentes a conduit à l'élaboration d'un crible fonctionnel en RNAi pour déterminer l'impact d'une diminution des niveaux de transcrits des JmjC sur le destin des CSH de la souris (chapitre 4). La découverte initiale de l'amine oxydase LSD1 et sa capacité de réverser la méthylation des histones a grandement ouvert la voie en ce sens, en plus de sa fonction dans la spécification des lignées hématopoïétiques. Il est fort intéressant de constater que le niveau d'expression de *Lsd1* est souvent élevé dans les blastes leucémiques, et que leur diminution par RNAi favorise un programme de différentiation au détriment de l'auto-renouvellement des cellules malignes [199, 200]. Ce phénotype est rapporté pour des leucémies induites par deux oncoprotéines de fusion distinctes, soit MLL-AF9 et PML-RARA. Le mécanisme sous-jacent n'est pas clairement établi, l'hypothèse avancée étant que de forts niveaux de *Lsd1* diminueraient la marque H3K4m2 au loci de déterminants de l'auto-renouvellement, tout en préservant la modification activatrice H3K4me3, augmentant le ratio H3K4me3//H3K4me2. Les auteurs soutiennent une moindre dépendance de LSD1 du système hématopoïétique normal, décrivant toutefois un tableau d'anémie sévère suivant sa diminution chez la souris. Ces données encouragent la poursuite de la caractérisation du rôle précis des HDM dans l'ontogénie et le cancer.

2. Sustained In Vitro Trigger of Self-Renewal Divisions in Hoxb4^{hi}Pbx1^{lo} Hemopoietic Stem Cells

Sonia Cellot[1], Jana Krosl[1], Jalila Chagraoui[1], Martin Sauvageau[1], R. Keith Humphries[2] & Guy Sauvageau[1,3]

[1]Laboratory of Molecular Genetics of Stem Cells, Institute for Research in Immunology and Cancer (IRIC), C.P. 6128 succursale Centre-Ville, Montréal, Québec H3C 3J7, Canada;

[2]Terry Fox Laboratories, British Columbia Cancer Agency, Vancouver, British Columbia and Department of Medicine, University of British Columbia, Vancouver, British Columbia;

[3]Department of Medicine and Division of Hematology and Leukemia Cell Bank of Quebec, Maisonneuve-Rosemont Hospital, Montréal, Québec, Canada

Corresponding Author:

Guy Sauvageau M.D., Ph.D.

Institute for Research in Immunology and Cancer (IRIC)

C.P. 6128, succursale Centre-Ville, Montréal, Québec

Canada H3C 3J7

Telephone: (514) 343-7134

Fax: (514) 343-7379

E-mail: [redacted]

Running head: Self-Renewal in *Hoxb4^{hi}Pbx1^{lo}* Stem Cells

Key words: Self-renewal; Cell cycle; Hoxb4; Pbx1

2.1 Contribution des co-auteurs

SC, JK, and GS planned and designed experiments. SC performed all experiments. JK contributed to cell culture and transplantation experiments. JC contributed to planning and execution of experiments involving flow cytometry, and analysis of results. MS contributed to execution of Q-PCR experiments, and analysis of results. SC and GS wrote the paper. RKH revised manuscript.

2.2 Summary

Factors that trigger and sustain self-renewal divisions in tissue stem cells remain poorly characterized. By modulating the levels of *Hoxb4* and its co-factor *Pbx1* in primary hematopoietic cells *(Hoxb4^{hi}Pbx1^{lo}*cells*)*, we report an *in vitro* expansion of mouse hematopoietic stem cells (HSCs) by 10^5-fold over 2 weeks, with subsequent preservation of HSC properties. Clonal analyses of the hematopoietic system in recipients of expanded HSCs indicate that up to 70% of *Hoxb4^{hi}Pbx1^{lo}* stem cells present at initiation of culture underwent self-renewal *in vitro*. In this setting, *Hoxb4* and its co-factor did not promote an increase in DNA synthesis, or a decrease in doubling time of Sca1$^+$Lin$^-$cells when compared to controls. Q-PCR analyses further revealed a down regulation of *Cdkn1b* (*p27^{Kip1}*) and *Mxd1* (*Mad1*) transcript levels in *Hoxb4^{hi}Pbx1^{lo}* primitive cells, accompanied by a more subtle increase in *c-myc* and reduction in *Ccnd3* (Cyclin D3). We thus put forward this strategy as an efficient *in vitro* HSC expansion tool, enabling a further step into the avenue of self-renewal molecular effectors.

2.3 Introduction

Integration of cell-autonomous factors and microenvironmental signals is believed to dictate the final outcome of HSC division (reviewd in (Moore and Lemischka, 2006)), namely to self-renew with preservation of stemness, or to engage in differentiation pathways. Dissection of the molecular mechanisms that regulate this delicate balance would greatly increase the probability of successful ex vivo expansion of HSCs. Following myeloablative HSC transplantation, the total stem cell reservoir of a recipient is replenished to only approximately 10% of the pre-transplantation levels ((Pawliuk et al., 1996; Sauvageau et al., 1995), see also supplementary Fig.2.S1)), indicating that HSCs present in the bone marrow (BM) graft display a limited expansion potential in vivo in this particular biological setting, probably in response to both intrinsic (cell-autonomous (Sauvageau et al., 1995)) and extrinsic (growth factors, cell-cell contact (Iscove and Nawa, 1997)) cues. In the same context HSCs engineered to overexpress *Hoxb4* can fully replenish the stem cell pool of recipients, and then maintain a normal supply of HSCs (~20,000 per mouse) for the duration of life (Thorsteinsdottir et al., 1999). *Hoxb4*-transduced HSCs can also expand in vitro by at least ~40-fold in a period of 12 days (Antonchuk et al., 2002), and by ~4-6-fold in 4 days in response to the recombinant TAT-HOXB4 protein (Amsellem et al., 2003; Krosl et al., 2003a).

Although HOXB4 binding to DNA is essential for HSC expansion (Beslu et al., 2004), other potential molecular interactions involved in this process remain undefined. The demonstrated effects of *Hoxb4* retroviral overexpression on stem cells in vivo can be enhanced by concomitantly decreasing intracellular levels of PBX1, a homeoprotein of the TALE subfamily and known DNA-binding cofactor of HOXB4 and other Hox proteins (Azpiazu and Morata, 1998; Chang et al., 1995; Medina-Martinez and Ramirez-Solis, 2003; Nygren et al., 2006; Popperl et al., 1995). Upon transplantation, these *Hoxb4* + antisense *Pbx1* doubly transduced HSCs (thereafter called $Hoxb4^{hi}Pbx1^{lo}$ HSCs) are significantly (20-50 times) more competitive than control $Hoxb4^{hi}$ cells (Krosl et al., 2003b), and interestingly, their functional integrity and responsiveness to in vivo signals that regulate HSC pool size appear unperturbed (see supplementary Fig. 2.S1).

The in vivo repopulating activity of $Hoxb4^{hi}Pbx1^{lo}$ HSCs thus appears to be tightly controlled by as yet non-identified physiological mechanisms. To circumvent these constraints, and to reveal the intrinsic potential for self-renewal (SR) divisions of HSCs, $Hoxb4^{hi}Pbx1^{lo}$ cells were cultured ex vivo for prolonged periods of time. We now present novel findings that document essentially exclusive induction of HSC self-renewal divisions in vitro, associated with slow proliferation rates in primitive cells, thus supporting the emerging evidence that these processes are ultimately linked (Cheng et al., 2000a; Cheng et al., 2000b; Miyake et al., 2005; Yu et al., 2006; Zhang et al., 2005). The levels of in vitro HSC expansion achieved parallel those documented in an accompanying paper

using *Hox* fusion genes. Together these results provide potent methods to enable sustained triggering of HSC self-renewal in vitro and open up new approaches to elucidate the key mechanisms involved.

2.4 Experimental procedures

Animals

(C57Bl/6J x C3H/HeJ)F1 or W^{41} recipients (expt. 1) and (C57Bl/6Ly-Pep3b x C3H/HeJ) F1 congenic donor mice were bred at a specific pathogen free (SPF) animal facility at the Institute for Research in Immunology and Cancer in Montreal. All animals were housed in ventilated cages and provided with sterilized food and acidified water.

Retroviral vectors

Generation of the MSCV-IRES-*GFP* and MSCV-*Hoxb4*-IRES-*GFP* (Antonchuk et al., 2001), MSCV-a/s *Pbx1b*-PGK-*YFP* (Krosl et al., 2003b), MSCV-PGK-neo and MSCV-*Hoxb4*-PGK-neo (Sauvageau et al., 1995), and MSCV-a/s *Pbx1b*-PGK-puro (Krosl et al., 1998) vectors were described before. For MSCV- *PBX1b*-PGK-*YFP*, a 1.4 kb fragment encoding *Pbx1b* ORF was blunted and subcloned into *Hpa*I site of MSCV-PGK-*YFP* (Krosl et al., 2003a).

Retroviral infection and transplantation of primary bone marrow cells

Generation of retrovirus producing GP+E-86 cells, and single or double infections of bone marrow cells were performed as previously described (Krosl et al., 2003a). Upon recovery from co-culture with retroviral producers, the proportions of transduced (GFP^+, YFP^+, or GFP^+/YFP^+) cells were determined by flow cytometry using MoFlo (Cytomation, Fort Collins, CO) or BD LSR II System (BD biosciences, San Jose, California.

In vitro culture and transplantation of primary bone marrow cells

Cultures comprised of bone marrow cell populations harvested from either GFP, or combined *Hoxb4* + a/s Pbx1 retroviral producers, were immediately initiated after co-culture at a density of 3 x 10^5 cells/mL, in media supplemented with 15% FCS, 6 ng/mL of IL-3, 10 ng/mL of IL-6, 100 ng/mL of SCF, 50 µg/mL of gentamycine and 10 µg/mL of ciprofloxacin. At 3 day-intervals, cells were counted and diluted with fresh media so that cell density was maintained between 3 x 10^5 and 2 x 10^6 cells/mL. Cell aliquots were taken at regular intervals to determine total cell counts and progenitor frequencies as assessed by plating cells in methycelullose containing 10 ng/mL of IL-3, 10 ng/mL of IL-6, 50 ng/mL of SCF, and 5U/mL of Epo and scoring colonies on day 7. Cytokines used in these experiments were prepared at IRIC as COS-cell supernatants. All other media components were purchased from GIBCO/Invitrogen Corp. (Burlington, ON, Canada).

Flow cytometry

Cells isolated from BM, spleen and thymus of transplantation chimeras were resuspended in PBS with 2% FCS and allophycocyanin (APC)-conjugated antibodies recognizing Mac-1, or B220, or CD8 cell surface markers, or phycoerithryn-Cy7 (PECy7)-conjugated anti-CD4 antibody (Pharmingen, Mississauga, ON) as previously described (Krosl et al., 2003b). Data were acquired using BD LSR II flow cytometer (BD Biosciences, San Jose, CA) and analyzed using FlowJo software (Tree Star Inc., Ashland, OR).

CRU assays

To determine the contributions of the transplanted transduced (GFP^+, YFP^+, and GFP^+/YFP^+) HSC to hemopoietic reconstitution at various intervals post transplantation, ~50 μL of blood obtained from the tail vein were incubated with excess ammonium chloride (StemCell Technologies, Vancouver, BC) to lyse erythrocytes, and the proportions of GFP^+, YFP^+, and GFP^+/YFP^+ blood cells were determined by flow cytometry. Mice that had greater than 2% GFP^+/YFP^+ cells in both, myeloid ($SSC^{hi}FSC^{low}$) and lymphoid ($SSC^{low}FSC^{hi}$) subpopulations were considered to be repopulated with at least 1 *Hoxb4*+a/sPbx1-transduced HSC. Fidelity of discrimination between myeloid and lymphoid cells was verified using cell surface staining to detect lineage specific markers (Mac-1 vs B-220). HSC numbers in primary recipients were evaluated as described (Sauvageau et al., 1995) using a limiting dilution transplantation-based assay (CRU assay), that detects cells with competitive, long-term lympho-myeloid repopulation capacity (Szilvassy et al., 1990).

CFC assays and *in vitro* expansion of myeloid clones

The frequencies of myeloid progenitors in BM and spleen cell populations of primary and secondary recipients were determined as described (Thorsteinsdottir et al., 2002). To generate clonal myeloid cell populations, well isolated multilineage mixed colonies were transferred from methylcellulose to liquid cultures and expanded for 14 days in IMDM, supplemented with 10 % FSC, IL-3 (10 ng/mL) , IL-6 (10 ng/mL) , IL-11 (100 ng/mL), SCF (100 ng/mL), and 10^{-5}M β-mercaptoethanol

Southern blot analysis of genomic DNA

High molecular weight DNA from the BM, spleen and thymus of transplantation chimeras, from myeloid clones and from lineage marker specific sorted cells was digested as indicated in figure legends. Probes used were 600 bp (nt 930-1525 of the ORF) Pvu II fragment of *PBX1*, 490 bp Sal I – Pml I fragment of *HOXB4* cDNA, and 730 bp full length *YFP* cDNA.

BrdU incorporation assay

BrdU incorporation studies of in vitro cultured BM cells were performed using the BD Pharmingen APC BrdU Flow Kit (BD Pharmingen, Mississauga, ON) as recommended by manufacturer. Briefly, one week upon removal from retroviral producer cells, aliquots of BM cells transduced with either MSCV-*Hoxb4*-IRES-*GFP,* MSCV-*Hoxb4*-PGK-*Neo* or MSCV-PGK-*Neo* vectors were incubated at a density of 1 x 10^6 cells/mL in culture

media containing 10 μM BrdU for 12 hours. Cells were first stained with R-Phycoerythrin (PE)-conjugated antibody specific for the Sca1 surface antigen (BD Pharmingen, Mississauga, ON), and then treated according to the manufacturer guidelines. Flow cytometric ata were acquired and analyzed as specified above.

Cell cycle analysis using Hoechst 33342 dye

After one week in culture, aliquots of BM cells transduced with either MSCV-*Hoxb4*-PGK-*Neo* or MSCV-PGK-*Neo* vectors were first incubated in media (DMEM+FCS2%+10mM Hepes pH 7.4) containing 5 μg/mL of Hoechst 33342 (Molecular Probe, Invitrogen) as suggested by manufacturer, and then stained using PE-conjugated anti-Sca1 and APC-conjugated anti-GR1 antibodies. 1,000,000 events per condition were acquired using UV-excitation source equipped BD LSR II flow cytometer (BD Biosciences, San Jose, CA) and data for both total and $Sca1^{+}Gr1^{-}$ gated cell populations were analyzed using ModFit software (Verity Software House, Topsham, Maine).

CFSE cell tracking studies

In vitro cultures of BM cells (C57Bl/6J-Ly5.2) transduced with either MSCV-*Hoxb4*-PGK-*Neo*, MSCV-*Hoxb4*-PGK-*Neo*+MSCV-a/s *PBX1b*-PGK-*Puro,* or MSCV-PGK-*Neo* were initiated following our standard protocol. Three days after harvest from retroviral producer cells, aliquots of cells were resuspended at a final density of $1x\ 10^6$ cells/mL in prewarmed PBS containing 0.1% BSA and 10 μM CFSE (carboxyfluorescein diacetate succinimidyl ester, CellTrace™ CFSE Cell Proliferation Kit, Molecular Probes/Invitrogen, Burlington, ON), and were then treated according to the manufacturer guidelines and published literature (Lyons and Parish, 1994; Oostendorp et al., 2000). Following CFSE uptake, cells were washed 3 X with fresh BM media, replated in the same media at a density of 5×10^5 cell/mL, and incubated for 4 additional days. The CFSE fluorescence was determined immediately after the treatment, and after 3-day culture. To assess mean CFSE fluorescence intensity in the primitive cell subpopulations, aliquots of cultures were stained using PE-conjugated anti Sca1 and APC-conjugated anti GR1 antibodies. Data were acquired using BD LSR II System (BD Biosciences, San Jose, California), and generation peaks were determined using ModFit software (Verity Software House, Topsham, Maine). On the 4^{th} day of CFSE incorporation, cells were sorted (BD FACSAria, BD Biosciences, San Jose, California) according to arbitrarily set gates encompassing high, medium and low levels of CFSE fluorescence intensity (see Fig 2.3D). Predetermined cell numbers were collected in individual tubes containing pure FCS. Cells were then pelleted and resuspended in DMEM + FCS 2% and content of each tube singly transplanted in a previously irradiated (800 cGy) mouse recipient (C57Bl/6J-Ly5.1-Pep3b). Peripheral blood reconstitution of animals was evaluated 3 months post transplantation using APC-conjugated anti-Ly5.2 antibodies described above.

Quantitative RT-PCR

Total RNA was isolated using Trizol ™ according to manufacturer's protocol (Invitrogen).

RNA was treated with DnaseI (Invitrogen) before cDNA synthesis. Reverse transcription of total RNA was performed using the MMLV-RT and random hexamers according to macufactuer's protocol (Invitrogen). The ABI Gene Expression Assay was performed to measure gene expression levels (c-Myc, c-Myb and Hoxb4, see suppl Table 1) using primer and probe sets from Applied Biosystems (ABI Assays on Demand, http://www.appliedbiosystems.com/). PCR reactions for 384 well plate formats were performed using 2 µl of cDNA samples (10-40 ng), 5 µl of the TaqMan Universal PCR Master Mix (Applied Biosystems, CA) and 0.5 µl of the TaqMan® Gene Expression Assays (20X) in a total volume of 10 µl. Gene expression levels were also measured (see suppl Table 2) by custom primers and TaqMan probes designed (Dr Sylvain Meloche laboratory) using the online version of PrimerQuest software (http://scitools.idtdna.com/Primerquest/). Default parameters for real time PRC were used to select the best primers and probes. In order to amplify only the cDNA, primers were located in different exons or in the splicing junction between two exons. PCR reactions were performed using 2 µl of cDNA samples (10-40 ng), 5 µl of the TaqMan PCR Master Mix (Applied Biosystems, CA), 10 pmol of each primer and 5 pmol of the TaqMan probe in a total volume of 10 µl. The ABI PRISM® 7900HT Sequence Detection System (Applied Biosystems) was used to detect the amplification level and was programmed to an initial step of 10 minutes at 95˚C, followed by 50 cycles of 15 seconds at 95˚C and 1 minute at 60˚C. All reactions were run in duplicate and the average values were used for quantification. GAPDH (glyceraldehyde-3-phosphate dehydrogenase) was used as endogenous control. The relative quantification of target genes was determined by using the ΔCT method. Briefly, the Ct (threshold cycle) values of target genes were normalized to the endogenous control gene (GAPDH) ($\Delta CT = Ct_{target} - Ct_{GAPDH}$) and compared with a calibrator (control Sca+Lin- cells): $\Delta\Delta CT = \Delta Ct_{Sample} - \Delta Ct_{Calibrator}$. Relative expression (RQ) was calculated using the Sequence Detection System (SDS) 2.2.2 software (Applied Biosystems) and the formula $RQ = 2^{-\Delta\Delta CT}$.

2.5 Results

Ex vivo expansion potential of HSC

The potential of *Hoxb4^{hi}Pbx1^{lo}* engineered HSCs to proliferate and expand under ex vivo conditions was investigated using the experimental strategy outlined in Fig. 2.1A (see figure legend for details). At initiation of culture, HSC or competitive repopulating unit (CRU) frequency {Szilvassy, 1990 #55} in the *Hoxb4^{hi}Pbx1^{lo}* group was 1 in 50,000 cells, or 0.002%, for an absolute number of 100 doubly transduced stem cells, in the same range as for the starting number of GFP control HSCs (i.e. 1 in 25,000 cells, or 150 CRUs). In a 12-day time span, total cell number expansion was comparable in 2 independent experiments between cultures initiated with *Hoxb4^{hi}Pbx1^{lo}* or control GFP cells, averaging 2-3 logs (Fig. 2.1B). However, morphologically undifferentiated cells were more prevalent in cultures initiated with *Hoxb4^{hi}Pbx1^{lo}* cells compared to control (Fig. 2.1C). This was reflected in the clonogenic progenitor frequencies, as assessed by plating cultured cells in semi-solid media, which were identical at initiation of culture for both groups (in the order of 1 colony-forming cell (CFC) per 150 cells). This frequency remained constant in the control group after 2 weeks, with an overall 100-fold CFC increase, as opposed to a 1000-1500-fold CFC expansion in the *Hoxb4^{hi}Pbx1^{lo}* groups, where the frequency increased to 1 in 3-15 cells (n=4 independent cultures, see Fig. 2.1B). In sharp contrast also, the stem cell frequency differed markedly between these 2 conditions. After 12 days of in vitro expansion, CRUs represented 1 in 50 cells or 2% of the *Hoxb4^{hi}Pbx1^{lo}* culture, for an absolute number of 1.2 x 10^7 CRUs in Exp.1 and 1.9 x 107 in Exp.2 (Fig. 2.1D), and a net 100,000-fold in vitro increment. In parallel, the CRU frequency in the GFP control group declined to 1 in 2 x 10^7 cells, or 25 CRUs, over the same time period, for a net 6-fold reduction (Fig. 2.1B, D). The in vitro stem cell enrichment in the *Hoxb4^{hi}Pbx1^{lo}* culture is illustrated in Fig. 2.1E where peripheral blood reconstitution by GFP and YFP (ie, *Hoxb4^{hi}Pbx1^{lo}*) cells at 4 months post transplantation, of a primary recipient of 5 expanded T+14 cells (Exp.2), is presented. In order to unambiguously conclude about the stem cell nature of the expanded CRUs, their in vivo functional properties were further investigated.

Preservation of functional integrity of expanded HSCs

The in vivo regenerative capacity of *Hoxb4^{hi}Pbx1^{lo}* HSCs that had undergone a 10^5-fold expansion in vitro was first evaluated. These experiments involved serial passages of transduced cells over several recipients during a 19-month period as depicted in Fig.2.1F. As estimated by the CRU assay, the *Hoxb4^{hi}Pbx1^{lo}* HSC frequency in a primary recipient 4 months post-transplantation of 4,000 cultured cells was 1 in 8,000, for a total stem cell pool size of ~25,000 cells per mouse, representing a net 100-fold expansion in vivo (Fig. 2.1F, second column of graphic). Bone marrow clonogenic progenitor activity of these primary animals was within normal limits, and the majority (>90%) of myeloid progenitors in these mice were derived from *Hoxb4^{hi}Pbx1^{lo}* cells as assessed by epifluorescence

and Southern blot analyses (data not shown). When a secondary mouse transplanted with the equivalent of 1-2 CRUs served as a donor for a series of tertiary recipients (Fig.2.1F, see 2^o mouse), it was inferred that bone marrow HSCs underwent an additional 1000-fold in vivo expansion in secondary recipient (Fig.2.1F, 3^{rd} column of graphic). Overall, the doubly transduced HSCs underwent a cumulative 10^{10} expansion following serial transplantations, in a time span of 19 months. Despite this level of expansion, the peripheral blood reconstitution in tertiary recipients of a single HSCs was measured to be ~ 4% at 4 months (data not shown). This output is consistent with previous observations (Thorsteinsdottir et al., 2002) and shows that these stem cells probably remained responsive to physiological mechanisms that regulate HSC proliferation.

The in vitro stem cell frequency measured after ~2 weeks of culture acquires relevance if the reported expansion is oligo- to poly-clonal in character, rather than secondary to an overtly proliferating single clone. Clonal analysis revealed at most 100 doubly-transduced CRU (likely fewer, see Fig. 2.2A legend) at initiation of culture in Exp. 1 and the recovery of at least 11 expanded HSCs in primary and secondary recipients (Fig. 2.2A-B). This type of analysis was not available for Exp. 2 but repeated in a 3^{rd} experiment where up to 77% of expanded CRU were recovered in recipients analyzed 16 weeks post-transplantation (Fig. 2.2A, C), a period deemed sufficient for the in vivo exhaustion of transplanted progenitors, hence ensuring that at this time all hematopoietic cells originated from long-term repopulating HSCs (Fig. 2.2C)

To further assess the functional integrity of the expanded HSCs, their ability to engage in terminal differentiation in various hematopoietic tissues was evaluated. A preliminary screen of peripheral blood hemoglobin concentration, white blood cell and platelet counts in long-term recipients of high doses of cultured cells reported values within normal limits (suppl Fig.2.3A-D). Peripheral blood reconstitution of lymphoid (T and B) and myeloid (granulocyte and monocyte) lineages was assessed in selected primary and secondary recipients (Exp.1) using flow cytometry (Fig. 2.3A). Final maturation of blood and BM cells in very long-term primary recipients (14 months, Exp.2) is shown in Fig.2.3B. As reported previously (Krosl et al., 2003b), *Hoxb4^{hi}Pbx^{lo}* HSCs differentiated into all aforementioned cell types, although in some instances, a significant proportion of recipients manifested a skewing of differentiation towards the myeloid lineage for the transplanted cells, possibly in a dose-dependent effect of Hoxb4 as previously reported (Schiedlmeier et al., 2003). This skewing in myeloid differentiation was not observed in primary recipients (n=138 mice) of long-term culture cells (up to 28 days) from Exp. 3. In this particular experiment, myeloid and T lymphoid differentiation was confirmed in all reconstituted animals from all transplantation intervals (T0; T+7; T+16 and T+28 post initiation of culture) using proviral integration pattern analysis (data not shown).

To further confirm the ability of expanded cells to differentiate in vivo, selected primary and secondary recipients from Exp.1 were sacrificed 4 months post transplantation to isolate and sort bone marrow-derived myeloid (Mac-1^+), splenic B ($B220^+$) and thymic T

($CD4^+/CD8^+$) cells. Clonal analysis of these sorted cell populations revealed that within the same animal, a particular clone could be traced in all of the three aforementioned cell lineages (see legend for Fig.2.3C), providing evidence for more than one common pluripotent parent HSC that gave rise to the mature progeny. Phenotypic analysis of myeloid, B- and T-cell compartments of tertiary recipients (n=40) revealed that *Hoxb4^{hi}Pbx^{lo}* HSCs maintained this differentiation potential upon serial transplantation (data not shown).

Together, these observations strongly suggest that despite the apparent maturation arrest observed in bulk expansion cultures (Fig.2.1C), in vitro expanded *Hoxb4^{hi}Pbx^{lo}* HSCs retained their ability to engage in differentiation pathways in vivo, as well as their potential for self-renewal divisions.

Hoxb4^{hi}Pbx1^{lo} HSCs: Proliferation or cell fate determination?

Rates of DNA synthesis and cell cycle progression in primitive fractions of control *neo* and *Hoxb4* over-expressing BM cell populations were examined within the first week of expansion, when control *neo* cultures still contained detectable repopulating HSCs. At day 8 of culture, similar rates of BrdU incorporation were observed in total cell populations of all groups (Fig. 2.4A). Within the $Sca1^+$ compartment, however, DNA synthesis appeared accentuated in the control group, where the majority of cells (81%) incorporated BrdU, (Fig. 2.4A upper panel), while DNA synthesis could only be detected in a minor fraction (24%) of $Sca1^+$ *Hoxb4* cells (Fig. 2.4A middle and lower panel). Cell cycle analyses (Fig.2.4B), in parallel, mirrored these findings in that *Hoxb4* $Sca1^+$ cell populations comprised similar proportions of cells in the $S/G_2/M$ transition compared to controls (16% vs 33% for *Hoxb4* and *neo*, respectively), again with a trend of fewer dividing cells among the *Hoxb4* transduced culture. Thus, the reported expansion of *Hoxb4^{hi}Pbx1^{lo}* HSCs could not be attributed to an overtly proliferating precursor pool. HSC depletion associated with certain in vitro culture conditions could also be counteracted by up-regulation of anti-apoptotic mechanisms. Annexin V staining performed on control *neo* and *Hoxb4^{hi}Pbx1^{lo}* $Scal^+Lin^-$ cells, however, showed less than 15% positivity in both conditions (data not shown, n=3 expts.).

A CFSE high-resolution cell tracking system was used to further characterize the proliferation pattern of cultured cells. This fluorescent dye irreversibly integrates the intracellular environment and distributes evenly between daughter cells, such that with each cell division the intensity of the emitted fluorescence is precisely halved. Sub-populations of *Hoxb4* overexpressing cells, with or without additional modulation of *Pbx1* levels, displayed characteristic distributions of CFSE intensity following incorporation of the dye at day 3 of culture (Fig. 2.4C). Indeed, profiles analyzed 72 hours later demonstrated a clear shift of generation peaks to the right, or high CFSE intensity levels, for $Sca1^+Lin^-$ cells (right lower panel), in contrast to a more Gaussian type of fluorescence distribution for the overall cell culture (left lower panels), again suggesting a slower pace of division in

the primitive fraction of *Hoxb4-a/sPbx1*-transduced cells. Division profiles of $Sca1^{+}Lin^{-}$ fractions of $Hoxb4^{hi}Pbx1^{lo}$ and *neo* control cells were strikingly opposed; whereas 95% of cells in the $Hoxb4^{hi}Pbx1^{lo}$ group had undergone less than 7 divisions, 80% of cells in the *neo* control group divided more than 7 times (compare red peaks in right upper and lower panels in Fig. 2.4C).

Functional relationship between CFSE retention and stem cell activity was sought in additional experiments. At day 7 of culture, 4 days post CFSE incorporation, sorting gates were arbitrarily set to define cell fractions with high, medium and low levels of fluorescence (Fig. 2.4D). In all examined populations, the boundaries for the highest CFSE levels encompassed between 1 and 2% of the total in vitro culture. Evaluation of clonogenic progenitor activity revealed that the greatest concentration of CFCs was found within the $CFSE^{high}$ fraction of $Hoxb4^{hi}Pbx1^{lo}$ containing cells, in a ratio of ~1:7 cells, and the frequency declined to ~1:100 cells in the low fluorescence group (supplementary Fig.2.S2). High progenitor content also correlated with higher CFSE fluorescent levels in control *neo* cultures, albeit the absolute CFC numbers in this culture were markedly reduced compared to *Hoxb4* populations (supplementary Fig. 2.S2).

Interestingly, when an identical dose of 5000 (day7) $Hoxb4^{hi}Pbx1^{lo}$ cells from each fluorescence sub-group was transplanted in primary mice, $CFSE^{high}$ cells were most effective in sustaining long-term hematopoietic in vivo reconstitution, as assessed by Ly5.2 reconstitution of peripheral blood at 3 months post transplant (Fig. 2.4E). Indeed, transplanted cells could be traced in graft recipients up to a limit dilution dose of 50 cells in the $CFSE^{high}$ fractions of cultures initiated with $Hoxb4^{hi}Pbx1^{lo}$ cells (not shown). It is important to note that CRU frequencies in these experiments are lower than those determined in Exp.1 and 2 (Fig 2.1B) because cultures were not maintained for 12-14 days, but rather for 6-7 days. A CRU assay performed at T+7 of Exp.2 revealed a CRU frequency of > 1 in 3000 cells at that time point. In contrast, occasional HSC output was measured (≤ 7% of Ly 5.2 cells in PB) from the $CFSE^{med}$ fraction with 5000 cells transplanted, whereas absolutely no detectable readout could be derived from the $CFSE^{lo}$ cells. Low levels of peripheral blood reconstitution activity could also be observed among the $CFSE^{high}$ cells of the control group, but only at the highest transplantation dose of 5000 cells (see Fig. 2.4E).

From a different perspective, transcriptionally regulated and key cell cycle integrators, particularly of the G_1 phase [**cyclin proteins**: Ccnd2 (CyclinD2), Ccnd3 (CyclinD3), Ccne2 (Cyclin E1), **Cip/Kip proteins**: Cdkn1a ($p21^{Cip1/Waf1}$), Cdkn1b ($p27^{Kip1}$), Cdkn1c ($p57^{Kip2}$), **INK4 proteins**: Cdkn2a ($p16^{INK4A}$), Cdkn2b ($p15^{INK4B}$), Cdkn2c ($p18^{INK4C}$), Cdkn2d ($p19^{INK4D}$), c-Myc and c-Myb], were assessed by quantitative RT-PCR performed on sorted $Sca^{+}Lin^{-}$ BM cells, following a week of culture of both control and test (*Hoxb4±a/sPbx1* transduced) cell fractions (Fig. 2.5A). A comparison of mean delta Ct values for the various transcripts (Fig. 2.5B) demonstrates a statistically significant 4-fold decrease ($p<0.005$) in the expression of Cdkn1b ($p27^{Kip1}$) in $Hoxb4^{hi}Pbx1^{lo}$ cells, and to a lesser degree, an upregulation of c-myc (2-fold, $p<0.05$) and 2-fold decrease ($p<0.05$) in Ccnd3

(CyclinD3). As a general trend, cyclin genes seem less transcribed in *Hoxb4* containing cells. Of note, in these independent triplicate cultures, we do not observe a significant decrease in Cdkn1a (p21$^{Cip1/Waf1}$) (Cheng et al., 2000b; Miyake et al., 2005), or an important change in c-myb (Sakamoto et al., 2006) or Ccne2 (Cyclin E1) (Berger et al., 2005) levels as may have been suggested by the litterature.

2.6 Discussion

Modulation of *Pbx1* levels in BM HSCs engineered to overexpress *Hoxb4* confers a marked competitive in vivo repopulating advantage to these cells (see Suppl. Fig.2.S1), yet they remain fully responsive to the intricate interplay of intrinsic and extrinsic physiological cues that regulate the stem cell reservoir (Krosl et al., 2003b). As presented in this study, perturbation of micro environmental conditions modifies the behaviour of theses cells, resulting in unrestrained symmetrical self-renewal divisions ex vivo, with a measured increment spanning several logs in magnitude, reminiscent of the HSC expansion potential displayed during ontogeny in the fetal liver between days ~9.5 and 14.5 post conception (Gekas et al., 2005), when the pool reaches almost its adult and lifelong size. Such manifestations of pure symmetrical divisions of pluripotent cells are time-restricted, and presumably highly regulated processes in vivo. Indeed, adult stem cells are highly preserved through asymmetrical divisions, giving rise to both an identical and a differentiated cell. Efforts to induce sustained ex vivo symmetrical divisions of adult tissue stem cells, as opposed to ES cells, remain elusive, with the exception of immunophenotypically defined neural stem cells (Conti et al., 2005), and functionally defined HSCs as suggested by this work.

A crucial point to ascertain in experiments involving tissue stem cells is the irrefutable assignment of pluripotent properties. In a two-week time span, we report a 100 000-fold in vitro expansion of *Hoxb4^{hi}Pbx1^{lo}* stem cells as functionally determined by CRU assays. Marked HSC enrichment in culture was evidenced by the high frequency (~1/50) at which these cells could long-term reconstitute the hematopoietic compartment of recipient hosts, as compared to the start of culture (1/500 000). According to clonality analyses, multiple doubly transduced CRUs engaged in sustained self-renewal divisions, as reflected by the pattern of retroviral genomic insertions of differentiated tissues in serially transplanted recipients (BM and thymus from Exp.1, see Fig. 2.2A), or of individual methylcellulose colonies arising from BM cells of primary animals (see Exp.3 in Fig. 2.2A). Indeed calculated ratios of clone recovery, ie comparing numbers of distinct *Hoxb4^{hi}Pbx1^{lo}* CRUs present at cessation of long-term culture to those of input, ranged between 11-77%, testifying that a significant proportion of transduced stem cells present in vitro contributed to the expansion. In Exp.1 for instance, based on CRU frequencies determined at T0 and corresponding double gene transfer rates assessed by epifluorescence, between 20-100 *Hoxb4^{hi}Pbx1^{lo}* CRUs were present at the start of culture. At least 11 distinct clones (refer

to Fig.2.2A and 2.2B) could be identified upon genomic DNA retroviral insertion patterns studies of secondary recipients of T+12 cells, implying that > 11% (up to 11/20, or 50%) of doubly transduced stem cells initially present in vitro engaged in self-renewal, and their progeny still traced upon serial adoptive transfer. This may also reflect the heterogeneity of the in vitro stem cell population regarding self-renewal potential. Given the large volume of cells present in vitro after a 2 week expansion, only a glimpse of total clones can be identified through retroviral signatures analysis, thus estimations can only under evaluate fractions of clones that engaged in self-renewal. Convincingly though, these rates are too significant to be associated with an epiphenomenon and preclude the possibility that a single marginal stem cell aberrantly divided in vitro and contributed exclusively to the read-out of functional assessments. Moreover, if recruitment of progenitors into the stem cell compartment accounted for the marked enrichment of HSCs in vitro, one would expect to distinguish significantly more signatures or clones at the end of culture, given the higher propensity of progenitors to retroviral infection compared to stem cells, and their relative abundance at initiation of culture (>30 000 CFCs vs 20-100 CRUs in Exp.1).

Given that cultures were initiated with at most ~20 *Hoxb4^{hi}Pbx1^{lo}* CRUs (a total of 100 stem cells were present considering single, double and no gene transfer), and assuming that all these cells maintained their stemness and contributed to the increase in stem cell numbers to some extent, one would assume an average of 17 divisions in a 12-day time span, or one self-renewal division of each stem cell approximately every 17 hours. In our experimental conditions, the vast majority of cultured bone marrow cells had incorporated BrdU within 12 hours, implying that *Hoxb4^{hi}Pbx1^{lo}* stem cells proliferated slower than their more differentiated progeny, but at a pace similar to their genetically non-modified counterparts (Uchida et al., 2003), and interestingly, to neural stem cells in vitro (Conti et al., 2005), for which 12-14 and 24 hr doubling times have been reported respectively. Following these substantial numbers of HSC divisions in vitro, fundamental stem cell characteristics were preserved, including in vivo engraftment, expansion, maintenance (cells probably revert to asymmetrical divisions post adoptive transfer, see Fig.2.6) and terminal differentiation, as assessed by retroviral insertion studies and immunophenotype.

Since multiple stem cells were recruited in the in vitro expansion compartment, seemingly without an accelerated proliferative impetus, it was hypothesized that Hoxb4 and Pbx1 may alter cell fate programs. Undeniably, a mitotic signal must be integrated for a cell to self-renew. By examining DNA synthesis, cell cycle phase distributions and tracking cell divisions in our experimental setting, *Hoxb4^{hi}Pbx1^{lo}* HSCs do divide, but they are not highly proliferative, and alternate mechanisms must be considered to explain the high frequency of self-renewal documented herein. Of note, apoptosis rates, as measured by Anexin-V studies, were comparable between control and *Hoxb4^{hi}Pbx1^{lo}* Sca+Lin- cells.

It must be emphasized that $CFSE^{med}$ BM cells, which had undergone ≥4 divisions in 72 hours, could also be traced in recipients mice (≤ 7% peripheral blood reconstitution). Although not as enriched in CRUs as the fraction of cells that highly retained the fluorescent dye (in the range of 1/5000 vs 1/50 for $CFSE^{high}$ cells), $CFSE^{med}$ BM cells comprised 30-40% of T+7 culture, thus the absolute number of stem cells in this compartment is not negligible. This corroborates the emerging concept that engrafment potential can be preserved upon stem cell division in vitro (Dykstra et al., 2006), perhaps contrary to initial observations (Oostendorp et al., 2000; Peters et al., 1996). Moreover, this sustains the idea that in vitro symmetrical self-renewal divisions are not restricted exclusively to rigorously defined stem cells, but may also occur in early progenitors, as indicated by the increment of multipotent precursors and highly proliferative colonies in culture (Fig.2.1, lowest impact of Hoxb4 over-expresion on differentiated cells), and as previously reported by others (Antonchuk et al., 2002). Our results also demonstrate that CFCs division kinetics mirrors that of CRUs (Suppl Fig2.S2). As opposed to asymmetrical divisions then, symmetry preserves cell fate or impedes cellular diversity, as can be strikingly evident by simple histological examination of $Hoxb4^{hi}Pbx1^{lo}$ cell cultures (Fig.2.1C). Fascinatingly, the literature provides with other elegant example of in vitro symmetrical divisions of early progenitors in other cell types (Shinin et al., 2006).

Altogether, our results support the established link between cell cycle modulation and self-renewal [e.g., p21, p27, etc., (Berger et al., 2005; Cheng et al., 2000a; Cheng et al., 2000b; Walkley et al., 2005; Yu et al., 2006; Yuan et al., 2004; Zhang et al., 2005) see also (Yuan et al., 2004)], and follow the postulate that cellular identity may dictate the pattern of progression through the cycle. Quantification analyses of RNA transcripts in the primitive hematopoietic compartment show a decrease in p27 and a rise in c-myc in Hoxb4 over expressing cells compared to controls, in agreement with the phenotype of the combined null *Mad1* (inhibitor of c-myc) and p27 mice that display an increase in HSC frequency and interestingly, an expanded pool of quiescent stem cells (Walkley et al., 2005). Generation of the pancreatic beta cell mass is also reported to be modulated by p27 (Georgia and Bhushan, 2006), and recently Notch1 signalling has been linked to p27 degradation (Sarmento et al., 2005). Notably, c-myc has been assigned a role in self-renewal (Cartwright et al., 2005) and overall chromatin structure (Knoepfler et al., 2006). Moreover, the documented decrease in Cyclin D3 in cultured cells sustaining self-renewal parallels the findings of Cyclin D3 null mice, reported to have a normal stem and progenitor pool, but a differentiation arrest (Sicinska et al., 2006).

What then defines the niche, or the proper combination of cell fate determinants that enables and sustains symmetrical self-renewal divisions? Many eloquent examples attempt to dissect this complex question in HSCs (BMP, Gfi-1, Ezh2, Smad7, Mph/Rae, and others) (Blank et al., 2006; Hock et al., 2004; Kamminga et al., 2006; Kim et al., 2004; Ying et al., 2003) and in ES cells (Oct4, Nanog, Sox2, reviewed in (Rao and Orkin, 2006)). Part of the answer may reside in proper chromatin configuration, integration of

specific proliferation, differentiation, senescence or apoptosis signals, as well as intracellular segregation of key regulator molecules. Nonetheless, a role for homeotic genes in cell fate decisions is indisputable, and perturbations in the C. elegans hox-meis-pbx complex were recently shown to alter the outcome of cellular division (Arata et al., 2006) S& . Data from foetal stromal cells and tissue stem cell profiling may continue to provide interesting candidates. For now, our data supports currently proposed patterns of lengthy cell cycle progression for hematopoietic stem cells (Calegari et al., 2005; Dykstra et al., 2006; Nygren et al., 2006), and agrees with the idea that unrestricted proliferation may override stemness. We have not assessed the length of time extensive self-renewal can be sustained in vitro, but HSC activity is still functionally detectable at 21-28 days of culture in our system (data not shown).

As already mentioned in the result section, some degree of skewing towards the myeloid lineage was observed in vivo upon transplantation of BM *Hoxb4*^{hi}*Pbx1*^{lo} long term culture cells, and as reported, a dosage effect of transcription factor may be incriminated to explain this observation (Schiedlmeier et al., 2003), and cell type specific differential transcription of the integrated provirus is also possible. As an alternate mechanism, ES cells that are highly passaged in vitro start to display impaired differentiation, presumably through genetic and epigenetic changes (Maitra et al., 2005). In our prolonged in vitro cultures, we have also sporadically documented the generation of leukemic HSCs (HSC-L), in a ratio inferior to normal HSCs [1/2500 (HSC-L) vs 1/50 (HSC)] after 2 weeks in culture, as assessed by standard CRU assays (data not shown), resulting in acute myeloid leukemia with short latency in primary and secondary recipients. Clonality analyses (based on Hoxb4 integrations) of BM cells from animals that succumbed to leukemia revealed that a maximum of 2 clones contributed to the disease (see Suppl. Fig.2.S4), confirming the low incidence of the event. More strikingly, whereas clones recovered from healthy mice harboured between 1.5-2.6 integrations per clone (see Suppl. Table 1 for details), leukemic clones carried 10-11 of these integrations (Suppl. Fig.2.S4), providing strong evidence to incriminate insertional mutagenesis as a major culprit in this process (statistically significant difference, $p<0.0001$). Accordingly, there was an association between retroviral transduction rates and leukemogenesis, with only one reported leukemia among 138 recipients in experiment 3, where double gene transfer was evaluated at 4%. To strengthen the argument, in vitro immortalization of primary hematopoietic cells by insertional mutagenesis, and a correlation to the number of integrations, has been rigorously documented (Du et al., 2005), and in vitro expansion of tissue stem cells (Conti et al., 2005) in the absence of retroviral gene transfer was not associated with malignant transformation in vivo.

During a 16-month period, *Hoxb4*^{hi}*Pbx1*^{lo} HSCs were subjected to a considerable proliferation pressure to achieve a cumulative 10^{10}-fold in vitro and in vivo expansion. Both, the cytokine-promoted proliferation in vitro (Vaziri et al., 1994) and repopulation of host following transplantation (Allsopp et al., 2001; Notaro et al., 1997) have been associated

with telomere shortening implicated in limiting the replicative lifespan of somatic cells. We did not assess telomere length in these cells, although ongoing studies (P. Lansdorp, Vancouver, BC) will determine the impact of Hoxb4 overexpression on telomere length in transduced HSCs. Central to the theme of the presented work however, remains the demonstration that pure symmetrical self-renewal divisions can be sustained in vitro under appropriate conditions, and that supraphysiological ex vivo expansions of tissue stem cells for therapeutic purposes should be envisioned with caution, even in retrovirus-free systems. We propose this in vitro model of stem cell enrichment as a valuable genetic tool to gain further insight into the self-renewal machinery, for instance through the isolation of protein complexes, to better dissect the critical interplay between cell fate determinants and cell cycle regulators, and to study other stem cell biological properties such as replicative senescence.

2.7 Figures

Figure 2.1. In vitro expansion of *Hoxb4^{hi}Pbx1^{lo}* HSC

(A) Diagrammatic representation of retroviral vectors and experimental strategy used in these experiments. In total 3 independent experiments (Exp.1-3) were performed. CRU frequency in cultures were assessed at different times (T) using limit dilution assays as follows: Exp.1: T0; T+12, T+19; Exp.2: T+3; T+14; Exp.3: T0, T+7, T+16, T+21*; T+28;. At each time point, between 20-35 primary recipients were transplanted per condition, except for * where only 3 mice were used.

FCS: Fetal Calf Serum; SF: Steel Factor

(B) Differential impact of Hoxb4 over-expression on the expansion of distinct cell fractions following 2 weeks of ex vivo culture. From Exp.1 and 2. CFC: colony-forming cell, CRU: competitive repopulating unit. *To calculate fold-expansion in Exp.2, CFCs and CRUs at initiation of culture were considered to be equivalent to those of Exp.1, even though 1/3 of mice or 1/10 of BM cells were used to begin the experiment. Hence, the fold-increase may be an underestimate.

(C) Wright stain of cellular preparations obtained from T+14 cultures initiated with GFP-transduced cells (left panel) or *Hoxb4^{hi}Pbx1^{lo}* cells (right panel). Note the reduction of differentiated cells (e.g., ring neutrophils) in right panel. Representative example shown from Exp.2.

(D) Histogram depicting the absolute HSC (CRU) numbers increment in the cultures initiated with GFP-transduced cells versus those with *Hoxb4^{hi}Pbx1^{lo}* cells. X-axis refers to number of days cells from Exp.1 and 2 were kept in culture. ¶ Total CRU value at T0 also includes untransduced and singly transduced cells. * Estimated value according to CRU frequency of Exp.1, see legend of (B).

(E) Representative FACS profile of GFP and YFP expression in peripheral blood (PB) cells from a primary mouse recipient of 5 *Hoxb4^{hi}Pbx1^{lo}* expanded cells after 14 days of culture. Recipient (Exp.2) was analyzed at 16 weeks post transplant.

(F) Summary of CRU expansion in serial transplantations of *Hoxb4^{hi}Pbx1^{lo}* BM cells revealing a cumulative 10^{10}-fold in vitro and in vivo expansion over a period of 19 months. From Exp.1.

Fig. 2.1

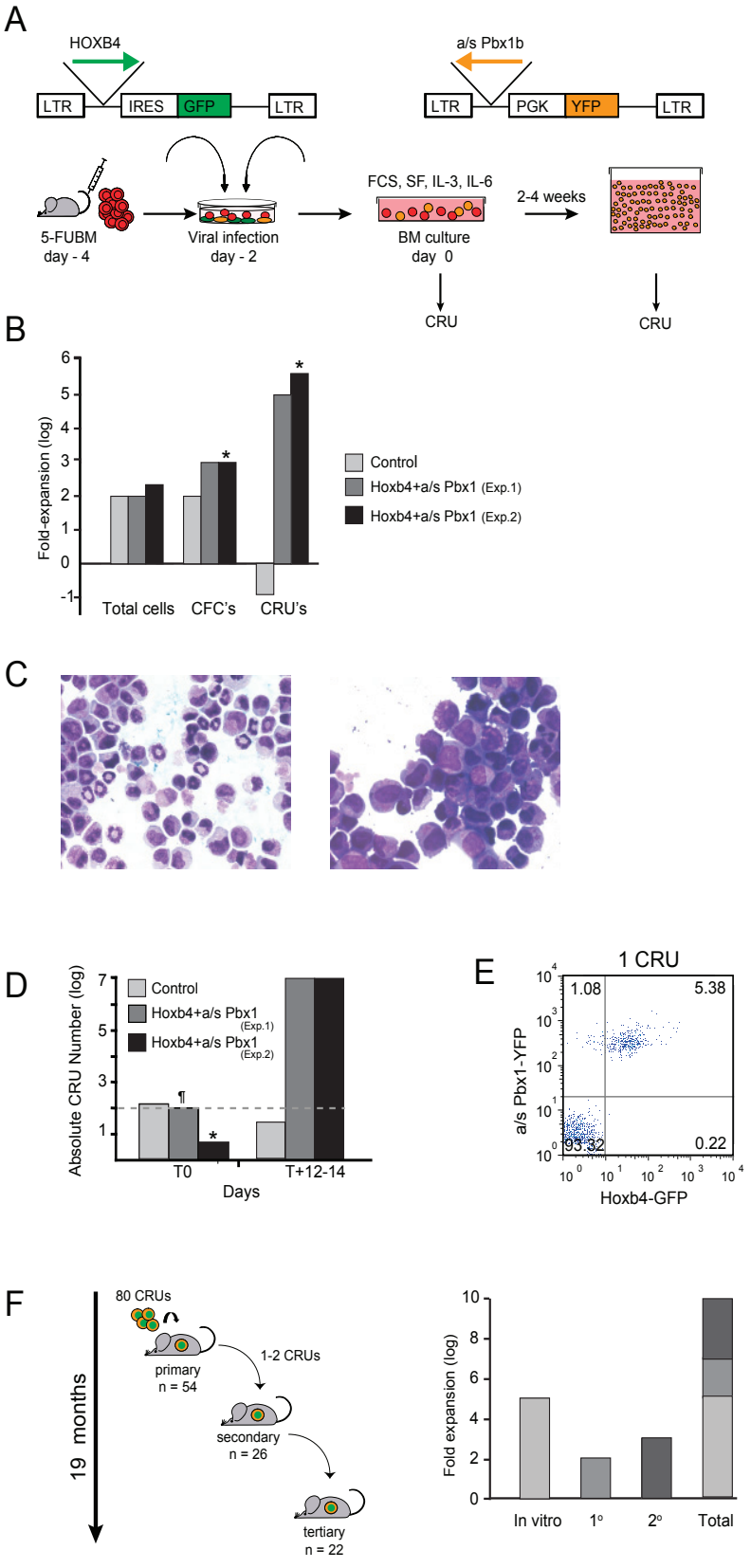
A
HOXB4
LTR
IRES
GFP
LTR
a/s Pbx1b
LTR
PGK
YFP
LTR
5-FUBM
day - 4
Viral infection
day - 2
FCS, SF, IL-3, IL-6
BM culture
day 0
2-4 weeks
CRU
CRU
B
Fold-expansion (log)
Total cells
CFC's
CRU's
Control
Hoxb4+a/s Pbx1 (Exp.1)
Hoxb4+a/s Pbx1 (Exp.2)
C
D
Absolute CRU Number (log)
Control
Hoxb4+a/s Pbx1 (Exp.1)
Hoxb4+a/s Pbx1 (Exp.2)
T0
T+12-14
Days
E
1 CRU
1.08
5.38
93.32
0.22
a/s Pbx1-YFP
Hoxb4-GFP
F
19 months
80 CRUs
primary
n = 54
1-2 CRUs
secondary
n = 26
tertiary
n = 22
Fold expansion (log)
In vitro
1°
2°
Total

Figure 2.2. Polyclonal and pluripotent character of expanded *Hoxb4^{hi}Pbx1^{lo}* HSCs

(A) Summary of *Hoxb4^{hi}Pbx1^{lo}* CRUs present at initiation (T0) and termination (T+12-16) of culture in the reported experiments, with CRUs at output over input numbers expressed as percentages on the far right column. T=0 CRUs calculated using CRU frequencies and transduction rates (Exp.1) or Southern Blot analyses of BM cells of primary recipients (Exp.3). Note that CRU numbers at T0 (<100) also include untransduced and singly transduced cells, hence the possible over estimation of *Hoxb4^{hi}Pbx1^{lo}* CRUs. T+12-16 CRUs calculated using Southern Blot analyses of BM cells of secondary recipients (Exp.1) or individually expanded myeloid colonies derived from BM cells of primary recipients (Exp.3).

(B) Clonal analyses of hemopoietic reconstitution were also performed on 1^{o} (mouse I) and 2^{o} (mice II-X) recipients of *Hoxb4+a/sPbx1* BM cells from Exp.1. Mice were sacrificed 4 months post transplantation. DNA extracted from BM, spleen and thymus was digested with HindIII and EcoRI , which released a constant fragment of 3 kb representing the integrated *Pbx1* provirus (see dotted line) and unique fragments for the integrated *Hoxb4* virus (see autoradiographic signals identifying specific integration sites). Hence, a GFP probe generated a single autoradiographic signal for all *a/sPbx1* proviral integrations (as indicated by the dotted lines), together with multiple bands denoting each *Hoxb4* proviral integration event (see bottom diagram). A primary recipient of 4000 cells of T+12 in vitro culture (0.0007% of the total cell population), mouse I, displayed an oligoclonal pattern of *Hoxb4* integration, reflecting the presence of several doubly transduced HSCs in the in vitro culture. Individual clones, labelled from “a” to “g”, can be distinguished among 2^{o} transplant recipients of BM cells from mouse I (clones “h” to “k” are not shown in this blot). Note that a given clone was sometimes present in more than one 2^{o} recipient, see for example clone “f” in mice III and IX, suggesting in vivo self-renewal of this HSC in the 1^{o} donor mouse.

(C) Primary recipients of day 16 in vitro culture *Hoxb4^{hi}Pbx1^{lo}* cells (from Exp.3) were sacrificed at 4 months post transplantation, their respective BM cells plated in methylcellulose (m.c.), and individual colonies were then expanded. Southern Blot analyses of genomic DNA extracted from these clones are presented; DNA was digested with restriction enzymes (HindIII and EcoRI) as in (B). Individual clones, labeled from “1” to “10”, can be distinguished among 3 transplant recipients of BM cells. Note that a given clone was sometimes present in different recipients, suggesting in vitro self-renewal of the parent HSC. Mice were sacrificed 4 months post transplantation to ensure in vivo exhaustion of transduced progenitors, and thus assure that each colony forming cell (CFC) in methylcellulose (m.c.) was stem cell derived. * Probable contamination from clone no 2.

Fig. 2.2

A

	T= 0 # CRU transduced	T+12-16 # CRU recovered	% of CRU that expanded
expt 1	< 100	> 11	> 11%
expt 2	nd	nd	nd
expt 3	≥ 13	≥ 10	77%

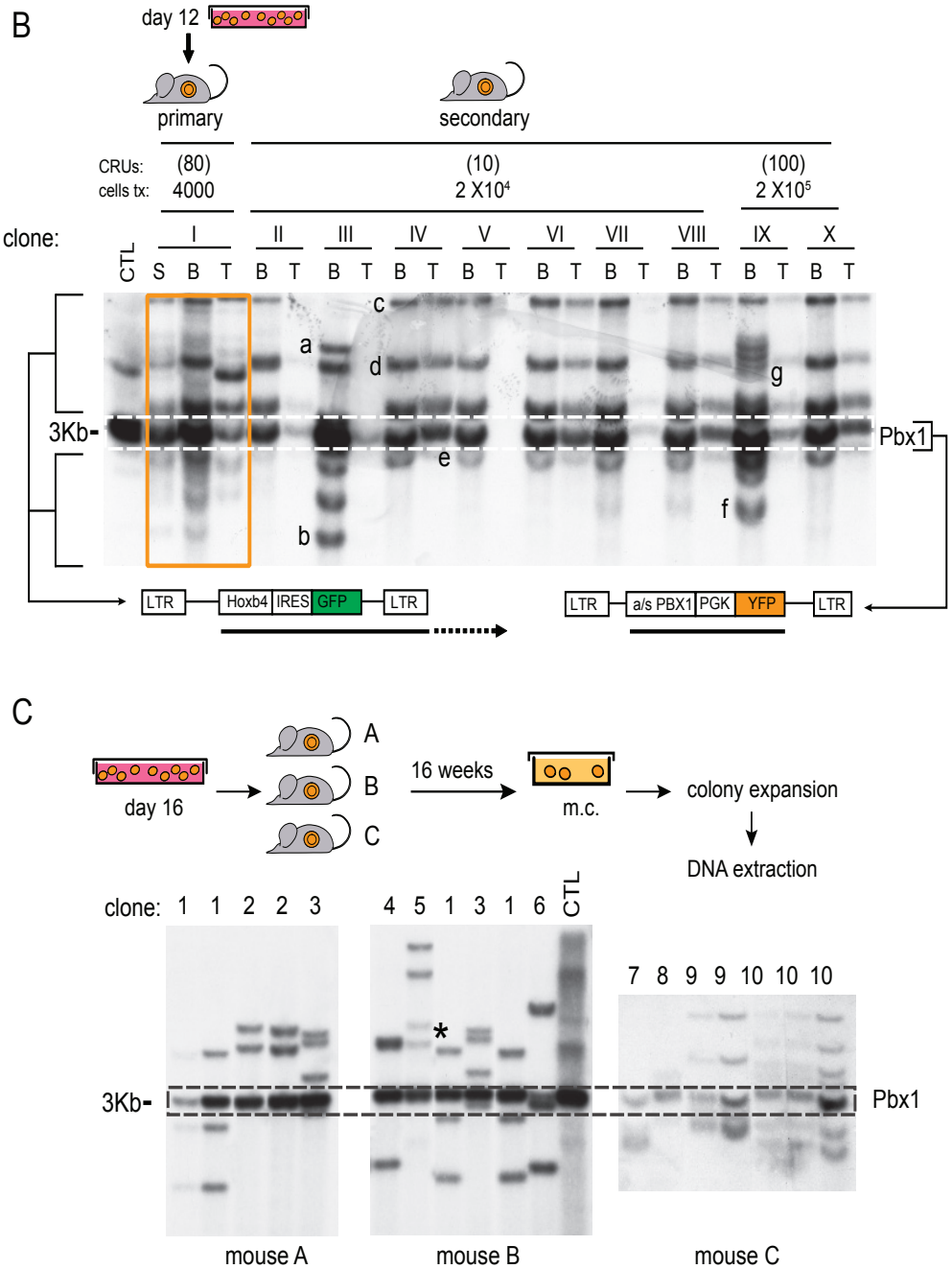

Figure 2.3. Differentiation potential analysis of in vitro and in vivo expanded CRUs.

(A) Representative FACS profiles of primary (top) and secondary (bottom) recipients of in vitro cultured T+12 *Hoxb4^{hi}Pbx1^{lo}* cells (Exp.1) showing myeloid (Mac-1) and lymphoid (B220, CD8) differentiation. Animals were sacrificed 4 months post transplantation. BM: bone marrow, Sp: spleen, Th: thymus.

(B) FACS prolifes of bone marrow (BM) and peripheral blood (PB) cells from a representative primary recipient of 500 T+14 *Hoxb4^{hi}Pbx1^{lo}* expanded cells (Exp.2), 14 months post transplantation. For the different lineage marker shown on the Y-axis (Gr1, Mac-1, Ter119, B220, CD8) and on the X-axis (CD4), gates are set on double positive GFP:YFP (Hoxb4:a/sPbx1) cells.

(C) Terminal differentiation capacity of in vitro expanded HSCs was further evaluated in a 1^{o} recipient (Exp.1) of 2,500 T+12 expanded cells and in serially transplanted 2^{o} recipients (left panel). Both, 1^{o} and 2^{o} recipients were sacrificed at 4 months post transplantation, and their hemopoietic cells sorted in B (B220^{+}), T (CD4^{+}/CD8^{+}) lymphoid and (Mac-1^{+}) myeloid lineages. Genomic DNA extracted from these populations was analyzed by Southern blot (right panel) as described in Fig 2.2A. Within a given animal, a common clone could be identified in all the aforementioned cell types, testifying that a common parental HSC gave rise to this differentiated lympho-myeloid progeny.

Fig. 2.3

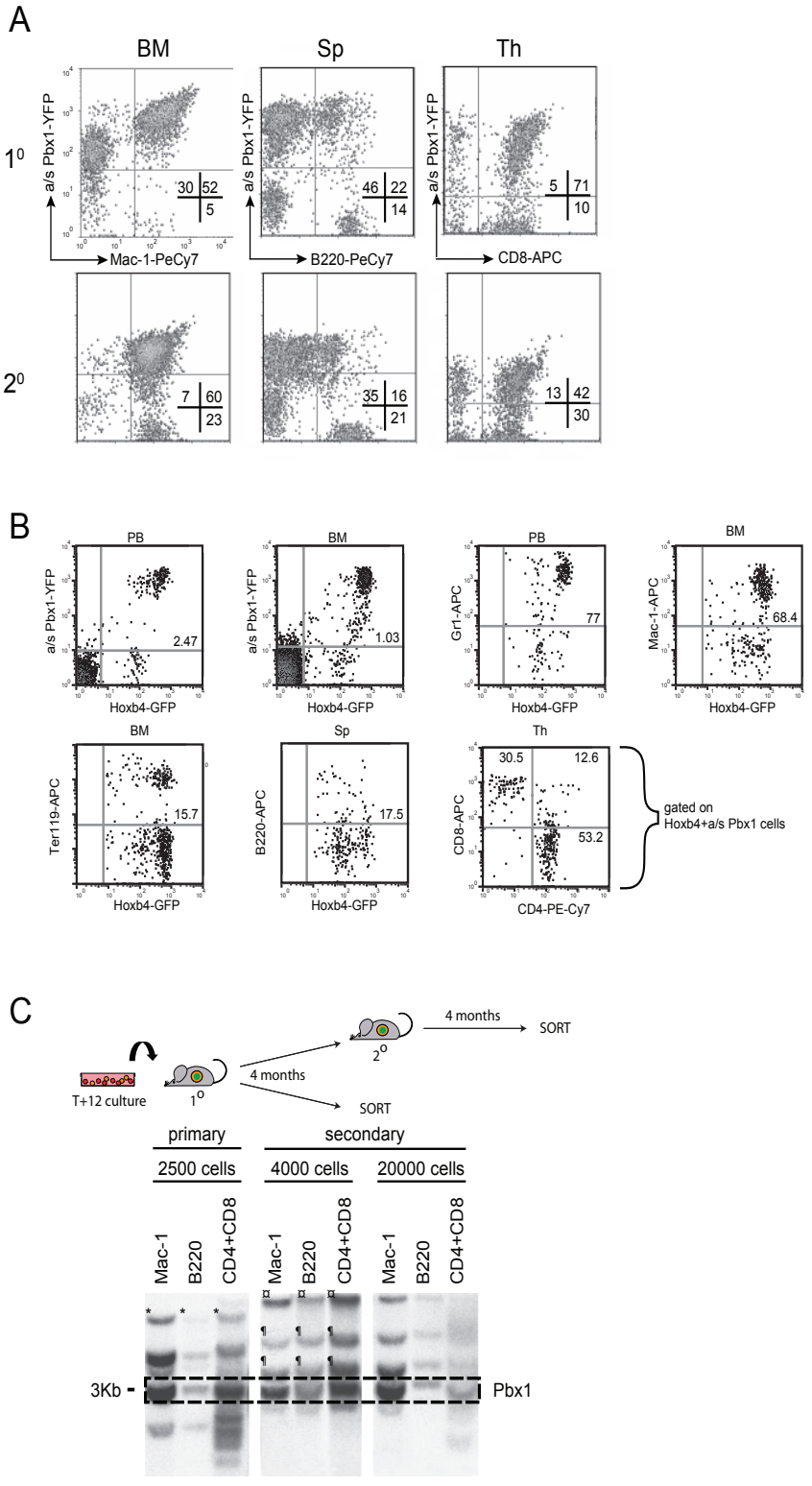
A
BM
Sp
Th
1⁰
2⁰
a/s Pbx1-YFP
Mac-1-PeCy7
B220-PeCy7
CD8-APC
30
52
5
46
22
14
5
71
10
7
60
23
35
16
21
13
42
30
B
PB
BM
Hoxb4-GFP
2.47
1.03
Gr1-APC
77
Mac-1-APC
68.4
Ter119-APC
15.7
Sp
B220-APC
17.5
Th
CD8-APC
CD4-PE-Cy7
30.5
12.6
53.2
gated on
Hoxb4+a/s Pbx1 cells
C
T+12 culture
1°
2°
4 months
SORT
primary
secondary
2500 cells
4000 cells
20000 cells
Mac-1
B220
CD4+CD8
3Kb
Pbx1

Figure 2.4. Division tracking of primitive hemopoietic cells

(A) In vitro BrdU incorporation assay performed on BM cells transduced with the indicated retroviruses and maintained in culture for 8 days. BrdU incorporation was estimated at ~80% in control and *Hoxb4*-transduced cells (total population). *Hoxb4*-transduced $Sca1^+$ cells contained a larger proportion of units that have not engaged in DNA synthesis than comparable controls (see ratio of upper/lower right quadrants in 1st (control) versus 2nd and 3rd (*Hoxb4*) panels). Representative result from n=1 experiment.

(B) Cell cycle phase distributions of $Sca1^+Lin^-$ cells in culture initiated with control or *Hoxb4*-transduced cells reinforce the results obtained in "A" since a smaller proportion of *Hoxb4*-transduced cells were found in S/G2/M than in control cultures. Representative result from n=3 independent experiments.

(C) CFSE labeling of $Hoxb4^{hi}Pbx1^{lo}$ versus control BM cells at day 3 of culture, and FACS profiles of cells analyzed at day 6 are shown. Number of events (y axis) is displayed against CFSE intensity (x axis), for both total cell populations (left panels) and $Sca1^+Lin^-$ subgroups. Similar patterns of division were observed in $Hoxb4^{hi}$ and $Hoxb4^{hi}Pbx1^{lo}$ groups, namely, increased proportions of cells with high fluorescence intensity or low numbers of divisions in the $Sca1^+Lin^-$ fraction, against a more Gaussian type of fluorescence distribution in the overall cell population (generation 7 peak illustrated in red for comparison), and in the control condition. When comparing $Sca1^+Lin^-$ subgroups of $Hoxb4^{hi}Pbx1^{lo}$ cells to that of control, 95% of cells in the former group had divided ≤ 7 times, whereas 80% of cells in the latter group divided ≥ 7 times. Representative result from n=2 independent experiments performed in triplicate.

(D) Gates used to sort CSFE labeled cells on day +7 of culture. Sorted cells were transplanted as depicted in "C" and results of this experiment are reported in "E".

(E) CFSE treated cells described in "D" according to CFSE fluorescence intensity levels, with arbitrarily set gates of high, medium and low intensity. The $CFSE^{high}$ cell fraction represented 1-2% of cells in all conditions examined (*neo*, *Hoxb4* or *Hoxb4+a/sPbx1* transduced cells). Cell subpopulations characterized by a distinct CFSE fluorescence intensity were evaluated for repopulation activity by transplanting between 50 to 5000 cells in myeloablated recipients, which were analyzed 3 months after transplantation. Long-term repopulating cells are found in greatest proportion in the $CFSE^{high}$ fractions, irrespective of genotype. Similar results were obtained for *Hoxb4* or *Hoxb4+a/sPbx1* groups. N=2 independent experiments with 3 recipients transplanted per CSFE fraction with representative shown.

Fig. 2.4

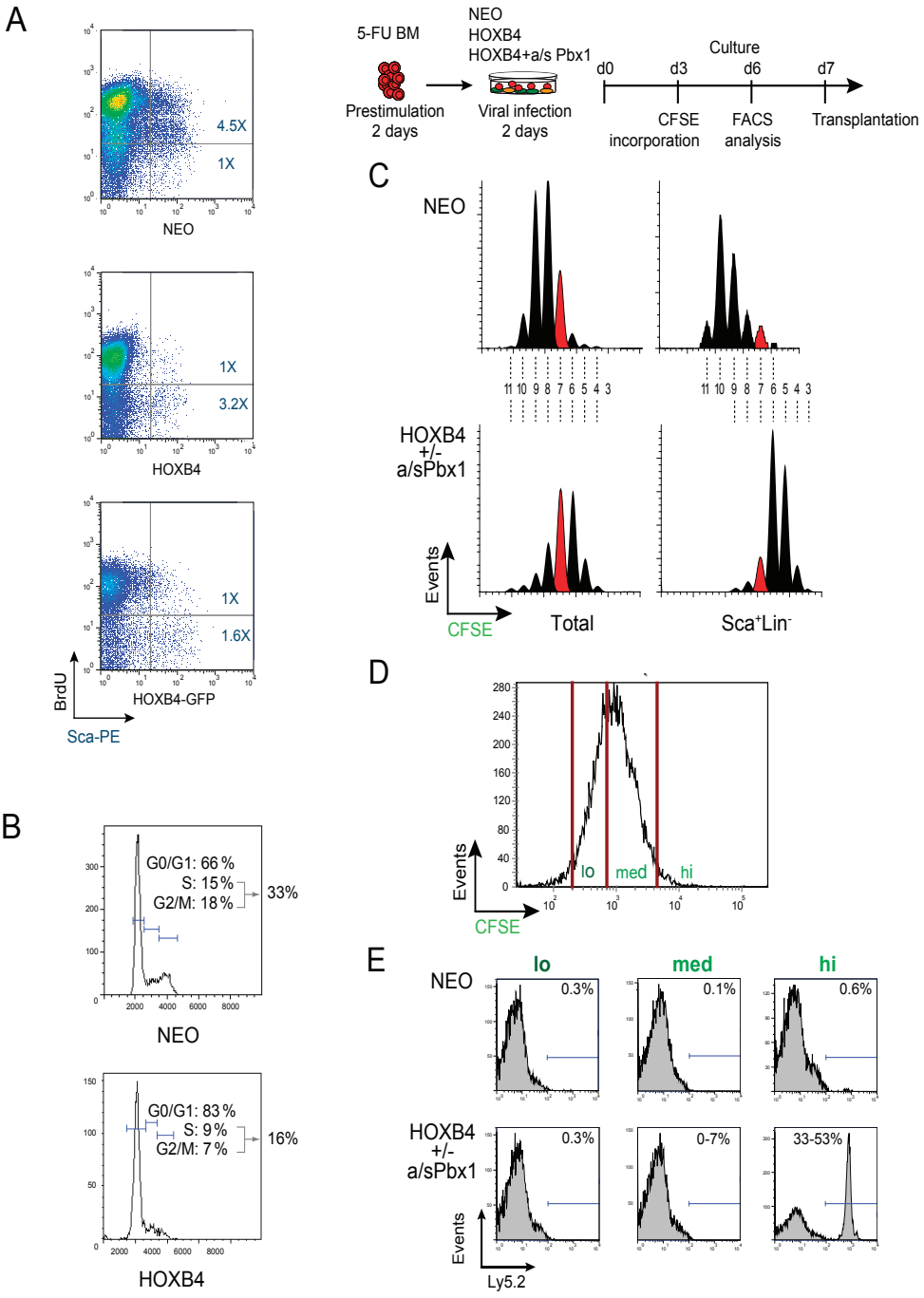
A
4.5X
1X
NEO
1X
3.2X
HOXB4
1X
1.6X
HOXB4-GFP
BrdU
Sca-PE
B
G0/G1: 66 %
S: 15 %
G2/M: 18 %
33%
NEO
G0/G1: 83 %
S: 9 %
G2/M: 7 %
16%
HOXB4
5-FU BM
Prestimulation
2 days
NEO
HOXB4
HOXB4+a/s Pbx1
Viral infection
2 days
Culture
d0
d3
d6
d7
CFSE
incorporation
FACS
analysis
Transplantation
C
NEO
HOXB4
+/-
a/sPbx1
Events
CFSE
Total
Sca+Lin-
D
Events
lo
med
hi
CFSE
E
lo
med
hi
NEO
0.3%
0.1%
0.6%
HOXB4
+/-
a/sPbx1
0.3%
0-7%
33-53%
Events
Ly5.2

Figure 2.5. Expression profiles of cell cycle related genes in primitive cells

(A) Sca+Lin- BM cells were sorted on T+7 of in vitro culture for the single transduced Hoxb4-GFP cell population, the double transduced Hoxb4-GFP + a/s Pbx1-YFP fraction (see test FACS profiles on the left) as well as for control GFP + YFP cells (see control FACS profiles on the right). Retroviral infections and cultures were performed in triplicates according to our standard protocol for 5-FU BM cells as described above (n= total of 60 mice).

(B) Analysis of selected genes by Quantitative RT-PCR. Results are presented as relative fold-differences in m-RNA expression as compared to control Sca+Lin- cell fraction. For all triplicate culture conditions, genes were analyzed in duplicates, and mean delta Ct values were compared between groups and their significance assed by independent t-test. Statistically significant differences are highlighted by a symbol. ¤ $p<0.05$, * $p<0.005$. For both Cdkn1a and Cdkn1c, one of the triplicate values was disregarded in the Hoxb4 group because it was considered as an outlier (delta Ct value differed by ≥ 4 units).

(C) Average delta Ct (threshold cycle) values for all genes. As an assessment of RNA quality, Ct values for the endogenous control gene (GAPDH) ranged between 15.3 and 26. ¶ Genes were considered not to be expressed for delta Ct values > 15.

Fig.2.5

A

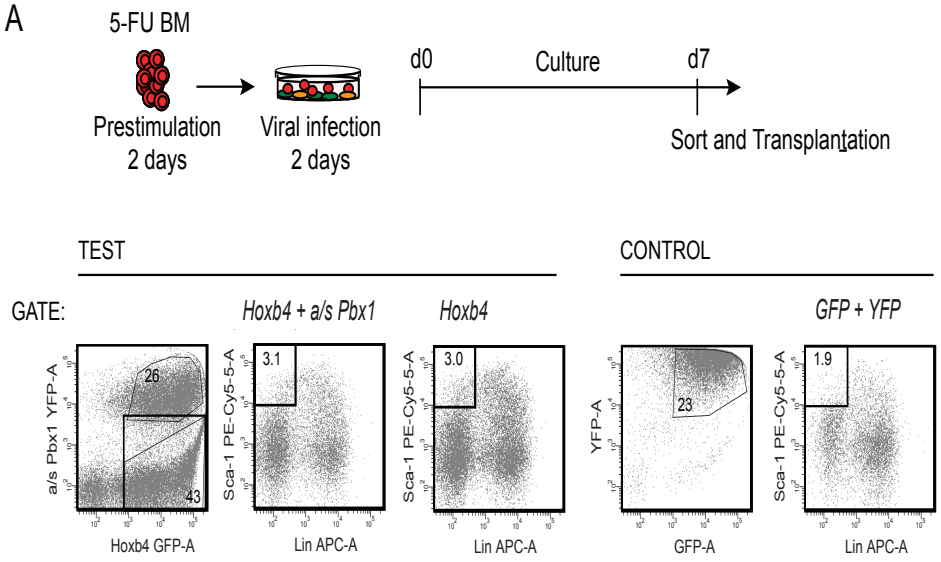

B

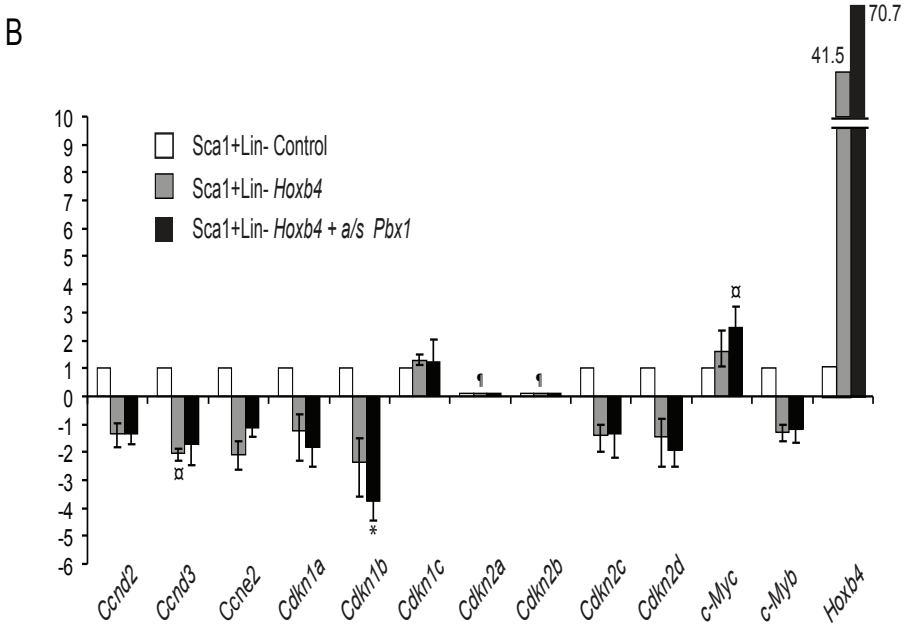

C

Average Delta Ct							¶	¶					
	Ccnd2	*Ccnd3*	*Ccne2*	*Cdkn1a*	*Cdkn1b*	*Cdkn1c*	*Cdkn2a*	*Cdkn2b*	*Cdkn2c*	*Cdkn2d*	*c-Myc*	*c-Myb*	*Hoxb4*
Sca1+Lin- Hoxb4	4.7	6.7	8.4	7.7	8.3	13.8	>15	>15	11.7	11.5	5.3	7.7	3.9
Sca1+Lin- Hoxb4 +a/s Pbx1	4.7	6.5	7.6	7.3	9.5	13.9	>15	>15	11.6	11.1	5.1	7.6	2.4
Sca1+Lin- Control	4.3	5.7	7.4	6.0	7.7	14.2	>15	>15	11.2	10.1	6.0	7.3	9.2

Figure 2.6. Model for in vitro and in vivo self-renewal division of *Hoxb4*^{hi}*Pbx1*^{lo} HSCs

Hoxb4 and *Pbx1* preferentially alter stem cell fate in vitro with increased probability of symmetrical self-renewal divisions of expansion, for the vast majority of HSCs present in culture, rather than accelerating the division rates of a few stem cells. Following a brief period of expansion in vivo post adoptive transfer, they can revert to asymmetrical divisions of maintenance and respond to physiological cues of the niche.

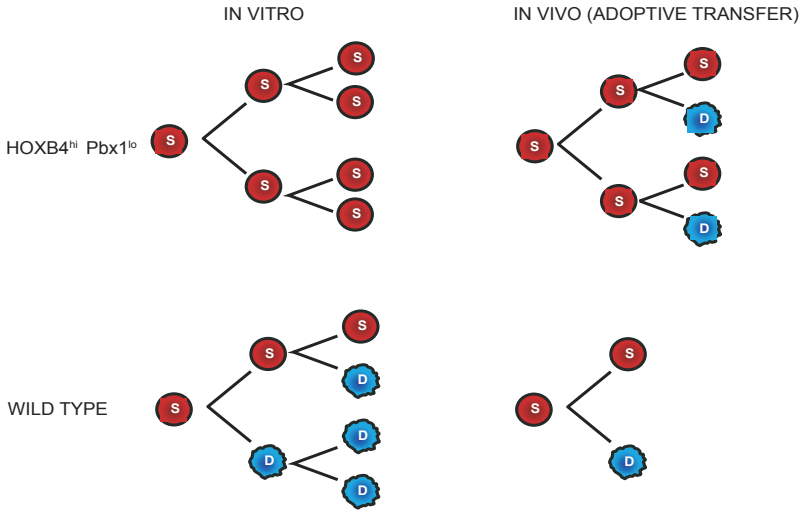

Supplementary Figure 2.S1. Maintenance of HSC pool size is a highly regulated process

HSC numbers significantly decline in vivo following myeloablative bone marrow (BM) transplantation to about 10% of normal levels (compare 1st and 2nd panel). Yet, when the BM graft consists of cells engineered to overexpress *Hoxb4* (panel 3), the stem pool size is replenished to normal levels, and not above, in the recipient animal, and this remains true for up to 1 year following transplantation (Thorsteinsdottir et al., 1999). If the graft contains similar fractions (~10%) of both *Hoxb4* and *Hoxb4+a/sPbx1* singly and doubly transduced cells (panel 4), the latter completely refill the stem cell pool, restrain the expansion of the single *Hoxb4* cells, but are still responsive to in vivo regulatory mechanisms that control HSC numbers (Krosl et al., 2003b). Hence the hypothesis that in vitro culture of these doubly transduced cells could release cells from in vivo physiological constraints and reveal their intrinsic expansion potential.

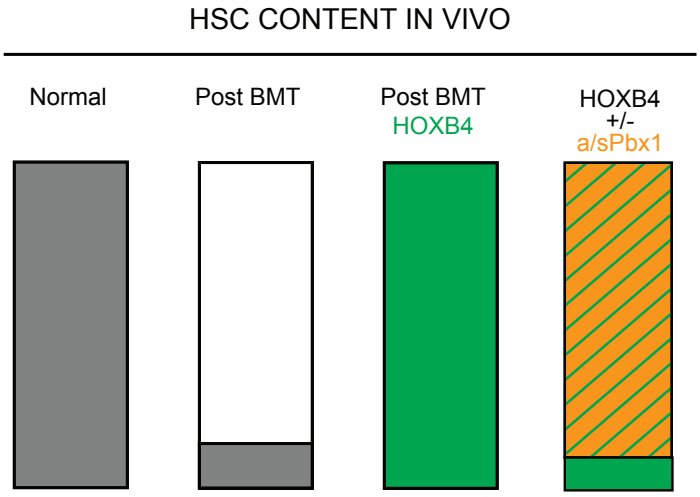

Supplementary Figure 2.S2. Progenitor frequency in CFSE^{+} sorted cells

The various CFSE^{+} cell-sorted subpopulations (see Fig.2.4D) were evaluated for colonogenic progenitor activity, and as established, marked increase in CFC frequency was found among *Hoxb4*-containing cells, but within this group, the small CFSE^{high} sorted cell fraction was enriched 50-fold with myeloid progenitors with respect to the CFSE^{low} counterpart. N=2 expt. performed in quadruplicate cultures. Error bar not indicated but within 15% of values.

CFC: colony forming cell; CFSE: carboxyfluoroscein diacetate succinimidyl ester.

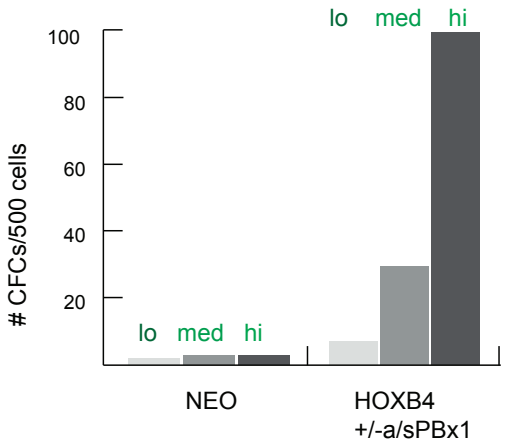

Supplementary Figure 2.S3. Hematological phenotype of high dose recipients of long-term cultured cells

(A) One million T+16 cultured *Hoxb4*^{hi}*Pbx1*^{lo} BM cells (Exp.3) were transplanted in each of 3 primary recipients (A, B and C), and animals were sacrificed after a 4-month interval for analysis.

(B) Southern Blot analysis of DNA retrieved from thymus (T), spleen (S) and bone marrow (BM) of these mice, as detailed in Fig.2.2A, revealed a polyclonal pattern of reconstitution, and common retroviral insertion signatures among the different tissues of a given mouse, suggesting that the graft contained pluripotent parental HSCs.

(C) Automated blood count values for the respective mice. Platelet counts could not be evaluated due to clotting in the samples, but appeared normal on blood smear examination (see D). WBC: white blood cell, Hg: hemoglobin, Plt: platelet, N:normal.

(D) Representative histological slides from peripheral blood (PB) and spleen (Sp) of mouse B, with no obvious pathological signs.

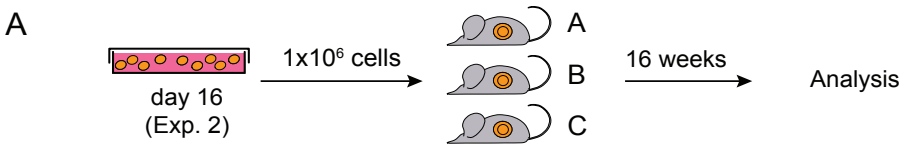

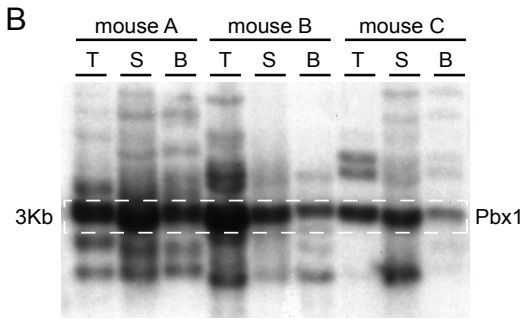

C

	WBC (10x^9/L)	Hb (g/L)	Plt (x10^9/L)
Control	6.8	170	N
Mouse A	11.2	142	N
Mouse B	8	142	N
Mouse C	4.6	152	N

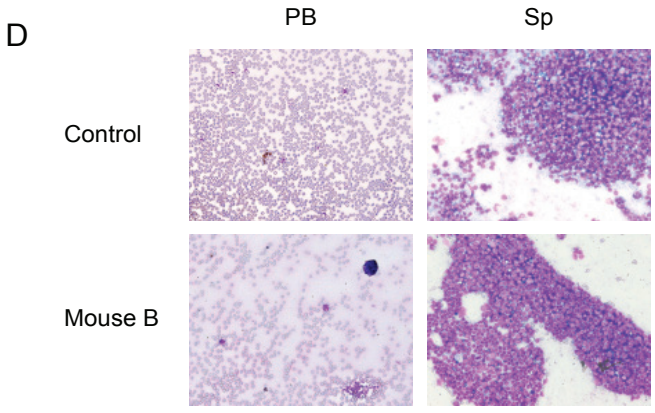

Supplementary Figure 2.S4. Clonality studies of leukemic mice

Southern Blot analyses of DNA extracted from BM cells of leukemic mice (Exp.1, low-dose recipients of T+12 culture cells) revealed multiple (~11) and identical retroviral genomic integrations, as opposed to their non-leukemic littermates [compare with low-dose recipients from Exp.1 in Fig.2.2B, or high-dose (Exp.3) in Suppl. Fig.2.S3B]. These mice received between 1 and 8 leukemic (L) CRU, present in culture at a frequency of 1/2500 cells, as estimated by the CRU assay at T+12 culture. This evokes the possibility of insertional mutagenesis as a mechanism underlying leukemic transformation.

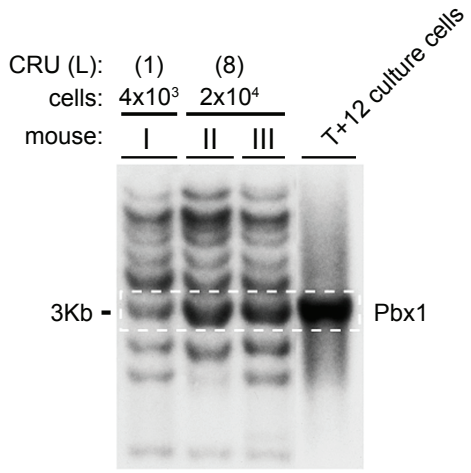

Table 2. S1. Clonal characteristics of hematopoietic clones in normal vs leukemic mice

	Normal mice #clones (#int/clone)	Leukemic mice #clones (#int/clone)
Exp.1	11 (1.5±0.5)	2 (11)
Exp.2	nd	nd
Exp.3	13 (2.6±1)	nd*

int: integrations; nd: not determined

Table 2.S2 List of primers used for Q-PCR reactions

GENES	OLIGO ID	TaqMan Assay ID	Primer A	Primer B	Probe
Ccnd2	T007		ATCTGTGGGCTTCAGCAGGATGAT	TTCAGCAGCAGAGCTTCGATTTGC	ATGTGGATTGTCTCAAAGCCTGCCAGGA
Ccnd3	T008		ATACTGGATGCTGGAGGTGTGTGA	AGCGATCCAGGTAGTTCATAGCCA	AGCAGCGCTGCGAGGAGGATGTCTT
Ccne2	T010		TCTGGAGGAATCAGCCCTTGCATT	TTGCCAAACCTCCTGTGAACATGC	TCCCTCACCTCTGCCAGATTTAAGCT
Cdkn1a	T022		TTGTCGCTGTCTTGCACTCTGGT	AGGGCCCTACCGTCCTACTAATTT	AAACGGAGGCAGACCAGCCTGACAGAAA
Cdkn1b	T023		AGAAATCTCTTCGGCCCGGTCAAT	GTCGAAATTCCACTTGCGCTGACT	AGAAGCACTGCCGGGATATGGAAGAA
Cdkn1c	T024		CGCGCAAACGTCTGAGATGAGTTA	AACCATCTCCGGTTCCTGCTACAT	TAGAGGCTAACGGCCAGAGAGAACTT
Cdkn2a	T025		TTCTTGGTGAAGTTCGTGCGATCC	TTGAGCAGAAGAGCTGCTACGTGA	TGCGCTCTGGCTTTCGTGAACATGTT
Cdkn2b	T026		ACCCTACCCAGTAAGACAAAGCCA	AGGGCCCGGGAACTTCATACAATA	TTTCTGCAGCTGGATCTGGTCCTTGA
Cdkn2c	T027		TGCGCTGCAGGTTATGAAACTTGG	AACATCAGCCTGGAACTCCAGCAA	TCATTCATGATGCTGCCAGAGCAGGT
Cdkn2d	T028		GCCTTGCAGGTCATGATGTTTGGA	AGTACCGGAGGCATCTTGGACATT	TGCTTTGGAGCTCCTGAAGCAAGGT
cMyc	TA076	Mm00487803_m1			
cMyb	TA081	Mm00501741_m1			
Hoxb4	TA084	Mm00657964_m1			
GAPDH		4352339E			

2.8 Acknowledgments

The authors acknowledge Amélie Faubert for her contribution to cell cycle and cell tracking studies. The constant help and support of Simon Girard and Nadine Mayotte was greatly appreciated. We also thank Mélanie Fréchette for her expertise and help with the maintenance and manipulation of the animals, Christian Charbonneau from the imagery plateform, Danièle Gagné from the flow cytometry platform, as well as Pierre Chagnon and Raphaelle Lambert from IRIC genomic platform for their expertise with quantitative RT-PCR. We would also acknowledge Dr. Trang Hoang for discussions and critical comments on the manuscript.

This work was supported by grants from the NIH to G.S., R.K.H. and Norman Iscove. S.C. was a recipient of a National Cancer Institute of Canada Post-MD Fellowship Award and now holds a CIHR Clinician-Scientist phase I Fellowship. G.S. holds a Canada Research Chair in Molecular Genetics of Stem Cells, and is a scholar of the Leukemia Lymphoma Society of America.

2.9 References

Allsopp, R. C., Cheshier, S., and Weissman, I. L. (2001). Telomere shortening accompanies increased cell cycle activity during serial transplantation of hematopoietic stem cells. J Exp Med *193*, 917-924.

Amsellem, S., Pflumio, F., Bardinet, D., Izac, B., Charneau, P., Romeo, P. H., Dubart-Kupperschmitt, A., and Fichelson, S. (2003). Ex vivo expansion of human hematopoietic stem cells by direct delivery of the HOXB4 homeoprotein. Nat Med *9*, 1423-1427.

Antonchuk, J., Sauvageau, G., and Humphries, R. K. (2002). HOXB4-induced expansion of adult hematopoietic stem cells ex vivo. Cell *109*, 39-45.

Arata, Y., Kouike, H., Zhang, Y., Herman, M. A., Okano, H., and Sawa, H. (2006). Wnt signaling and a Hox protein cooperatively regulate psa-3/Meis to determine daughter cell fate after asymmetric cell division in C. elegans. Dev Cell *11*, 105-115.

Azpiazu, N., and Morata, G. (1998). Functional and regulatory interactions between Hox and extradenticle genes. Genes Dev *12*, 261-273.

Berger, C., Pallavi, S. K., Prasad, M., Shashidhara, L. S., and Technau, G. M. (2005). A critical role for cyclin E in cell fate determination in the central nervous system of Drosophila melanogaster. Nat Cell Biol *7*, 56-62.

Beslu, N., Krosl, J., Laurin, M., Mayotte, N., Humphries, K. R., and Sauvageau, G. (2004). Molecular interactions involved in HOXB4-induced activation of HSC self-renewal. Blood *104*, 2307-2314.

Blank, U., Karlsson, G., Moody, J. L., Utsugisawa, T., Magnusson, M., Singbrant, S., Larsson, J., and Karlsson, S. (2006). Smad7 promotes self-renewal of hematopoietic stem cells in vivo. Blood.

Calegari, F., Haubensak, W., Haffner, C., and Huttner, W. B. (2005). Selective lengthening of the cell cycle in the neurogenic subpopulation of neural progenitor cells during mouse brain development. J Neurosci *25*, 6533-6538.

Cartwright, P., McLean, C., Sheppard, A., Rivett, D., Jones, K., and Dalton, S. (2005). LIF/STAT3 controls ES cell self-renewal and pluripotency by a Myc-dependent mechanism. Development *132*, 885-896.

Chang, C. P., Shen, W. F., Rozenfeld, S., Lawrence, H. J., Largman, C., and Cleary, M. L. (1995). Pbx proteins display hexapeptide-dependent cooperative DNA binding with a subset of Hox proteins. Genes Dev *9*, 663-674.

Cheng, T., Rodrigues, N., Dombkowski, D., Stier, S., and Scadden, D. T. (2000a). Stem cell repopulation efficiency but not pool size is governed by p27(kip1). Nat Med *6*, 1235-1240.

Cheng, T., Rodrigues, N., Shen, H., Yang, Y., Dombkowski, D., Sykes, M., and Scadden,

D. T. (2000b). Hematopoietic stem cell quiescence maintained by p21cip1/waf1. Science *287*, 1804-1808.

Conti, L., Pollard, S. M., Gorba, T., Reitano, E., Toselli, M., Biella, G., Sun, Y., Sanzone, S., Ying, Q. L., Cattaneo, E., and Smith, A. (2005). Niche-independent symmetrical self-renewal of a mammalian tissue stem cell. PLoS Biol *3*, e283.

Du, Y., Jenkins, N. A., and Copeland, N. G. (2005). Insertional mutagenesis identifies genes that promote the immortalization of primary bone marrow progenitor cells. Blood *106*, 3932-3939.

Dykstra, B., Ramunas, J., Kent, D., McCaffrey, L., Szumsky, E., Kelly, L., Farn, K., Blaylock, A., Eaves, C., and Jervis, E. (2006). High-resolution video monitoring of hematopoietic stem cells cultured in single-cell arrays identifies new features of self-renewal. Proc Natl Acad Sci U S A *103*, 8185-8190.

Gekas, C., Dieterlen-Lievre, F., Orkin, S. H., and Mikkola, H. K. (2005). The placenta is a niche for hematopoietic stem cells. Dev Cell *8*, 365-375.

Georgia, S., and Bhushan, A. (2006). p27 Regulates the Transition of {beta}-Cells From Quiescence to Proliferation. Diabetes *55*, 2950-2956.

Hock, H., Hamblen, M. J., Rooke, H. M., Schindler, J. W., Saleque, S., Fujiwara, Y., and Orkin, S. H. (2004). Gfi-1 restricts proliferation and preserves functional integrity of haematopoietic stem cells. Nature *431*, 1002-1007.

Iscove, N. N., and Nawa, K. (1997). Hematopoietic stem cells expand during serial transplantation in vivo without apparent exhaustion. Curr Biol *7*, 805-808.

Kamminga, L. M., Bystrykh, L. V., de Boer, A., Houwer, S., Douma, J., Weersing, E., Dontje, B., and de Haan, G. (2006). The Polycomb group gene Ezh2 prevents hematopoietic stem cell exhaustion. Blood *107*, 2170-2179.

Kim, J. Y., Sawada, A., Tokimasa, S., Endo, H., Ozono, K., Hara, J., and Takihara, Y. (2004). Defective long-term repopulating ability in hematopoietic stem cells lacking the Polycomb-group gene rae28. Eur J Haematol *73*, 75-84.

Knoepfler, P. S., Zhang, X. Y., Cheng, P. F., Gafken, P. R., McMahon, S. B., and Eisenman, R. N. (2006). Myc influences global chromatin structure. Embo J *25*, 2723-2734.

Krosl, J., Austin, P., Beslu, N., Kroon, E., Humphries, R. K., and Sauvageau, G. (2003a). In vitro expansion of hematopoietic stem cells by recombinant TAT-HOXB4 protein. Nat Med *9*, 1428-1432.

Krosl, J., Baban, S., Krosl, G., Rozenfeld, S., Largman, C., and Sauvageau, G. (1998). Cellular proliferation and transformation induced by HOXB4 and HOXB3 proteins involves cooperation with PBX1. Oncogene *16*, 3403-3412.

Krosl, J., Beslu, N., Mayotte, N., Humphries, R. K., and Sauvageau, G. (2003b). The

competitive nature of HOXB4-transduced HSC is limited by PBX1: the generation of ultra-competitive stem cells retaining full differentiation potential. Immunity *18*, 561-571.

Lyons, A. B., and Parish, C. R. (1994). Determination of lymphocyte division by flow cytometry. J Immunol Methods *171*, 131-137.

Maitra, A., Arking, D. E., Shivapurkar, N., Ikeda, M., Stastny, V., Kassauei, K., Sui, G., Cutler, D. J., Liu, Y., Brimble, S. N.*, et al.* (2005). Genomic alterations in cultured human embryonic stem cells. Nat Genet *37*, 1099-1103.

Medina-Martinez, O., and Ramirez-Solis, R. (2003). In vivo mutagenesis of the Hoxb8 hexapeptide domain leads to dominant homeotic transformations that mimic the loss-of-function mutations in genes of the Hoxb cluster. Dev Biol *264*, 77-90.

Miyake, N., Brun, A. C., Magnusson, M., Miyake, K., Scadden, D. T., and Karlsson, S. (2005). HOXB4-induced self-renewal of hematopoietic stem cells is significantly enhanced by p21 deficiency. Stem Cells.

Moore, K. A., and Lemischka, I. R. (2006). Stem cells and their niches. Science *311*, 1880-1885.

Notaro, R., Cimmino, A., Tabarini, D., Rotoli, B., and Luzzatto, L. (1997). In vivo telomere dynamics of human hematopoietic stem cells. Proc Natl Acad Sci U S A *94*, 13782-13785.

Nygren, J. M., Bryder, D., and Jacobsen, S. E. (2006). Prolonged cell cycle transit is a defining and developmentally conserved hemopoietic stem cell property. J Immunol *177*, 201-208.

Oostendorp, R. A., Audet, J., and Eaves, C. J. (2000). High-resolution tracking of cell division suggests similar cell cycle kinetics of hematopoietic stem cells stimulated in vitro and in vivo. Blood *95*, 855-862.

Pawliuk, R., Eaves, C., and Humphries, R. K. (1996). Evidence of both ontogeny and transplant dose-regulated expansion of hematopoietic stem cells in vivo. Blood *88*, 2852-2858.

Peters, S. O., Kittler, E. L., Ramshaw, H. S., and Quesenberry, P. J. (1996). Ex vivo expansion of murine marrow cells with interleukin-3 (IL-3), IL-6, IL-11, and stem cell factor leads to impaired engraftment in irradiated hosts. Blood *87*, 30-37.

Popperl, H., Bienz, M., Studer, M., Chan, S. K., Aparicio, S., Brenner, S., Mann, R. S., and Krumlauf, R. (1995). Segmental expression of Hoxb-1 is controlled by a highly conserved autoregulatory loop dependent upon exd/pbx. Cell *81*, 1031-1042.

Rao, S., and Orkin, S. H. (2006). Unraveling the transcriptional network controlling ES cell pluripotency. Genome Biol *7*, 230.

Sakamoto, H., Dai, G., Tsujino, K., Hashimoto, K., Huang, X., Fujimoto, T., Mucenski,

M., Frampton, J., and Ogawa, M. (2006). Proper levels of c-Myb are discretely defined at distinct steps of hematopoietic cell development. Blood *108*, 896-903.

Sarmento, L. M., Huang, H., Limon, A., Gordon, W., Fernandes, J., Tavares, M. J., Miele, L., Cardoso, A. A., Classon, M., and Carlesso, N. (2005). Notch1 modulates timing of G1-S progression by inducing SKP2 transcription and p27 Kip1 degradation. J Exp Med *202*, 157-168.

Sauvageau, G., Thorsteinsdottir, U., Eaves, C. J., Lawrence, H. J., Largman, C., Lansdorp, P. M., and Humphries, R. K. (1995). Overexpression of HOXB4 in hematopoietic cells causes the selective expansion of more primitive populations in vitro and in vivo. Genes Dev *9*, 1753-1765.

Schiedlmeier, B., Klump, H., Will, E., Arman-Kalcek, G., Li, Z., Wang, Z., Rimek, A., Friel, J., Baum, C., and Ostertag, W. (2003). High-level ectopic HOXB4 expression confers a profound in vivo competitive growth advantage on human cord blood CD34+ cells, but impairs lymphomyeloid differentiation. Blood *101*, 1759-1768.

Shinin, V., Gayraud-Morel, B., Gomes, D., and Tajbakhsh, S. (2006). Asymmetric division and cosegregation of template DNA strands in adult muscle satellite cells. Nat Cell Biol *8*, 677-687.

Sicinska, E., Lee, Y. M., Gits, J., Shigematsu, H., Yu, Q., Rebel, V. I., Geng, Y., Marshall, C. J., Akashi, K., Dorfman, D. M.*, et al.* (2006). Essential role for cyclin d3 in granulocyte colony-stimulating factor-driven expansion of neutrophil granulocytes. Mol Cell Biol *26*, 8052-8060.

Szilvassy, S. J., Humphries, R. K., Lansdorp, P. M., Eaves, A. C., and Eaves, C. J. (1990). Quantitative assay for totipotent reconstituting hematopoietic stem cells by a competitive repopulation strategy. Proc Natl Acad Sci U S A *87*, 8736-8740.

Thorsteinsdottir, U., Mamo, A., Kroon, E., Jerome, L., Bijl, J., Lawrence, H. J., Humphries, K., and Sauvageau, G. (2002). Overexpression of the myeloid leukemia-associated Hoxa9 gene in bone marrow cells induces stem cell expansion. Blood *99*, 121-129.

Thorsteinsdottir, U., Sauvageau, G., and Humphries, R. K. (1999). Enhanced in vivo regenerative potential of HOXB4-transduced hematopoietic stem cells with regulation of their pool size. Blood *94*, 2605-2612.

Uchida, N., Dykstra, B., Lyons, K. J., Leung, F. Y., and Eaves, C. J. (2003). Different in vivo repopulating activities of purified hematopoietic stem cells before and after being stimulated to divide in vitro with the same kinetics. Exp Hematol *31*, 1338-1347.

Vaziri, H., Dragowska, W., Allsopp, R. C., Thomas, T. E., Harley, C. B., and Lansdorp, P. M. (1994). Evidence for a mitotic clock in human hematopoietic stem cells: loss of telomeric DNA with age. Proc Natl Acad Sci U S A *91*, 9857-9860.

Walkley, C. R., Fero, M. L., Chien, W. M., Purton, L. E., and McArthur, G. A. (2005).

Negative cell-cycle regulators cooperatively control self-renewal and differentiation of haematopoietic stem cells. Nat Cell Biol *7*, 172-178.

Ying, Q. L., Nichols, J., Chambers, I., and Smith, A. (2003). BMP induction of Id proteins suppresses differentiation and sustains embryonic stem cell self-renewal in collaboration with STAT3. Cell *115*, 281-292.

Yu, H., Yuan, Y., Shen, H., and Cheng, T. (2006). Hematopoietic stem cell exhaustion impacted by p18 INK4C and p21 Cip1/Waf1 in opposite manners. Blood *107*, 1200-1206.

Yuan, Y., Shen, H., Franklin, D. S., Scadden, D. T., and Cheng, T. (2004). In vivo self-renewing divisions of haematopoietic stem cells are increased in the absence of the early G1-phase inhibitor, p18INK4C. Nat Cell Biol *6*, 436-442.

Zhang, J., Attar, E., Cohen, K., Crumpacker, C., and Scadden, D. (2005). Silencing p21(Waf1/Cip1/Sdi1) expression increases gene transduction efficiency in primitive human hematopoietic cells. Gene Ther *12*, 1444-1452.

3. An RNAi screen identifies Msi2 and Prox1 as having opposite roles in the regulation of hematopoietic stem cell activity

Hope KJ[1], Cellot S[1], Ting SB[1,3], MacRae T[1], Mayotte N[1], Iscove NN[2], Sauvageau G[1].

[1]Molecular Genetics of Stem Cells Laboratory, Institute of Research in Immunology and Cancer (IRIC), University of Montreal, Montreal, Quebec H3C 3J7, Canada.

[2]Ontario Cancer Institute, Princess Margaret Hospital, University Health Network, University of Toronto, Toronto Medical Discovery Tower, 101 College Street, Toronto, ON M5G 1L7, Canada

[3]Current address: Immune Signalling Laboratory, Cancer Immunology Research Division, and Department of Clinical Hematology, Peter MacCallum Cancer Centre, St. Andrews Place, East Melbourne, Victoria 3001, Australia

Corresponding Author:

Guy Sauvageau M.D., Ph.D.

Institut de Recherche en Immunologie et Cancérologie

C.P. 6128, succursale Centre-Ville, Montréal, Québec

Canada H3C 3J7

Telephone: (514) 343-7134

Facsimile: (514) 343-7379

E-mail: [redacted]

3.1 Contribution des co-auteurs

KJH, SC and GS planned and designed experiments. The selection of gene candidates was performed solely by KJH. KJH and SC performed all experiments. SC did not contribute to experiments pertaining to Figure 3.4D and 3.5C. SBT contributed to isolation of hematopoietic stem cells and to studies involving overexpression of Msi2. TM contributed to planning, execution and analysis of Q-RT-PCR, and to the cloning of shRNA constructs. NM contributed to cell culture and gene transduction. NNI contributed to semiquantitative RT-PCR assays (Figure 3.5C) and in manuscript revision. KJH, SC and GS contributed to manuscript preparation.

3.2 Summary

In this study, we describe an *in vivo* RNA interference functional genetics approach to evaluate the role of 20 different conserved polarity factors and fate determinants in mouse hematopoietic stem cell (HSC) activity. In total, this screen revealed 3 enhancers and 1 suppressor of HSC-derived reconstitution. *Pard6a*, *Prkcz* and *Msi2* shRNA-mediated depletion significantly impaired HSC repopulation. An *in vitro* promotion of differentiation was observed following the silencing of these genes, consistent with their function in regulating HSC self-renewal. Conversely, *Prox1* knockdown led to *in vivo* accumulation of primitive and differentiated cells. HSC activity was also enhanced *in vitro* when *Prox1* levels were experimentally reduced, identifying it as a potential antagonist of self-renewal. HSC engineered to overexpress *Msi2* or *Prox1* showed the reverse phenotype to those transduced with corresponding shRNA vectors. Gene expression profiling studies identified a number of known HSC and cell cycle regulators as potential downstream targets to *Msi2* and *Prox1*.

3.3 Introduction

A detailed understanding of the molecular machinery that controls hematopoietic stem cell (HSC) self-renewal is critical for the development of novel regenerative therapies and treatments aimed at reigning in leukemic stem cells (LSC). While great strides have been made toward a molecular understanding of self-renewal in ES cells, it has proven more challenging to pinpoint the genes directing this process in HSCs. Insight into the regulatory mechanisms of HSC self-renewal may be provided by examining its mode of division. During homeostasis, for example, the HSC must divide in such a way as to maintain its numbers while also producing all required mature cells.

In other stem cell systems including those of *Drosophila melanogaster* and *Caenorhabditis elegans,* where stem cells can be unambiguously identified as well as spatially located within their endogenous niche, the maintenance of appropriate numbers of primitive cells and diverse downstream cell types is known to occur through conserved mechanisms of asymmetric cell division (ACD). As such, ACDs represent one of the critical mechanisms of self-renewal regulation in these systems. One mode of ACD relies on signaling from a specialized niche to maintain the primitive cell state of only the daughter cell directly in contact with it (Knoblich, 2008). Alternatively, an ACD can occur by the initial polarization of the primitive mother cell followed by the asymmetric segregation and acquisition of intracellular fate determinants upon division (Knoblich, 2008). In this case, the loss or mutation of specific determinants normally acquired by the stem cell results in a depletion of stem cell numbers and the accumulation of differentiated cell types. Conversely, both daughter cells will maintain the stem cell state in situations where determinants of differentiation are depleted. Indeed, a connection between the maintenance of asymmetric divisions and tumour suppression has recently been provided in the fly system. In one example, depletion of any of 4 such determinants (*lgl*, *mira*, *prospero*, *brat*) in the *Drosophila* larval neuroblast (NB) leads to predominantly symmetric self-renewal divisions such that both daughter cells behave like NBs whose unchecked self-renewal often leads to the formation of larval brain tumours (Betschinger et al., 2006; Bilder, 2004; Lee et al., 2006).

Although it is generally assumed that HSCs undergo asymmetric self-renewal divisions in order to facilitate the balance between primitive and differentiated cells at steady state, it has been difficult to conclusively validate this as the exclusive mode of division largely due to the absence of an antigen that unambiguously distinguishes HSCs from their immediate more committed daughter cells. Several groups have shown that single hematopoietic progenitor cells (HPCs) cultured *in vitro* can give rise to daughters with different *in vitro* potentials/fates (Beckmann et al., 2007; Brummendorf et al., 1998; Ema et al., 2000; Punzel et al., 2002; Takano et al., 2004). While these results are consistent with the expected outcome of an ACD, asymmetric fates could also have been post-mitotically imposed following an initially symmetric division. More recently, the Reya group

has utilized the approach of time lapse imaging to track individual HPCs during division (Wu et al., 2007). They made use of an EGFP transgene under the control of activated Notch to first demonstrate that, at a population level, expression of GFP on cells in culture corresponded with their primitive potential *in vivo*. By relying on decreased GFP expression as an indicator of differentiation, they were able to correlate differential cell fate of paired daughter cells in culture with the asymmetric acquisition of the Numb protein, a known ACD determinant in other cell types (Cayouette and Raff, 2002). Nonetheless, this study did not address the functional importance of the numb determinant in these cells and therefore could not conclude whether its presence or absence was a cause or consequence of differential fate specification.

Due to the aforementioned difficulty in specifically pinpointing HSCs in culture, it remains difficult to rely solely on visualization of primitive hematopoietic cell divisions to determine whether a polarization and segregation of specific cell fate determinants underlies the asymmetric/symmetric self-renewal of these cells. The existence of markers that unequivocally define leukemic stem cells (LSC) are also lacking, making it equally as challenging to use this strategy in isolation to assess whether deregulation of fate determinants could contribute to the pathogenesis of hematopoietic malignancies by disrupting the balance between self-renewal and differentiation. As has been done for ACD determinants in other systems, we opted instead to utilize a functional approach that explores the consequences of the downregulation of potentially critical fate determinants in HSCs. Specifically, we developed a functional genetics approach taking advantage of systematic RNAi to interrogate the HSC-specific function of polarity proteins and cell fate determinants implicated in the ACD of other stem cell model systems. Using this strategy we identified 3 genes essential for proper HSC function and 1 gene as an HSC antagonist.

3.4 Experimental Procedures

Construction of shRNA retroviral vectors. For each gene target (see Table 3. S1), 2-3 shRNAs were designed as single stranded oligonucleotides also incorporating mir-30 flanking arms using the RNAi Central shRNA design tool at **http://katahdin.cshl.org:9331/RNAi_web/scripts/main2.pl**. See Supplemental Experimental Procedures for additional details.

Mice. (C57Bl/6J-Ly5.2 x C3H/HeJ) F1 recipient mice and (C57Bl/6J-Ly5.1 Pep3b x C3H/HeJ) F1 congenic donor mice were bred in a specific pathogen-free animal facility.

Bone marrow cell culture, retroviral infection and transplantation. Generation of retrovirus-producing GP+E-86 cells was performed as previously described (Krosl et al., 2003). These cells were seeded in 96-well plates such that a single ecotropic pseudotyped retrovirus was produced per well. See Supplemental Experimental Procedures for details.

Evaluation of donor–derived reconstitution and immunophenotyping. At intervals 50 µl blood samples obtained from tail vein puncture were incubated with excess ammonium chloride (StemCell Technologies, BC, Canada) to lyse erythrocytes. Cells were then analyzed by flow cytometry as detailed in the Supplemental Experimental Procedures.

Competitive repopulating unit (CRU) assay. CRU assays were carried out to quantify the number of HSCs present either after a 7 day *in vitro* incubation or within the grafts of primary mice transplanted 30 weeks earlier with day 0 transduced cells. Both cultured cells and freshly harvested bone marrow were subjected to flow cytometry to determine GFP% and Ly5.1%. For each sample, a range of cell doses was transplanted into 2-5 sub-lethally irradiated (800 cGy, ^{137}Cs gamma radiation) C57Bl/6J-Ly5.2 recipients along with $1.0x10^5$ congenic Ly5.2 competitor cells. The level of Ly5.1 reconstitution was evaluated 12 weeks (primary bone marrow cells) or 14-16 weeks later (day 7 cells) by flow cytometric assessment of peripheral blood (see Evaluation of donor-derived reconstitution and immunophenotyping section). Recipients with ≥1% myelo-lymphoid donor-derived cells were considered to be repopulated by at least 1 CRU. Assessment of the frequency of CRUs in each sample was carried out by applying Poisson statistics to the proportion of negative mice at different dilutions.

Progenitor assays. Cells were harvested from culture at various time points (day 0 or days 6-9) and plated in 1% methylcellulose diluted with DMEM and supplemented with

10% FBS, 5.7% bovine serum albumin (BSA), 2mM glutamine, 200μg/mL transferrin, 10^{-4}M β-mercaptoethanol, 10 ng IL-3, 10ng/mL IL-6, 50ng/mL SF and 5U/mL erythropoietin (EPO). GFP+ and GFP- progenitors were enumerated and scored 7-9 days later. Pictures of colonies were taken on a Leica fluorescence microscope.

Microarray hybridization and analyses. Following infection of HSC-enriched cells with shRNAs (as outlined) cells were kept in culture for a period of 8 days. After trizol extraction, 10 μg of RNA was reversed transcribed using SuperScript Double-Stranded cDNA Synthesis Kit (Invitrogen) according to the manufacturer's instructions. For the control (shLuciferase) samples, 1 μg of purified cDNA was labeled with Cy5-labeled 9mers (Trilink technologies) using 3'-5' exo- Klenow fragment (NEB), while the test (shProx1) samples were labeled with Cy3-labeled 9mers. Two-colour hybridizations on NimbleGen 385K eukaryotic expression arrays were carried out using 6 μg of Cy5-labeled control and 6 μg of Cy3-labeled test cDNA using the NimbleGen hybridization kit as recommended by the manufacturer. Arrays were scanned at 5 μm resolution using a GenePix4000B scanner (Molecular Devices). Data from scanned images were extracted using NimbleScan 2.5 extraction software (NimbleGen Systems, Inc.) and analysed using Genespring .GX version 7.3

Statistical tests. The significance of differences was determined by a one-tailed Student's t test.

3.5 Results

Selection of Candidate Genes

A list of 71 candidates involved in different aspects of polarity establishment and cell fate specification was assembled through a literature review of model organisms and subsequent documented expression in stem cell and leukemia databases (Faubert et al., 2004) (Ting SB *et al*., in preparation). The selection of a smaller subset of these genes was facilitated by Q-RT-PCR evaluation of the expression level of each candidate in a subset of murine bone marrow highly enriched for HSCs (Ting SB *et al*., in preparation). Genes were ranked based on their level of expression and the reproducibility of this expression over multiple experiments. Based on this data, 20 of the most highly expressed genes which had not previously been reported in loss of function studies were selected for downregulation (Table 3. S1)

Design of the primary screen

For the primary screening approach depicted in Figure 3.3. 1a, a total of 2 to 3 shRNAs were designed per gene and subsequently introduced into a retroviral vector encoding GFP to permit tracking of transduced cells *in vivo*. HSC-enriched $Lin^{-}150^{+}48^{-}$ cells (representing ~60 functional long-term repopulating HSC (LTR-HSC) or competitive repopulation units (CRU)) were infected over 5 days by co-culture with the retroviral producer cells in an arrayed 96-well format, i.e. 1 shRNA per well. This infection protocol was optimized to yield an average of 59% gene transfer (Figure 3.S1). Directly following infection, the *in vivo* reconstituting potential of $1/4^{th}$ of each well was evaluated through duplicate competitive repopulating assays involving the co-transplantation of 1.5×10^5 congenic bone marrow competitor cells into irradiated recipients. HSC activity was next monitored by flow cytometric evaluation of the extent of GFP^{+} cells in the peripheral blood sampled at early (4 and 8 weeks) and late (16-20 weeks) post-transplant time points. The screen made use of the principle that when two distinctly marked but functionally equivalent HSC populations are co-transplanted, their resultant grafts will be present at levels directly proportional to their input numbers.

Primary screen and validation

In preliminary studies with a control shRNA vector (i.e., shLuciferase), we found that it is critical to take into account the initial gene transfer efficiency in order to accurately identify shRNAs that positively or negatively impact on LTR-HSC activity (Figure 3.S1). Based on these results, we excluded experiments in which shRNA gene transfer were below 25% and, in each case, repeated the given shRNA transduction until results were achieved with higher level transduction. Moreover, we had to adapt our selection criteria

to maximize the identification of hits in experiments where gene transfer was between 25-75% (see Figure 3.1b, left panel) from those where it exceeded this value (above 75%: Figure 3.1b, right panel). Indeed, at the 20 week time point in the primary screen, significant fluctuations from the initial ratio of infected to non-infected cells were detectable when gene transductions ranged from 25-75% (Figure 3.S1b, see dotted red and green lines in left panel of Figure 3.1b). In contrast, this ratio remained much more stable in experiments where higher gene transfer (>75%) was achieved, necessitating the measurement of GFP as a percentage of the total peripheral blood (Figure 3.S1b, see dotted green line in Figure 3.1c). Based on these two distinct sets of criteria adjusted for the differences in gene transfer (summarized in Supplemental experimental procedures), we found that 12 shRNAs were associated with a perturbation in LTR-HSC activity (see * in Figure 3.1b right and left panels). Ten of these 12 shRNAs, namely 3-shPard6a, 1-shMapre3, 2-shCtnna1, 1-shMsi2, 1-shLgl1, 1-shNumb, 2-shNumb, 2-shPard6a, 3-shMapre3 and 1-shPrkcz appeared to antagonize LTR-HSC repopulation activity. The remaining 2 shRNAs, 2-shProx1 and 3-shProx1 were associated with increased levels of repopulation. In total, these 12 hits targeted 8 different genes with *Numb*, *Mapre3* and *Prox1* each identified by 2 different shRNA sequences (Figure 3.1d).

To confirm that the observed effects of each shRNA hit were specific to knockdown of the target transcript we first examined the residual mRNA levels. Flow sorted GFP^+ cells were harvested directly from the remaining material within wells used for transplantation. Importantly, for 8 of the 12 shRNAs, transcripts were reduced from 60 to 7% the levels present in either the corresponding GFP^- fraction or in GFP^+ cells from shLuciferase control wells (Figure 3.1c). The remaining shRNAs, directed against the *Mapre3*, *Lgl1* and *Ctnna1* genes, were removed from further consideration as they induced little to no appreciable knockdown suggesting that their ability to decrease reconstitution may have been the result of off-target effects. Each shRNA hit was also retested in at least two independent validation experiments which resulted in the further elimination of hairpins against 2 additional genes (*Num*b and *Anapc5*) as their effects were not reproducible (data not shown). It is important to note that this lack of reproducibility is not an artifact of insufficient shRNA levels since gene transduction was in every case above 65%. We next tested if the genes that were eliminated from further study were effectively knocked down by at least one of the shRNA sequences. The results from these experiments show that of 8 excluded genes tested, 7 were targeted by one or more hairpins with at least a 40% knockdown efficiency, signifying an overall low frequency of false negatives for the primary screen (Figure 3.S1c).

In summary, the primary screen and subsequent validation tests identified 4 hairpins to *Msi2*, *Pard6a* and *Prkcz* as candidate suppressors and 2 additional shRNAs to *Prox1* as potential enhancers of LTR-HSC activity.

Msi2, Par6a and Prkcz positively regulate HSC activity

In independent experiments, cells infected with the control shRNA to luciferase were stably maintained to 20 weeks while few to no remaining cells with shRNAs against the candidate positive regulators were present at the end of the transplant (Figure 3.2a-b). Moreover, at least two unique and effective (>45% knockdown) shRNAs, directed against *Msi2*, *Pard6a* and *Prkcz* were consistently able to substantially reduce and in some cases completely eliminate transduced cells from the donor graft (Figure 3.2b and Figure 3.S2). Importantly, for *Msi2* we were also able to generate shRNA constructs which gave a graded reduction in transcript levels. We show that at the 16 week time point post-transplant, the decrease in repopulation mediated by these is directly proportional to the level of *Msi2* transcript knockdown (Figure 3.2c). Together, these results demonstrate that the observed loss in transduced cell-mediated reconstitution is specific to target transcript loss and is not due to off-target effects.

Although the direct promotion of HSC commitment and differentiation would accurately explain the shRNA-induced defects in repopulation, these results could be accounted for by a number of alternate mechanisms; effects on downstream progenitor cells, increased apoptosis, altered cell cycle properties, or an inability to properly home to the bone marrow following intravenous transplantation. We explored each of these possibilities in turn. It should be noted that while we present below results of these experiments with one hairpin against each gene, similar results were observed in each case with a second, independent shRNA (data not shown).

Colony forming assays established immediately following the infection period indicated that the total colony output of GFP^+ shRNA-transduced cells was the same as their untransduced counterparts and matched that of shluciferase transduced cells (Figure 3.2d). Colonies generated by $shRNA^+$ cells also showed no alteration in size with respect to controls. Moreover, control levels of high proliferative potential (HPP) colonies were also observed upon candidate knockdown, indicating the proliferative capacity of progenitors was maintained (Figure 3.2d). In all cases there was no significant skewing in the lineages of shRNA-infected progenitors when colonies were scored by type (Figure 3.2e). These results show that proliferation and differentiation of myeloid and erythroid progenitors are unaffected by knockdown of the candidate genes.

Following a 10-12 day culture period, reduction of *Msi2*, *Prkcz* and less significantly *Pard6a*, induced a greater proportion of differentiated myeloid cells as measured by both size and granularity as well as presence of the antigens Gr-1 and CD11b, in comparison to control shLuciferase cultures (Figure 3.2f, left and middle). In accordance with this apparent skewing towards differentiation in culture, progenitor numbers were also decreased in shRNA transduced cells relative to controls at this time point (Figure 3.2f, right). Despite their presence at low levels, mature cells of both the B and T lineage

were also detectable in the bone marrow and thymus within residual RNAi grafts with knockdown of any of the three hits (data not shown). Together these data indicate that shRNA-infected lymphomyeloid progenitors are able to successfully differentiate into mature downstream cell types and further suggests that knockdown of *Msi2*, *Pard6a* and *Prkcz* enhances the production of mature cells at the expense of progenitors.

Hoechst staining carried out immediately following the infection of $Lin^{-}CD150^{+}48^{-}$ cells indicated that silencing of *Msi2*, *Pard6a* or *Prkcz* elicited no change in the cell cycle profiles of gated $Sca\text{-}1^{+}Gr\text{-}1^{-}$ cells when compared to those of control cultures. Similarly, no abnormalities were observed when cell cycle analysis was carried out on the bulk population of shRNA-transduced cells after an additional 5 days of culture (data not shown). In addition, for all candidate shRNAs as assessed by Annexin V staining, there was no increase in apoptosis in the transduced cell population either in comparison to non-transduced counterparts or shluciferase transduced controls (Figure 3.S3a).

To test for a potential shRNA-induced defect in homing capacity we transplanted 5-FU bone marrow cells infected with hairpins to each candidate positive regulator. Twenty-four hours post-transplant, homing efficiency was determined by evaluating the total number of donor GFP^{+} cells as well as the number of donor GFP^{-} and GFP^{+} colony-forming cells present in the bone marrow. This analysis indicated that knockdown of the candidates did not impair the absolute homing efficiency of bulk transduced cells (Figure 3. S3c) nor did it inhibit the ability of GFP^{+} CFCs or more primitive HPPs to transit to the bone marrow (Figure 3.2g and Figure 3.S3b). Cumulatively, these experiments serve to demonstrate that the GFP^{+} graft depletion observed with shRNA hits is not the result of overt inhibitory effects on progenitor cells, alteration of the cell cycle, promotion of cell death or homing to the bone marrow.

In line with the above data and in further support of a role for these factors in the regulation of very primitive cells, we observed in almost all cases a modest graft at the 4-6 week time point that was progressively depleted over time. Such transitory repopulation is consistent with early contribution by short-lived progenitors followed by the gradual loss of donor cells due to a lack of LTR-HSCs that would normally provide the reserve to supply stable donor hematopoiesis (Adolfsson et al., 2001; Christensen and Weissman, 2001; Zhao et al., 2000). This, in combination with an increased propensity towards *in vitro* differentiation following their knockdown, suggests that *Msi2*, *Pard6a* and *Prkcz* could directly alter HSC or primitive cell fate choices towards more commitment/differentiation decisions, however, *in vivo* studies including direct measurements of LTR-HSC cycle status and apoptosis levels will be important in conclusively validating this potential mechanism.

In vivo HSC self-renewal is increased upon Prox1 knockdown

To confirm the positive effects of *Prox1* knockdown on donor repopulation and to characterize the reconstitution kinetics, we carried out several independent experiments examining the contribution of shProx1 transduced cells to the recipient peripheral blood at multiple time points post-transplant. With 2-shProx1, which achieves more than 80% knockdown, we observed in all cases a steady increase in both the percentage of GFP^+ cells within the $Ly5.1^+$ graft as well as the GFP% within the peripheral blood. At the 20 week end-point, peripheral blood sampling showed GFP^+ cells comprised the majority of the graft, representing a proportional 1.6-fold increase over the %GFP on the day of transplant. In contrast, control transduced GFP^+ cells exhibited a slight decrease over time and at the transplant endpoint comprised approximately 50% less of the total peripheral blood than did $shProx1^+$ cells (Figure 3.3a,b and data not shown). Similar results were observed with a second independent shRNA (3-shProx1, Figure 3.S4b). Importantly, *in vivo* knockdown is restricted to the GFP^+ as compared to GFP^- donor cells when assessed at 35 weeks post-transplant, indicating that GFP expression is not silenced and continues to reliably mark shRNA transduced cells in mice at late transplant time points (Figure 3.3b right).

Despite the progressive accumulation of shProx1 infected cells, we observed no block in the differentiative capacity of these cells. The GFP^+ portion of donor grafts appeared to be multilineage in nature, with mature erythroid, myeloid, B and T lymphoid cells observed in similar proportions as shluciferase controls in the blood, bone marrow and thymus (Figure 3.3c and data not shown). Surprisingly, however, we found that the phenotypically primitive compartment of *Prox1* shRNA grafts was significantly expanded. The expression of CD150, Sca-1 and c-kit combined with an absence of surface CD48 and lineage antigens has been shown to be reliable in discriminating HSCs from more committed cell types in repopulated recipients (Yilmaz et al., 2006). When tested for by flow cytometric evaluation of recipient bone marrow, the shRNA transduced GFP^+ fraction of $CD45.1^+$ donor grafts exhibited a 4-fold expansion of this compartment. In contrast, shluciferase controls had a similar proportion of these primitive cells in both the GFP^- and GFP^+ fractions (Figure 3.3d,e). Preliminary secondary transplantations of BM harvested from single shLuciferase and shProx1 primary mice at limiting dilution indicated that *Prox1* knockdown gives an in vivo fold expansion of repopulating cells 118x that of control transduced cells (data not shown). These results are consistent with the concept that the elevated levels of phenotypic HSCs following *Prox1* RNAi is due to enhanced in vivo HSC self-renewal, however, conclusive validation of this hypothesis will require more detailed quantitative studies.

Prox1 RNAi enhances HSC activity *in vitro*

The observed increase in HSC numbers *in vivo* by *Prox1* knockdown prompted us to explore the possibility that reduction of *Prox1* could also expand primitive cells *in vitro*.

To address this we kept cells in culture for an additional seven days following the infection period. At this point, we observed an accumulation of shProx1^{+} cells that appear primitive or blast-like in nature, a finding similar to that seen following overexpression of the potent HSC expanding NupHD fusion protein or other agonists of HSC self-renewal (Deneault et al., 2009). In contrast, shLuciferase control cultures were comprised of predominantly more mature and differentiated myeloid cells (Figure 3.4a). A similar assessment of primitiveness through immunophenotyping showed *Prox1* knockdown increased the proportion of Lin^{-}Sca-1^{+} cells in D7-12 cultures (18.0 ± 1.7% for 3-shProx1 versus 9.0 ± 1.1% for shLuciferase controls, Figure 3.4a). Similar results were also observed for 2-shProx1 (data not shown).

To directly test the *in vivo* output of *Prox1* shRNA-transduced cells, we transplanted 1/8th of the contents of 7-day 96-well cultures in competition with 1.5x10^{5} congenic bone marrow cells. Strikingly, we observed that the engraftment level was consistently and significantly enhanced with *Prox1* knockdown cells relative to control shRNAs. It is important to note that in these experiments the percent gene transfer for shProx1 was significantly lower than for shLuciferase controls (63.0% vs 92.0%, Figure 3.4b). We therefore normalized the %GFP cells in the peripheral blood to the amount of input GFP^{+} shluciferase cells to provide a better estimate of the actual difference in repopulating ability of shProx1^{+} cells in relation to controls. In fact, in relation to shLuciferase, *Prox1* knockdown cells exhibit an impressive 5.1x more GFP^{+} cells per input GFP^{+} cell (data not shown). We then made use of the Mean Activity of Stem cell (MAS) calculation, described by Ema and Nakauchi, to quantify the proliferative output per input LTR-HSC, taking into account the initial difference in gene transfer (Ema and Nakauchi, 2000). In fact, decreased levels of *Prox1*by 2-shProx1 and 3-shProx1 mediated a remarkable 9.1 and 5.6-fold higher MAS respectively, than controls, values similar to that achieved by cultured HOXB4 overexpressing cells (Figure 3.4b).

We next quantified the actual HSC output mediated by *Prox1* silencing through *in vivo* limiting dilution analyses. These results indicated that RNAi against the *Prox1* gene yields a 6.9x greater frequency of HSC per equivalent proportion of control wells and a 5.2x greater frequency of HSCs per total cells (Figure 3.4c, Table 3. S4). Interestingly, cells infected with either 2-shProx1 or 3-shProx1 do exhibit a slight increase in the proportion of cells in S and G2/M *in vitro* (Figure 3.4d and data not shown), however as the frequency of HSCs also increase as a percentage of total cells in these cultures as compared to controls, we conclude that HSC expansion must be due in part to altered fate decisions toward more HSC renewal divisions.

Candidate gene expression in primitive hematopoietic cell subsets

Given the potent effects of each hit on primitive hematopoietic cells, we wanted to explore the possibility that they were expressed differentially within these cell types. We

addressed this by carrying out both quantitative and semi-quantitative RT-PCR on HSC subsets, progenitors and more committed subsets.

The existence of a distinct intermediate term repopulating or ITR-HSC has recently been described which is distinguished from LTR-HSC by the fact that its multilineage grafts exhaust by 20-24 weeks post-transplant (Benveniste et al., 2003; Benveniste et al., 2010; Dykstra et al., 2007; Kent et al., 2009; Kiel et al., 2005). *Msi2* levels as measured by Q-RT-PCR are found to be highest in both LTR- and ITR-HSCs and significantly lower in multipotent progenitors (MPP) (Figure 3.5a, left). It should be noted that similar patterns of expression were seen with *Prox1, Pard6a* and *Prkcz* however expression levels were not as high and the differential expression between these subsets was not as pronounced (Figure 3.S5a).

If *Msi2* expression could be considered specific to more primitive hematopoietic cells, its transcript levels might also be expected to increase in cultures of symmetrically expanding HSCs such as those initiated following NupHD overexpression. Indeed we observed a reproducible 3.5x increase in *Msi2* expression in NupHD cells in comparison to controls (Figure 3.5b). The *Msi2* paralogue *Msi1*, has documented roles in the maintenance of a variety of different stem cells types (Okano et al., 2005), however we observed that it was expressed at extremely low to undetectable levels in primitive hematopoietic cells and was neither detected in shLuciferase cultures nor upregulated in NupHD overexpressing cells (data not shown).

In addition, semi-quantitative RT-PCR *Msi2* expression analyses in the cycling and non-cycling LTR- and ITR-HSC subsets of 11 independent experiments show that it is predominantly expressed in LTR- versus ITR-HSC regardless of the cycle status, however, some experiments exhibited variable differential expression between these subsets. We have also documented the relative expression of *Msi2* in more committed and very transiently reconstituting STR-HSC and MPP populations where it is reduced in comparison to LTR- and ITR-HSC subsets. Its expression is further decreased in committed and mature cell types (with the exception of BFU-Es and to some extent B and T cells). Similar analyses of both *Pard6a* and *Prkcz* in these same cell subsets also shows that the expression profile of these two is similarly low in STR-HSC and MPP populations and higher in LTR- and ITR-HSC subsets, while *Prkcz* becomes expressed at higher levels again as cells reach maturity (Figure 3.S5b). We speculate that the observed lower expression of the identified hits in more committed stem and progenitor types could indicate a decreased dependence on these genes for proper functioning of these cell types, a concept which is consistent with their maintenance despite the shRNA-mediated silencing of these genes.

Modulation of gene expression by *Msi2* and *Prox1*

We next characterized the expression levels of a panel of candidate target genes following both *Msi2* knockdown and overexpression in HSC-enriched populations. These results showed that modulation of *Msi2* levels has an effect on the expression of regulators im-

plicated in HSC self-renewal and cycling. In particular, we found that in response to *Msi2* overexpression, the self-renewal agonists *HoxA9* and *HoxA10* were significantly elevated as were the Sonic hedgehog and Notch signalling effectors, *Gli1* and *Hes1*. Similarly *Cyclin D1* and *Cdk2* were upregulated and *p19*, *p16* and *p21* exhibited a parallel decrease. Importantly, some of these genes showed the opposite expression profile following *Msi2* knockdown.

These findings suggested that *Msi2* may in fact contribute to enhanced HSC activity when overexpressed. This hypothesis was confirmed in a subsequent experiment in which HSCs were engineered, by retroviral gene transfer, to overexpress *Msi2* then cultured as described (Deneault et al., 2009) or using a similar scaled-up approach (see Methods). Upon analysis, we found that the 16-week post-transplant repopulation levels of *Msi2* overexpressing HSCs were indeed significantly higher than controls (Fig. 5e).

For *Prox1* we carried out similar overexpression experiments and found that cells engineered to express high levels of this gene are lost in short-term cultures (at day 0, 5% versus 25% live, immature cells remain for *Prox1* overexpression versus vector-alone). The small number of cells obtainable from these experiments precluded gene expression analysis.

Using HSC-enriched populations infected with shRNA vectors to *Prox1* as described above, we obtained sufficient material to carry out microarray-based global gene expression profiling. In total, 86 genes were greater than 2-fold upregulated following *Prox1* knockdown while another 96 genes were 2-fold downregulated when compared to shLuciferase-transduced control cells (Table 3. S5). Q-RT-PCR expression studies performed on 29 genes verified the differential expression of 14/19 upregulated and 3/10 downregulated transcripts, respectively (Figure 3.5f). Interestingly, expression of several known markers of HSCs (*Esam1*, *Jag2*, *Vwf* and *Aldh1a2*) was elevated following *Prox1* knockdown (Hess et al., 2004; Palmqvist et al., 2007, Kent, 2009 #72; Yokota et al., 2009). Other genes normally detected on mature myeloid cells (*Cfh* and *Msr1*) or inhibitory to progenitor proliferation and survival (*RhoE*) were downregulated (Gu et al., 2005; Inada et al., 1983; Krieger et al., 1993).

3.6 Discussion

We report here the completion of an RNAi screen that rigorously tested for and identified both negative and positive HSC regulators from within an initial candidate list of genes chosen for their conserved roles in polarity and asymmetric cell division. In determining these genes, initial shRNA hits from a primary RNAi screen were subjected to thorough validation tests. In total, we identified 4 bona fide novel regulators from a list of 20 of such genes verified to be expressed in primitive hematopoietic subsets. This 20% hit rate further substantiates the success and validity of our approach and highlights the previously unappreciated role that such genes may have in regulating HSC activity.

Specifically, we demonstrate that *Msi2*, *Pard6a* and *Prkcz* are critical positive regulators of hematopoietic repopulation as knockdown of each transcript dramatically impaired late transplant reconstitutions. We show that in all three cases, this effect is mediated at the level of primitive hematopoietic cells and is not due to negative effects on progenitor cells, elevated apoptosis, alterations in the cell cycle or homing defects. The increased propensity for transduced primitive HSCs/HPCs to commit, as evidenced by the premature differentiation that occurs following their *in vitr*o culture, is suggestive that the observed repopulation defects may be due, at least in part, to a shift towards differentiation as opposed to self-renewal decisions.

Pard6a is one of 4 mammalian pard6 proteins that are homologues of the *Caenorhabditis elegans* PARD6 gene, originally identified in this organism for its importance, in conjunction with other partition defective or par proteins in specifying polarity of the early embryo (Watts et al., 1996). Since the discovery of their importance in this process, the PAR proteins have been shown to be involved in virtually all biological processes that require establishment of polarity. Mammalian Pard6 and Pard3 can co-exist in a complex also containing atypical protein kinase C (aPKC) and cdc42 (Joberty et al., 2000; Lin et al., 2000). It is particularly striking that given their close association and interdependence in other settings, our screen identified both *Pard6a* and *Prkcz* (one of 2 mammalian homologues of *aPKC*) as necessary for the maintenance of HSCs. This finding would further suggest that Pard6a and Prkcz may maintain their conserved association with one another in hematopoietic cells. Whether the significant reduction in HSC numbers upon *Pard6a* or *Prkcz* depletion is due to the loss of their normal asymmetrical polarization remains to be determined. Support for the concept that Prkcz does indeed polarize asymmetrically in mammalian hematopoietic ACDs was recently provided by Chang et al. 2007, who showed that during T cell division, Prkcz is asymmetrically concentrated at the cell pole opposite the immunological synapse (Chang et al., 2007). Our study demonstrates the critical importance of these two conserved proteins in the maintenance of HSCs and provides the impetus to further explore their roles in potentially regulating the polarity of these cells.

Msi2 is one of two mammalian members of the conserved Musashi family of RNP-type RNA binding proteins, originally identified as critical for the ACD of the drosophila sensory organ precursor and more recently shown to be essential to germline stem cell identity (Nakamura et al., 1994; Siddall et al., 2006). In the mammalian setting, *Msi1* has been identified as a putative marker of both intestinal and breast stem cells (Clarke et al., 2005; Kayahara et al., 2003; Potten et al., 2003). As well as being highly expressed in CNS stem cells, *Msi1* and *Msi2* appear to have a critical and compensatory role in the maintenance of these cells (Sakakibara et al., 2002). Our study shows that this does not appear to be the case in the hematopoietic system as *Msi1* transcripts are barely detectable in hematopoietic cells including the same HSC-enriched subpopulations in which *Msi2* is present at high levels. Neither did we detect *Msi1* expression in HSCs expanded by NupHD overexpression while *Msi2* levels in contrast were significantly elevated. Importantly, we have shown that *Msi2* is predominantly expressed in highly purified LTR and ITR-HSC subsets. We suggest that this narrow profile of expression, combined with a similarly elevated transcript level in HSCs expanded in culture, indicates that *Msi2* represents a novel functional marker of primitive HSCs. In combination with our functional data, further demonstrating the necessity of *Msi2* in the maintenance of these HSCs and illustrating the enhanced stem cell activity imposed by its overexpression, we therefore propose that Msi2 is a regulator of the self-renewal process in stem cells of the hematopoietic system. The elevated expression of a number of known stem cell agonists and indicators of Notch and Sonic Hedgehog signalling following *Msi2* overexpression provide important insight into the mechanisms by which it carries out this regulation. It is particularly significant that we found the Notch effector *Hes1* among these genes given that others have shown that Msi1 binds the 3'UTR of the Notch inhibitor *Numb*, mediating its translational repression, thereby enhancing Notch signalling (Imai et al., 2001; Okano et al., 2002).

As well as identifying novel positive HSC regulators, the RNAi screen also elucidated shRNAs to *Prox1*, which led to reproducible and significant accumulation of transduced cells *in vivo*. Phenotypic and functional assays confirmed an enhanced expansion of the HSC compartment within shProx1^{+} grafts. This expanded pool of HSCs could explain the increased competitiveness of shProx1 GFP^{+} cells. Importantly, the ability of *Prox1* knockdown to modulate self-renewal versus differentiation decisions was not restricted to the *in vivo* case. Consistent with a conserved role in the promotion of differentiation at the expense of stem cell maintenance *Prox1,* an atypical homeodomain containing transcription factor, has been shown to be involved in promoting the differentiation of progenitor cells in a variety of lineage contexts (Dyer, 2003; Risebro et al., 2009; Wigle et al., 1999; Wigle et al., 2002). Our results are consistent with a conserved role for *Prox1* in the promotion of differentiation at the expense of stem cell maintenance. In the fly, protein and transcript for the Prox1 homologue prospero is present in both the NB stem cell and its GMC daughter, however, its nuclear localization only within the GMC acts

to repress stem cell and cell cycle genes and upregulate differentiation promoting genes facilitating loss of stemness (Choksi et al., 2006). It will now be of interest to explore the localization of the Prox1 protein itself during hematopoietic stem and progenitor cell division to elucidate whether a differential localization could also underlie its functions in hematopoiesis. Importantly, we do observe transcriptional changes upon *Prox1* knock-down which are consistent with it initiating a program of enhanced proliferation and primitive cell self-renewal.

While significant efforts have been put into the dissection of the molecular regulation of HSC self-renewal, the identification of critical determinants has been modest. In this context, it is particularly intriguing that by focusing on a class of genes historically over-looked as important regulators of HSC biology, we have identified 4 important determi-nants of HSC behaviour. Our findings have important implications for our understanding of HSC biology as, given their known roles in polarity and/or asymmetric cell division, it is likely the genes we have identified point to a previously unappreciated role for these particular mechanisms in mediating HSC fate decisions. As such, future work examin-ing the specific function of these factors in primitive hematopoietic cell polarization or as asymmetrically segregating determinants will be essential.

Determinants which regulate HSC self-renewal may also represent critical targets in the onset and/or propagation of hematopoietic malignancies. Along these lines, Msi2 has been identified as a translocation partner to in several cases of chronic and acute myeloid leukemias (Barbouti et al., 2003; De Weer et al., 2008) while Prox1 reduction or mutation has also been described in a number of primary leukemia samples and cell lines (Nagai et al., 2003). It will therefore be interesting to explore whether misregulation of these genes, which are critical in normal HSC regulation, also have roles in the biology of leukemic stem cells.

3.7 Figures

Figure 3.1. Identification of polarity proteins and fate determinants that regulate hematopoietic repopulation. a. Experimental design of primary screen and validation steps. b. Primary screen results at 20 weeks post-transplant. For constructs which achieved a gene transfer of 25-75% (left panel), significant loss or accumulation of transduced cells was determined by normalizing the percent of GFP^+ cells within the donor peripheral blood graft at 20 weeks to the corresponding percent GFP at day 0. Upper and lower thresholds were established as the mean ± 1.5 standard deviations determined from multiple experiments with shLuciferase controls transduced over the 25-75% range (see Figure 3.S1b, Supplementary experimental methods). In cases where gene transfer was >75% (right panel), values are shown as the percent GFP of the total peripheral blood. The mean from multiple shLuciferase experiments was 54% (black line) with a lower threshold value at 1.5 SD shown by the dashed line (see Figure 3.S1b, Supplementary text). Cases with gene transfer ratios between 65-75% were manually inspected for increases in output/input GFP ratios also occurring with at least one other independent shRNA. c. Q-RT-PCR assessment of relative transcript levels remaining in GFP^+ cells sorted at day0-day1 from 2-3 independent experiments. ShRNAs achieving less than 40% transcript knockdown were eliminated from further study. Data is presented as mean ± SEM d. Summary of the results of the primary and validation screens from candidate selection to final hit confirmation. * indicate hits that fall above or below cutoffs.

Figure 3.1

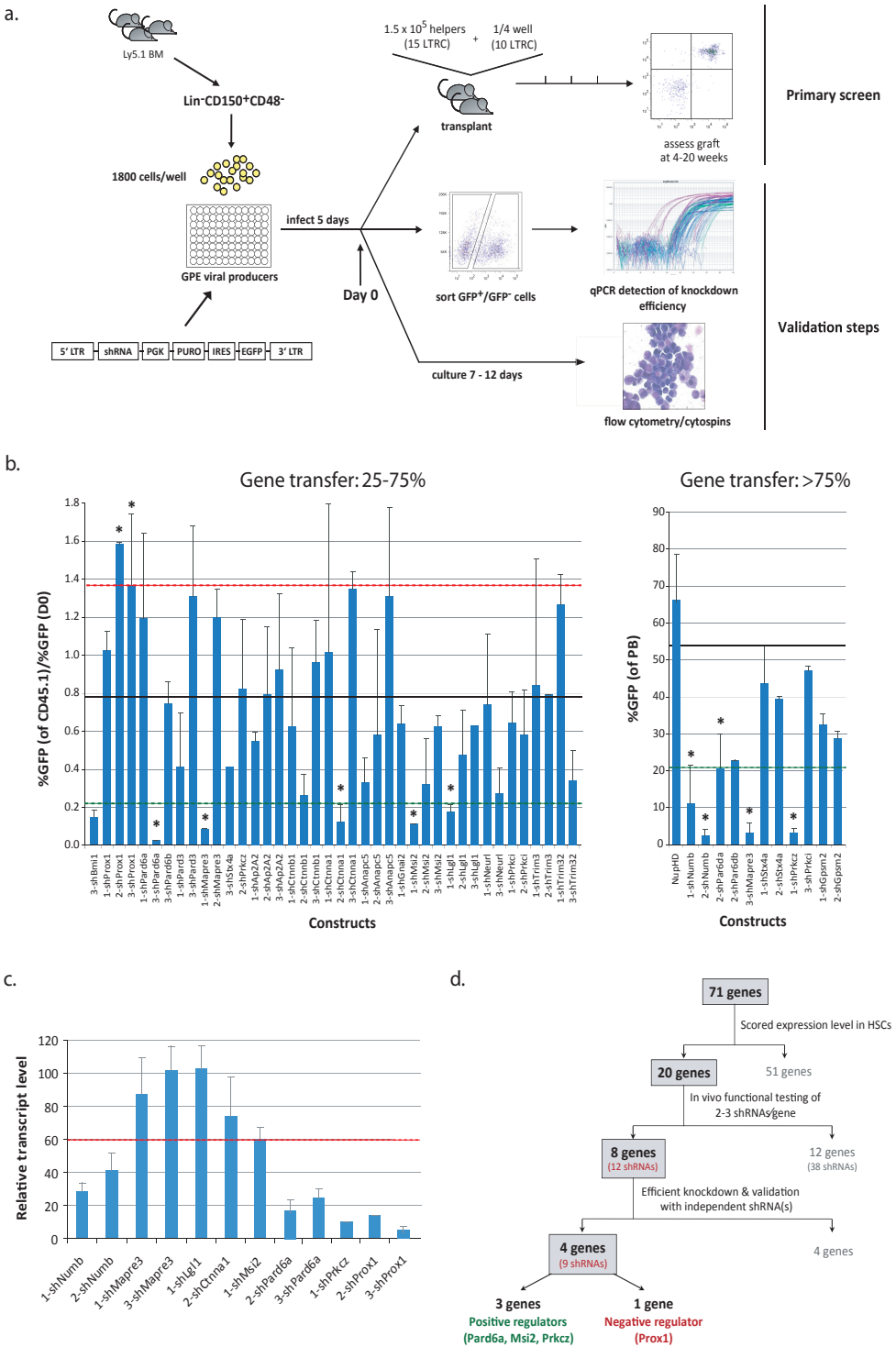
a.
Ly5.1 BM
Lin-CD150+CD48-
1800 cells/well
infect 5 days
GPE viral producers
5' LTR
shRNA
PGK
PURO
IRES
EGFP
3' LTR
Day 0
1.5 x 10^5 helpers (15 LTRC)
1/4 well (10 LTRC)
transplant
assess graft at 4-20 weeks
Primary screen
sort GFP+/GFP- cells
qPCR detection of knockdown efficiency
culture 7 - 12 days
flow cytometry/cytospins
Validation steps
b.
Gene transfer: 25-75%
%GFP (of CD45.1)/%GFP (D0)
Constructs
Gene transfer: >75%
%GFP (of PB)
Constructs
c.
Relative transcript level
1-shNumb
2-shNumb
1-shMapre3
3-shMapre3
1-shIgl1
2-shCtcna1
1-shMsi2
2-shPard6a
3-shPard6a
1-shPrkcz
2-shProx1
3-shProx1
d.
71 genes
Scored expression level in HSCs
20 genes
51 genes
In vivo functional testing of 2-3 shRNAs/gene
8 genes
(12 shRNAs)
12 genes
(38 shRNAs)
Efficient knockdown & validation with independent shRNA(s)
4 genes
(9 shRNAs)
4 genes
3 genes
Positive regulators
(Pard6a, Msi2, Prkcz)
1 gene
Negative regulator
(Prox1)

Figure 3.2. Characterizing the nature of repopulation impairment by *Msi2*, *Pard6a* and *Prkcz* shRNAs. a. Flow cytometric analysis of peripheral blood sampled from representative recipients of shLuciferase and shMsi2 transduced cells at 4 (middle) and 20 (right) weeks post-transplant. Gene transfer percentages assessed immediately following infection (D0) are also shown (left). b. Quantitative assessment of shRNA-induced defects in repopulation. shMsi2 and shPar6a results (49 and 51% gene transduction respectively) results are displayed as a ratio of the GFP% within the donor graft (at the indicated time point) to the GFP% at D0. Results for shRNAs to *Prkcz* are presented as %GFP of total peripheral blood as initial GFP% at D0 were consistently above 80%. (6-shMsi2, n=5; 3-shPar6a, n=6; 1-shPrkcz, n=4; 3 experiments each for 6-shMsi2 and 3-shPard6a, 2 experiments for 1-shPrkcz). In each case, the cumulative effect of each hairpin was tested against at least 6 mice transplanted with shLuciferase transduced cells that were infected to similar levels on D0. c. Evaluation of repopulation following graded levels of *Msi2* knockdown. Q-RT-PCR evaluation of *Msi2* knockdown by 4 separate shRNAs (left). At 20 weeks post-transplant, repopulation (shown at right) decreased in direct proportion to knockdown levels (2-shMsi2, n=6; 1-shMsi2, n=5; 4-shMsi2, n=5; 6-shMsi2, n=5, except for 4-sh-Msi2 (2 experiments), results are shown from 3 separate experiments). d. Bright field (left-upper panels) and fluorescence images (left-lower panels) of typical high proliferative potential (HPP) shLuciferase and shMsi2 GFP^+ colonies (left panels). Colony forming activity of GFP^+ transduced cells plated immediately following infection (right). (n=2 for each dataset). e. Lineage distribution of colonies generated by shRNA transduced progenitors (n=2-4). f. Morphology of representative shLuciferase and shMsi2 transduced cells following a 10-day culture period (left). Flow cytometric evaluation of the percentage of cells positive for the differentiation antigen Gr-1 (middle) (n=3-10 for each shRNA). Day 10 CFC output of GFP^+ cells right) (n=3-8 for each shRNA). g. Bone marrow homing efficiency of GFP^+ shRNA transduced progenitors at 24 hours post-transplant. Results are presented as the proportion of GFP^+ colonies recovered from recipient bone marrow relative to the %GFP colonies input. Values for d, f and g are represented as mean ± SEM. Total CFC output in d and f is shown as relative to corresponding untransduced cells. * indicate p values below 0.05.

Figure 3.2

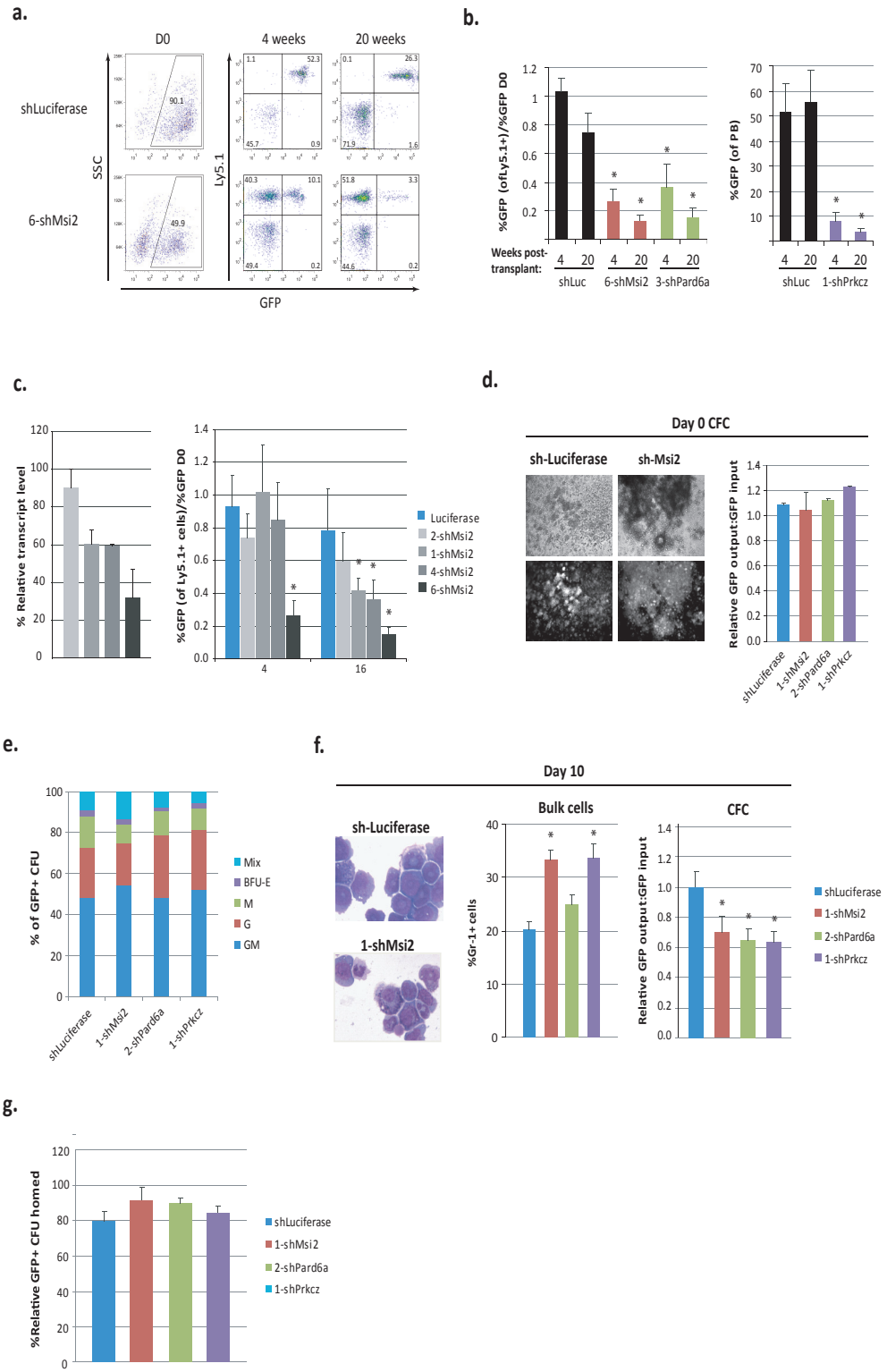
a.
D0
4 weeks
20 weeks
shLuciferase
6-shMsi2
SSC
Ly5.1
GFP
b.
%GFP (ofLy5.1+)/%GFP D0
Weeks post-transplant:
shLuc
6-shMsi2
3-shPard6a
%GFP (of PB)
1-shPrkcz
c.
% Relative transcript level
%GFP (of Ly5.1+ cells)/%GFP D0
Luciferase
2-shMsi2
1-shMsi2
4-shMsi2
6-shMsi2
d.
Day 0 CFC
sh-Luciferase
sh-Msi2
Relative GFP output:GFP input
shLuciferase
1-shMsi2
2-shPard6a
1-shPrkcz
e.
% of GFP+ CFU
Mix
BFU-E
M
G
GM
f.
Day 10
sh-Luciferase
1-shMsi2
Bulk cells
%Gr-1+ cells
CFC
Relative GFP output:GFP input
g.
%Relative GFP+ CFU homed

Figure 3.3. Evaluation of the role of *Prox1* in regulating HSC numbers *in vivo*. a. Representative flow cytometric analysis of donor reconstitution in recipients of shLuciferase and 2-shProx1 transduced cells at 4 (middle) and 20 (right) weeks post-transplant. D0 transduction efficiencies for each shRNA are also shown (left). b. Quantitative assessment of *Prox1* shRNA-induced enhancement in repopulation (left). Results are shown in comparison to shLuciferase controls transduced over a similar range. (Data is summarized from 4 independent experiments: shLuciferase, n=17; 2-shProx1, n=7). Evaluation of knockdown in donor GFP^+ and GFP^- cells taken from two mice transplanted with 2-shProx1 transduced cells 35-weeks prior is shown at right. c. Percentages of donor GFP^+ cells expressing B220, Gr-1 and CD3 in peripheral blood at 25-40 weeks post-transplant. d. Flow cytometry plots depicting the level of $CD150^+Sca^+kit^+$ as a percentage of Lin^-CD48^- cells from GFP^+ or GFP^- bone marrow of representative recipients at 25 weeks post-transplant (left). e. Cumulative results illustrate the elevated percentage of $Lin^-CD150^+CD48^-Sca^+kit^+$ cells within shProx1 GFP^+ grafts as compared to GFP^+ shLuciferase grafts or GFP^- cells. (shLuciferase GFP^+, n=3; GFP^-, n=12; 2-shProx1 GFP^+, n=2; 3-shProx1, n=4). Values are represented as mean ± SEM. * $p < 0.05$.

Figure 3.3

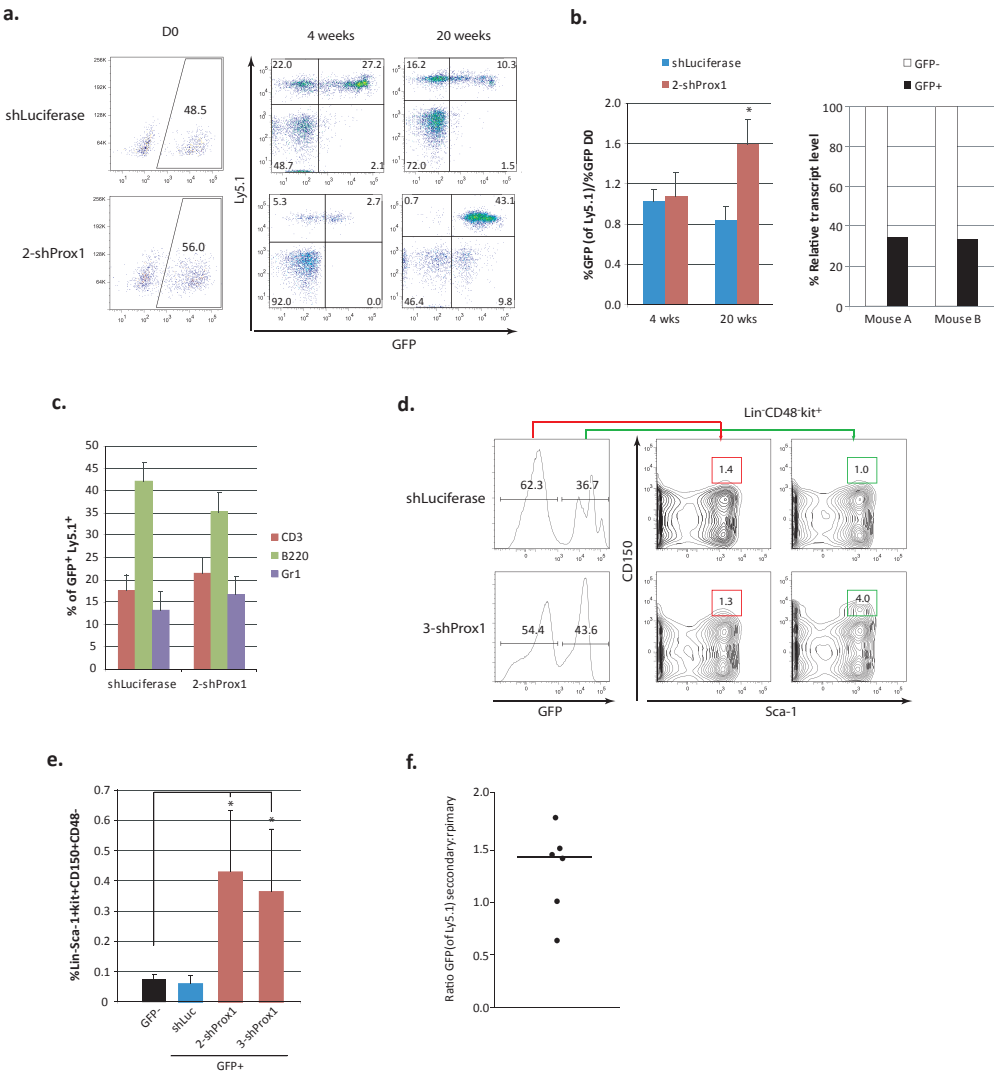
a.
D0
4 weeks
20 weeks
shLuciferase
2-shProx1
48.5
56.0
22.0
27.2
48.7
2.1
16.2
10.3
72.0
1.5
5.3
2.7
92.0
0.0
0.7
43.1
46.4
9.8
Ly5.1
GFP
b.
shLuciferase
2-shProx1
%GFP (of Ly5.1)/%GFP D0
4 wks
20 wks
GFP-
GFP+
% Relative transcript level
Mouse A
Mouse B
c.
% of GFP+ Ly5.1+
CD3
B220
Gr1
shLuciferase
2-shProx1
d.
Lin-CD48-kit+
shLuciferase
3-shProx1
62.3
36.7
54.4
43.6
1.4
1.0
1.3
4.0
CD150
GFP
Sca-1
e.
%Lin-Sca-1+kit+CD150+CD48-
GFP-
shLuc
2-shProx1
3-shProx1
GFP+
f.
Ratio GFP(of Ly5.1) seccondary:primary

Figure 3.4. Determining the potential for *Prox1* downregulation to induce *in vitro* HSC expansion. a. Morphological examination of transduced cells cultured for 7-10 days following infection with NupHD or shRNAs directed against *Prox1* or *Luciferase*. Flow cytometric evaluation of the percentage of Gr-1^{-}Sca^{+} cells within the transduced population of 7-10 day cultures (bottom right) (shLuciferase, n=5; 3-shProx1, n=5). b. Assessment of the *in vivo* repopulation contribution by 1/8th the contents of 7-day shProx1 or control shRNA 96-well cultures. Results are presented as the mean %GFP within the recipient peripheral blood at the indicated time points and are representative of data from n=8, 6 and 3 mice for shLuc, 2-shProx1 and 3-shProx1 respectively (2 separate experiments for shLuc and 2-shProx1). Mean activity of stem cells (MAS) values calculated as outlined in Methods (Bone marrow cell culture, retroviral infection and transplantation section). (shLuciferase, n=8; 2-shProx1, n=6; 3-shProx1, n=3; HOXB4, n=3). c. Limiting dilution analysis of the HSC frequency in 7-day cultured 2-shProx1, shLuciferase and HOXB4 cells. HSC frequencies are displayed beside the corresponding curve. d. Cell cycle analysis of GFP^{+} cells infected with shRNAs to *Prox1* or *Luciferase* after 5 days of culture. Representative profiles are shown on the left while the quantitative assessment of the percentage of cells at different phases of the cell cycle is depicted on the right (shLuciferase, n=3; 3-shProx1, n=4; NupHD, n=3). Data is shown as mean ± SEM. * indicate p values below 0.05.

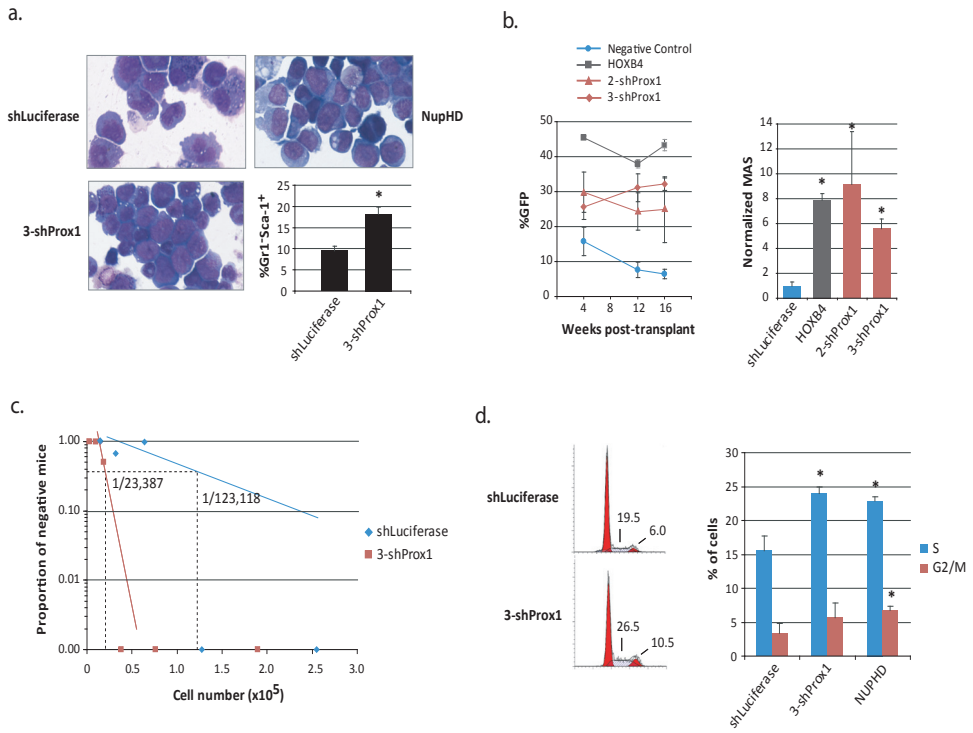

Figure 3.5. Endogenous expression of *Msi2* and effects on gene expression following their *Msi2* or *Prox1* modulation. a. Q-RT-PCR analysis of *Msi2* in the indicated stem and progenitor fractions isolated from two separate sorts. *Msi2* levels were normalized to *Gapdh*. b. Q-RT-PCR evaluation of the expression level of *Msi2* in control and Nup-PHD-overexpressing cells following 10 days of culture. c. Semi-quantitative RT-PCR assessment of *Msi2* transcript levels in the hematopoietic lineage hierarchy. Corresponding *Gapdh* levels are shown in Figure 3.S5. d. Q-RT-PCR evaluation of expression changes of candidate target genes following *Msi2* overexpression (left) and knockdown (right). e. Assessment of *in vivo* repopulation contribution by equivalent proportions of day-7 cultures initiated with HSCs overexpressing *Msi2* or infected with control empty vector (MSCV). Results are presented as the mean %Ly5.1^{+} cells within the recipient peripheral blood at the indicated time points and are representative of data from 7 mice per condition. f. Q-RT-PCR validation of the differential expression of targets, identified by microarray as being altered 2-fold in expression following *Prox1* knockdown. In d and f, dashed green and red lines indicate 2-fold greater or decreased expression relative to control MSCV (overexpression experiments) or shLuciferase (knockdown experiments) transduced cells respectively. * indicate p values below 0.05.

Figure 3.5

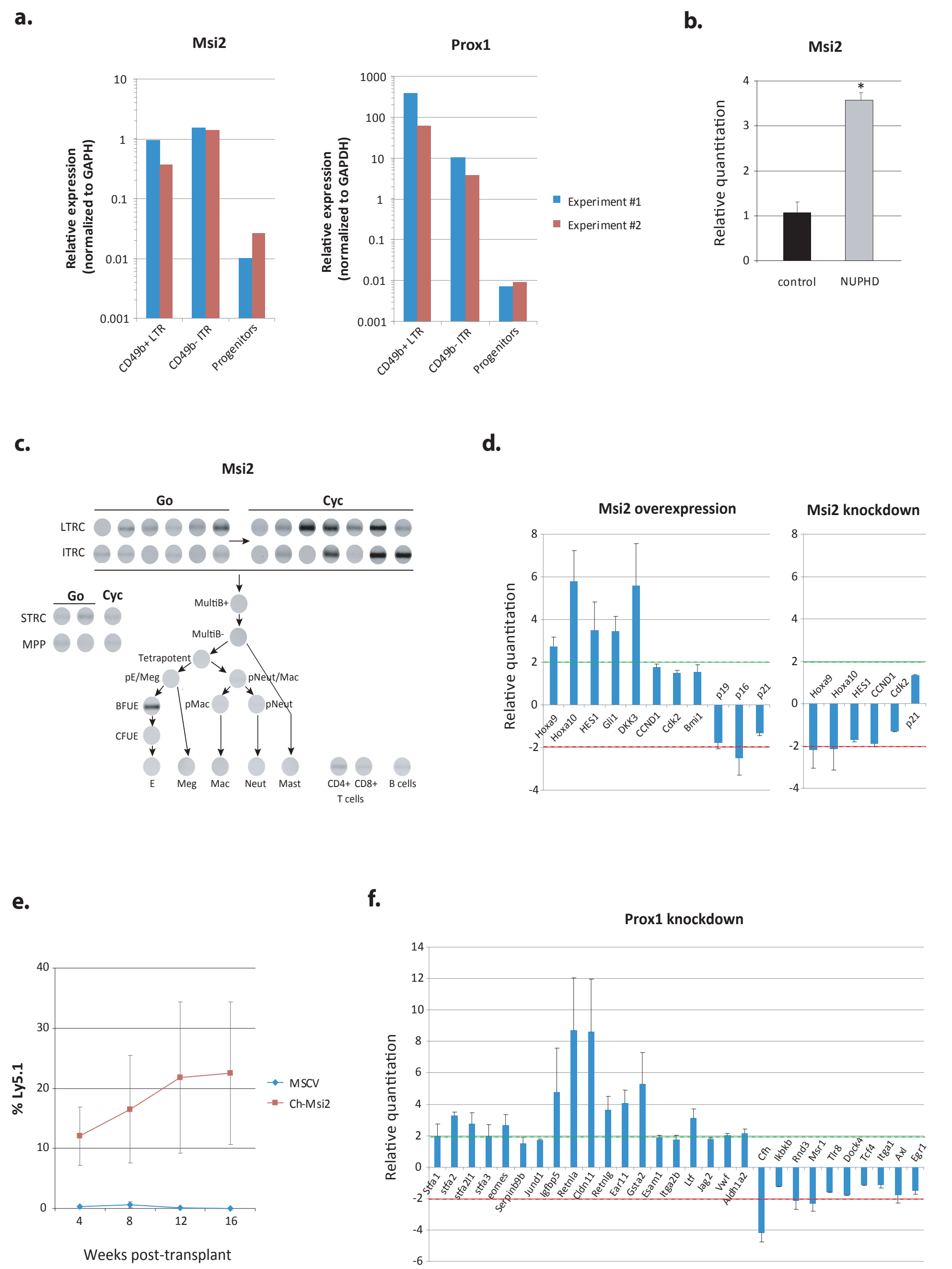
a.
Msi2
Prox1
Relative expression (normalized to GAPH)
Relative expression (normalized to GAPDH)
CD49b+ LTR
CD49b- ITR
Progenitors
Experiment #1
Experiment #2
b.
Msi2
Relative quantitation
control
NUPHD
c.
Msi2
Go
Cyc
LTRC
ITRC
STRC
MPP
MultiB+
MultiB-
Tetrapotent
pE/Meg
pNeut/Mac
BFUE
pMac
pNeut
CFUE
E
Meg
Mac
Neut
Mast
CD4+ CD8+
T cells
B cells
d.
Msi2 overexpression
Msi2 knockdown
Relative quantitation
Hoxa9
Hoxa10
HES1
Gli1
DKK3
CCND1
Cdk2
Bmi1
p19
p16
p21
e.
% Ly5.1
MSCV
Ch-Msi2
Weeks post-transplant
f.
Prox1 knockdown
Relative quantitation
Sfa1
sfa2
sfa2l1
sfa3
eomes
Serpinb9b
Jund1
Igfbp5
Retnla
Cldn11
Retnlg
Ear11
Gsta2
Esam1
Itga2b
Ltf
Jag2
Vwf
Aldh1a2
Cfh
Ikbkb
Rnd3
Msr1
Tlr8
Dock4
Tcf4
Itga1
Axl
Egr1

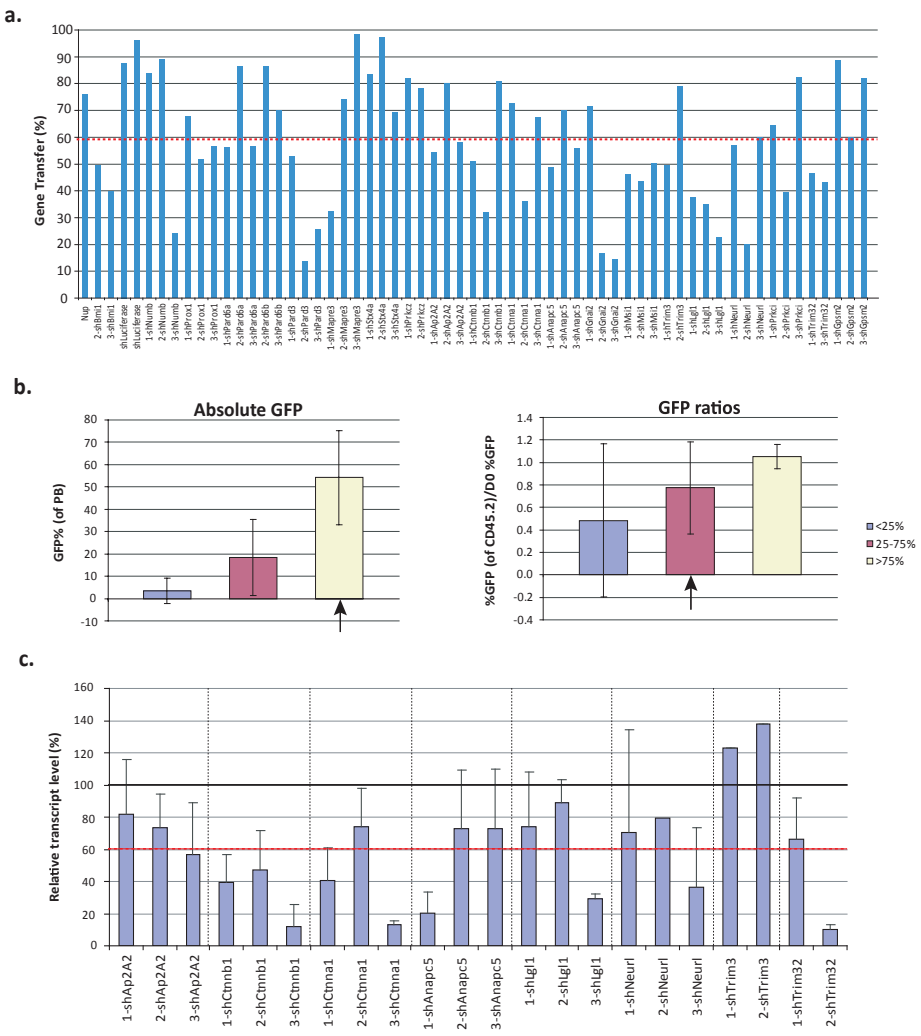

Figure 3.S1: Optimization of primary screen parameters. a. Gene transfer efficiency. Range of retroviral gene transfer efficiencies as determined by flow cytometry on the day of transplantation (day 0). Mean indicated by dashed line. **b. Establishing the control range of GFP+ repopulation at various gene transfer efficiencies**. HSCs were infected with shLuciferase at a range of gene transfers (from 16% - 96%, with each gene transfer in between differing by approximately 5%). All data shown was obtained by flow cytometric assessment of peripheral blood at 20 weeks post-transplant. The percentage of GFP+ cells is indicated in the left panel. At right, GFP+ contribution is measured as a ratio of the %GFP+ cells in the donor CD45.1 graft to the day 0 GFP percentage. Values shown are mean ± SD. (<25%, n=8; 26-75%, n=21, >75%, n=7). Arrows indicate the method of GFP measurement utilized to define hits in the screen when gene transfers were >75% (left panel) and 25-75% (right panel). **c. Assessment of transcript knockdown for eliminated genes**. For a subset of genes that did not fall above or below the established cutoffs we performed qRT-PCR evaluation of transcript levels at day 0 with all shRNAs (2-3) directed against each gene. Dashed line represents a threshold of 40% knockdown. Of 8 genes tested, only trim3 (targeted in the screen by 2 shRNAs) was not targeted by at least one shRNA giving the threshold level of transcript reduction.

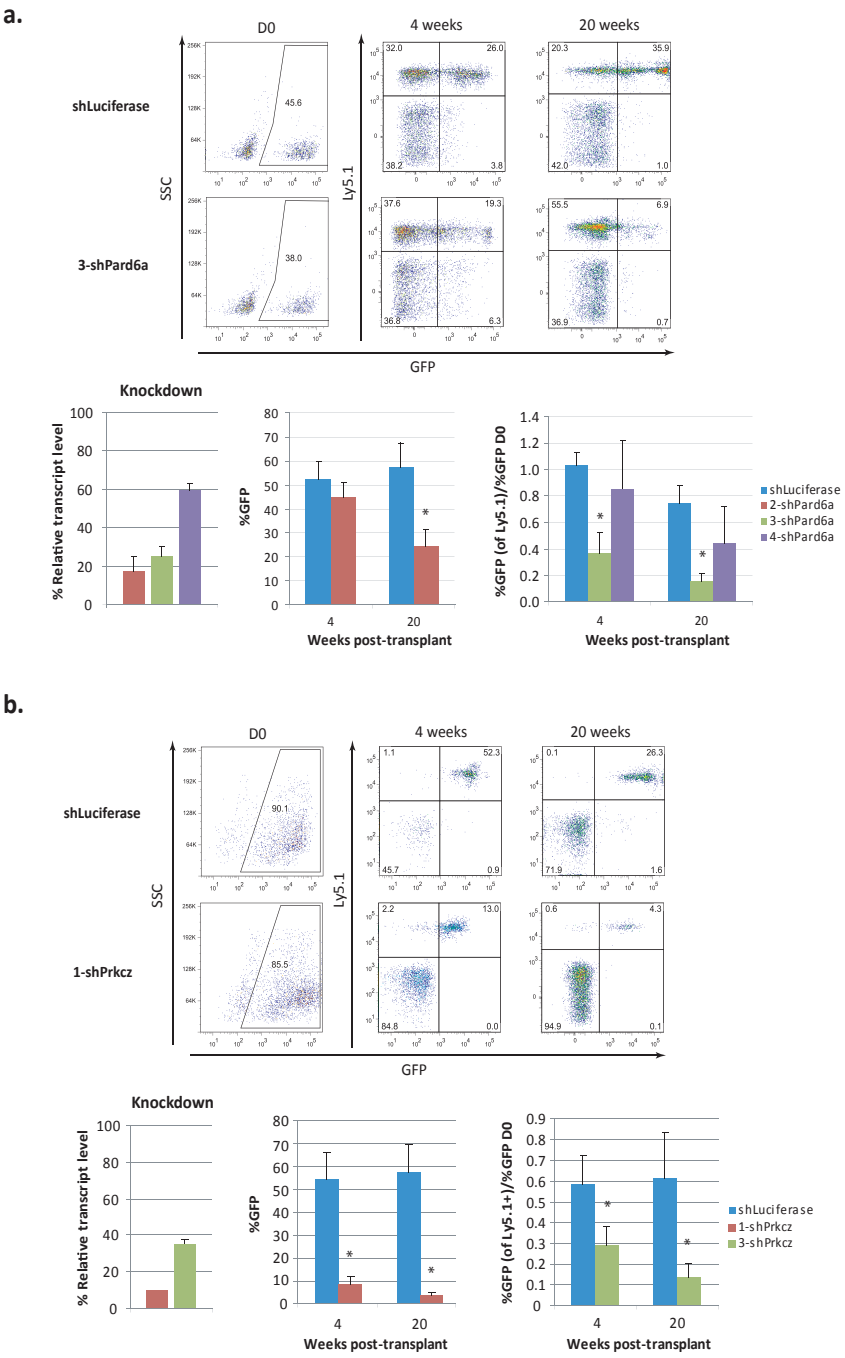

Figure 3.S2: Confirmation of Pard6a and Prkcz shRNA specificity. a, b. Assessment of shRNA-induced defects in repopulation using independent hairpins against Pard6a (**a**) and Prkcz (**b**). Representative flow plots immediately following infection and at 4 and 20 weeks post-transplant are shown in upper panels. Knockdown is shown in lower left panels alongside cumulative repopulation results (lower middle and lower right panels) in comparison to shLuciferase controls transduced over a similar range. Values shown are mean ± SEM (shLuciferase, n≥4; 2-shPard6a, n=5; 3-shPard6a, n=6; 4-shPard6a, n=3; 1-shPrkcz , n=4; 3-shPrkcz, n=3) * p=0.05.

a.

	AnnexinV$^+$ cells	
Sample	**% of GFP$^+$**	**% of GFP$^-$**
shLuciferase	3.0	8.6
shMsi2 A	2.9	4.8
shMsi2 B	4.9	9.5
shPar6da A	3.2	13.9
shPard6a B	3.0	4.4
shPrkcz A	3.7	2.2
shPrkcz B	3.8	2.2

b.

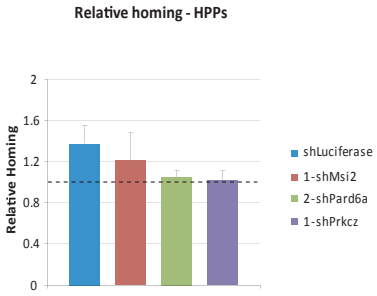

c.

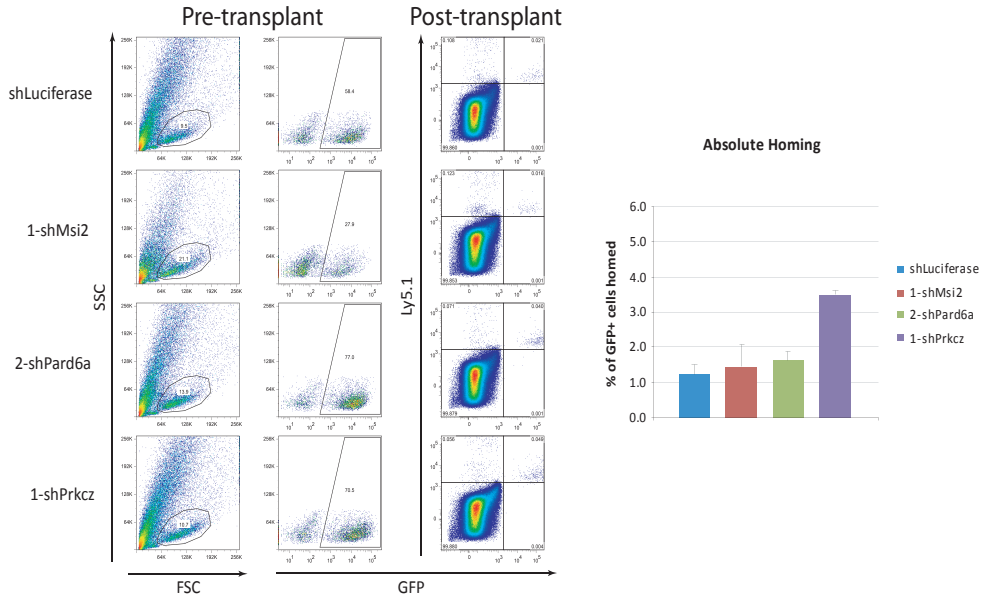

Figure 3.S3: Apoptosis and primitive cell homing assessment. a. Flow cytometric evaluation of the percentage of Annexin V$^+$ cells within the PI$^-$ subset of day 0 GFP$^+$ and GFP$^-$ cells for each candidate shRNA. A and B refer to two independent experiments. **b.** Twenty-four hour bone marrow homing efficiencies of high proliferative potential (HPP) colony forming cells. Data shown is the GFP% of harvested HPPs (including GEMM-type colonies) relative to the input HPP GFP%. **c.** Pre- and 24 hours post-transplant flow cytometry plots indicating the percentage of live, GFP+, and Ly5.1+ cells in representative samples (left). Percentage of GFP$^+$ cells present in recipient bone marrow (right, n=3 per condition). Values represent Mean +/- SEM.

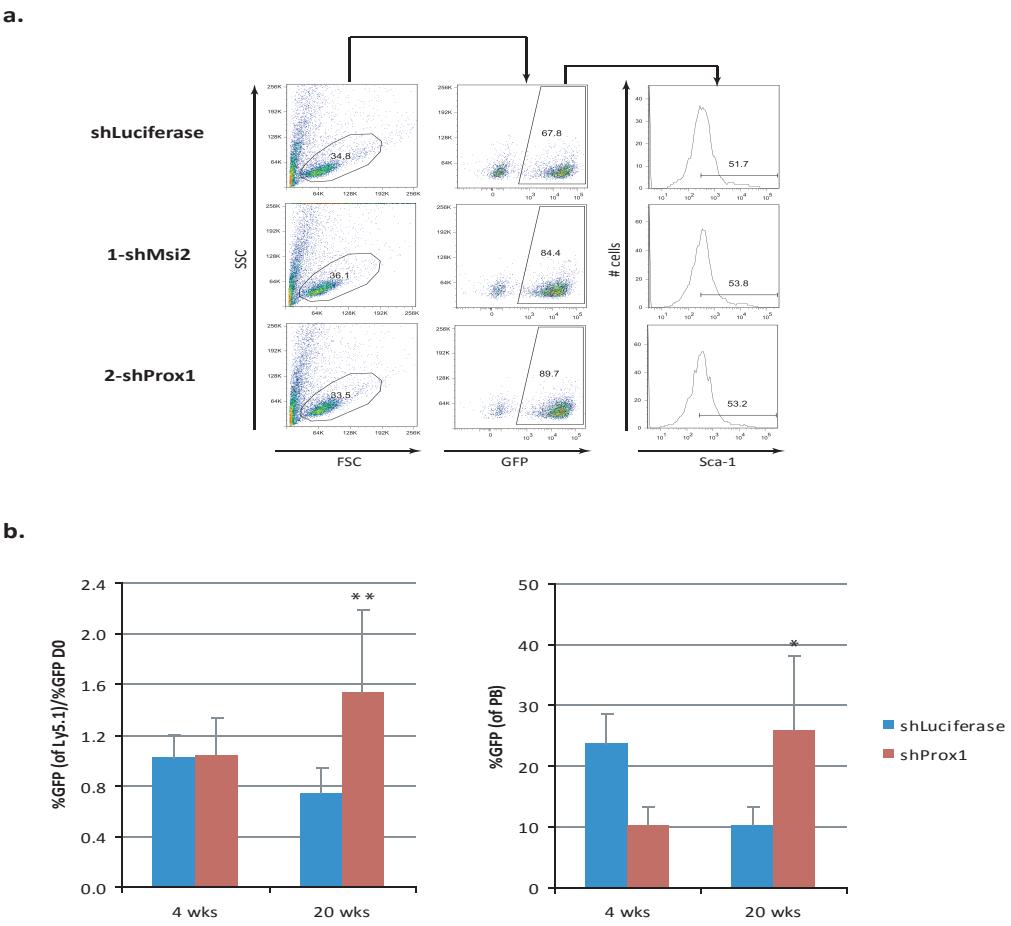

Figure 3.S4: Confirmation of Prox1 shRNA specificity. a. Representative flow cytometry plots of test cells (1-shMsi2 and 2-shProx1) versus controls immediately post-infection (day 0) indicate little change in cell phenotype over the course of infection. Note that in all cases the GFP+ cells were exclusively Gr-1- and contained approximately the same proportion of Sca-1+ cells. **b.** Quantitative assessment of Prox1 shRNA-induced enhancement in repopulation using a second independent hairpin (3-shProx1) to that shown in Figure 3b. Results are shown in comparison to shLuciferase controls transduced over a similar range. Values shown are mean ± SEM (shLuciferase, n=10; 3-shProx1, n=4) ** p=0.07, * p=0.05.

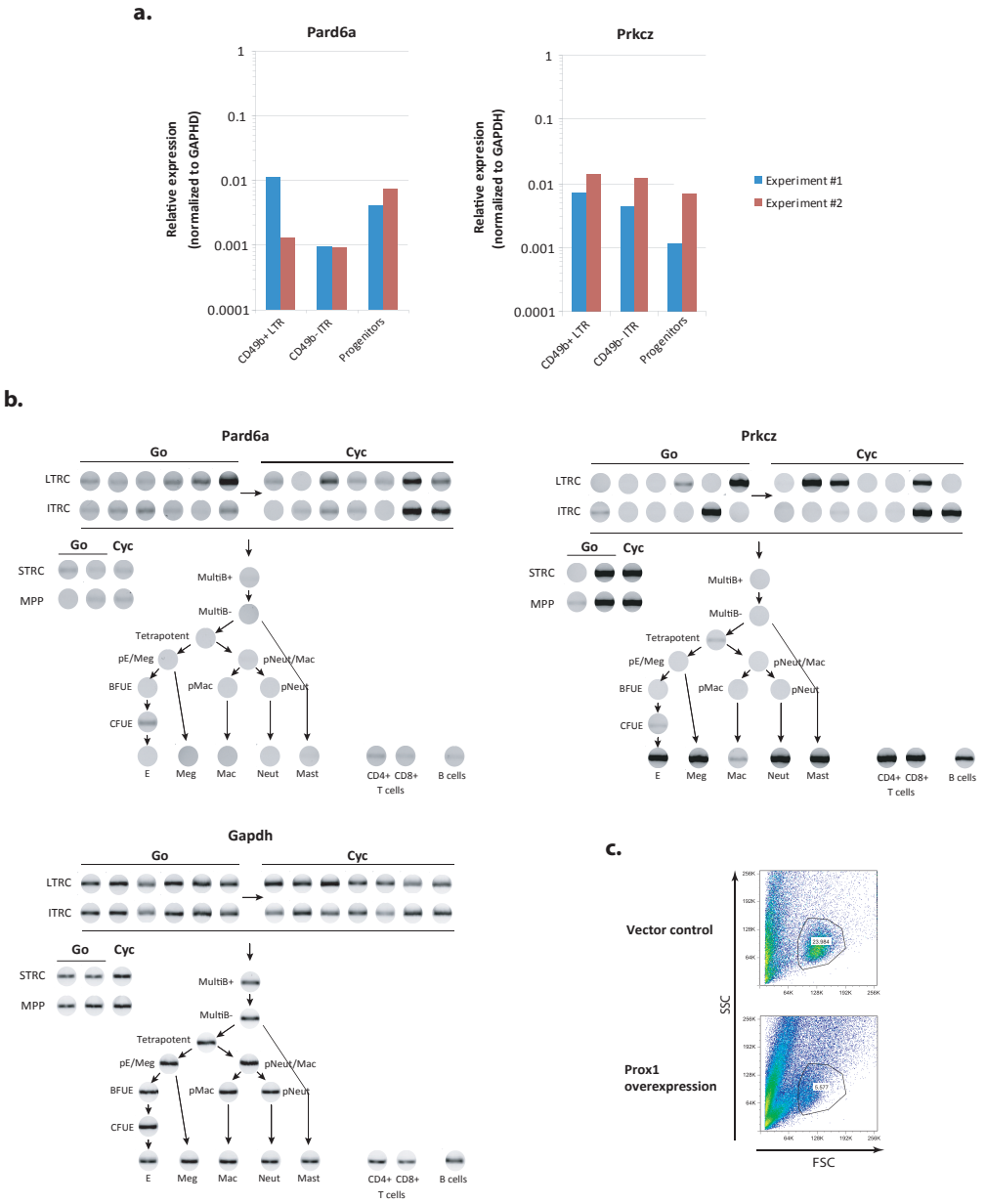

Figure 3.S5: Evaluation of endogenous Pard6a and Prkcz hematopoietic expression and effects of Prox1 overexpression. a. QPCR relative quantitation of Pard6a (left) and Prkcz (right) levels in sorted hematopoietic stem and progenitor cells (data shown as relative to GAPDH expression). **b.** Semi-quantitative assessment of Pard6a and Prkcz transcript levels in purified hematopoietic subsets ranging from primitive to mature hematopoietic cells of all three lineages. GAPDH levels in each subset are shown for comparison. **c.** Representative flow cytometry plots showing increased death and differentiation observed upon Prox1 overexpression.

Sample	Previously tested	Loss impairs cell division	Eliminated for technical reasons	Chosen for final list
Akt1	X			
Anapc5				X
Ap2a2				X
Apc	X			
AurkA		X		
AurkB		X		
Bicd1			X	
Cdc42	X			
Cdk2	X			
Ctnna1				X
Ctnnb1				X
CylinB1		X		
Ect2		X		
Gfi-1	X			
Gnai2				X
Gnb2			X	
Gpsm2				X
Lgl1				X
Mapre3				X
MgcRacGap	X			
Msi2				X
Myo6		X		
Neurl				X
Numb				X
Pard3**				X
Pard6a				X
Pard6b				X
Prkci				X
Prkcz				X
Prox1				X
Pten	X			
PTP1B	X			
PTP2A		X		
Rsn	X			
Scrb			X	
Spin1	X			
Stat3	X			
Stau1			X	
Stx4A				X
TC-PTP	X			
Trim3				X
Trim32				X
Tuba1		X		
Ywhab		X		

Table 3.S1. Candidate gene selection criteria. Candidate genes with a ΔCt of >9.0 (with respect to GAPDH) were first filtered out. A review of the literature on the remaining genes enabled the further exclusion of those whose loss or reduced function alters cell survival or division. Genes having previously been tested in a loss-of-function context in hematopoietic stem cell function were also eliminated from further study. Four genes were not tested as a result of various technical difficulties. Candidates that satisfied all criteria (listed in rightmost column) were tested in the primary shRNA screen. ** technical difficulties precluded Q-RT-PCR assessment of Pard3. We therefore relied on previously documented reports of Pard3 expression in primitive murine bone marrow and fetal liver subsets (reviewed in Faubert *et al*. 2004).

Gene	Oligo name	Oligo Sequence
Luciferase	shLuciferase	TGCTGTTGACAGTGAGCGCCGATATGGGCTGAATACAAATTAGTGAAGCCACAGATGTAATTTGTATTCAGCCCATATCGTTGCCTACTGCCTCGGA
NA	shScrambled	TGCTGTTGACAGTGAGCGCAAGGTTAAGTCGCCCTCGCTCTAGTGAAGCCACAGATGTAGAGCGAGGGCGACTTAACCTTATGCCTACTGCCTCGGA
Anapc5	1-shAnapc5	TGCTGTTGACAGTGAGCGCACACAGCCTGTCAGAACTTATTAGTGAAGCCACAGATGTAATAAGTTCTGACAGGCTGTGTTTGCCTACTGCCTCGGA
	2-shAnapc5	TGCTGTTGACAGTGAGCGCATTGTCAGTATCTTTGTTAAGTAGTGAAGCCACAGATGTACTTAACAAAGATACTGACAATTTGCCTACTGCCTCGGA
	3-shAnapc5	TGCTGTTGACAGTGAGCGCGCACTAACTGTTCTTCTAAAGTAGTGAAGCCACAGATGTACTTTAGAAGAACAGTTAGTGCTTGCCTACTGCCTCGGA
Ap2A2	1-shAp2A2	TGCTGTTGACAGTGAGCGACCTGACTGAGTGCTTGGAGACTAGTGAAGCCACAGATGTAGTCTCCAAGCACTCAGTCAGGCTGCCTACTGCCTCGGA
	2-shAp2A2	TGCTGTTGACAGTGAGCGATTGCACTATGTCTTGCAGTAATAGTGAAGCCACAGATGTATTACTGCAAGACATAGTGCAAGTGCCTACTGCCTCGGA
	3-shAp2A2	TGCTGTTGACAGTGAGCGCGCACTAGGTGTGGTCAGTTATTAGTGAAGCCACAGATGTAATAACTGACCACACCTAGTGCTTGCCTACTGCCTCGGA
Ctnna1	1-shCtnna1	TGCTGTTGACAGTGAGCGCCCACATTAACTTCTTGGTCACTAGTGAAGCCACAGATGTAGTGACCAAGAAGTTAATGTGGTTGCCTACTGCCTCGGA
	2-shCtnna1	TGCTGTTGACAGTGAGCGCTGGCTGCATCTGTTGAACAAGTAGTGAAGCCACAGATGTACTTGTTCAACAGATGCAGCCAATGCCTACTGCCTCGGA
	3-shCtnna1	TGCTGTTGACAGTGAGCGCCCCAATAAAGTCCATTAAGAATAGTGAAGCCACAGATGTATTCTTAATGGACTTTATTGGGATGCCTACTGCCTCGGA
Ctnnb1	1-shCtnnb1	TGCTGTTGACAGTGAGCGCGGACTGCCTGTTGTGGTTAAATAGTGAAGCCACAGATGTATTTAACCACAACAGGCAGTCCATGCCTACTGCCTCGGA
	2-shCtnnb1	TGCTGTTGACAGTGAGCGATGTCTGAACGTGCATTGTGATTAGTGAAGCCACAGATGTAATCACAATGCACGTTCAGACACTGCCTACTGCCTCGGA
	3-shCtnnb1	TGCTGTTGACAGTGAGCGACCAGTGTGGGTGAATACTTTATAGTGAAGCCACAGATGTATAAAGTATTCACCCACACTGGCTGCCTACTGCCTCGGA
Gnai2	1-shGnai2	TGCTGTTGACAGTGAGCGACCTGGCTTTGTCCAACACCAGTAGTGAAGCCACAGATGTACTGGTGTTGGACAAAGCCAGGGTGCCTACTGCCTCGGA
	2-shGnai2	TGCTGTTGACAGTGAGCGACCACAGGCCTCCCAGTCTAAATAGTGAAGCCACAGATGTATTTAGACTGGGAGGCCTGTGGCTGCCTACTGCCTCGGA
	3-shGnai2	TGCTGTTGACAGTGAGCGCTGACAGCATCTGCAACAACAATAGTGAAGCCACAGATGTATTGTTGTTGCAGATGCTGTCAATGCCTACTGCCTCGGA
Gpsm2	1-shGpsm2	TGCTGTTGACAGTGAGCGAGCAACTTCAGGGATGCAGTTATAGTGAAGCCACAGATGTATAACTGCATCCCTGAAGTTGCCTGCCTACTGCCTCGGA
	2-shGpsm2	TGCTGTTGACAGTGAGCGCCCAGAGGGCCAGTTTCAGTAATAGTGAAGCCACAGATGTATTACTGAAACTGGCCCTCTGGTTGCCTACTGCCTCGGA
	3-shGpsm2	TGCTGTTGACAGTGAGCGAACACACTACCTCCTCGGCAACTAGTGAAGCCACAGATGTAGTTGCCGAGGAGGTAGTGTGTGTGCCTACTGCCTCGGA
Lgl1	1-shLlgl1	TGCTGTTGACAGTGAGCGCGCTGTCACACTCCATGCTGAGTAGTGAAGCCACAGATGTACTCAGCATGGAGTGTGACAGCATGCCTACTGCCTCGGA
	2-shLlgl1	TGCTGTTGACAGTGAGCGACTCCTGACCCTGCTAGATGACTAGTGAAGCCACAGATGTAGTCATCTAGCAGGGTCAGGAGGTGCCTACTGCCTCGGA
	3-shLlgl1	TGCTGTTGACAGTGAGCGAGCCTACACCCTTCTGATTAAATAGTGAAGCCACAGATGTATTTAATCAGAAGGGTGTAGGCCTGCCTACTGCCTCGGA
Lgl2	1-shLlgl2	TGCTGTTGACAGTGAGCGAGCCCAGGCTGTGAATACCAAGTAGTGAAGCCACAGATGTACTTGGTATTCACAGCCTGGGCCTGCCTACTGCCTCGGA
	2-shLlgl2	TGCTGTTGACAGTGAGCGATGTCTGTCTGTCTGTCCTGACTAGTGAAGCCACAGATGTAGTCAGGACAGACAGACAGACAGTGCCTACTGCCTCGGA
	3-shLlgl2	TGCTGTTGACAGTGAGCGCCCTTGCAAAGCTATAACGAAATAGTGAAGCCACAGATGTATTTCGTTATAGCTTTGCAAGGATGCCTACTGCCTCGGA
Mapre3	1-shMapre3	TGCTGTTGACAGTGAGCGAAGTGAGAATCTGAGTCGCCATTAGTGAAGCCACAGATGTAATGGCGACTCAGATTCTCACTGTGCCTACTGCCTCGGA
	2-shMapre3	TGCTGTTGACAGTGAGCGCTTTGACAAAGTCATTGGTATATAGTGAAGCCACAGATGTATATACCAATGACTTTGTCAAATTGCCTACTGCCTCGGA
	3-shMapre3	TGCTGTTGACAGTGAGCGAGCTGATATGAGGAAAGGGAAGTAGTGAAGCCACAGATGTACTTCCCTTTCCTCATATCAGCCTGCCTACTGCCTCGGA
Msi2	1-shMsi2	TGCTGTTGACAGTGAGCGAAGAGCATACCTGGATGTCCAGTAGTGAAGCCACAGATGTACTGGACATCCAGGTATGCTCTCTGCCTACTGCCTCGGA
	2-shMsi2	TGCTGTTGACAGTGAGCGAGCGCTTCCATTGCCGTCTCACTAGTGAAGCCACAGATGTAGTGAGACGGCAATGGAAGCGCCTGCCTACTGCCTCGGA
	3-shMsi2	TGCTGTTGACAGTGAGCGAACCCAGCAAGTGTAGATAAAGTAGTGAAGCCACAGATGTACTTTATCTACACTTGCTGGGTCTGCCTACTGCCTCGGA
	4-shMsi2	TGCTGTTGACAGTGAGCGACCGGATTTGCTCCTAGCTATGTAGTGAAGCCACAGATGTACATAGCTAGGAGCAAATCCGGGTGCCTACTGCCTCGGA
	6-shMsi2	TGCTGTTGACAGTGAGCGCGCAAGTGTAGATAAAGTATTATAGTGAAGCCACAGATGTATAATACTTTATCTACACTTGCTTGCCTACTGCCTCGGA
Neurl	1-shNeurl	TGCTGTTGACAGTGAGCGACCACTGTGTTTGTGAATAAAGTAGTGAAGCCACAGATGTACTTTATTCACAAACACAGTGGCTGCCTACTGCCTCGGA
	2-shNeurl	TGCTGTTGACAGTGAGCGAGCCGAGACCATCTTCATCAAGTAGTGAAGCCACAGATGTACTTGATGAAGATGGTCTCGGCCTGCCTACTGCCTCGGA
	3-shNeurl	TGCTGTTGACAGTGAGCGAGCCACTGTGTTTGTGAATAAATAGTGAAGCCACAGATGTATTTATTCACAAACACAGTGGCCTGCCTACTGCCTCGGA
Numb	1-shNumb	TGCTGTTGACAGTGAGCGCGCACATTTACTGGAATATAAATAGTGAAGCCACAGATGTATTTATATTCCAGTAAATGTGCTTGCCTACTGCCTCGGA
	2-shNumb	TGCTGTTGACAGTGAGCGCGGCCTTACAATCAAATGTAAGTAGTGAAGCCACAGATGTACTTACATTTGATTGTAAGGCCATGCCTACTGCCTCGGA
	3-shNumb	TGCTGTTGACAGTGAGCGAGCAGAAGATCTGAAGAGGAATTAGTGAAGCCACAGATGTAATTCCTCTTCAGATCTTCTGCCTGCCTACTGCCTCGGA
Pard3	1-shPard3	TGCTGTTGACAGTGAGCGCTGACTTTCAGTGGTGTTTAAGTAGTGAAGCCACAGATGTACTTAAACACCACTGAAAGTCATTGCCTACTGCCTCGGA
	2-shPard3	TGCTGTTGACAGTGAGCGACCTGCGAATCTTGATATGAAATAGTGAAGCCACAGATGTATTTCATATCAAGATTCGCAGGCTGCCTACTGCCTCGGA
	3-shPard3	TGCTGTTGACAGTGAGCGCCCCATTTATGTCAAGAATATCTAGTGAAGCCACAGATGTAGATATTCTTGACATAAATGGGATGCCTACTGCCTCGGA
Pard6a	1-shPard6a	TGCTGTTGACAGTGAGCGACCTCTCAGTCTGGTGAACATTTAGTGAAGCCACAGATGTAAATGTTCACCAGACTGAGAGGGTGCCTACTGCCTCGGA
	2-shPard6a	TGCTGTTGACAGTGAGCGATCTCAGTCTGGTGAACATTAATAGTGAAGCCACAGATGTATTAATGTTCACCAGACTGAGAGTGCCTACTGCCTCGGA
	3-shPard6a	TGCTGTTGACAGTGAGCGACCTCTCAGTCTGGTGAACATTTAGTGAAGCCACAGATGTAAATGTTCACCAGACTGAGAGGGTGCCTACTGCCTCGGA
Pard6b	1-shPard6b	TGCTGTTGACAGTGAGCGCTGTGGGTAGGTGATAGCATAGTAGTGAAGCCACAGATGTACTATGCTATCACCTACCCACAATGCCTACTGCCTCGGA
	2-shPard6b	TGCTGTTGACAGTGAGCGAACAGTGTGGATCATGGGATAATAGTGAAGCCACAGATGTATTATCCCATGATCCACACTGTCTGCCTACTGCCTCGGA
	3-shPard6b	TGCTGTTGACAGTGAGCGAACTGAGTTTCTCCTCTCACACTAGTGAAGCCACAGATGTAGTGTGAGAGGAGAAACTCAGTGTGCCTACTGCCTCGGA
Prkci	1-shPrkci	TGCTGTTGACAGTGAGCGCGCTGAGCTTGTGATGATTTAATAGTGAAGCCACAGATGTATTAAATCATCACAAGCTCAGCATGCCTACTGCCTCGGA
	2-shPrkci	TGCTGTTGACAGTGAGCGAAGCTCCTATGTCATAGCTAACTAGTGAAGCCACAGATGTAGTTAGCTATGACATAGGAGCTCTGCCTACTGCCTCGGA
	3-shPrkci	TGCTGTTGACAGTGAGCGCCGTCAATGACGATGAGGATATTAGTGAAGCCACAGATGTAATATCCTCATCGTCATTGACGATGCCTACTGCCTCGGA
Prkcz	1-shPrkcz	TGCTGTTGACAGTGAGCGAGCCATGAAGGTGGTAAAGAAGTAGTGAAGCCACAGATGTACTTCTTTACCACCTTCATGGCGTGCCTACTGCCTCGGA
	2-shPrkcz	TGCTGTTGACAGTGAGCGCTGAGTTGAGCTGCTAAGATAATAGTGAAGCCACAGATGTATTATCTTAGCAGCTCAACTCATTGCCTACTGCCTCGGA
	3-shPrkcz	TGCTGTTGACAGTGAGCGAGCTCTGTGTCTCCTATTGATCTAGTGAAGCCACAGATGTAGATCAATAGGAGACACAGAGCCTGCCTACTGCCTCGGA
Prox1	1-shProx1	TGCTGTTGACAGTGAGCGCTGTCACCAAGTCCTTTGTAAGTAGTGAAGCCACAGATGTACTTACAAAGGACTTGGTGACAATGCCTACTGCCTCGGA
	2-shProx1	TGCTGTTGACAGTGAGCGCGGAAACCCTGTGCTTTGTCACTAGTGAAGCCACAGATGTAGTGACAAAGCACAGGGTTTCCTTGCCTACTGCCTCGGA
	3-shProx1	TGCTGTTGACAGTGAGCGATCAGACAATGAGATGTGTGAGTAGTGAAGCCACAGATGTACTCACACATCTCATTGTCTGAGTGCCTACTGCCTCGGA
Stx4a	1-shStx4a	TGCTGTTGACAGTGAGCGCTTTGTCGAGCTCATCAACAAGTAGTGAAGCCACAGATGTACTTGTTGATGAGCTCGACAAATTGCCTACTGCCTCGGA
	2-shStx4a	TGCTGTTGACAGTGAGCGAGTGCAGGACTTCCAAATTTAGTAGTGAAGCCACAGATGTACTAAATTTGGAAGTCCTGCACCTGCCTACTGCCTCGGA
	3-shStx4a	TGCTGTTGACAGTGAGCGCCCTGTTTGTCTGGGATACATGTAGTGAAGCCACAGATGTACATGTATCCCAGACAAACAGGATGCCTACTGCCTCGGA
Trim3	1-shTrim3	TGCTGTTGACAGTGAGCGAACCCTCAGTCTGCTCTCTGATTAGTGAAGCCACAGATGTAATCAGAGAGCAGACTGAGGGTGTGCCTACTGCCTCGGA
	2-shTrim3	TGCTGTTGACAGTGAGCGACCACGGTTGCACTTTATTTATTAGTGAAGCCACAGATGTAATAAATAAAGTGCAACCGTGGGTGCCTACTGCCTCGGA
Trim32	1-shTrim32	TGCTGTTGACAGTGAGCGAAGCTATCATCTGAGAAGATATTAGTGAAGCCACAGATGTAATATCTTCTCAGATGATAGCTGTGCCTACTGCCTCGGA
	2-shTrim32	TGCTGTTGACAGTGAGCGCGGCCAGTTTGTGGTGACTGACTAGTGAAGCCACAGATGTAGTCAGTCACCACAAACTGGCCATGCCTACTGCCTCGGA
	3-shTrim32	TGCTGTTGACAGTGAGCGCGGAGTTTATAGGTTAGAATTATAGTGAAGCCACAGATGTATAATTCTAACCTATAAACTCCTTGCCTACTGCCTCGGA

PCR primers	Sequence
mir30-F	CAGAAGGCTCGAGAAGGTATATTGCTGTTGACAGTGAGCG
mir30-R	CTAAAGTAGCCCCTTGATTCCGAGGCAGTAGGCA

Table 3.S2. shRNA oligonucleotides and PCR primers. The shRNA sequences designed to target each candidate gene are shown in addition to the sequences of the forward and reverse PCR primers used for their amplification and subsequent subcloning

Primary mouse	GFP cell dose	# repopulated mice/ # transplanted mice	HSC Frequency			Number of HSCs	Fold Expansion
			Frequency	Lower limit	Upper limit		
shLuciferase	1.7E+05	1/3	1/470,897	1/3,324,574	1/66,698	7	0.9
	1.7E+04	0/3					
NUPHD	1.7E+05	2/2	1/65,215	1/334,589	1/12,711	2637	329.7
	8.7E+03	0/3					
	8.7E+02	0/3					
2-shProx1	2.0E+06	2/2	1/96,181	1/392,823	1/25,549	849	106.2
	4.1E+05	3/3					
	4.1E+04	1/3					
	4.1E+03	0/3					
	4.1E+02	0/2					

Table 3.S3. Evaluation of CRU numbers in primary mice. Data was obtained from peripheral blood sampled at 12 weeks post-transplant. Secondary recipients were considered positive if donor lymphoid and myeloid repopulation was at least 1% in the blood. Upper and lower frequencies were determined based on a 95% CI. In evaluating the number of tranduced HSCs in each primary mouse we assumed a whole bone marrow mass of $2x10^8$ cells. *In vivo* fold expansion of CRUs was determined by dividing the total number of HSCs (second to last column) by 8 input CRU.

Sample	Cell dose	% of well	# repopulated mice/ # transplanted mice	Frequency (per cells)			Frequency (per culture %)			Total # HSC at 7 days
				Frequency	Upper limit	Lower limit	Frequency	Upper limit	Lower limit	
HOXB4	384375	12.5%	1/1 (33.5)	NA	1	23809	NA	<.00001%	0.77%	130*
	153750	5.0%	3/3 (50.9+6.3)							
	76875	2.5%	3/3 (42.6+10.7)							
	38438	1.3%	3/3 (19.5+6.8)							
	9609	0.3%	2/2 (10.3+0.6)							
shLuciferase	255000	20.0%	1/1 (46.6)	123118	45604	332382	9.70%	3.60%	26.10%	10
	127500	10.0%	2/2 (1.4+0.1)							
	63750	5.0%	0/3							
	31875	2.5%	1/3 (7.4)							
	15000	1.3%	0/2							
3-shProx1	190000	12.5%	2/2 (14.5+7.3)	23387	10817	50566	1.54%	0.71%	3.33%	65
	76000	5.0%	3/3 (6.2+2.4)							
	38000	2.5%	4/4 (36.6+19.3)							
	19000	1.3%	1/2 (2.2)							
	9500	0.6%	0/4							
	4750	0.3%	0/1							

Table 3.S4. Evaluation of CRU numbers following *in vitro* culture. Data was obtained from peripheral blood sampled at 14 weeks post-transplant. Recipients were considered positive if donor repopulation was above 1% in the blood. The mean CD45.1% (± SEM) of positive mice is shown in brackets. Upper and lower frequencies per cell and per culture percentage were determined based on a 95% CI. * value represents the minimum number of CRUs.

3.8 Acknowledgments

We thank M. Frechette and A. Fournier for technical assistance with mouse transplantations, D. Gagné from the IRIC flow cytometry platform, R. Lambert from the IRIC genomic platform for help with quantitative RT-PCR and J. Landry for technical assistance with microarray experiments. The authors also thank J. Krosl for discussions and critical comments about the manuscript. This work was supported by the Canadian Institute of Health Research (CIHR) Team Grant in Hematopoietic Stem Cell Self-Renewal: From Genes to Bedside (Grant number 154290). G.S. holds a Canada Research Chair on molecular genetics of stem cells; K.H. and S.C. are recipients of a CIHR Post-doctoral fellowship and Clinician Scientist award, respectively; S.B.T. is the recipient of National Health Medical Research Council, Royal Australian College of Physicians and CIHR Post-doctoral fellowships. IRIC is supported in part by the Canadian Center of Excellence in Commercialization and Research (CECR), the Canada Foundation for Innovation (CFI), and the Fonds de Recherche en Santé du Québec (FRSQ).

3.9 References

Adolfsson, J., Borge, O. J., Bryder, D., Theilgaard-Monch, K., Astrand-Grundstrom, I., Sitnicka, E., Sasaki, Y., and Jacobsen, S. E. (2001). Upregulation of Flt3 expression within the bone marrow Lin(-)Sca1(+)c-kit(+) stem cell compartment is accompanied by loss of self-renewal capacity. Immunity *15*, 659-669.

Barbouti, A., Hoglund, M., Johansson, B., Lassen, C., Nilsson, P. G., Hagemeijer, A., Mitelman, F., and Fioretos, T. (2003). A novel gene, MSI2, encoding a putative RNA-binding protein is recurrently rearranged at disease progression of chronic myeloid leukemia and forms a fusion gene with HOXA9 as a result of the cryptic t(7;17)(p15;q23). Cancer Res *63*, 1202-1206.

Beckmann, J., Scheitza, S., Wernet, P., Fischer, J. C., and Giebel, B. (2007). Asymmetric cell division within the human hematopoietic stem and progenitor cell compartment: identification of asymmetrically segregating proteins. Blood *109*, 5494-5501.

Benveniste, P., Cantin, C., Hyam, D., and Iscove, N. N. (2003). Hematopoietic stem cells engraft in mice with absolute efficiency. Nat Immunol *4*, 708-713.

Benveniste, P., Frelin, C., Janmohamed, S., Barbara, M., Herrington, R., Hyam, D., and Iscove, N. N. (2010). Intermediate term hematopoietic stem cells with extended but time-limited reconstitution potential. Cell Stem Cell in press *xx-xx*.

Betschinger, J., Mechtler, K., and Knoblich, J. A. (2006). Asymmetric segregation of the tumor suppressor brat regulates self-renewal in Drosophila neural stem cells. Cell *124*, 1241-1253.

Bilder, D. (2004). Epithelial polarity and proliferation control: links from the Drosophila neoplastic tumor suppressors. Genes Dev *18*, 1909-1925.

Brummendorf, T. H., Dragowska, W., Zijlmans, J., Thornbury, G., and Lansdorp, P. M. (1998). Asymmetric cell divisions sustain long-term hematopoiesis from single-sorted human fetal liver cells. J Exp Med *188*, 1117-1124.

Cayouette, M., and Raff, M. (2002). Asymmetric segregation of Numb: a mech-

anism for neural specification from Drosophila to mammals. Nat Neurosci *12*, 1265-1269.

Chang, J. T., Palanivel, V. R., Kinjyo, I., Schambach, F., Intlekofer, A. M., Banerjee, A., Longworth, S. A., Vinup, K. E., Mrass, P., Oliaro, J.*, et al.* (2007). Asymmetric T lymphocyte division in the initiation of adaptive immune responses. Science *315*, 1687-1691.

Choksi, S. P., Southall, T. D., Bossing, T., Edoff, K., de Wit, E., Fischer, B. E., van Steensel, B., Micklem, G., and Brand, A. H. (2006). Prospero acts as a binary switch between self-renewal and differentiation in Drosophila neural stem cells. Dev Cell *11*, 775-789.

Christensen, J. L., and Weissman, I. L. (2001). Flk-2 is a marker in hematopoietic stem cell differentiation: a simple method to isolate long-term stem cells. Proc Natl Acad Sci U S A *98*, 14541-14546.

Clarke, R. B., Spence, K., Anderson, E., Howell, A., Okano, H., and Potten, C. S. (2005). A putative human breast stem cell population is enriched for steroid receptor-positive cells. Dev Biol *277*, 443-456.

De Weer, A., Speleman, F., Cauwelier, B., Van Roy, N., Yigit, N., Verhasselt, B., De Moerloose, B., Benoit, Y., Noens, L., Selleslag, D.*, et al.* (2008). EVI1 overexpression in t(3;17) positive myeloid malignancies results from juxtaposition of EVI1 to the MSI2 locus at 17q22. Haematologica *93*, 1903-1907.

Deneault, E., Cellot, S., Faubert, A., Laverdure, J. P., Frechette, M., Chagraoui, J., Mayotte, N., Sauvageau, M., Ting, S. B., and Sauvageau, G. (2009). A functional screen to identify novel effectors of hematopoietic stem cell activity. Cell *137*, 369-379.

Dyer, M. A. (2003). Regulation of proliferation, cell fate specification and differentiation by the homeodomain proteins Prox1, Six3, and Chx10 in the developing retina. Cell Cycle *2*, 350-357.

Dykstra, B., Kent, D., Bowie, M., McCaffrey, L., Hamilton, M., Lyons, K., Lee, S. J., Brinkman, R., and Eaves, C. (2007). Long-term propagation of distinct hematopoietic differentiation programs in vivo. Cell Stem Cell *1*, 218-229.

Ema, H., and Nakauchi, H. (2000). Expansion of hematopoietic stem cells in the developing liver of a mouse embryo. Blood *95*, 2284-2288.

Ema, H., Takano, H., Sudo, K., and Nakauchi, H. (2000). In vitro self-renewal division of hematopoietic stem cells. J Exp Med *192*, 1281-1288.

Faubert, A., Lessard, J., and Sauvageau, G. (2004). Are genetic determinants of asymmetric stem cell division active in hematopoietic stem cells? Oncogene *23*, 7247-7255.

Gu, Y., Zheng, Y., and Williams, D. A. (2005). RhoH GTPase: a key regulator of hematopoietic cell proliferation and apoptosis? Cell Cycle *4*, 201-202.

Hess, D. A., Meyerrose, T. E., Wirthlin, L., Craft, T. P., Herrbrich, P. E., Creer, M. H., and Nolta, J. A. (2004). Functional characterization of highly purified human hematopoietic repopulating cells isolated according to aldehyde dehydrogenase activity. Blood *104*, 1648-1655.

Imai, T., Tokunaga, A., Yoshida, T., Hashimoto, M., Mikoshiba, K., Weinmaster, G., Nakafuku, M., and Okano, H. (2001). The neural RNA-binding protein Musashi1 translationally regulates mammalian numb gene expression by interacting with its mRNA. Mol Cell Biol *21*, 3888-3900.

Inada, S., Brown, E. J., Gaither, T. A., Hammer, C. H., Takahashi, T., and Frank, M. M. (1983). C3d receptors are expressed on human monocytes after in vitro cultivation. Proc Natl Acad Sci U S A *80*, 2351-2355.

Joberty, G., Petersen, C., Gao, L., and Macara, I. G. (2000). The cell-polarity protein Par6 links Par3 and atypical protein kinase C to Cdc42. Nat Cell Biol *2*, 531-539.

Kayahara, T., Sawada, M., Takaishi, S., Fukui, H., Seno, H., Fukuzawa, H., Suzuki, K., Hiai, H., Kageyama, R., Okano, H., and Chiba, T. (2003). Candidate markers for stem and early progenitor cells, Musashi-1 and Hes1, are expressed in crypt base columnar cells of mouse small intestine. FEBS Lett *535*, 131-135.

Kent, D. G., Copley, M. R., Benz, C., Wohrer, S., Dykstra, B. J., Ma, E., Cheyne, J., Zhao, Y., Bowie, M. B., Zhao, Y*., et al.* (2009). Prospective isolation and molecular characterization of hematopoietic stem cells with durable self-renewal potential. Blood *113*, 6342-6350.

Kiel, M. J., Yilmaz, O. H., Iwashita, T., Yilmaz, O. H., Terhorst, C., and Morrison, S. J. (2005). SLAM family receptors distinguish hematopoietic stem and progenitor cells and reveal endothelial niches for stem cells. Cell *121*, 1109-1121.

Knoblich, J. A. (2008). Mechanisms of asymmetric stem cell division. Cell *132*, 583-597.

Krieger, M., Acton, S., Ashkenas, J., Pearson, A., Penman, M., and Resnick, D. (1993). Molecular flypaper, host defense, and atherosclerosis. Structure, binding properties, and functions of macrophage scavenger receptors. J Biol Chem *268*, 4569-4572.

Krosl, J., Beslu, N., Mayotte, N., Humphries, R. K., and Sauvageau, G. (2003). The competitive nature of HOXB4-transduced HSC is limited by PBX1: the generation of ultra-competitive stem cells retaining full differentiation potential. Immunity *18*, 561-571.

Lee, C. Y., Robinson, K. J., and Doe, C. Q. (2006). Lgl, Pins and aPKC regulate neuroblast self-renewal versus differentiation. Nature *439*, 594-598.

Lin, D., Edwards, A. S., Fawcett, J. P., Mbamalu, G., Scott, J. D., and Pawson, T. (2000). A mammalian PAR-3-PAR-6 complex implicated in Cdc42/Rac1 and aPKC signalling and cell polarity. Nat Cell Biol *2*, 540-547.

Nagai, H., Li, Y., Hatano, S., Toshihito, O., Yuge, M., Ito, E., Utsumi, M., Saito,

H., and Kinoshita, T. (2003). Mutations and aberrant DNA methylation of the PROX1 gene in hematologic malignancies. Genes Chromosomes Cancer *38*, 13-21.

Nakamura, M., Okano, H., Blendy, J. A., and Montell, C. (1994). Musashi, a neural RNA-binding protein required for Drosophila adult external sensory organ development. Neuron *13*, 67-81.

Ohta, H., Sekulovic, S., Bakovic, S., Eaves, C. J., Pineault, N., Gasparetto, M., Smith, C., Sauvageau, G., and Humphries, R. K. (2007). Near-maximal expansions of hematopoietic stem cells in culture using NUP98-HOX fusions. Exp Hematol *35*, 817-830.

Okano, H., Imai, T., and Okabe, M. (2002). Musashi: a translational regulator of cell fate. J Cell Sci *115*, 1355-1359.

Okano, H., Kawahara, H., Toriya, M., Nakao, K., Shibata, S., and Imai, T. (2005). Function of RNA-binding protein Musashi-1 in stem cells. Exp Cell Res *306*, 349-356.

Palmqvist, L., Pineault, N., Wasslavik, C., and Humphries, R. K. (2007). Candidate genes for expansion and transformation of hematopoietic stem cells by NUP98-HOX fusion genes. PLoS One *2*, e768.

Pawliuk, R., Eaves, C., and Humphries, R. K. (1996). Evidence of both ontogeny and transplant dose-regulated expansion of hematopoietic stem cells in vivo. Blood *88*, 2852-2858.

Potten, C. S., Booth, C., Tudor, G. L., Booth, D., Brady, G., Hurley, P., Ashton, G., Clarke, R., Sakakibara, S., and Okano, H. (2003). Identification of a putative intestinal stem cell and early lineage marker; musashi-1. Differentiation *71*, 28-41.

Punzel, M., Zhang, T., Liu, D., Eckstein, V., and Ho, A. D. (2002). Functional analysis of initial cell divisions defines the subsequent fate of individual human CD34(+)CD38(-) cells. Exp Hematol *30*, 464-472.

Risebro, C. A., Searles, R. G., Melville, A. A., Ehler, E., Jina, N., Shah, S., Pallas,

J., Hubank, M., Dillard, M., Harvey, N. L.*, et al.* (2009). Prox1 maintains muscle structure and growth in the developing heart. Development *136*, 495-505.

Sakakibara, S., Nakamura, Y., Yoshida, T., Shibata, S., Koike, M., Takano, H., Ueda, S., Uchiyama, Y., Noda, T., and Okano, H. (2002). RNA-binding protein Musashi family: roles for CNS stem cells and a subpopulation of ependymal cells revealed by targeted disruption and antisense ablation. Proc Natl Acad Sci U S A *99*, 15194-15199.

Siddall, N. A., McLaughlin, E. A., Marriner, N. L., and Hime, G. R. (2006). The RNA-binding protein Musashi is required intrinsically to maintain stem cell identity. Proc Natl Acad Sci U S A *103*, 8402-8407.

Takano, H., Ema, H., Sudo, K., and Nakauchi, H. (2004). Asymmetric division and lineage commitment at the level of hematopoietic stem cells: inference from differentiation in daughter cell and granddaughter cell pairs. J Exp Med *199*, 295-302.

Thorsteinsdottir, U., Sauvageau, G., and Humphries, R. K. (1999). Enhanced in vivo regenerative potential of HOXB4-transduced hematopoietic stem cells with regulation of their pool size. Blood *94*, 2605-2612.

Watts, J. L., Etemad-Moghadam, B., Guo, S., Boyd, L., Draper, B. W., Mello, C. C., Priess, J. R., and Kemphues, K. J. (1996). par-6, a gene involved in the establishment of asymmetry in early C. elegans embryos, mediates the asymmetric localization of PAR-3. Development *122*, 3133-3140.

Wigle, J. T., Chowdhury, K., Gruss, P., and Oliver, G. (1999). Prox1 function is crucial for mouse lens-fibre elongation. Nat Genet *21*, 318-322.

Wigle, J. T., Harvey, N., Detmar, M., Lagutina, I., Grosveld, G., Gunn, M. D., Jackson, D. G., and Oliver, G. (2002). An essential role for Prox1 in the induction of the lymphatic endothelial cell phenotype. Embo J *21*, 1505-1513.

Wu, M., Kwon, H. Y., Rattis, F., Blum, J., Zhao, C., Ashkenazi, R., Jackson, T.

L., Gaiano, N., Oliver, T., and Reya, T. (2007). Imaging hematopoietic precursor division in real time. Cell Stem Cell *1*, 541-554.

Yilmaz, O. H., Kiel, M. J., and Morrison, S. J. (2006). SLAM family markers are conserved among hematopoietic stem cells from old and reconstituted mice and markedly increase their purity. Blood *107*, 924-930.

Yokota, T., Oritani, K., Butz, S., Kokame, K., Kincade, P. W., Miyata, T., Vestweber, D., and Kanakura, Y. (2009). The endothelial antigen ESAM marks primitive hematopoietic progenitors throughout life in mice. Blood *113*, 2914-2923.

Zhao, Y., Lin, Y., Zhan, Y., Yang, G., Louie, J., Harrison, D. E., and Anderson, W. F. (2000). Murine hematopoietic stem cell characterization and its regulation in BM transplantation. Blood *96*, 3016-3022.

4. RNAi screen identifies Jarid1b as a major regulator of mouse HSC self-renewal

S. Cellot[1,2,5], K. J. Hope[1], M. Sauvageau[1], J. Chagraoui[1], E. Deneault[1], T. MacRae[1], N. Mayotte[1], J. R. Landry[1], S. B. Ting[1], J. Krosl[1], A. Thompson[1], K. Humphries[6] and Guy Sauvageau[1,2,3,4]*

[1]Institute for Research in Immunology and Cancer (IRIC), Université de Montreal, Montreal, Quebec, Canada H2W 1R7; [2]Faculty of Medicine, Université de Montreal, H3C 3J7; [3]Division of Hematology, Maisonneuve-Rosemont Hospital, Montreal, H1T 2M2; [4]Leukemia Cell Bank of Quebec, Maisonneuve-Rosemont Hospital, Montreal, H1T 2M2; [5]Division of Hematology, Ste-Justine Hospital, Montreal, H3T 1C5. [6]Terry Fox Laboratory, British Columbia Cancer Agency, and Department of Medicine, University of British Columbia, Vancouver, BC.

Running title: Jarid1b negatively influences self-renewal

*Correspondence:

Guy Sauvageau

Université de Montreal

C.P.6128, succursale Centre-Ville

Montreal, Quebec, Canada H3C 3J7

E-mail : [redacted]

4.1 Contribution des co-auteurs

S.C. and G.S. established the gene candidate list. M.S., J.C and S.C. contributed to isolation and functional assessment of highly purified HSC populations used for expression profile studies of gene candidates. S.C., K.J.H. and G.S. planned and performed the initial screen. S.C., K.J.H. and N.M. designed and performed validation experiments. S.C., N.M., K.J.H., S.B.T., J.C., E.D. J.K. and M.S. contributed to HSC isolation experiments required for initial screen, validation experiments and subsequent experiments. S.C. and N.M. performed confirmation experiments for shJarid1b-transduced cells including cell culture, progenitor assays and FACS. T.M. and S.C. performed RNA extraction and Q-RT-PCR analyses involving shJarid1b transduced cells. S.C., N.M. and J.C. performed LDA experiments and analyses of long-term recipient mice. A.T. optimized all Q-RT-PCR TaqMan dual-labelled probe assays for HoxA gene expression studies. E.D. performed Southern Blot analyses. J.R.L., T.M., S.C. and K.J.H. performed ChIP-chip experiments. M.S. and N.M. performed experiments involving co-transduction of NA10hd and shRNA constructs. S.C. and J.K. wrote paper.

4.2 Summary

Histone methylation is a dynamic and reversible process proposed to directly impact on stem cell fate. The Jumonji (JmjC) domain-containing family of demethylases comprises 27 members which can demethylate mono-, di- and tri-methylated lysine residues of histone (or non-histone) targets. To evaluate their role in regulation of hematopoietic stem cell (HSC) behaviour we performed a RNAi-based screen and found that demethylases JARID1B (H3K4) and JHDM1F (H3K9) play opposing roles in regulation of HSC activity. Decrease in *Jarid1b* levels correlated with an *in vitro* expansion of HSC with preserved long term *in vivo* lympho-myeloid differentiation potential. *Jarid1b* knockdown was associated with an increase in expression levels of 5' *Hoxa* cluster genes and *CxCl5*, and reduced levels of *Pu.1, Egr1* and *Cav1*. shRNA against *Jhdmlf*, in contrast, impaired hematopoietic reconstitution of bone marrow cells. Together, our studies identified *Jarid1b* as a negative, and *Jhdmlf* as a positive regulator of HSC activity.

4.3 Introduction

Blood tissue homeostasis is finely orchestrated by cyclical outputs from multipotent hematopoietic stem cells (HSC) which ensure sustained production of lineage committed cells throughout life. The pool of long-lived HSC is preserved due to their inherent capacity to undergo self-renewal divisions. Ultimately, cell fate decisions emanate from integrated influences of various nuclear factors, including chromatin modifiers, that regulate access of transcriptional machinery to various genomic loci. As the basic chromatin unit consists of intertwined DNA, histone and non-histone proteins, both nucleic acids and amino acids can be covalently modified by epigenetic effectors. DNA methyltransferases (DNMTs) modify carbon-5 of cytosine bases within cytosine-guanosine dinucleotides (CpG) frequently located in or in proximity of promoters [1]. In mammalian cells, the mechanism and effectors of DNA demethylation are less well understood, but recent reports suggest this process likely requires activity TET enzyme family [2,3]. Post-translational modifications of histones include methylation, acetylation, phosphorylation, ubiquitination, sumoylation or ADP-ribosylation (reviewed in [4]. Together, epigenetic modifications introduce changes in local chromatin topography that affect docking and/or activity of transcriptional complexes and subsequently alter patterns of gene expression in developmental stage and cell context-specific manner.

Methylation of histone residues represents a classical paradigm linking epigenetics to cell fate and identity. This is best illustrated by the antagonistic forces of Polycomb (PcG) and Trithorax (Trx) group protein complexes on regulation of key developmental loci such as *Hox* gene clusters (reviewed in [5]. In general, the activity of PcG protein complexes PRC2 and PRC1 have been associated with gene silencing, and Trx complexes (compass-like or MLL, Mixed Lineage Leukemia, complexes) with gene activation. The histone methyltransferase (HMT) EZH2 (Enhancer of Zeste Homolog 2), of the PRC2 complex catalyzes tri-methylation of lysine 27 of histone H3 (H3K27me3). This covalent mark serves as a docking site for the PRC1 complex which mono-ubiquitinates lysine 119 of histone H2A (H2AK119Ub) and thus initiates gene silencing. MLL (MLL1 to 5) containing complexes counteract these epigenetic marks via tri-methylation of lysine 4 in histone H3 (H3K4me3) at transcription start sites, a mark associated with active gene transcription [6], and recruitment of H3K27me3 demethylases UTX and JMJD3 [7-9]. Additional Trx-mediated modifications such as acetylation of H3K27 (H3K27Ac) and di-methylation of H3K36 (H3K36me2) further oppose the PcG mediated gene repression. In embryonic stem cells (ESC), many loci encoding developmental regulators carry both, the H3K27me3 (OFF) and H3K4me3 (ON) epigenetic cues, poised for repression or activation depending on cell specific context [10,11].

Identification of histone demethylating enzymes and their ability to disrupt the thermodynamically stable N-CH3 bond support the model predicting that histone methylation

status evolves through highly dynamic and finely regulated processes (reviewed in [12]. Histone demethylases (HDM) integrate into multi-unit complexes, comprising other chromatin modifiers and nuclear factors, and the combinatorial outcome likely dictates transcriptional repression or activation. Histone methylation can occur either on lysine (K) or on arginine (R) residues. Removal of a methylation mark can occur via enzymatic reactions of amine oxidation, deimination and hydroxylation. Demethylation of arginine residues is carried out by the peptidyl arginine deiminase (PADI) enzyme family which convert the positively charged arginine into neutral citrulline (reviewed in [13]. The lysine specific demethylase 1 (LSD1/KDM1A)-related HDM can demethylate mono- and di-, but not trimethylated lysine residues. LSD1 acts as part of a multiprotein complex comprising other nuclear factors proposed to modulate the activity of holoenzyme. The possibility that trimethylated lysine residues represent permanent histone modifications was further disproved by the discovery of the Jumonji C (JmjC) domain-containing HMD capable of removing all three lysine methylation states by an oxydative reaction requiring α-ketoglutarate and iron (Fe^{2+}) as cofactors. To date, 27 JmjC family members have been identified in mammalian cells, and their characterization remains under intense scrutiny. Like the LSD1 family of HDMs, JmjC/JARID1 proteins act as components of multisubunit complexes, and the non-catalytic protein domains were proposed to mediate protein-protein interactions involved in regulation of demethylase activity and/or target specificity (reviewed in [14]). In addition, JMJD6 was reported to demethylate arginine residues [15] and bacterial Jumonji domain-containing AlkB protein is involved in DNA demethylation and repair [16,17] suggesting that JmjC substrates likely also include non-histone targets.

Activity of JmjC proteins results in dynamic changes of chromatin landscape which enable expression of distinct gene subsets required for diverse cellular processes such as self-renewal [18], proliferation [19], differentiation [20-24], cellular senescence [25,26] and cancer development [27-30]. In light of these findings, an established *in vivo* RNAi based screening strategy [31] was undertaken to assess the impact of JmjC gene down-regulation on adult primary HSC cell fate. We identify *Jarid1b* as a negative regulator of HSC self-renewal and progenitor cell expansion, while *Jhdm1f* positively influences blood reconstitution. Results from these experiments and possible downstream functional networks involved are presented in this paper.

4.4 Experimental procedures

Construction of shRNA retroviral vectors

For each gene target, 3-5 shRNAs were designed as single stranded oligonucleotides also incorporating miR-30 flanking arms using the RNAi Central shRNA design tool at http://katahdin.cshl.org:9331/RNAi_web/scripts/main2.pl and our previously established methodology [31].

Mice

C57BL/6J (Ly5.2$^+$) transplant recipients and C57BL/6Ly-Pep3b (Ly5.1$^+$) congenic bone marrow donor mice were bred and manipulated in a specific pathogen-free animal facility. Experimental procedures were revised and approved by the University of Montreal animal ethics committee (Comité de Déontologie de l'Expérimentation sur les Animaux de l'Université de Montréal).

Flow cytometry

Negative selection of hematopoietic lineage marker (GR-1$^+$, B220$^+$, Ter119$^+$) expressing cells (Lin$^-$) was performed as described [31]. Lin$^-$ bone marrow fraction was subsequently stained with PE-Cy7-conjugated anti-cKit, PE-Cy5-conjugated anti-Sca1 (eBioscience), PE-conjugated anti-CD150 (BioLegend) and FITC-conjugated anti-CD48 (BD Biosciences) antibodies, followed by isolation of HSC-enriched PE-Cy5-Sca1$^+$/PE-Cy7-cKit$^+$/PE-CD150$^+$/FITC-CD48$^-$/APC-Lin$^-$ cell population. Day E14.5d.p.c. fetal liver derived HSCs were purified from the Lin$^-$ cell populations by isolating the fraction of PE-Cy5-Sca1$^+$/PE-CD11b$^+$/PE-Cy7-CD150$^+$/FITC-CD48$^-$/APC-Lin$^-$ cells. Cells were sorted using the FACSAria cell sorter (Becton-Dickinson, San Jose, CA, USA). Proportions of transduced (GFP$^+$) transplant-derived (L5.1$^+$) peripheral blood leukocytes [32] and contribution of these cells to reconstitution of hematopoietic lineages [31,32] were determined as described**.**

HSC/progenitor cell culture, retroviral infection and transplantation

Suspension cell cultures of HSC/progenitor cell enriched populations, generation of retrovirus-producing GP+E-86 cells and infection of the sorted HSC/progenitor cells were performed as described [32]. For validation assays, 1500 CD150$^+$CD48$^-$ Lin$^-$ bone marrow derived cells were introduced in co-culture with retroviral producers in 96-well plates [32]. After 5-day incubation (day 0), the total cell content of each well was harvested, and partitioned for transplantation and cell culture. 1/8 of cell suspension, together with 150,000 freshly isolated bone marrow cells, was transplanted in sublethally irradiated congenic recipients (n=2 for each shRNA species). The remaining ½ of cell suspension was cultured for additional 7 days , then proportions of the recovered cells corresponding to 1/8 of the cell input were transplanted in 3 recipient mice (day 7). Exceptions from this design were Jhdmf1 knockdown validation experiments. To compensate for the shJhdmf1-associated loss of reconstituting activity, ¼ of day 0 cell suspensions was transplanted in each of the

3 recipients, and no continuing suspension cultures were initiated.

Clonogenic progenitor cell assays

The total numbers and distributions of myeloid clonogenic progenitors in various cell populations recovered from the 5-day co-culture with retroviral producers (day 0), or from the subsequent suspension cultures (day 7) were determined as described [31].

Microphotograpy

Images of Wright-stained cytospin cell preparations were acquired using a Leica DMIRB microscope with an HCXPL FluotarL 40×/0.6 numeric aperture objective (Leica) and a Retiga EX-i camera (Q-Imaging). Images were transformed directly into TIFF files using Adobe Photoshop Version 6.0 (Adobe Systems). In situ images of colonies in semisolid media were acquired using the same set up, but using the HC Pl Fluotar 10X/0.30, Ph 1 lens.

Competitive repopulating unit (CRU) assay

CRU frequencies in the sorted input HSC-enriched populations, and in cultures of sh-Luc- (n=1) or shJarid 1b-transduced cells (n=2) were determined using the in vivo limit dilution approach. Briefly, 24,000 $CD150^{+}CD48^{-}Lin^{-}Ly5.1^{+}$ sorted cells were co-cultured with retroviral producers for 5 days. After additional 7-day in vitro incubation, the proportion of GFP^{+} (hairpin-transduced) cells in each culture was determined, and populations with gene transfer efficiency >95% were selected for the *in vivo* limiting dilution assays. Different fractions of the recovered cells were transplanted into a series of sublethally irradiated (800 cGy, $^{137}\gamma$-Cs – radiation source) congenic $Ly5.2^{+}$recipients, together with $1.5x10^{5}$ $Ly5.2^{+}$ competitor bone marrow cells. At 20 and 51 weeks after transplantation, the proportions of transplant-derived ($Ly5.1^{+}$, for all cohorts of recipient mice) GFP^{+} (for recipients of hairpin-transduced cells) peripheral blood leukocytes were determined by flow cytometry. Recipients with > 0.2% myelo-lymphoid donor-derived cells were considered to be repopulated by at least 1 CRU. The frequency of CRU in each sample was calculated using Limit Dilution Analysis software (StemCell Technologies).

Q-RT-PCR assessment of JmjC gene expression in HSC enriched populations

Total RNA was isolated using Trizol™ according to the manufacturer's protocol (Invitrogen, CA) and treated with Dnase-I (Invitrogen, Carlsbad, CA) before cDNA synthesis. Reverse transcription of total RNA was performed using the MMLV-RT and random hexamer primers according to the manufacturer's protocol (Invitrogen). The cDNA was then amplified with the Taqman® PreAmp Master Mix for 12 cycles prior to Q-RT-PCR. Pre-amplification of the cDNA was performed according to the manufacturer's protocol (Applied Biosystems). Gene expression was assessed by Q-RT-PCR using the Roche LightCycler® 480 System (Roche, Basel, Switzerland). Reactions were performed in 384-well plates for 50 amplification cycles (95°C 10 s; 60°C 10 s; 72°C 10 s). Reference Taqman® gene assay (*Hprt*) was purchased from Applied Biosystems (Carlsbad, CA). Histone

demethylase gene expression assays were designed using Roche Universal ProbeLibrary Assay Design software (Advanced Primer3 settings) and were tested for maximum amplification efficiency by standard curve analysis (Efficiency = 0.98 to 1.1). For a given cDNA sample, threshold cycle (Ct) values were determined using the Advanced Relative Quantification algorithm for each target gene (Ct_{target}) as well as *Hprt* endogenous reference gene ($Ct_{reference}$). As a control for reliability of Ct values generated for each target and reference gene studied, each plate also comprised control cDNA samples. Reactions were performed in triplicate using cDNA from 2-3 independent samples. Average values were used for quantification. Primer and probe sequences are listed in Supplementary Table 2.

ChIP-chip analysis

shLuc and shJarid 1b cells recovered on day 7 (Fig. 4.5C) were fixed in PBS containing 1% formaldehyde for 10 min, then reaction was quenched with 125 mM glycine. Cells were lysed in hypotonic buffer (10 mM NaCl, 10 mM TRIS-Cl pH 8, 0.2% NP40 buffer), then nuclei were pelleted, resuspended lysis buffer (50 mM TRIS-Cl pH 8, 10 mM EDTA, 1% SDS), and sonicated to shear the DNA. To reduce the nonspecific IgG binding, the resulting material was pre-cleared using rabbit IgG and Protein G Sepharose adsorbtion. Chomatin immunoprecipitation of the pre-cleared material was performed using anti HistoneH3 (AbCam), or anti H3tri-MeK4 (Millipore) antibodies and Protein-G Sepharose. DNA-protein complexes were eluted with 100 mM $NaHCO_3$ and 1%SDS, treated with 0.3M NaCl and 3µg/mL RNaseA to reverse cross-links, and digested with Proteinase K to remove the protein. ChIP material was amplified using the WGA2 kit as recommended by manufacturer (Sigma), and purified through a QiaQuick column (Qiagen). For the input material (no IP), 1 µg of amplified DNA was labelled with Cy5-labelled 9mers (Trilink technologies) using 3'-5' exo- Klenow fragment (NEB), while the IP samples (shLuc or shJarid1b) were labelled with Cy3-labelled 9mers. Two-colour hybridizations on NimbleGen MM8 Deluxe Promoter HX1 arrays were carried out using 34µg of Cy5-labeled input and 34µg of Cy3-labeled test ChIP DNA using the NimbleGen hybridization kit as recommended by the manufacturer. Arrays were scanned at 5 µm resolution using a GenePix4000B scanner (Molecular Devices). Data extraction and peak finding analysis was done using NimbleScan 2.5 and visualized in the UCSC genome browser.

shRNA-mediated knockdown in NA10hd transduced HSCs

1500 purified $CD150^+CD48^-Lin^-$ bone marrow cells were co-cultured with irradiated (40 Gy) GP+E86 cells producing MSCV-NUP98-HOXA10HD-IRES-Puromycin (NA10HD) virus. After 4-day co-culture, cells were harvested and cultured for 6 days in the presence of Puromycin. Cells were then harvested and stained with APC/Cy7-conjugated anti-CD43 (BioLegend), APC-conjugated anti-Sca1, PE/Cy7-conjugated anti-Gr1 and PE/Cy5-conjugated anti-F4/80 (eBioscience). The sorted NA10-transduced $Sca1^+CD43^+Gr1^-F4/80^-$ cell subpopulation was co-cultured with GP+E86 cells producing shLuc, sh3Jarid1b or sh1Moz recombinant retroviruses. After 4 days, the nonadherent cells were recovered and

expanded for additional 6 days. To assess the extent of differentiation in these cultures, cells were stained with PE/Cy7-conjugated anti-Gr1 and PE/Cy5-conjugated anti F4/80-PE/Cy5 antibodies. Data were acquired using BD LSRII cytometer and FACSDiva Version 4.1 software (BD Biosciences PharMingen), and analyzed using the FlowJo Version 7.6.4 software (TreeStar).

4.5 Results

JmjC gene expression in HSC-enriched populations

We first assessed expression profiles of all JmjC genes in mouse bone marrow and fetal liver long-term repopulating (LTR)-HSC enriched populations. To ensure that our JmjC candidate survey accurately reflected expression of these genes in the LTR-HSC compartment, only sorted cell populations comprising ≥30% of functionally defined LTR-HSC, as evaluated by competitive repopulation (CRU) assays [33] (Supplementary Table 1), were processed for cDNA synthesis and gene expression studies. Results from these experiments indicated that all JmjC gene transcripts, except *Hairless*, can be detected at relatively high levels in these HSC-enriched populations (Fig. 4.1A). Of note, also well expressed in the primitive cell fractions was the gene encoding for the histone acetyltransferase MOZ (MYST3). This gene was reported to be essential for HSC expansion [34,35], and was therefore chosen as a control for our functional screen. Transcripts of four JmjC genes, namely *Jarid1b*, *Jmjd2d*, *Fbxl10* and *Jmjd1c*, were notably enriched for in the examined HSC-enriched fractions relative the total, non-separated bone marrow cell populations (Fig. 4.1B). In contrast, *Jhdm1d*, *Hspbap1*, *Hairless* were preferentially expressed in more mature cells. The differential transcript abundance of *Jarid1b*, *Jmjd2d*, *Fbxl10* and *Jmjd1c* in the primitive cell compartment questioned their implication in HSC biology, and these candidates were prioritized in our functional studies. They were thus assigned an arbitrary expression score value of one, while genes that were preferentially expressed in mature cells were attributed negative scores (Fig. 4.1B, lower panel).

Functional *in vivo* RNAi-based primary screen

To assess the potential role of JmjC demethylating enzymes in HSC biology, we designed an shRNA based screen which tested 23 of the 27 known *JmjC* mouse genes (Fig. 4.1C). In these experiments, shRNA *Luciferase* (shLuc) was used as a control, while shRNA *Moz* (shMoz) and *Nup98Hoxa10-homeodomain* (NA10hd) overexpression were used as controls for the loss and gain of HSC activity, respectively (data not shown for NA10hd, and [36,37]). An average of 3-5 different shRNA were tested per gene candidate. HDM-directed shRNA sequences (n=112, Supplementary Table 3) were subcloned in a LMP retroviral vector (Fig. 4.1D) and functionally assessed *in vivo* using our previously described procedure [31] and summarized Fig. 4.1D). The biological impact of each shRNA on HSC activity was evaluated by serial sampling of peripheral blood from the transplant recipient mice at early (4 weeks) and late (16-20 weeks) time points. Criteria for hit (shRNA) identification were based on the establishment of a "selection threshold scoring system" described in Fig. 4.2A. Overall, six hits were identified: *Jarid1b, Jmjd2a Jhdm1f* and *Jmjd1b* (selection threshold score (STS) of 2); *Hif1an* (STS of 3) and *Jarid1a* (STS of 4). Four of these genes, namely *Jarid1a, Jarid1b, Jmjd2a*, *Hif1an,* were identified as potential negative regulators of HSC activity (Fig. 4.2B, green shaded areas), while *Jhdm1f* and *Jmjd1b* (Fig. 4.2, red area), as putative positive regulators.

JmjC HDM knockdown validation experiments

Hit validation was restricted to proven JmjC domain containing histone demethylases. HIF1AN demethylase, for example, targets the transcription factor HIF1α, and was therefore not included in the validation steps of this study. For technical considerations we also limited our validation studies of the potential positive regulators to *Jhdm1f*. The increased hematopoietic reconstitution levels observed with shRNA mediated knockdown of the three remaining hits (*Jarid1a, Jarid1b, Jmjd2a*) prompted us to examine how the transduced HSC would behave *in vitro*, where control HSC normally rapidly exhaust [32]. For these validation experiments, sorted HSC-enriched populations were seeded in 96-well plates on retroviral producers, and HSC activity was monitored over a 7 day period as depicted in Fig. 4.3A. A gain-of-function phenotype for *Jarid1a* or *Jmjd2a* could not be confirmed upon shRNA transduction and prolonged *in vitro* culture (data not shown).

Conversely, reducing *Jarid1b* levels in HSC populations clearly conferred a competitive advantage to the freshly transduced cells when compared to shLuc controls (Fig. 4.3B, left panel: n=3 different shRNA to Jarid1b, day 0 transplanted cells). Importantly, a positive impact on HSC activity was even more noticeable for cells transplanted after one week of *in vitro* culture (Fig. 4.3B, middle and right panels, cells transplanted after 7-day culture), a time point at which our previous studies demonstrated a clear reduction of the background stochastic noise. Proportions of shRNA-transduced (GFP^+) peripheral blood cells in recipients of shJarid1b-transduced cells remained well above those determined for shLuc controls. This advantage was sustained for a follow-up interval of 10 months (Fig. 4.3B). Knockdown efficiencies of biologically active shRNA (sh2,3,4-Jarid1b) were determined for freshly transduced cells, and the Q-RT-PCR-based assays revealed a 40 to 50% decrease in Jarid1b mRNA levels compared to controls (Fig. 4.3C). For loss-of-fucntion validation experiments (Fig. 4.3D), greater numbers of freshly infected cells were used for transplantation (1/4 vs 1/8 well, day 0 cells only, Fig. 4.1D vs 4.3A), and confirmed decreased HSC activity phenotype associated with shRNA against *Jhdm1f* (3 different constructs, Fig. 4.3D) relative to control cells. Validation experiments thus uncovered one negative (*Jarid1b*) and one positive (*Jhdm1f*) regulator of HSC activity (Fig.4.3E). The striking impact of *Jarid1b* knockdown on blood reconstitution oriented research towards elucidation of the JARID1B-modulated cellular and molecular responses, and the effects of *Jhdm1f* knockdown were not further analyzed.

Jarid1b knockdown decreases hematopoietic cell differentiation in vitro

Sh2- or sh3Jarid1b-transduced primitive hematopoietic cell populations had a ~1.5-2-fold proliferative advantage *in vitro* compared to shLuc controls, while *Moz* knockdown halted expansion of the transduced cells (Fig. 4.4A, left panel). The expanded shJarid1b-transduced populations comprised high proportions of morphologically immature cells (Fig. 4.4A, right panel), and lower percentages of differentiated ($Gr1^+$) myeloid cells than

shLuc controls (Fig. 4.4B). Moreover, fractions of primitive ($Gr1^-$) shJarid1b-transduced cells were comparable to that determined in response to NA10hd, a well characterized enhancer of *in vitro* HSC/progenitor cell expansion, while a marked elevation in differentiation was observed for shMoz loss-of-function control (Fig. 4.4B). During the 7-day culture period, the numbers of shJarid1b-transduced clonogenic progenitor cells (colony forming cell, CFC) increased ~3-fold compared to shLuc and shMoz controls (Fig.4.4C). *Jarid1b* knockdown enhanced the proliferative activity of individual CFC as evidenced by the increase in sizes of colonies compared to shMoz controls (Fig.4.4D), and promoted expansion of the highly proliferative granulocyte-macrophage progenitors (Fig. 4.4E). Although the total CFC contents of shLuc and shMoz control cultures were comparable (Fig. 4.4C), and both cell populations differentiated in granulocytes and macrophages (Fig. 4.4E), the antiproliferative effect of *Moz* knockdown was evident from the decrease in sizes of shMoz clones compared to shLuc controls (data not shown).

Modulations of *Jarid1b* levels could promote *in vitro* primitive cell expansion by inhibiting cell fate commitment pathways, including differentiation, senescence and apoptosis, or by favoring cell cycle progression. Accordingly, expression levels of genes implicated in these pathways were determined in expanded shJarid1b and shMoz-cells, and compared to shLuc controls. Q-RT-PCR assays involving selected canditates revealed a marked downregulation of differentiation associated genes *Hairless* (*Hr*) and *Pu.1* in shJarid1b-cells compared to shMoz control (Fig. 4.4F). No major changes in expression levels of genes regulating senescence (*Cdkn2a* (*p16*) and *Cdkn2d* (*p19*)) or apoptosis (*Bcl2*, *Mcl1*) were detected in shJarid1b-cells, while modest increases in *c-Myc* and decreases in *Mad1* levels resembled those determined for *Hoxb4*-overexpressing cells (data not shown, and [38]. *Moz* knockdown was, however, clearly associated with upregulation of *Hr*, *Cdkn2a* and *Cdkn2d* expression. Together, these observations suggest that *Jarid1b* knockdown likely promoted *in vitro* expansion of HSC/progenitors by suppressing their differentiation, while cells remained permissive to cell cycle re-entry. In contrast, reduced dosage of *Moz* enforced commitment to differentiation and senescence cell fate pathways.

Jarid1b negatively regulates HSC self-renewal

Following a 7-day *in vitro* culture interval (Fig. 4.3A), transplanted shJarid1b-transduced cells (GFP^+) sustained production of peripheral blood cells at levels superior to those of controls over extended periods of time (Fig. 4.3B). All recipients of shJarid1b-cells had normal numbers of total bone marrow mononuclear cells (MNC), and no splenomegaly was observed (Fig. 4.5A, top panels). Contributions of the transduced (GFP^+) shLuc- and shJarid1b-cells to myeloid progenitor cell compartments were comparable (Fig. 4.5A, left bottom panel), but we observed ~8-10-fold increase in the frequencies of shJarid1b-multilineage progenitors (Colony Forming Unit-Granulocyte, Erythroid, Macrophage, Megakaryocyte, CFU-GEMM) compared to controls (Fig. 4.5A, right bottom panel). This difference in immature progenitor cell content remained benign, and no leukemia development was observed during the 12 month observation period. Moreover, the

transplanted shJarid1b-cells generated normal proportions of myeloid ($Mac1^+/CD11b^+$), B-lymphoid ($B220^+/CD45R^+$) and T-lymphoid ($CD4^+$, $CD8^+$) progeny (Fig. 4.5B), suggesting that the *in vivo* differentiation ability of the transduced cells was not affected.

These observations suggested that the enhanced reconstitution capacity of shJarid1b-bone marrow cells could result from enhanced activity in the progenitor cell compartment, but did not exclude the possibility that *Jarid1b* knockdown altered HSC cell fate decisions to favour self-renewal divisions leading to expansion of HSC populations. To address this issue, we introduced equal numbers of HSC-enriched ($CD150^+CD48^-Lin^-$) cell populations in co-culture with shLuc or shJarid1b retroviral producers, and determined HSC frequencies in samples immediately after cell sorting and after a cumulative 12-day *ex vivo* culture period (Fig. 4.5C, top panel), using the competitive repopulation assay (CRU). CRU numbers in cell populations recovered from shLuc cultures (Fig. 4.5C, green bar) were comparable to those determined for the input cell population (Fig. 4.5C, red bar) suggesting no major gain or loss of HSCs during the *in vitro* incubation. In contrast, the CRU numbers in shJarid1b cultures increased 8- to 20-fold above the numbers determined for either the corresponding shLuc samples, or for the sorted cells before the start of shJarid1b infection (Fig. 4.5C, blue bars), suggesting that *Jarid1b* knockdown promoted the *in vitro* expansion of long term-repopulating HSCs.

To verify the multipotency of these expanded HSC we performed Southern blot analyses of shJarid1b proviral integrations in DNA isolated from hematopoietic tissues of transplant recipients. Analyses revealed a common integration pattern shared between bone marrow (mostly myeloid, erythroid and B cells), thymus (mostly T cells) and spleen (B and T cells) cells of individual recipient (Fig. 4.5D, representative recipients) thus demonstrating that the ancestral cell(s) had the ability to generate all major blood lineages. Variations in positions, numbers and intensity of autoradiographic bands also suggested oligoclonal nature of hematopoietic reconstitution.

Impact of *Jarid1b* knockdown on 5' *Hoxa* gene expression

Two sets of observations prompted us to assess the effect of *Jarid1b* knockdown on expression of *Hoxa* cluster genes in HSC/progenitor cell populations: i, the impact of *Jarid1b* knockdown on *in vitro* mouse HSC expansion is similar to the effect observed with Hox gene overexpression [36,38]; and ii, JmjC members KDM6A (UTX) and KDM6B (JMJD3) have been recognized as positive regulators of Hox gene expression [25]. Q-RT-PCR assays revealed that *Jarid1b* knockdown induced a 2 to 5-fold increase in 5' *Hoxa* gene (*Hoxa5* to *Hoxa11*) expression levels compared to controls (Fig. 4.6A). *Jarid1b* knockdown also correlated with downregulation of the previously reported putative JARID1 targets [39-41] *Cav1*, *Sash1* and *Egr1*, and an increase in *Cxcl5* mRNA levels (Fig. 4.6B). We also analyzed the impact of shJarid1b on other known regulators of HSC activity, such as *Hes1*, *Meis1* and *Mll1* [42-45], and found no detectable differences between shJarid1b and control shLuc-cells. Of note, *Moz* knockdown, used in this study as a negative control for HSC

activity, resulted in a decrease in expression levels of these stemness-associated genes (Fig. 4.6C).

JARID1B has been proposed to target H3K4me3 [46] and to possess inherent specificity for removal of this modification associated with active gene transcription [47]. Given the up-regulation of *Hoxa* gene expression in the context of reduced *Jarid1b* dosage, we next compared the abundance of the H3K4me3 mark along *Hoxa* loci of shJarid1b and control shLuc-cells. We noted a similar, albeit not identical, pattern of enrichment for this mark at the 3' end of *Hoxa* gene cluster (*Hoxa1* to *Hoxa4*) in both conditions (Fig. 4.6D). However, consistent with the increased 5' *Hoxa* gene (*Hoxa5* to *Hoxa11*) expression detected in shJarid1b-cells (Fig. 4.6A), we also found a distinct enrichment for H3K4me3 peaks in the 5' portion of the *Hoxa* cluster of these cells compared to shLuc controls (Fig. 4.6D). This suggests that JARID1B may play an active role in the epigenetic regulation of *Hoxa* gene expression.

Study of epistasis between *Jarid1b* and *Nup98Hoxa10-homeodomain*

We postulated that *Jarid1b* could restrain HSC self-renewal by regulating, in addition to *Hoxa* cluster, also a number of other multipotency-associated genes. We examined, therefore, if *Jarid1b* knockdown could further reduce the probability of lineage commitment and/or differentiation in the context of *Hoxa* overexpressing HSC. To address this issue, HSC/progenitor cell populations were first transduced with the potent stimulator of self-renewal *NUP98Hoxa10-homeodomain* (NA10hd). The HSC-enriched populations ($Sca1^+CD43^+$ $Gr1^-F4/80^-$) of NA10hd-transduced cells were then infected with shJarid1b, shMoz, or control shLuc, and the effects of these hairpins on differentiation were measured by evaluating the proportions of mature $GR1^+$ $F4/80^+$ cell fractions in each condition (Fig. 4.6E). Results from these experiments showed that the combined effects of *NA10hd* overexpression and *Jarid1b* knockdown on differentiation were additive, and resulted in suppression of *in vitro* differentiation significantly ($p<0.0001$; Student t-test) below the levels determined for control NA10hd+shLuc-cells (Fig. 4.6F). In contrast, shMoz overrode the maturation arrest imposed by NA10hd overexpression, and enforced differentiation above the levels determined for controls (Fig. 4.6F). These observations suggested that in addition to *Hoxa* gene expression JARID1B likely also regulates other loci implicated in HSC cell fate.

Together, results presented in this report identify *Jarid1b* as a negative regulator of *in vitro* HSC expansion, and suggest a role for this histone demethylase in regulation of hematopoietic cell differentiation.

4.6 Discussion

In these studies, a putative role for the JmjC class of genes in HSC biology was queried through an RNAi mediated knockdown approach. Following the established pipeline strategy from HSC isolation and infection to *in vivo* functional assessment of hematopoietic reconstitution, the presented screen highlighted *Jarid1b* as a negative and *Jhmd1f* as a positive modulator of HSC activity.

Akin to *Hox* gene overexpression, differentiation was restrained in cultures initiated with shJarid1b-transduced HSC as evidenced by more primitive cell morphology, reduced granulocytic maturation, and greater expansion of clonogenic progenitors relative to control conditions. After transplantation, *ex vivo* expanded HSC were able to resume normal lympho-myeloid differentiation in recipient mice, in the absence of lineage skewing or myeloproliferative disorders for up to one year. Through CRU assay based quantifications of HSC frequencies, we showed a one log *ex vivo* expansion of shJarid1b-transduced HSC, suggesting that modulations of this gene can indeed influence stem cell fate decisions. Analyses of retroviral insertion patterns of DNA extracted from long-term recipient mice of shJarid1b-transduced cells confirmed the oligoclonal origin of the repopulating HSC pool, and the inherent multipotency of parental stem cells.

Mechanistically, the competitive advantage conferred to shJarid1b-transduced HSC could be at least in part attributed to the selective up-regulation of 5' *Hoxa* genes. Segmental transcription of this chromosomal region is well documented [48], and particularly targeted by epigenetic regulators such as MLL or its derived fusion oncoproteins, both in normal and leukemic stem cells [49,50]. Interestingly, the 5' *Hoxa* cluster is also targeted by the fusion oncoprotein NUP98-JARID1A in a mouse model system of myeloid leukemia [51]. In agreement with the proposed substrate specificity of JARID1B for H3K4me3 [41], we noted enrichment for this epigenetic mark on 5' *Hoxa* genes. It could thus be envisioned that JARID1B contributes to the negative regulation of *Hoxa* gene expression, and that its knockdown lifts this inhibition, ultimately leading to increased HSC activity. However, enhancement of NA10hd-induced maturation arrest with concomitant reductions in *Jarid1b* levels argues for regulation of additional cell fate determinants by this JmjC candidate to account for the HSC phenotype documented herein. Recent reports further support a role for JARID1B in transcriptional regulation of cell fate associated genes. In a model of myeloid differentiation, PU.1 induction of transcription factor EGR2 was reported to recruit JARID1B to the miR-17-92 promoter site, resulting in H3H4 demethylation and transcriptional silencing of the cluster required for proper monocyte maturation [21]. Transcripts of the miR-17-92 cluster are enriched for in the most primitive hematopoietic cell compartment and down-regulated upon differentiation [52-54]. In accordance, high levels of miR-17-92 expression were detected in patients with acute myeloid leukemia [55] suggesting that JARID1B activity is essential for proper differentiation of hematopoietic

cells. Supporting this possibility, Schmitz et al. [22] recently reported that *Jarid1b* depletion prevents neuronal differentiation of ESC by indirectly preventing H3K4 demethylation and silencing of loci comprising pluripotency and germ cell-associated genes.

Of note, transcript levels of *Jarid1b* are preferentially enriched for in HSC (Fig. 4.1B), suggesting either a role in preventing unrestricted self-renewal divisions, or in enabling timely and cell type specific downregulation of cell fate associated genes upon lineage commitment. Interestingly, 1q32 anomalies, which include *Jarid1b*, are common genetic mutations found in cells of chronic myeloid leukemia (CML) patients during disease progression characterized by block in myeloid differentiation [56,57]. This observation supports the hypothesis that low *Jarid1b* levels maintain stem cell fate, which combined with the proliferative activity of BCR-ABL, could result in development of overt acute leukemia. In our studies, transplant recipients of shJarid1b-transduced cells never developed leukemia. However, all our *Jarid1b* hairpins achieved similar, ~50% gene knockdown, and more drastic outcomes after complete *Jarid1b* depletion cannot be ruled out. Two *Jarid1b* null alleles have recently been described. Deletion of *Jarid1b* exon 1 was reported to result in death of mutant embryos between days E4.5 and E7.5 post conception [58], suggesting that *Jarid1b* is essential for early embryonic development. Mutant mice carrying a *Jarid1b* null allele generated by deletion of exon 6 were, in contrast, viable and exhibited no gross abnormalities [22], implying that *Jarid1b* activity is redundant, and can be compensated for by other *Jarid1* members. Precise elucidation of the role *Jarid1b* gene dosage plays in HSC and leukemia development will thus likely require analyses of HSC-specific *Jarid1b* deletion.

Overall, our studies point to a cellular and developmental stage specific effect of *Jarid1b* levels in modulation of HSC cell fate. A proposed working model integrating our results is presented in Fig. 4.7. To sustain stem cell fate, integrated influences from various epigenetic effectors should promote an active state of transcription at multipotency loci (Fig.4.7 upper panel). Activity of chromatin modifiers, including JARID1B, should culminate in maintenance of the H3K4me3 epigenetic mark on these loci, and exclusion of repressive marks, such as H3K9me3 or H3K27me3. Whether JHDM1F activity influences the methylation status of H3K9 or HSC fate decisions remain to be explored. On the contrary, removal of the active H3K4me3 epigenetic mark, potentially by JARID1B, could repress transcription of "stemness" genes and favor lineage commitment (Fig. 4.7, lower panel).

4.7 Figures

Figure 4.1. JmjC gene expression in HSC/progenitor cell populations and selection for RNAi screen. A) Transcript levels of histone demethylases (HDM) in HSC enriched cell populations. Results show ΔCT values determined by quantitative (Q) RT-PCR assays and represent average ± SEM of 5 independently sorted HSC populations (bone marrow, n=3; E14.5 d.p.c. fetal liver, n=2). Frequencies of long term-repopulating HSCs in these populations are shown in Supplementary table 1. **B)** Comparison of HDM transcript levels detected in HSCs and total bone marrow cell populations. Relative transcript quantities (RQ) are shown in log2 scale, and represent the ΔCT (HSC)/ΔCT(bone marrow) ratio determined by quantitative RT-PCR assays (average ± SEM, n=3). Expression score was determined from expression levels (ΔCT) and differential expression (RQ) of individual HDM: gene not expressed in HSC, -2; expressed in mature cells, -1; expressed in HSC, +1; others, 0. **C)** List of the 23 HDM candidates tested in primary screen. HDMs sub-families sharing similarities outside the catalytic domain are denoted by different shading. Left column, the revised current terminology; central column, synonyms; right column, proposed substrate specificity [12,59]. Four HDM genes were excluded from the screen: *Jarid1d* and *Uty* map to chromosome Y and are thus likely not required for regulation of HSC activity; *Pla3g4b* belongs to the cytosolic phospholipase A2 family; *Jhdm1e* knockdown could not be achieved by any hairpin in two independent experiments. **D)** Schema of shRNA retroviral vector backbone (top), and experimental outline (bottom) of the primary screen at the bottom. At 16 week after transplantation, increase in the proportion of GFP^+ peripheral blood leukocytes above their input levels reflects knockdown of a negative regulator of HSC activity (green box), and the inverse outcome denotes a positive HSC regulator (red box).

Figure 4.1

A

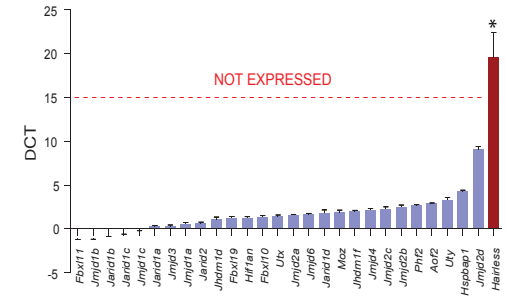

B

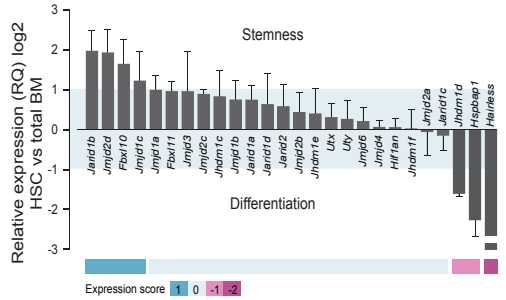

C

NAME	SYNONYMS	SUBSTRATE
KDM2A	JHDM1A / FBXL11	H3K36me$^{2/1}$
KDM2B	JHDM1B / FBXL10	H3K36me$^{2/1}$, H3K4me^{3}
	JHDM1D / KIAA1718	H3K9me$^{2/1}$, H3K27me$^{2/1}$
	JHDM1F / PHF8	H3K9me$^{2/1}$ / H4K20me^{1}
KDM3A	JMJD1A / JHDM2A / TSGA	H3K9me$^{2/1}$
KDM3B	JMJD1B	H3K9me$^{2/1}$
	JMJD1C	
	HR	
KDM4A	JMJD2A / JHDM3A	H3K9me$^{3/2}$, H3K36me$^{2/1}$
KDM4B	JMJD2B / JHDM3B	H3K9me$^{3/2}$, H3K36me$^{2/1}$
KDM4C	JMJD2C / JHDM3C / GASC1	H3K9me$^{3/2}$, H3K36me$^{2/1}$
KDM4D	JMJD2D / JHDM3D	H3K9me$^{3/2}$, H3K36me$^{2/1}$
KDM5A	JARID1A	H3K4me$^{3/2}$
KDM5B	JARID1B	H3K4me$^{3/2}$
KDM5C	JARID1C	H3K4me$^{3/2}$
	JARID2	
KDM6A	UTX	H3K27me$^{3/2}$
KDM6B	JMJD3	H3K27me$^{3/2}$
	JMJD4	
	JMJD5	
	JMJD6 / PTDSR / PSR	H3R2me^{2}, H4R3me^{2}
	HSPBAP1	
	HIF1AN	HIF1a-N803

D

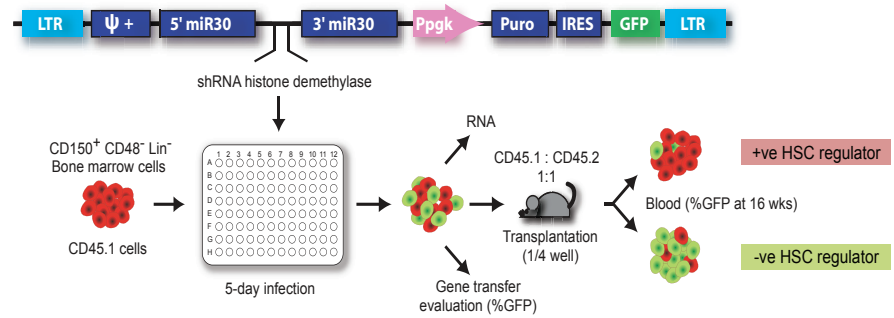

Figure 4.2. HDM hit identification. A) The selection threshold score for genes was calculated from the expression score (Fig. 4.1B) and HSC activity score or biological score, (Fig. 4.2B). Biological score represents the number of shRNAs per HDM which modulate HSC activity in 2 recipients above or below the 95% confidence interval range established for control shLuc cells (dotted blue lines in Fig. 4.2B-C). Selection threshold score of 2 and above identifies hits selected for validation experiments. **B)** Contributions of GFP$^+$ (shRNA-transduced) cells to peripheral blood reconstitution of recipients at 20 weeks after transplantation. Results are presented as proportions GFP$^+$ cells within the transplant-derived (Ly5.1$^+$) peripheral blood cells and are normalized for the gene transfer efficiency determined on the day of transplantation (day 0). Green shaded areas, suppressors of HSC activity; red shaded areas, enhancers of HSC activity.

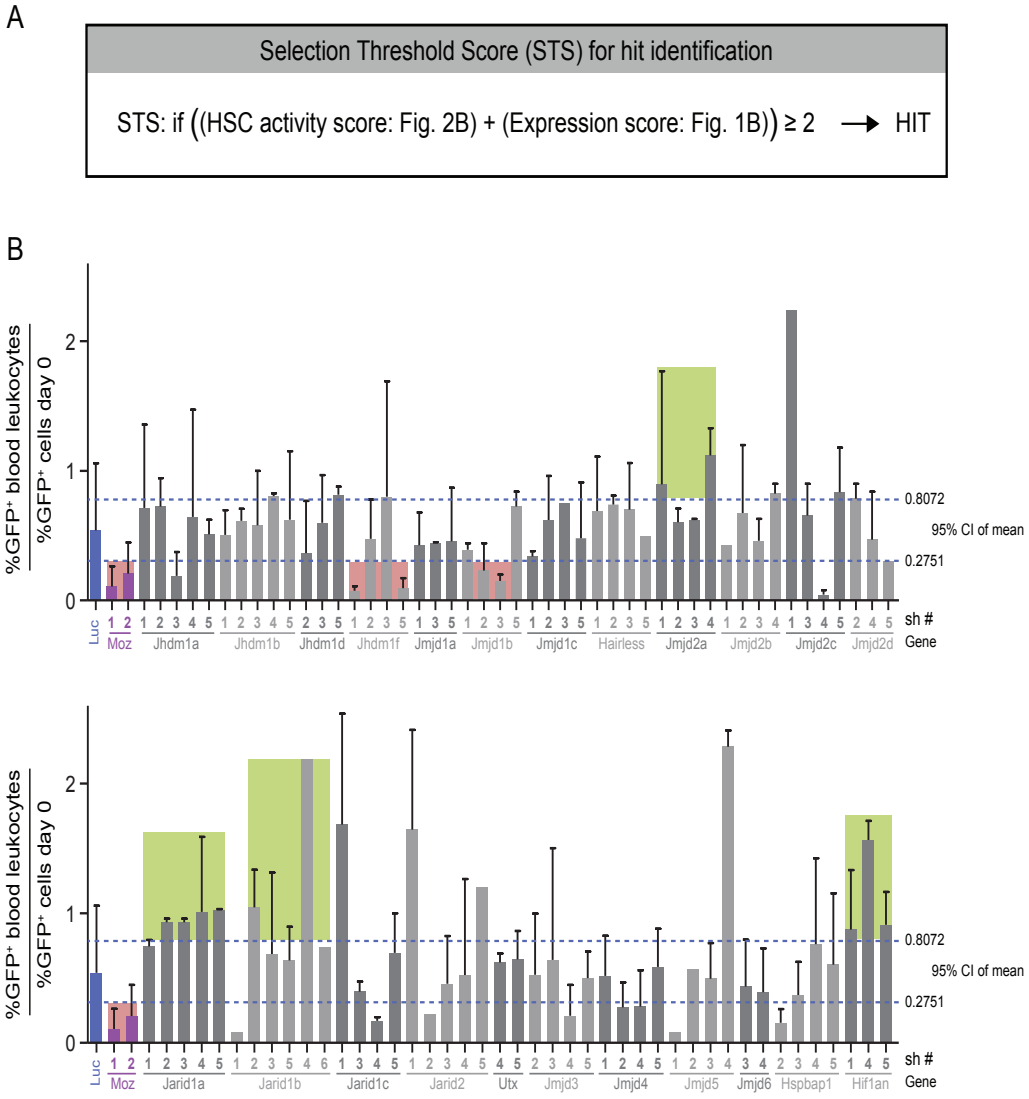

Figure 4.3. Validation assays for identified hits. A) Schema of experimental design. **B)** Long-term contribution of GFP^+ ($shLuc^+$, or $shJarid1b^+$, or $NA10hd^+$) cells to peripheral blood reconstitution of recipients. Left panel: recipients of day 0 cells; central and right panel, recipients of day 7 cells. NA10hd, cells engineered to overexpress NUP98Hoxa10-homeodomain fusion protein and green fluorescent protein (GFP). **C)** Evaluation of *Jarid1b* knockdown in GFP^+ shJarid1b-transduced cells compared to shLuc controls. Results represent average ± SEM (n=4) RQ values determined for 3 different hairpins. **D)** Long-term contribution of GFP^+ ($shLuc^+$, or $shMoz^+$, or $shJhdmf1^+$) cells to peripheral blood reconstitution in recipients of day 0 cells. Each recipient received a ¼ of the transduced cell population, or twice the number of input cells transplanted for validation experiment shown in Fig. 4.3A. E) Summary of screen results.

Figure 4.3

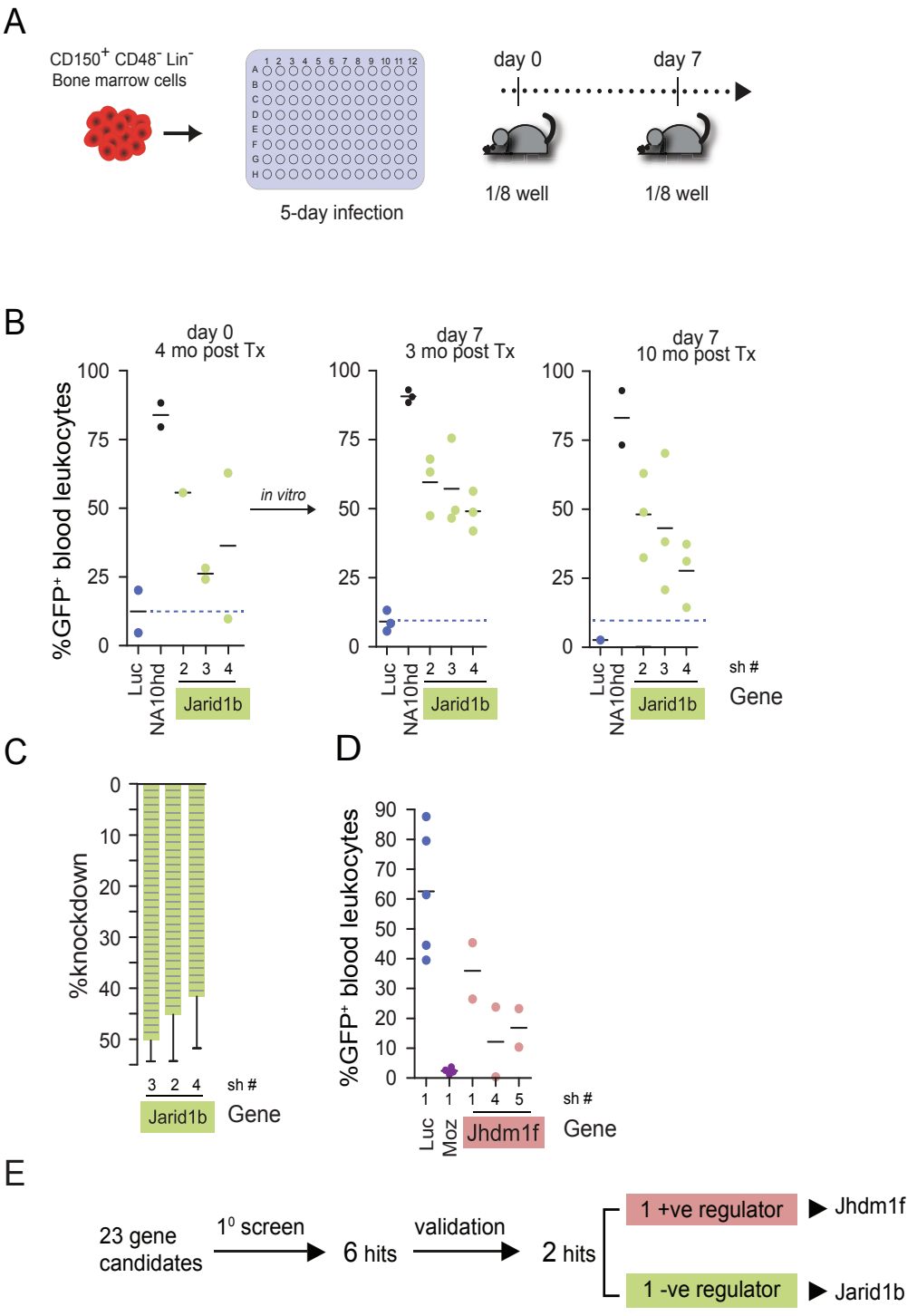
A
CD150+ CD48- Lin-
Bone marrow cells
5-day infection
day 0
day 7
1/8 well
1/8 well
B
day 0
4 mo post Tx
day 7
3 mo post Tx
day 7
10 mo post Tx
%GFP+ blood leukocytes
in vitro
Luc
NA10hd
Jarid1b
sh #
Gene
C
%knockdown
Jarid1b
D
%GFP+ blood leukocytes
Luc
Moz
Jhdm1f
E
23 gene candidates
1⁰ screen
6 hits
validation
2 hits
1 +ve regulator
Jhdm1f
1 -ve regulator
Jarid1b

Figure 4.4. *Jarid 1b* knockdown decreases hematopoietic cell differentiation *in vitro*. **A)** Left panel**:** *Jarid1b* knockdown increases yields of mononuclear cells in cultures initiated with shJarid-transduced HSC/progenitor cell populations (mean ±SD, n=2). Right panel: Wright-stained cytospin preparations of cells on day 9 of culture, 40x magnification. **B)** shJarid1b suppresses *in vitro* differentiation of HSC/progenitor cell populations. Proportions of $Gr1^+$ cells on day 9 of culture were determined by flow cytometry. Each dot represents an independent culture. **C)** Jarid1b knockdown enhances *in vitro* expansion of myeloid colony forming cells (CFC). The increase in CFC numbers was calculated from MNC and CFC numbers determined on days 2 and 9 (mean ± SD, n=2) **D)** Images of the predominant colony types. shJarid1b, colony forming unit granulocyte-macrophage (CFU-GM), high proliferative potential; shMoz, colony forming unit macrophage (CFU-M), low proliferation. Left panels, bright field; right panels, epifluorescence. **E)** Proportions of the highly proliferative CFU-GM in cultures of shRNA-transduced cells (mean ± SD, n=2). **F)** Q-RT-PCR-based comparison of cell fate-associated transcript levels in day 7 (Fig. 4.3A) shJarid1b and shMoz-cells compared to shLuc controls (mean ± SD, n=2).

Fig. 4.4

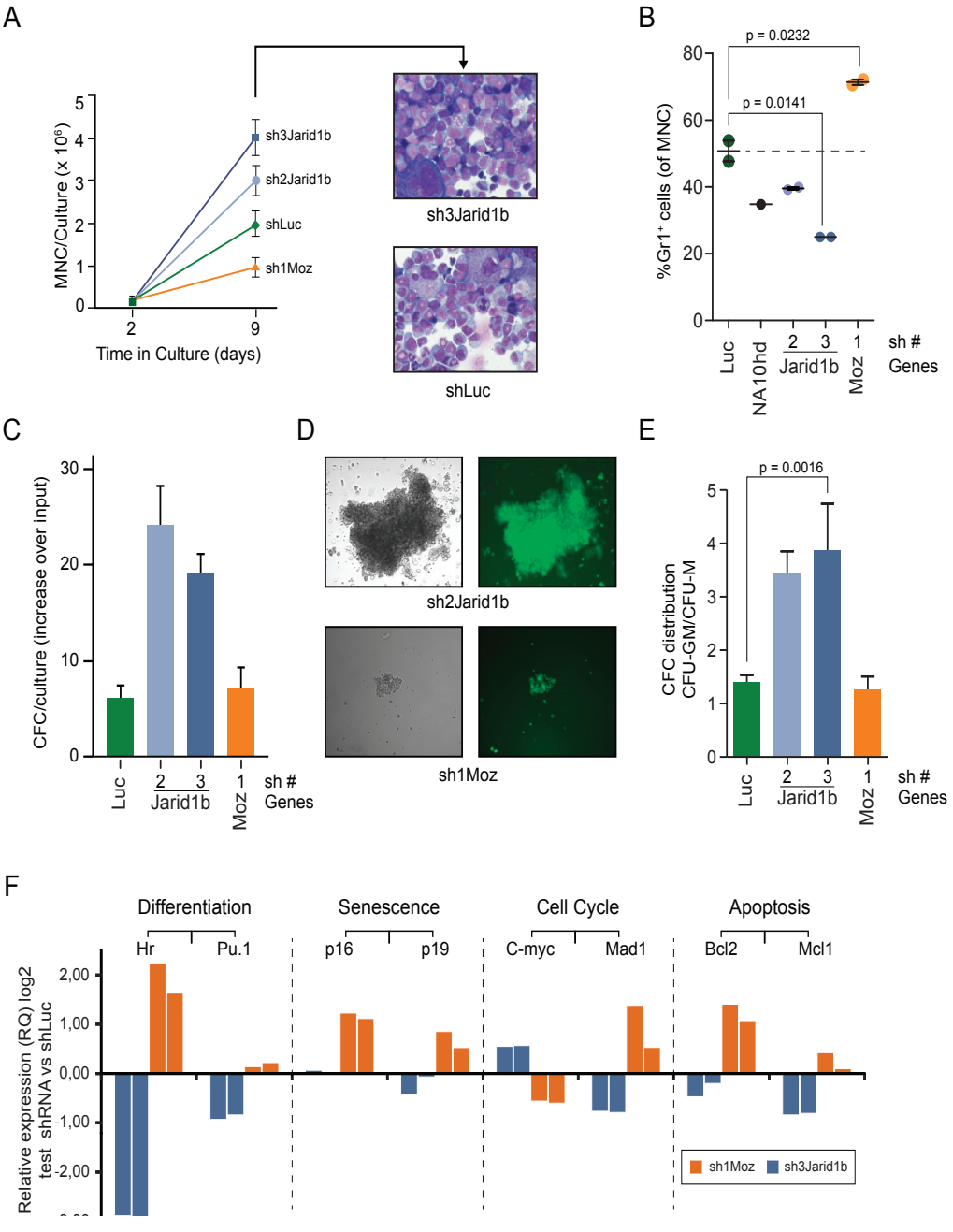
A
MNC/Culture (x 10⁶)
Time in Culture (days)
sh3Jarid1b
sh2Jarid1b
shLuc
sh1Moz
sh3Jarid1b
shLuc
B
p = 0.0232
p = 0.0141
%Gr1⁺ cells (of MNC)
Luc
NA10hd
2 3
Jarid1b
1
Moz
sh #
Genes
C
CFC/culture (increase over input)
Luc
2 3
Jarid1b
1
Moz
sh #
Genes
D
sh2Jarid1b
sh1Moz
E
p = 0.0016
CFC distribution
CFU-GM/CFU-M
Luc
2 3
Jarid1b
1
Moz
sh #
Genes
F
Differentiation
Hr
Pu.1
Senescence
p16
p19
Cell Cycle
C-myc
Mad1
Apoptosis
Bcl2
Mcl1
Relative expression (RQ) log2
test shRNA vs shLuc
sh1Moz
sh3Jarid1b

Figure 4.5. *In vitro*-expanded shJrarid1b-HSC retain long-term *in vivo* multipotency. A) Analysis of hematopoietic tissues in recipients of day 7 cells (Fig. 4.3B) at 1 year after transplantation. Upper panels: left, spleen weight; right, the total numbers of bone marrow cells pooled from pelvis, femur and tibia. Lower panels: left, CFC frequency in the GFP^+ bone marrow cell populations; right, proportions of GFP^+ multilineage progenitors (Colony Forming Unit-Granulocyte, Erythrocyte, Monocyte, Megakaryocyte, CFU-GEMM). Dots in the upper left plot represent the numbers of individual mice for which all the described parameters were analyzed. B) Contribution of day 7 (Fig. 4.3A) shJarid 1b (GFP^+) cells to reconstitution of myeloid ($Mac1^+$), B-lymphoid ($B220^+$) and T-lymphoid lineage ($CD4^+$, $CD8^+$) at 1 year after transplantation. An example of typical reconstitution observed in all recipients (n>10) is shown. C) Jarid1b knockdown promotes the *in vitro* expansion of LTR-HSC. Upper panel, experimental outline. Lower panel, CRU numbers in freshly sorted (i.e., input) and day 7 shRNA-transduced cell populations (mean ± SE). shJarid1b CRUs were determined in 2 independent experiments. D) Clonal analysis of proviral integrations in DNA isolated from hematopoietic tissues of mouse from shJarid1b cohort introduced in Fig. 4.5C. DNA was digested with EcoRI which cuts once within the provirus such that each DNA fragment recognized by the ^{32}P-labelled *Gfp* probe represents a unique integration event. Mouse ID#, the total dose of transplanted cells, and the estimated number of transplanted CRU are shown on top. T, thymus; S, spleen; BM, bone marrow.

Figure 4.5

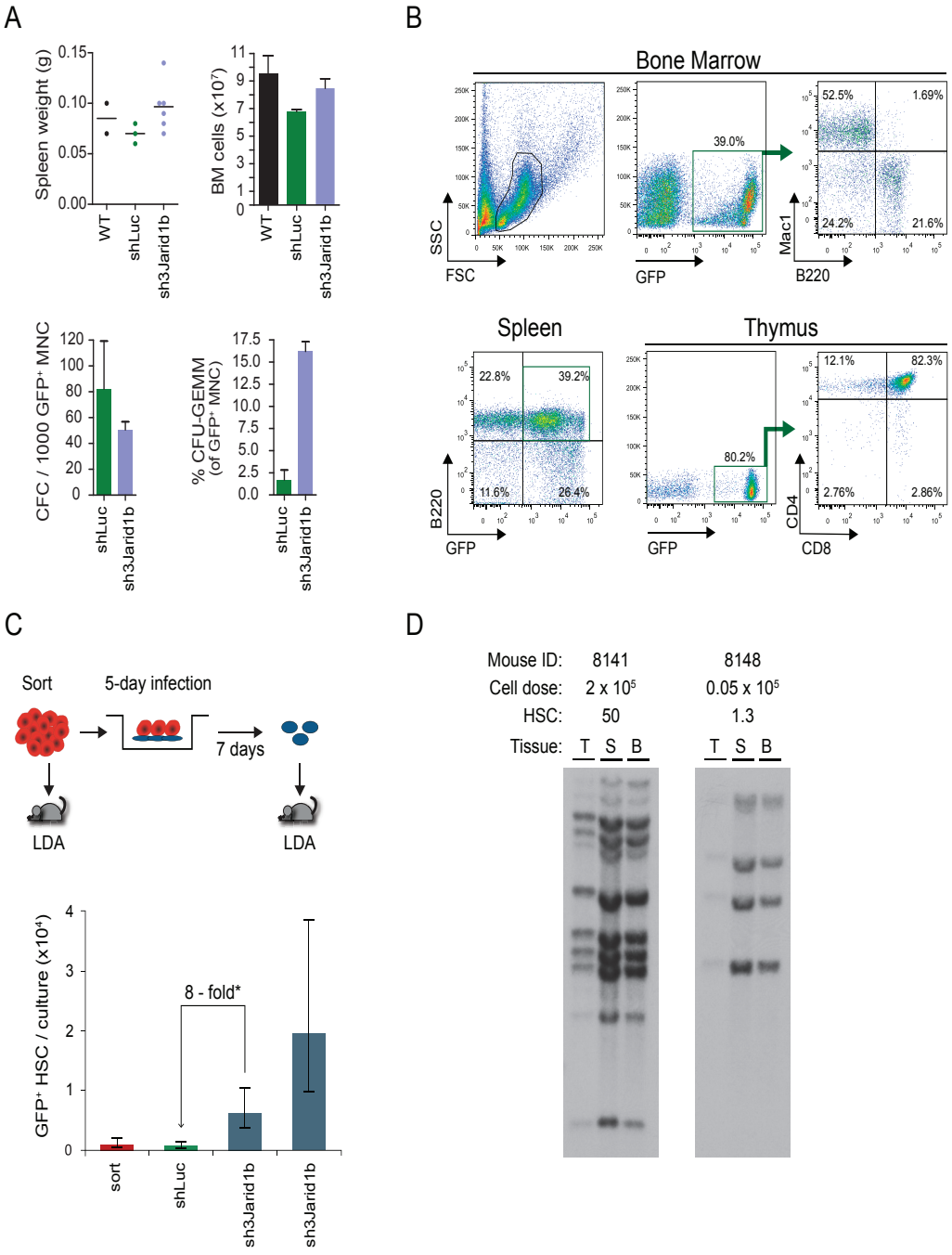
A
Spleen weight (g)
0.15
0.10
0.05
0.00
WT
shLuc
sh3Jarid1b
BM cells (x10⁷)
11
9
7
5
3
1
0
WT
shLuc
sh3Jarid1b
CFC / 1000 GFP⁺ MNC
120
100
80
60
40
20
0
shLuc
sh3Jarid1b
% CFU-GEMM (of GFP⁺ MNC)
17.5
15.0
12.5
10.0
7.5
5.0
2.5
0.0
shLuc
sh3Jarid1b
B
Bone Marrow
SSC
FSC
GFP
39.0%
Mac1
B220
52.5%
1.69%
24.2%
21.6%
Spleen
B220
GFP
22.8%
39.2%
11.6%
26.4%
Thymus
GFP
80.2%
CD4
CD8
12.1%
82.3%
2.76%
2.86%
C
Sort
5-day infection
7 days
LDA
LDA
GFP⁺ HSC / culture (x10⁴)
4
3
2
1
0
8 - fold*
sort
shLuc
sh3Jarid1b
sh3Jarid1b
D
Mouse ID: 8141 8148
Cell dose: 2 x 10⁵ 0.05 x 10⁵
HSC: 50 1.3
Tissue: T S B T S B

Figure 4.6. *Jarid1b* knockdown modulates molecular mechanisms implicated in maintenance of stemness. A) Relative quantities of *Hoxa* gene transcripts in shJarid1b-cells compared to shLuc controls. **B)** Independent experiment as described for Fig. 4.6A, but including transcripts of some previously identified JARID1B target genes. **C)** Relative quantities of transcripts denoting activity of genes implicated in maintenance of stemness in shJarid1b compared to shMoz-cells. RNA for all Q-RT-PCR assays was isolated from day 7 (Fig. 4.5C) cells. **D)** Enrichment of H3K4me3 marks (orange peaks) at 5'*Hoxa* loci in shJarid1b cells. Chromatin immunoprecipitation was was carried out using day 7 (Fig. 4.5C) shJarid1b or shLuc-cells. **E)** Experimental strategy for generation of *Nup98Hoxa10-homeodomain* (NA10hd) plus shRNA overexpressing cells. Following Puromycin selection, the $Sca1^{+}CD43^{-}$ $Gr1^{-}F4/80^{-}$ NA10hd-transduced cells were infected with shLuc-, shMoz-, and shJarid1b 1b-carrying retroviruses. **F)** Jarid1b knockdown suppresses differentiation of NA10hd overexpressing cells. Proportions of $Gr1^{+}F4/80^{+}$ (i.e. differentiated) cells in cultures were determined by flow cytometry on day 7 after shRNA transduction. Each dot represents individual culture comprising the transduced progeny of 1,500 $CD150^{+}CD48^{-}Lin^{-}$ bone marrow cells.

Figure 4.6

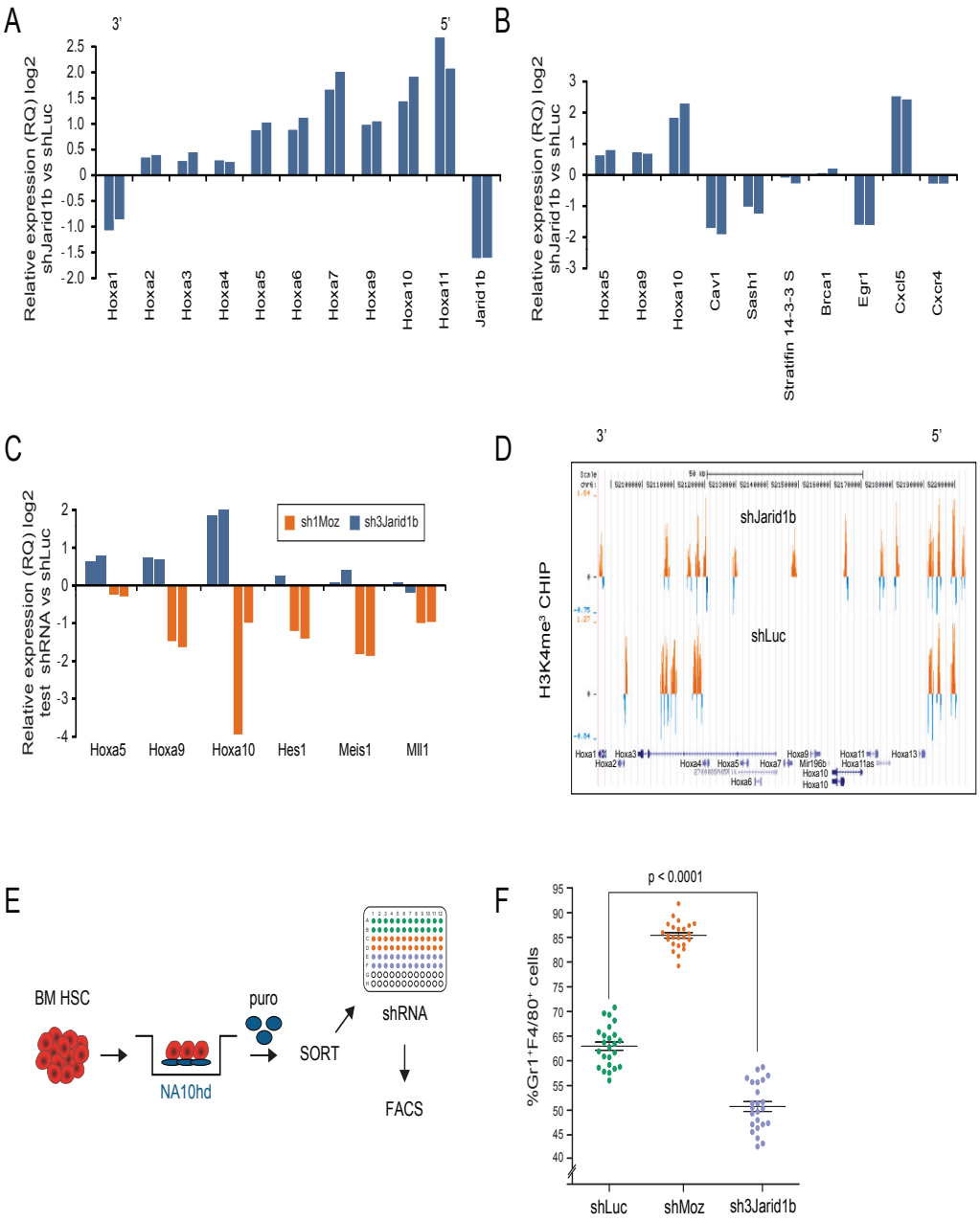
A
3'
5'
Relative expression (RQ) log2 shJarid1b vs shLuc
Hoxa1
Hoxa2
Hoxa3
Hoxa4
Hoxa5
Hoxa6
Hoxa7
Hoxa9
Hoxa10
Hoxa11
Jarid1b
B
Relative expression (RQ) log2 shJarid1b vs shLuc
Hoxa5
Hoxa9
Hoxa10
Cav1
Sash1
Stratifin 14-3-3 S
Brca1
Egr1
Cxcl5
Cxcr4
C
Relative expression (RQ) log2 test shRNA vs shLuc
sh1Moz
sh3Jarid1b
Hoxa5
Hoxa9
Hoxa10
Hes1
Meis1
Mll1
D
3'
5'
H3K4me3 CHIP
shJarid1b
shLuc
E
BM HSC
puro
NA10hd
SORT
shRNA
FACS
F
p < 0.0001
%Gr1+F4/80+ cells
shLuc
shMoz
sh3Jarid1b

Figure 4.7. Proposed model for JARID1B activity in modulation of HSC fate. Grey shaded area: JARID1B erases the tri-methyl marks of H3K4 at stemness loci and represses activity of multipotency genes. Pink area: Decrease in JARID1B activity shifts balance in favour of histone methylases, preserving the active H3K4me3 mark at stemness loci to sustain multipotency.

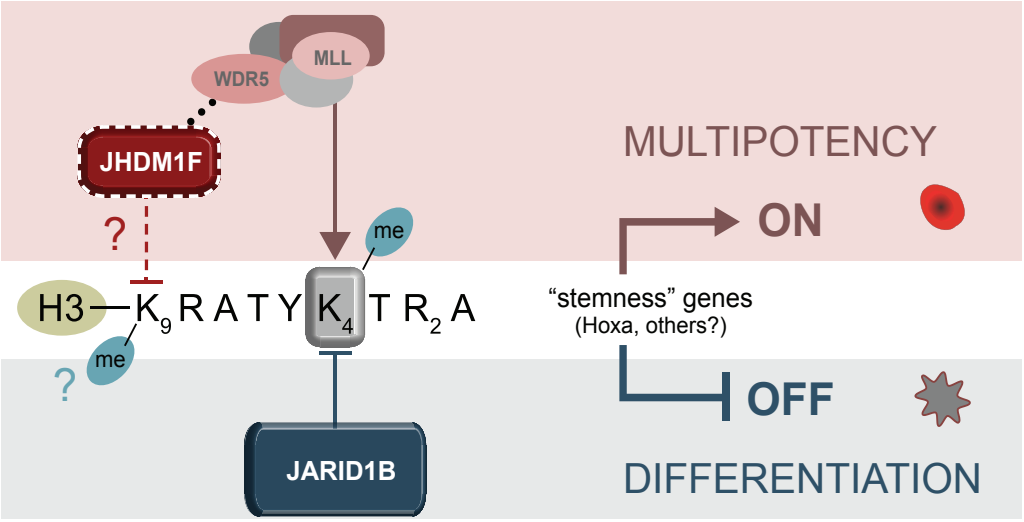

Table 4.S1. LTR-HSC frequencies (λ) of cells soted populations used for exression profile studies (Fig. 4.1)

soted cell population name	tissue (age)	HSC λ	markers for cell sorting
3wks BM2 KLSS	bone marrow (3 weeks)	1:2	CD150+ CD48- Sca1+ cKit+ Lin- (B220, Ter119, Gr1)
3wks BM1 SLAMSM	bone marrow (3 weeks)	1:4	CD150+ CD48- Sca1+ Mac1+ Lin- (B220, Ter119, Gr1)
4wks BM2 KLSS	bone marrow (4 weeks)	1:2	CD150+ CD48- Sca1+ cKit+ Lin- (B220, Ter119, Gr1)
4wks BM2 SLAMSM	bone marrow (4 weeks)	1:3	CD150+ CD48- Sca1+ Mac1+ Lin- (B220, Ter119, Gr1)
FL1 SLAMSM	fetal liver (E14.5)	1:2	CD150+ CD48- Sca1+ cKit+ Lin- (B220, Ter119, Gr1)

Table 4.S2: Pimers used for Q-RT-PCR assays (Exiquon Universal Probe library assays) Fig. 4.1, 4.3, 4.4 and 4.6

gene	revised name	NCBI ID	primer-A	primer-B
Jhdm1a / FbxI11	Kdm2a	NM_001001984	gctgcatctgcaacgagata	ttcagcaacccctctccat
Jhdm1b / FbxI10	Kdm2b	NM_001003953	gggcaggagtgttgacaatta	tatctctggcggtcaatcg
Jhdm1c / FbxI19		NM_172748	tgtctccaaaaagcagctcat	cacccagaaagcaccaactc
Jhdm1d / KIAA1718	Kdm7a	NM_001033430	tggatgtggaacgttatgtagg	gcacttttggtctgtcaggat
Jhdm1e / Phf2		NM_011078	aggtcatggacgaagaagca	gaagtgctctgggagttcgt
Jhdm1f / Phf8		NM_177201	cctgactatgctgccctcac	cctggatggcctcttgagt
Jmjd1a/ Jhdm2a / Tsga	Kdm3a	NM_001038695	ggacccaagacagcaaaatact	tggtaagttctgcttatgacatcc
Jmjd1b	Kdm3b	NM_001081256	ccccctggatacaggcata	gtaggctggctttgctcttc
Jmjd1c		XM_975833.2	gagtgctggaaacaaggacag	ggtggtctccaaaatccaga
Hairless		NM_021877	gcaacaagaggaacagagagg	gcaggatgtatccacaagtctg
Jmjd2a / Jhdm3a	Kdm4a	NM_172382	tggattgagtatggcaagca	tggagatcttcaccatatcttttct
Jmjd2b / Jhdm3b	Kdm4b	NM_172132	ggccagaagaggaaaacca	tcagcttagagaaaggggttgt
Jmjd2c / Jhdm3c / Gasc1	Kdm4c	NM_144787	ccagatccccaatgacactt	gcttagaacctcaggcaattct
Jmjd2d / Jhdm3d	Kdm4d	NM_173433	gaaggcgcaaataagtacgg	ggctactgggtgcacagac
Jarid1a / Rbp2	Kdm5a	BC010717	gatgtccccaaaggagactg	caaaggcttctcgaggtttg
Jarid1b/ Plu-1	Kdm5b	NM_152895	gagcagactgggatctgtaagg	gacatcacaagcgaatggtg
Jarid1c	Kdm5c	NM_013668	agtgacagtaagcggcacct	aggttccaaccacttgtagca
Jarid1d		NM_011419	gaaaaggcccatttttgctta	tgcctcacgtattataacttccaa
Jarid2		NM_021878	gcacttgtgctacctgtcca	tccaggcagaacacgacat
Utx	Kdm6a	NM_009483	cgtgaggtttcatgaagatgg	gagattcgtagcagcgaaca
Uty		NM_009484	gtggcatgggaggataaatg	tgtcttttgagaattgctttcatta
Jmjd3	Kdm6b	NM_001017426	cccatcaccgtcatcagg	ttggtggagaaaaggcctaa
Jmjd4		NM_178659	gaaggactacatccaagggagtt	tccaagtcattcaccaaggag
Jmjd5		NM_029842.4	gatcagcctgccaccaag	gggtaccatccgctctaaca
Jmjd6 / Ptdsr / Psr		NM_033398	ttccagctcgtcagactcg	ccatgctgcaggttctcc
Hspbap1		NM_175111	ggcaagcagatacggttcag	tcggtttcatactgaggaactg
Hif1an/Fih		NM_176958	gcctctatccataccctgtcc	caggattgtcaaagtccacct
Aof2/Lsd1	Kdm1a	NM_133872	agctgacgtttgaagccact	ctcggtggacaagcacagta
Myst3/Moz		NM_001081149	aagaggccgtctaaagaggaa	ggctttaggacaggagtgtca
Bcl2		NM_009754	ggagacgagttcaacgaaactt	aacagttgtaagataaccatttgagg
Brca1		NM_009764.3	tttagtcagcttgctgaagagc	ttgaaaaactaaaaccatttgtaagc
Cav1		NM_001243064	ccagggaaacctcctcaga	ccggatgggaacagtgtaga
Cxcl5		NM_009141.2	cctggtccgggatcttgt	catgaatggcgagatggaa
Cxcr4		NM_009911.3	tggaaccgatcagtgtgagt	gggcaggaagatcctattga
Egr1		NM_007913	ccctatgagcacctgaccac	tcgtttggctgggataactc
Hes1		NM_008235	acaccggacaaaccaaagac	cgcctcttctccatgatagg
Hoxa9		NM_010456	tccctgactgactatgcttgtg	gttggcagccgggttatt
Mad1		NM_010751	ggagcgctctgactctgatag	tcgtccgagtcactcacg
Mcl1		NM_008562	tgaaagctgaagtacagacaggat	actgcgctctccaagtcttc
Meis1		NM_010789.2	tcacactggccttaaagaggat	ccataatggggtaggtcgtc
Mll1		NM_001081049	gcagtgtttggggagagc	gagccaaaacctaagaactgct
Pu.1		NM_011355	ggagaagctgatggcttgg	caggcgaatcttttttcttgc
Sash1		NM_175155.4	atggctcctacccgacatt	tcatccgactgctctcttga
Stratifin 14-3-3 s		NM_018754	aaagggtgtggcgaagacta	agaagagttgggcgtggtc

Pimers used for Q-RT-PCR assays (TaqMan Dual-labelled probe assays (FAM-TAMRA)

	Forward	Reverse	Probe
Hoxa1	CCTTGGCAGTGGCGACTCT	GCGCAGGATTGGAAAGTTGT	CGAGCTTACCCCTCTGACCATGGGAT
Hoxa2	TCGCTGAGTGCCTGACATCT	AAAGCGTCGAGGTCTTGATTG	CCCCCTGTCGCTGATACATTTCAAAGTTCA
Hoxa3	CAATGGGTTCGCTTACAATGC	AGGCAGGTCGATGGTACTCAAC	CAGCCATACGCGCCGTCCG
Hoxa4	CCGGAGAATGAAGTGGAAGAAA	GCCGAGGCAGTGTTGGAA	CACAAACTTCCCAACACCAAGATGCGA
Hoxa5	TAGTTCCGTGAGCGAACAATTC	GCTGAGATCCATGCCATTGTAG	CTCGGCGAGCATGCACTCCG
Hoxa6	CCTATTTTGTGAATCCCACTTTC	CAGCTGGCCCAAGAAGGA	CCTGCCCAGCGGCCAGGA
Hoxa7	ACGCGCTTTTTAGCAAATATACG	GGGTGCAAAGGAGCAAGAAG	CTTCTCTCTTCCAAAATGCCGAGCCG
Hoxa10	CACAGGCCACTTCGTGTTCTT	TTGTCCGCAGCATCGTAGAG	TGCGCAGAACATCAAAGAAGAGAGCTCC
Hoxa11	AGATTTCTCCAGCCTCCCTTCTT	TGGAGGAGTAGGAGTATGTCATTGG	CCCCAGACCCCGTCTTCGCG
C-myc	TTGAAGGCTGGATTTCCTTTGGGC	TTGAAGGCTGGATTTCCTTTGGGC	CCTCAACGTGAACTTCACCAACAGGA
p16 (Cdkn2a)	TTCTTGGTGAAGTTCGTGCGATCC	TTGAGCAGAAGAGCTGCTACGTGA	TGCGCTCTGGCTTTCGTGAACATGTT
p19 (Cdkn2d)	GCCTTGCAGGTCATGATGTTTGGA	AGTACCGGAGGCATCTTGGACATT	TGCTTTGGAGCTCCTGAAGCAAGGT

Table 4.S3_ Oligo sequences_shRNAs_demethylases

Oligo name	Oligo Sequence
sh1 Myst3	TGCTGTTGACAGTGAGCGAAGCCTTACTTTCTTTATATACTAGTGAAGCCACAGATGTAGTATATAAAGAAAGTAAGGCTCTGCCTACTGCCTCGGA
sh2 Myst3	TGCTGTTGACAGTGAGCGATGCCAGACACTGCAGAGTTACTAGTGAAGCCACAGATGTAGTAACTCTGCAGTGTCTGGCAGTGCCTACTGCCTCGGA
sh3 Myst3	TGCTGTTGACAGTGAGCGAAGACACTATCCGCTTCTCAAGTAGTGAAGCCACAGATGTACTTGAGAAGCGGATAGTGTCTCTGCCTACTGCCTCGGA
sh4 Myst3	TGCTGTTGACAGTGAGCGAACCCAGTTTCTCTGTATATACTAGTGAAGCCACAGATGTAGTATATACAGAGAAACTGGGTCTGCCTACTGCCTCGGA
sh5 Myst3	TGCTGTTGACAGTGAGCGCCCAGCCAGTCTGCATCATCATTAGTGAAGCCACAGATGTAATGATGATGCAGACTGGCTGGATGCCTACTGCCTCGGA
sh1 Jarid1a	TGCTGTTGACAGTGAGCGCACACAGAATCTGCTGGATGATTAGTGAAGCCACAGATGTAATCATCCAGCAGATTCTGTGTTTGCCTACTGCCTCGGA
sh2 Jarid1a	TGCTGTTGACAGTGAGCGAAGAGCCTATCTGCTAAAGGACTAGTGAAGCCACAGATGTAGTCCTTTAGCAGATAGGCTCTCTGCCTACTGCCTCGGA
sh3 Jarid1a	TGCTGTTGACAGTGAGCGAACTTTGGATGTCATGAAGAAATAGTGAAGCCACAGATGTATTTCTTCATGACATCCAAAGTGTGCCTACTGCCTCGGA
sh4 Jarid1a	TGCTGTTGACAGTGAGCGAAGTCAGACTCTGGAGAAGTAATAGTGAAGCCACAGATGTATTACTTCTCCAGAGTCTGACTGTGCCTACTGCCTCGGA
sh5 Jarid1a	TGCTGTTGACAGTGAGCGCTGAGAGAATCAGTTGTTCAAATAGTGAAGCCACAGATGTATTTGAACAACTGATTCTCTCAATGCCTACTGCCTCGGA
1-shJarid1b	TGCTGTTGACAGTGAGCGCGCAGAGGCTATGAATATTAAATAGTGAAGCCACAGATGTATTTAATATTCATAGCCTCTGCTTGCCTACTGCCTCGGA
2-shJarid1b	TGCTGTTGACAGTGAGCGCGCAGTTTATATTGTGGAATAATAGTGAAGCCACAGATGTATTATTCCACAATATAAACTGCATGCCTACTGCCTCGGA
3-shJarid1b	TGCTGTTGACAGTGAGCGACGCCAGTGTGTGGAGCATTATTAGTGAAGCCACAGATGTAATAATGCTCCACACACTGGCGGTGCCTACTGCCTCGGA
4-shJarid1b	TGCTGTTGACAGTGAGCGCTGGGAGTAATTGATTCTGAAATAGTGAAGCCACAGATGTATTTCAGAATCAATTACTCCCAATGCCTACTGCCTCGGA
5-shJarid1b	TGCTGTTGACAGTGAGCGCACACACACTCACTTCATGTAATAGTGAAGCCACAGATGTATTACATGAAGTGAGTGTGTGTTTGCCTACTGCCTCGGA
sh6 JARID1B	TGCTGTTGACAGTGAGCGCCCTCACTGTCTGTAGCCATAATAGTGAAGCCACAGATGTATTATGGCTACAGACAGTGAGGATGCCTACTGCCTCGGA
sh7 JARID1B	TGCTGTTGACAGTGAGCGACTACATCATGTGAAAGAATTGTAGTGAAGCCACAGATGTACAATTCTTTCACATGATGTAGGTGCCTACTGCCTCGGA
sh8 JARID1B	TGCTGTTGACAGTGAGCGCTCAGTCTCTCTGGTTGTGGACTAGTGAAGCCACAGATGTAGTCCACAACCAGAGAGACTGATTGCCTACTGCCTCGGA
sh1 Jarid1c	TGCTGTTGACAGTGAGCGACCTGAGAAACTGGACCTGAACTAGTGAAGCCACAGATGTAGTTCAGGTCCAGTTTCTCAGGGTGCCTACTGCCTCGGA
sh2 Jarid1c	TGCTGTTGACAGTGAGCGCCCTCTGCAAGTGCTCCAGTAGTAGTGAAGCCACAGATGTACTACTGGAGCACTTGCAGAGGTTGCCTACTGCCTCGGA
sh3 Jarid1c	TGCTGTTGACAGTGAGCGCTCTCACCAACTTCTCTCTAACTAGTGAAGCCACAGATGTAGTTAGAGAGAAGTTGGTGAGATTGCCTACTGCCTCGGA
sh4 Jarid1c	TGCTGTTGACAGTGAGCGCAGAGTGAAACTGAACTATTTGTAGTGAAGCCACAGATGTACAAATAGTTCAGTTTCACTCTTTGCCTACTGCCTCGGA
sh5 Jarid1c	TGCTGTTGACAGTGAGCGATGGAAGAAGGTGGTTATGAAATAGTGAAGCCACAGATGTATTTCATAACCACCTTCTTCCACTGCCTACTGCCTCGGA
sh1 JARID2	TGCTGTTGACAGTGAGCGATGCCAGTACCTGCTTTCCTATTAGTGAAGCCACAGATGTAATAGGAAAGCAGGTACTGGCAGTGCCTACTGCCTCGGA
sh2 JARID2	TGCTGTTGACAGTGAGCGCTCTCAGAATGAGCAAGGAAAGTAGTGAAGCCACAGATGTACTTTCCTTGCTCATTCTGAGATTGCCTACTGCCTCGGA
sh3 JARID2	TGCTGTTGACAGTGAGCGAAGAAAGAGCCTGCTCACAAACTAGTGAAGCCACAGATGTAGTTTGTGAGCAGGCTCTTTCTCTGCCTACTGCCTCGGA
sh4 JARID2	TGCTGTTGACAGTGAGCGCGGCAAGAATATGCTGGGCAAATAGTGAAGCCACAGATGTATTTGCCCAGCATATTCTTGCCATGCCTACTGCCTCGGA
sh5 JARID2	TGCTGTTGACAGTGAGCGCGTGCCTGATTTCATTAGGAAATAGTGAAGCCACAGATGTATTTCCTAATGAAATCAGGCACATGCCTACTGCCTCGGA
sh1 JHDM1a	TGCTGTTGACAGTGAGCGCACTGCCTGTCTGATGAGAAACTAGTGAAGCCACAGATGTAGTTTCTCATCAGACAGGCAGTATGCCTACTGCCTCGGA
sh2 JHDM1a	TGCTGTTGACAGTGAGCGCTGCGTGTCTCTCCTCCGTTAATAGTGAAGCCACAGATGTATTAACGGAGGAGACACGCAATGCCTACTGCCTCGGA
sh3 JHDM1a	TGCTGTTGACAGTGAGCGCCCAGACCCTGTTCTTCCTAAGTAGTGAAGCCACAGATGTACTTAGGAAGAACAGGGTCTGGTTGCCTACTGCCTCGGA
sh4 JHDM1a	TGCTGTTGACAGTGAGCGCGCACAGGCTGTGCTATCCCAGTAGTGAAGCCACAGATGTACTGGGATAGCACAGCCTGTGCTTGCCTACTGCCTCGGA
sh5 JHDM1a	TGCTGTTGACAGTGAGCGCGATGAGAAACTGATACAGAAGTAGTGAAGCCACAGATGTACTTCTGTATCAGTTTCTCATCATGCCTACTGCCTCGGA
sh1 JHDM1b	TGCTGTTGACAGTGAGCGCCCTGTGCCTGTCCTTCTTCAATAGTGAAGCCACAGATGTATTGAAGAAGGACAGGCACAGGTTGCCTACTGCCTCGGA
sh2 JHDM1b	TGCTGTTGACAGTGAGCGCTGCCAGACCCTGATTTCACAGTAGTGAAGCCACAGATGTACTGTGAAATCAGGGTCTGGCATTGCCTACTGCCTCGGA
sh3 JHDM1b	TGCTGTTGACAGTGAGCGATGTGAGCAATTCATAGCTGAATAGTGAAGCCACAGATGTATTCAGCTATGAATTGCTCACAGTGCCTACTGCCTCGGA
sh4 JHDM1b	TGCTGTTGACAGTGAGCGCGTGGACTCACCTTACCGAATTTAGTGAAGCCACAGATGTAAATTCGGTAAGGTGAGTCCACTTGCCTACTGCCTCGGA
sh5 JHDM1b	TGCTGTTGACAGTGAGCGCACCAAGAATCAGGTAGAATAATAGTGAAGCCACAGATGTATTATTCTACCTGATTCTTGGTATGCCTACTGCCTCGGA
1-shJHDM1d (3' UTR)	TGCTGTTGACAGTGAGCGAAGACTGTATTTCCTTTGGAAATAGTGAAGCCACAGATGTATTTCCAAAGGAAATACAGTCTGTGCCTACTGCCTCGGA
2-shJHDM1d	TGCTGTTGACAGTGAGCGCGCCGATGAAATCATTGTAAAGTAGTGAAGCCACAGATGTACTTTACAATGATTTCATCGGCATGCCTACTGCCTCGGA
3-shJHDM1d (3' UTR)	TGCTGTTGACAGTGAGCGAACTCACTGAGTGCTCAGAAATTAGTGAAGCCACAGATGTAATTTCTGAGCACTCAGTGAGTGTGCCTACTGCCTCGGA
sh4 JHDM1d	TGCTGTTGACAGTGAGCGCTGTCTTAGTTTCCTGTCTTATTAGTGAAGCCACAGATGTAATAAGACAGGAAACTAAGACATTGCCTACTGCCTCGGA
sh5 JHDM1d	TGCTGTTGACAGTGAGCGCCCTAACAAGGTGCTGAATTAGTAGTGAAGCCACAGATGTACTAATTCAGCACCTTGTTAGGATGCCTACTGCCTCGGA
sh1 JHDM1f	TGCTGTTGACAGTGAGCGATCAGATGAAGTGATTCTGAAGTAGTGAAGCCACAGATGTACTTCAGAATCACTTCATCTGAGTGCCTACTGCCTCGGA
sh2 JHDM1f	TGCTGTTGACAGTGAGCGCGTCCTCAATGTCATTAGTTTGTAGTGAAGCCACAGATGTACAAACTAATGACATTGAGGACTTGCCTACTGCCTCGGA
sh3 JHDM1f	TGCTGTTGACAGTGAGCGAAGACCCAATGTGCAGAAGTACTAGTGAAGCCACAGATGTAGTACTTCTGCACATTGGGTCTCTGCCTACTGCCTCGGA
sh4 JHDM1f	TGCTGTTGACAGTGAGCGATCTCTTTGAGTGCTGGAGTAGTAGTGAAGCCACAGATGTACTACTCCAGCACTCAAAGAGAGTGCCTACTGCCTCGGA
sh5 JHDM1f	TGCTGTTGACAGTGAGCGCGGCATGAATATGATCAATATATAGTGAAGCCACAGATGTATATATTGATCATATTCATGCCTTGCCTACTGCCTCGGA
sh1 JMJD1a	TGCTGTTGACAGTGAGCGCGCAGCCAATGTCATGGTTTATTAGTGAAGCCACAGATGTAATAAACCATGACATTGGCTGCATGCCTACTGCCTCGGA
sh2 JMJD1a	TGCTGTTGACAGTGAGCGAACAGACAGGTTGCTTGGAAACTAGTGAAGCCACAGATGTAGTTTCCAAGCAACCTGTCTGTGTGCCTACTGCCTCGGA
sh3 JMJD1a	TGCTGTTGACAGTGAGCGATTTGATGATCTGATGGCCAACTAGTGAAGCCACAGATGTAGTTGGCCATCAGATCATCAAACTGCCTACTGCCTCGGA
sh4 JMJD1a	TGCTGTTGACAGTGAGCGCTGGAGTATGTGTAGATTGCTATAGTGAAGCCACAGATGTATAGCAATCTACACATACTCCAATGCCTACTGCCTCGGA
sh5 JMJD1a	TGCTGTTGACAGTGAGCGAAAGTAGACCTAGTCAATTGTATAGTGAAGCCACAGATGTATACAATTGACTAGGTCTACTTCTGCCTACTGCCTCGGA
sh1 JMJD1b	TGCTGTTGACAGTGAGCGAGCTGTTAATGTGATGGTGTATTAGTGAAGCCACAGATGTAATACACCATCACATTAACAGCGTGCCTACTGCCTCGGA
sh2 JMJD1b	TGCTGTTGACAGTGAGCGAACACACAGTGTCAGACTCAAGTAGTGAAGCCACAGATGTACTTGAGTCTGACACTGTGTGTCTGCCTACTGCCTCGGA
sh3 JMJD1b	TGCTGTTGACAGTGAGCGCTCCCAGTTTGTGCTCATTGAATAGTGAAGCCACAGATGTATTCAATGAGCACAAACTGGGAATGCCTACTGCCTCGGA
sh4 JMJD1b	TGCTGTTGACAGTGAGCGAGCTCTTTCTGTGCTGCCTCAATAGTGAAGCCACAGATGTATTGAGGCAGCACAGAAAGAGCGTGCCTACTGCCTCGGA
sh5 JMJD1b	TGCTGTTGACAGTGAGCGACAACATAAGGTGATGACTTACTAGTGAAGCCACAGATGTAGTAAGTCATCACCTTATGTTGCTGCCTACTGCCTCGGA
sh1 JMJD1c	TGCTGTTGACAGTGAGCGCCCTGATTCTGTGAAGTCTAAATAGTGAAGCCACAGATGTATTTAGACTTCACAGAATCAGGATGCCTACTGCCTCGGA
sh2 JMJD1c	TGCTGTTGACAGTGAGCGCGTTGTCAATGTCCTAGTCTATTAGTGAAGCCACAGATGTAATAGACTAGGACATTGACAACATGCCTACTGCCTCGGA
sh3 JMJD1c	TGCTGTTGACAGTGAGCGCGGAGAGAGACTGAACAAATACTAGTGAAGCCACAGATGTAGTATTTGTTCAGTCTCTCTCCATGCCTACTGCCTCGGA
sh4 JMJD1c	TGCTGTTGACAGTGAGCGCACAGATTACCTCAAACCAGAATAGTGAAGCCACAGATGTATTCTGGTTTGAGGTAATCTGTTTGCCTACTGCCTCGGA
sh5 JMJD1c	TGCTGTTGACAGTGAGCGAACAGAGGATCAGCTACATAAATAGTGAAGCCACAGATGTATTTATGTAGCTGATCCTCTGTGTGCCTACTGCCTCGGA
sh1 JMJD2A	TGCTGTTGACAGTGAGCGCGCTCACACTCTGGAAGCAAACTAGTGAAGCCACAGATGTAGTTTGCTTCCAGAGTGTGAGCTTGCCTACTGCCTCGGA
sh2 JMJD2A	TGCTGTTGACAGTGAGCGAACACAGAGTCTGTCTGGAAATTAGTGAAGCCACAGATGTAATTTCCAGACAGACTCTGTGTCTGCCTACTGCCTCGGA
sh3 JMJD2A	TGCTGTTGACAGTGAGCGACGCGATACAGTGAATTTGAAGTAGTGAAGCCACAGATGTACTTCAAATTCACTGTATCGCGGTGCCTACTGCCTCGGA
sh4 JMJD2A	TGCTGTTGACAGTGAGCGAACAGAGTCTGTCTGGAAATACTAGTGAAGCCACAGATGTAGTATTTCCAGACAGACTCTGTGTGCCTACTGCCTCGGA
sh5 JMJD2A	TGCTGTTGACAGTGAGCGATCAGACCAAATTATTTCTAATTAGTGAAGCCACAGATGTAATTAGAAATAATTTGGTCTGAGTGCCTACTGCCTCGGA
sh1 JMJD2B	TGCTGTTGACAGTGAGCGAAGGCCTCAAGTGATGAAGAAGTAGTGAAGCCACAGATGTACTTCTTCATCACTTGAGGCCTCTGCCTACTGCCTCGGA
sh2 JMJD2B	TGCTGTTGACAGTGAGCGAGGCCAGATCGTCATCACCAAGTAGTGAAGCCACAGATGTACTTGGTGATGACGATCTGGCCCTGCCTACTGCCTCGGA
sh3 JMJD2B	TGCTGTTGACAGTGAGCGAACAGCTGATCTTAAATGACAATAGTGAAGCCACAGATGTATTGTCATTTAAGATCAGCTGTCTGCCTACTGCCTCGGA
sh4 JMJD2B	TGCTGTTGACAGTGAGCGCGCTGAGCGCTTCCTATTCAAATAGTGAAGCCACAGATGTATTTGAATAGGAAGCGCTCAGCTTGCCTACTGCCTCGGA
sh5 JMJD2B	TGCTGTTGACAGTGAGCGACCGCTGTCTGTGGTCAAGCAGTAGTGAAGCCACAGATGTACTGCTTGACCACAGACAGCGGGTGCCTACTGCCTCGGA

Table 4.S3_ Oligo sequences_shRNAs_demethylases (suite)

Oligo name	Oligo Sequence
sh1 JMJD2C	TGCTGTTGACAGTGAGCGCTCCCAGAAGCTCTTAGTGAAGTAGTGAAGCCACAGATGTACTTCACTAAGAGCTTCTGGGATTGCCTACTGCCTCGGA
sh2 JMJD2C	TGCTGTTGACAGTGAGCGCACACTTTAGATGAAGAGTTACTAGTGAAGCCACAGATGTAGTAACTCTTCATCTAAAGTGTATGCCTACTGCCTCGGA
sh3 JMJD2C	TGCTGTTGACAGTGAGCGCCGGGACTGTTCACGCAATACATAGTGAAGCCACAGATGTATGTATTGCGTGAACAGTCCCGATGCCTACTGCCTCGGA
sh4 JMJD2C	TGCTGTTGACAGTGAGCGACAGGTAGCGAGTGATGAAGAATAGTGAAGCCACAGATGTATTCTTCATCACTCGCTACCTGCTGCCTACTGCCTCGGA
sh5 JMJD2C	TGCTGTTGACAGTGAGCGAACATATTAGTTGCTTCTGTAATAGTGAAGCCACAGATGTATTACAGAAGCAACTAATATGTCTGCCTACTGCCTCGGA
sh1 JMJD2D	TGCTGTTGACAGTGAGCGCGTTGAGTTTCTGCAAGCTAAATAGTGAAGCCACAGATGTATTTAGCTTGCAGAAACTCAACATGCCTACTGCCTCGGA
sh2 JMJD2D	TGCTGTTGACAGTGAGCGACCACAGCAAGTCTTCTTTATTTAGTGAAGCCACAGATGTAAATAAAGAAGACTTGCTGTGGCTGCCTACTGCCTCGGA
sh3 JMJD2D	TGCTGTTGACAGTGAGCGATCGCCCACTGTGCTTAAGGAGTAGTGAAGCCACAGATGTACTCCTTAAGCACAGTGGGCGAGTGCCTACTGCCTCGGA
sh4 JMJD2D	TGCTGTTGACAGTGAGCGACCAGGCAGTCTTATGACAATATAGTGAAGCCACAGATGTATATTGTCATAAGACTGCCTGGCTGCCTACTGCCTCGGA
sh5 JMJD2D	TGCTGTTGACAGTGAGCGCTGATATTTCGTCCAACCAAAGTAGTGAAGCCACAGATGTACTTTGGTTGGACGAAATATCATTGCCTACTGCCTCGGA
sh1 JMJD3	TGCTGTTGACAGTGAGCGCGCCCAGTCTGTGAAACCCAAGTAGTGAAGCCACAGATGTACTTGGGTTTCACAGACTGGGCATGCCTACTGCCTCGGA
sh2 JMJD3	TGCTGTTGACAGTGAGCGAGCACTCGATGCCTCATTCATATAGTGAAGCCACAGATGTATATGAATGAGGCATCGAGTGCCTGCCTACTGCCTCGGA
sh3 JMJD3	TGCTGTTGACAGTGAGCGAGCCCAGGGTCTCCTTCCCAAATAGTGAAGCCACAGATGTATTTGGGAAGGAGACCCTGGGCCTGCCTACTGCCTCGGA
sh4 JMJD3	TGCTGTTGACAGTGAGCGACCAGAGACTGTCACCTGGAAATAGTGAAGCCACAGATGTATTTCCAGGTGACAGTCTCTGGCTGCCTACTGCCTCGGA
sh5 JMJD3	TGCTGTTGACAGTGAGCGCCGCCAGGCCACCAAGAGAATATAGTGAAGCCACAGATGTATATTCTCTTGGTGGCCTGGCGTTGCCTACTGCCTCGGA
sh6 JMJD3	TGCTGTTGACAGTGAGCGCTGAGATTCTCTCTATGGGCTTTAGTGAAGCCACAGATGTAAAGCCCATAGAGAGAATCTCATTGCCTACTGCCTCGGA
sh1 JMJD4	TGCTGTTGACAGTGAGCGAACACACCCTGTCATCCCTAAGTAGTGAAGCCACAGATGTACTTAGGGATGACAGGGTGTGTCTGCCTACTGCCTCGGA
sh2 JMJD4	TGCTGTTGACAGTGAGCGCGGAGAGCATCTTCTTCAGAAGTAGTGAAGCCACAGATGTACTTCTGAAGAAGATGCTCTCCATGCCTACTGCCTCGGA
sh3 JMJD4	TGCTGTTGACAGTGAGCGCAGGCCTTGTGTGATAGATATTTAGTGAAGCCACAGATGTAAATATCTATCACACAAGGCCTATGCCTACTGCCTCGGA
sh4 JMJD4	TGCTGTTGACAGTGAGCGATTCGAGTATCTGCAGCAGAAGTAGTGAAGCCACAGATGTACTTCTGCTGCAGATACTCGAAGTGCCTACTGCCTCGGA
sh5 JMJD4	TGCTGTTGACAGTGAGCGATCCAAGACTCTCATCCTCTAGTAGTGAAGCCACAGATGTACTAGAGGATGAGAGTCTTGGAGTGCCTACTGCCTCGGA
sh1 JMJD5	TGCTGTTGACAGTGAGCGCGCTCCTGATGTCATGTTAGAGTAGTGAAGCCACAGATGTACTCTAACATGACATCAGGAGCTTGCCTACTGCCTCGGA
sh2 JMJD5	TGCTGTTGACAGTGAGCGCGCTGATCATGTCAGAGGACACTAGTGAAGCCACAGATGTAGTGTCCTCTGACATGATCAGCATGCCTACTGCCTCGGA
sh3 JMJD5	TGCTGTTGACAGTGAGCGAACACACCAGCTCCCAGGAAAGTAGTGAAGCCACAGATGTACTTTCCTGGGAGCTGGTGTGTCTGCCTACTGCCTCGGA
sh4 JMJD5	TGCTGTTGACAGTGAGCGATCCCAGACTCTCATGACAGTCTAGTGAAGCCACAGATGTAGACTGTCATGAGAGTCTGGGACTGCCTACTGCCTCGGA
sh5 JMJD5	TGCTGTTGACAGTGAGCGCGCTGGCAAGCTGCTCAGAGACTAGTGAAGCCACAGATGTAGTCTCTGAGCAGCTTGCCAGCTTGCCTACTGCCTCGGA
sh1 PTDSR (jmjd6)	TGCTGTTGACAGTGAGCGAAGTGTGAATCTGGGTCAGAAGTAGTGAAGCCACAGATGTACTTCTGACCCAGATTCACACTCTGCCTACTGCCTCGGA
sh2 PTDSR (jmjd6)	TGCTGTTGACAGTGAGCGACCGCTGTCTGTGCCAGGATATTAGTGAAGCCACAGATGTAATATCCTGGCACAGACAGCGGCTGCCTACTGCCTCGGA
sh3 PTDSR (jmjd6)	TGCTGTTGACAGTGAGCGATCGGTTAAGATGAAGATGAAGTAGTGAAGCCACAGATGTACTTCATCTTCATCTTAACCGAGTGCCTACTGCCTCGGA
sh4 PTDSR (jmjd6)	TGCTGTTGACAGTGAGCGCACCCTTTACCTATTTAATAAATAGTGAAGCCACAGATGTATTTATTAAATAGGTAAAGGGTTTGCCTACTGCCTCGGA
sh5 PTDSR (jmjd6)	TGCTGTTGACAGTGAGCGAAGGATGACTGTGTGAGCAAAGTAGTGAAGCCACAGATGTACTTTGCTCACACAGTCATCCTGTGCCTACTGCCTCGGA
sh1 UTX	TGCTGTTGACAGTGAGCGAACTGTGGATCTCCTGGGAGATTAGTGAAGCCACAGATGTAATCTCCCAGGAGATCCACAGTGTGCCTACTGCCTCGGA
sh2 UTX	TGCTGTTGACAGTGAGCGCGCTACGAATCTCTAATCTTAATAGTGAAGCCACAGATGTATTAAGATTAGAGATTCGTAGCATGCCTACTGCCTCGGA
sh3 UTX	TGCTGTTGACAGTGAGCGACCGCTTTCGGTGATGAGGAAATAGTGAAGCCACAGATGTATTTCCTCATCACCGAAAGCGGCTGCCTACTGCCTCGGA
sh4 UTX	TGCTGTTGACAGTGAGCGCCCTCTCACACTGCTACCTCAGTAGTGAAGCCACAGATGTACTGAGGTAGCAGTGTGAGAGGATGCCTACTGCCTCGGA
sh5 UTX	TGCTGTTGACAGTGAGCGCGCACATAGACTAAGAAATAAATAGTGAAGCCACAGATGTATTTATTTCTTAGTCTATGTGCATGCCTACTGCCTCGGA
sh1 hairless	TGCTGTTGACAGTGAGCGACCAGCTCTTGTTATACTTAACTAGTGAAGCCACAGATGTAGTTAAGTATAACAAGAGCTGGCTGCCTACTGCCTCGGA
sh2 hairless	TGCTGTTGACAGTGAGCGACCTCTCTCTGTGAGCTGCTAGTAGTGAAGCCACAGATGTACTAGCAGCTCACAGAGAGAGGGTGCCTACTGCCTCGGA
sh3 hairless	TGCTGTTGACAGTGAGCGACTTCTGACTCTGTAGGTCTACTAGTGAAGCCACAGATGTAGTAGACCTACAGAGTCAGAAGGTGCCTACTGCCTCGGA
sh4 hairless	TGCTGTTGACAGTGAGCGAAGCAAGCCTGTGAATCAGAAGTAGTGAAGCCACAGATGTACTTCTGATTCACAGGCTTGCTGTGCCTACTGCCTCGGA
sh5 hairless	TGCTGTTGACAGTGAGCGAAGTGATGACCGCATTACCAACTAGTGAAGCCACAGATGTAGTTGGTAATGCGGTCATCACTGTGCCTACTGCCTCGGA
sh1 Hspbap1	TGCTGTTGACAGTGAGCGAACAGTTTCTCTGCATACATAGTAGTGAAGCCACAGATGTACTATGTATGCAGAGAAACTGTGTGCCTACTGCCTCGGA
sh2 Hspbap1	TGCTGTTGACAGTGAGCGAGTTCATGGTGTGATTAAATATTAGTGAAGCCACAGATGTAATATTTAATCACACCATGAACGTGCCTACTGCCTCGGA
sh3 Hspbap1	TGCTGTTGACAGTGAGCGCAGTCTTTCTCTGATTCATCACTAGTGAAGCCACAGATGTAGTGATGAATCAGAGAAAGACTTTGCCTACTGCCTCGGA
sh4 Hspbap1	TGCTGTTGACAGTGAGCGCGGTCTTGGTTTGTTAGGTAAGTAGTGAAGCCACAGATGTACTTACCTAACAAACCAAGACCATGCCTACTGCCTCGGA
sh5 Hspbap1	TGCTGTTGACAGTGAGCGATGAGCCTTACTGCTGAATAAGTAGTGAAGCCACAGATGTACTTATTCAGCAGTAAGGCTCAGTGCCTACTGCCTCGGA
sh1 Hif1an	TGCTGTTGACAGTGAGCGCCCATATAGAGTCATTACTAAATAGTGAAGCCACAGATGTATTTAGTAATGACTCTATATGGTTGCCTACTGCCTCGGA
sh2 Hif1an	TGCTGTTGACAGTGAGCGACTCCTCTGTCTCCTTTCATAATAGTGAAGCCACAGATGTATTATGAAAGGAGACAGAGGAGCTGCCTACTGCCTCGGA
sh3 Hif1an	TGCTGTTGACAGTGAGCGAACCCATAAGTTCTTATACTATTAGTGAAGCCACAGATGTAATAGTATAAGAACTTATGGGTGTGCCTACTGCCTCGGA
sh4 Hif1an	TGCTGTTGACAGTGAGCGATTACTGCGTGTGCTCAGTTACTAGTGAAGCCACAGATGTAGTAACTGAGCACACGCAGTAACTGCCTACTGCCTCGGA
sh5 Hif1an	TGCTGTTGACAGTGAGCGCGCTATCTCAGTCCTTGGTAAGTAGTGAAGCCACAGATGTACTTACCAAGGACTGAGATAGCATGCCTACTGCCTCGGA

4.8 Acknowledgements

Authors acknowledge Mélanie Fréchette and Andrea Evelyn Mejia Alfaro for their assistance with animal care and transplantation experiments; IRIC's technological platform members: Danièle Gagné from Flow Cytometry Core Facility for help with cell sorting; Christian Charbonneau from Bio-imaging Core Facility for assistance with image acquisition and figure preparation; Raphaëlle Lambert, Pierre Chagnon and Simon Drouin from Genomic Core Facility for Q-RT-PCR and ChIP-chip experiments. This work was supported by grants from the Canadian Institute for Health Research (CIHR), the Canadian Cancer Society Research Institute and Fonds de Recherche en Santé du Québec (FRSQ) to GS. GS holds a Canada Research Chair in the Molecular Genetics of Stem Cells. SC is recipient of a CIHR Clinician-Scientist Fellowship Award and a Cole Foundation Transition Award. KH is recipient of a CIHR Post-Doctoral fellowship Award and a Cole Foundation Award. S.B.T. is recipient of National Health and Medical Research Council of Australia (NHMRC), Royal Australian College of Physicians and CIHR Post-doctoral Fellowships.

4.9 References

1. Fatemi M, Pao MM, Jeong S, et al. Footprinting of mammalian promoters: use of a CpG DNA methyltransferase revealing nucleosome positions at a single molecule level. *Nucleic Acids Res*. 2005;33(20):e176. Prepublished on 2005/11/30 as DOI 33/20/e176 [pii]

10.1093/nar/gni180.

2. He YF, Li BZ, Li Z, et al. Tet-mediated formation of 5-carboxylcytosine and its excision by TDG in mammalian DNA. *Science*. 2011;333(6047):1303-1307. Prepublished on 2011/08/06 as DOI science.1210944 [pii]

10.1126/science.1210944.

3. Ito S, Shen L, Dai Q, et al. Tet proteins can convert 5-methylcytosine to 5-formylcytosine and 5-carboxylcytosine. *Science*. 2011;333(6047):1300-1303. Prepublished on 2011/07/23 as DOI science.1210597 [pii]

10.1126/science.1210597.

4. Kouzarides T. Chromatin modifications and their function. *Cell*. 2007;128(4):693-705. Prepublished on 2007/02/27 as DOI S0092-8674(07)00184-5 [pii]

10.1016/j.cell.2007.02.005.

5. Mills AA. Throwing the cancer switch: reciprocal roles of polycomb and trithorax proteins. *Nat Rev Cancer*. 2010;10(10):669-682. Prepublished on 2010/09/25 as DOI nrc2931 [pii]

10.1038/nrc2931.

6. Barski A, Cuddapah S, Cui K, et al. High-resolution profiling of histone methylations in the human genome. *Cell*. 2007;129(4):823-837. Prepublished on 2007/05/22 as DOI S0092-8674(07)00600-9 [pii]

10.1016/j.cell.2007.05.009.

7. De Santa F, Totaro MG, Prosperini E, Notarbartolo S, Testa G, Natoli G. The histone H3 lysine-27 demethylase Jmjd3 links inflammation to inhibition of polycomb-mediated gene silencing. *Cell*. 2007;130(6):1083-1094. Prepublished on 2007/09/11 as DOI S0092-8674(07)01082-3 [pii]

10.1016/j.cell.2007.08.019.

8. Issaeva I, Zonis Y, Rozovskaia T, et al. Knockdown of ALR (MLL2) reveals ALR target genes and leads to alterations in cell adhesion and growth. *Mol Cell Biol*. 2007;27(5):1889-1903. Prepublished on 2006/12/21 as DOI MCB.01506-06 [pii]

10.1128/MCB.01506-06.

9. Lee MG, Villa R, Trojer P, et al. Demethylation of H3K27 regulates polycomb

recruitment and H2A ubiquitination. *Science*. 2007;318(5849):447-450. Prepublished on 2007/09/01 as DOI 1149042 [pii]

10.1126/science.1149042.

10. Azuara V, Perry P, Sauer S, et al. Chromatin signatures of pluripotent cell lines. *Nat Cell Biol*. 2006;8(5):532-538. Prepublished on 2006/03/30 as DOI ncb1403 [pii]

10.1038/ncb1403.

11. Mikkelsen TS, Ku M, Jaffe DB, et al. Genome-wide maps of chromatin state in pluripotent and lineage-committed cells. *Nature*. 2007;448(7153):553-560. Prepublished on 2007/07/03 as DOI nature06008 [pii]

10.1038/nature06008.

12. Cloos PA, Christensen J, Agger K, Helin K. Erasing the methyl mark: histone demethylases at the center of cellular differentiation and disease. *Genes Dev*. 2008;22(9):1115-1140. Prepublished on 2008/05/03 as DOI 22/9/1115 [pii]

10.1101/gad.1652908.

13. Di Lorenzo A, Bedford MT. Histone arginine methylation. *FEBS Lett*. 2011;585(13):2024-2031. Prepublished on 2010/11/16 as DOI 10.1016/j.febslet.2010.11.010.

14. Secombe J, Eisenman RN. The function and regulation of the JARID1 family of histone H3 lysine 4 demethylases: the Myc connection. *Cell Cycle*. 2007;6(11):1324-1328. Prepublished on 2007/06/15 as DOI 4269 [pii].

15. Chang B, Chen Y, Zhao Y, Bruick RK. JMJD6 is a histone arginine demethylase. *Science*. 2007;318(5849):444-447. Prepublished on 2007/10/20 as DOI 318/5849/444 [pii]

10.1126/science.1145801.

16. Falnes PO, Johansen RF, Seeberg E. AlkB-mediated oxidative demethylation reverses DNA damage in Escherichia coli. *Nature*. 2002;419(6903):178-182. Prepublished on 2002/09/13 as DOI 10.1038/nature01048

nature01048 [pii].

17. Trewick SC, Henshaw TF, Hausinger RP, Lindahl T, Sedgwick B. Oxidative demethylation by Escherichia coli AlkB directly reverts DNA base damage. *Nature*. 2002;419(6903):174-178. Prepublished on 2002/09/13 as DOI 10.1038/nature00908

nature00908 [pii].

18. Loh YH, Zhang W, Chen X, George J, Ng HH. Jmjd1a and Jmjd2c histone H3 Lys 9 demethylases regulate self-renewal in embryonic stem cells. *Genes Dev*. 2007;21(20):2545-2557. Prepublished on 2007/10/17 as DOI 21/20/2545 [pii]

10.1101/gad.1588207.

19. Hayami S, Yoshimatsu M, Veerakumarasivam A, et al. Overexpression of the JmjC histone demethylase KDM5B in human carcinogenesis: involvement in the proliferation of cancer cells through the E2F/RB pathway. *Mol Cancer*. 2010;9:59. Prepublished on 2010/03/17 as DOI 1476-4598-9-59 [pii]

10.1186/1476-4598-9-59.

20. Jepsen K, Solum D, Zhou T, et al. SMRT-mediated repression of an H3K27 demethylase in progression from neural stem cell to neuron. *Nature*. 2007;450(7168):415-419. Prepublished on 2007/10/12 as DOI 10.1038/nature06270.

21. Pospisil V, Vargova K, Kokavec J, et al. Epigenetic silencing of the oncogenic miR-17-92 cluster during PU.1-directed macrophage differentiation. *EMBO J*. 2011;30(21):4450-4464. Prepublished on 2011/09/08 as DOI emboj2011317 [pii]

10.1038/emboj.2011.317.

22. Schmitz SU, Albert M, Malatesta M, et al. Jarid1b targets genes regulating development and is involved in neural differentiation. *EMBO J*. 2011;30(22):4586-4600. Prepublished on 2011/10/25 as DOI emboj2011383 [pii]

10.1038/emboj.2011.383.

23. Sen GL, Webster DE, Barragan DI, Chang HY, Khavari PA. Control of differentiation in a self-renewing mammalian tissue by the histone demethylase JMJD3. *Genes Dev*. 2008;22(14):1865-1870. Prepublished on 2008/07/17 as DOI 22/14/1865 [pii]

10.1101/gad.1673508.

24. Strobl-Mazzulla PH, Sauka-Spengler T, Bronner-Fraser M. Histone demethylase JmjD2A regulates neural crest specification. *Dev Cell*. 2010;19(3):460-468. Prepublished on 2010/09/14 as DOI S1534-5807(10)00384-9 [pii]

10.1016/j.devcel.2010.08.009.

25. Agger K, Cloos PA, Rudkjaer L, et al. The H3K27me3 demethylase JMJD3 contributes to the activation of the INK4A-ARF locus in response to oncogene- and stress-induced senescence. *Genes Dev*. 2009;23(10):1171-1176. Prepublished on 2009/05/20 as DOI 23/10/1171 [pii]

10.1101/gad.510809.

26. Tzatsos A, Paskaleva P, Lymperi S, et al. Lysine-specific demethylase 2B (KDM2B)-let-7-enhancer of zester homolog 2 (EZH2) pathway regulates cell cycle progression and senescence in primary cells. *J Biol Chem*. 2011;286(38):33061-33069. Prepublished on 2011/07/16 as DOI M111.257667 [pii]

10.1074/jbc.M111.257667.

27. He J, Nguyen AT, Zhang Y. KDM2b/JHDM1b, an H3K36me2-specific demethylase, is required for initiation and maintenance of acute myeloid leukemia. *Blood*. 2011;117(14):3869-3880. Prepublished on 2011/02/12 as DOI blood-2010-10-312736 [pii]

10.1182/blood-2010-10-312736.

28. Liu G, Bollig-Fischer A, Kreike B, et al. Genomic amplification and oncogenic properties of the GASC1 histone demethylase gene in breast cancer. *Oncogene*. 2009;28(50):4491-4500. Prepublished on 2009/09/29 as DOI onc2009297 [pii]

10.1038/onc.2009.297.

29. Northcott PA, Nakahara Y, Wu X, et al. Multiple recurrent genetic events converge on control of histone lysine methylation in medulloblastoma. *Nat Genet*. 2009;41(4):465-472. Prepublished on 2009/03/10 as DOI ng.336 [pii]

10.1038/ng.336.

30. Xiang Y, Zhu Z, Han G, et al. JARID1B is a histone H3 lysine 4 demethylase up-regulated in prostate cancer. *Proc Natl Acad Sci U S A*. 2007;104(49):19226-19231. Prepublished on 2007/12/01 as DOI 0700735104 [pii]

10.1073/pnas.0700735104.

31. Hope KJ, Cellot S, Ting SB, et al. An RNAi screen identifies Msi2 and Prox1 as having opposite roles in the regulation of hematopoietic stem cell activity. *Cell Stem Cell*. 2010;7(1):101-113. Prepublished on 2010/07/14 as DOI S1934-5909(10)00289-4 [pii]

10.1016/j.stem.2010.06.007.

32. Deneault E, Cellot S, Faubert A, et al. A functional screen to identify novel effectors of hematopoietic stem cell activity. *Cell*. 2009;137(2):369-379. Prepublished on 2009/04/22 as DOI S0092-8674(09)00325-0 [pii]

10.1016/j.cell.2009.03.026.

33. Szilvassy SJ, Humphries RK, Lansdorp PM, Eaves AC, Eaves CJ. Quantitative assay for totipotent reconstituting hematopoietic stem cells by a competitive repopulation strategy. *Proc Natl Acad Sci U S A*. 1990;87(22):8736-8740. Prepublished on 1990/11/01 as DOI.

34. Katsumoto T, Aikawa Y, Iwama A, et al. MOZ is essential for maintenance of hematopoietic stem cells. *Genes Dev*. 2006;20(10):1321-1330. Prepublished on 2006/05/17 as DOI 10.1101/gad.1393106.

35. Thomas T, Corcoran LM, Gugasyan R, et al. Monocytic leukemia zinc finger protein is essential for the development of long-term reconstituting hematopoietic stem cells. *Genes Dev*. 2006;20(9):1175-1186. Prepublished on 2006/05/03 as DOI 10.1101/gad.1382606.

36. Ohta H, Sekulovic S, Bakovic S, et al. Near-maximal expansions of hematopoietic stem cells in culture using NUP98-HOX fusions. *Exp Hematol*. 2007;35(5):817-830. Prepublished on 2007/06/20 as DOI.

37. Sekulovic S, Gasparetto M, Lecault V, et al. Ontogeny stage-independent and high-level clonal expansion in vitro of mouse hematopoietic stem cells stimulated by an engineered NUP98-HOX fusion transcription factor. *Blood*. 2011;118(16):4366-4376. Prepublished on 2011/08/26 as DOI blood-2011-04-350066 [pii]

10.1182/blood-2011-04-350066.

38. Cellot S, Krosl J, Chagraoui J, Meloche S, Humphries RK, Sauvageau G. Sustained in vitro trigger of self-renewal divisions in Hoxb4hiPbx1(10) hematopoietic stem cells. *Exp Hematol*. 2007;35(5):802-816. Prepublished on 2007/06/20 as DOI.

39. Christensen J, Agger K, Cloos PA, et al. RBP2 belongs to a family of demethylases, specific for tri-and dimethylated lysine 4 on histone 3. *Cell*. 2007;128(6):1063-1076. Prepublished on 2007/02/27 as DOI S0092-8674(07)00182-1 [pii]

10.1016/j.cell.2007.02.003.

40. Klose RJ, Yan Q, Tothova Z, et al. The retinoblastoma binding protein RBP2 is an H3K4 demethylase. *Cell*. 2007;128(5):889-900. Prepublished on 2007/02/27 as DOI S0092-8674(07)00194-8 [pii]

10.1016/j.cell.2007.02.013.

41. Yamane K, Tateishi K, Klose RJ, et al. PLU-1 is an H3K4 demethylase involved in transcriptional repression and breast cancer cell proliferation. *Mol Cell*. 2007;25(6):801-812. Prepublished on 2007/03/17 as DOI S1097-2765(07)00146-3 [pii]

10.1016/j.molcel.2007.03.001.

42. Hisa T, Spence SE, Rachel RA, et al. Hematopoietic, angiogenic and eye defects in Meis1 mutant animals. *EMBO J*. 2004;23(2):450-459. Prepublished on 2004/01/10 as DOI 10.1038/sj.emboj.7600038.

43. Jude CD, Climer L, Xu D, Artinger E, Fisher JK, Ernst P. Unique and independent roles for MLL in adult hematopoietic stem cells and progenitors. *Cell Stem Cell*. 2007;1(3):324-337. Prepublished on 2008/03/29 as DOI S1934-5909(07)00060-4 [pii]

10.1016/j.stem.2007.05.019.

44. Kunisato A, Chiba S, Nakagami-Yamaguchi E, et al. HES-1 preserves purified hematopoietic stem cells ex vivo and accumulates side population cells in vivo. *Blood*. 2003;101(5):1777-1783. Prepublished on 2002/10/31 as DOI 10.1182/blood-2002-07-2051

2002-07-2051 [pii].

45. McMahon KA, Hiew SY, Hadjur S, et al. Mll has a critical role in fetal and adult

hematopoietic stem cell self-renewal. *Cell Stem Cell*. 2007;1(3):338-345. Prepublished on 2008/03/29 as DOI S1934-5909(07)00068-9 [pii]

10.1016/j.stem.2007.07.002.

46. Pedersen MT, Helin K. Histone demethylases in development and disease. *Trends Cell Biol*. 2010;20(11):662-671. Prepublished on 2010/09/25 as DOI S0962-8924(10)00179-0 [pii]

10.1016/j.tcb.2010.08.011.

47. Li Q, Shi L, Gui B, et al. Binding of the JmjC demethylase JARID1B to LSD1/NuRD suppresses angiogenesis and metastasis in breast cancer cells by repressing chemokine CCL14. *Cancer Res*. 2011;71(21):6899-6908. Prepublished on 2011/09/23 as DOI 0008-5472.CAN-11-1523 [pii]

10.1158/0008-5472.CAN-11-1523.

48. Rinn JL, Kertesz M, Wang JK, et al. Functional demarcation of active and silent chromatin domains in human HOX loci by noncoding RNAs. *Cell*. 2007;129(7):1311-1323. Prepublished on 2007/07/03 as DOI S0092-8674(07)00659-9 [pii]

10.1016/j.cell.2007.05.022.

49. Dorrance AM, Liu S, Yuan W, et al. Mll partial tandem duplication induces aberrant Hox expression in vivo via specific epigenetic alterations. *J Clin Invest*. 2006;116(10):2707-2716. Prepublished on 2006/09/19 as DOI 10.1172/JCI25546.

50. Krivtsov AV, Armstrong SA. MLL translocations, histone modifications and leukaemia stem-cell development. *Nat Rev Cancer*. 2007;7(11):823-833. Prepublished on 2007/10/25 as DOI 10.1038/nrc2253.

51. Wang GG, Song J, Wang Z, et al. Haematopoietic malignancies caused by dysregulation of a chromatin-binding PHD finger. *Nature*. 2009;459(7248):847-851. Prepublished on 2009/05/12 as DOI nature08036 [pii]

10.1038/nature08036.

52. Fontana L, Pelosi E, Greco P, et al. MicroRNAs 17-5p-20a-106a control monocytopoiesis through AML1 targeting and M-CSF receptor upregulation. *Nat Cell Biol*. 2007;9(7):775-787. Prepublished on 2007/06/26 as DOI ncb1613 [pii]

10.1038/ncb1613.

53. Ventura A, Young AG, Winslow MM, et al. Targeted deletion reveals essential and overlapping functions of the miR-17 through 92 family of miRNA clusters. *Cell*. 2008;132(5):875-886. Prepublished on 2008/03/11 as DOI S0092-8674(08)00267-5 [pii]

10.1016/j.cell.2008.02.019.

54. Xiao C, Srinivasan L, Calado DP, et al. Lymphoproliferative disease and autoimmunity in mice with increased miR-17-92 expression in lymphocytes. *Nat Immunol*. 2008;9(4):405-414. Prepublished on 2008/03/11 as DOI ni1575 [pii]

10.1038/ni1575.

55. Li Z, Lu J, Sun M, et al. Distinct microRNA expression profiles in acute myeloid leukemia with common translocations. *Proc Natl Acad Sci U S A*. 2008;105(40):15535-15540. Prepublished on 2008/10/04 as DOI 0808266105 [pii]

10.1073/pnas.0808266105.

56. Karrman K, Sallerfors B, Lenhoff S, Fioretos T, Johansson B. Cytogenetic evolution patterns in CML post-SCT. *Bone Marrow Transplant*. 2007;39(3):165-171. Prepublished on 2007/01/11 as DOI 1705560 [pii]

10.1038/sj.bmt.1705560.

57. Shah NK, Wagner J, Santos G, Griffin CA. Karyotype at relapse following allogeneic bone marrow transplantation for chronic myelogenous leukemia. *Cancer Genet Cytogenet*. 1992;61(2):183-192. Prepublished on 1992/07/15 as DOI 0165-4608(92)90084-L [pii].

58. Catchpole S, Spencer-Dene B, Hall D, et al. PLU-1/JARID1B/KDM5B is required for embryonic survival and contributes to cell proliferation in the mammary gland and in ER+ breast cancer cells. *Int J Oncol*. 2011;38(5):1267-1277. Prepublished on 2011/03/04 as DOI 10.3892/ijo.2011.956.

59. Allis CD, Berger SL, Cote J, et al. New nomenclature for chromatin-modifying enzymes. *Cell*. 2007;131(4):633-636. Prepublished on 2007/11/21 as DOI S0092-8674(07)01359-1 [pii]

10.1016/j.cell.2007.10.039.

5. DISCUSSION

5.1 Impact des modulations de *Hoxb4* et de son cofacteur *Pbx1* sur le destin des CSH

Les résultats des travaux présentés au chapitre 2 démontrent qu'il est possible pour des CSH adultes de soutenir en culture des divisions symétriques d'auto-renouvellement (AR), engendrant une expansion cellulaire significativement élevée (5 log). Ces données témoignent entre autre de l'important potentiel de prolifération des CSH, et de leur capacité de préservation de leur identité. La magnitude de l'expansion des CSH documentée corrobore les résultats d'un groupe de collaborateurs, générés de façon indépendante en employant une stratégie alterne de modulation des gènes *Hox* [57]. En effet, au lieu de moduler de façon concomitante les niveaux d'un gène *Hox* et d'un de ses principaux cofacteurs de liaison à l'ADN, l'équipe du Dr Humphries à fusionner le domaine de transactivation de la nucléoporine *Nup98* directement à la portion homéodomaine de *Hoxa10* (NA10hd). Ce faisant, la surexpression de NA10hd dans les CSH altère significativement le programme transcriptionnel, leur conférant une propriété accrue d'AR, similaire à la transduction des cellules par Hoxb4 et Pbx1 anti-sens.

Les stratégies d'expansion des CSH *in vitro* peuvent bien entendu éventuellement servir à répondre à des besoins cliniques, comme la thérapie cellulaire, mais leur application en recherche est tout aussi d'intérêt. En effet, les bases moléculaires qui sous-tendent l'AR demeurent difficiles à définir, en partie en raison des limites imposées pour l'obtention d'une masse critique de CSH pour fins d'analyses biochimiques. À titre d'exemple, avec la stratégie de purification de CSH utilisée dans les deux cribles présentés dans cette thèse, la récolte de la moelle d'une cinquantaine de souris permettait l'isolation de ~200 000 cellules CD150+CD48-Lin-, soit ~8000 CSH. Des outils facilitant leur expansion ouvriraient donc la porte à plusieurs types d'investigations moléculaires. Bien qu'une expansion de plusieurs logs des CSH soit pertinente dans un contexte de recherche, une telle magnitude n'est pas requise pour les applications cliniques. Pour une plus grande utilisation du sang de cordon en transplantation, par exemple, un modeste accroissement du nombre de CSH en culture suffirait. D'ailleurs, un mot de prudence s'impose en poussant à l'extrême les limites de l'AR pour des fins thérapeutiques. Des études rigoureuses, mesurant l'impact fonctionnel à long-terme de niveaux très élevés d'AR, sur le plan de la sénescence ou du potentiel de transformation maligne, par exemple, devront être effectuées au préalable [201].

5.2 Crible en RNAi comme stratégie d'identification de déterminants de l'auto-renouvellement

Hormis les modèles de souris transgéniques permettant de caractériser les répercussions de la délétion complète d'un gène chez l'animal, l'étude de facteurs modulant l'activité des CSH s'est longtemps basée sur la surexpression de gènes à l'aide de vecteurs rétroviraux [23]. L'amélioration des techniques de purification et de culture des CSH ont permis d'élaborer des stratégies de crible, et d'étudier ainsi plusieurs gènes de façon concomitante [27] utilisant un système de micro-cultures, tel qu'utilisé au laboratoire pour évaluer l'impact de la surexpression de 104 facteurs nucléaires dans les CSH (voir annexe 4). Ce système s'est avéré particulièrement efficace pour mettre en évidence des phénotypes de gain-de-fonction, notamment en allongeant le temps de culture *in vitro*, favorisant l'épuisement des CSH contrôles, et diminuant ainsi le bruit de fond [27]. Or, pour détecter des déterminants essentiels de l'AR, la technique d'interférence de l'ARN (RNAi) [202] et l'utilisation de constructions de shRNA dirigés contre des cibles spécifiques, offrent des avantages. Notemment, elle permet de mesurer l'effet d'une diminution des niveaux de transcrit d'un gène donné sur l'activité des CSH, et de repérer ainsi plus facilement les phénotypes de perte-de-fonction (régulateurs positifs de l'AR) que dans un contexte de surexpression.

Cette approche comporte aussi ses limites et se veut complémentaire à la stratégie de surexpression. Notamment, pour la mise en évidence d'un phénotype de perte-de-fonction, la prolongation du temps de culture n'est pas nécessaire, et devient même nuisible. En contrepartie, la réduction du temps de culture augmente le bruit de fonds, contaminé par l'activité stochastique des CSH contrôles, encore présentes en nombre significatif dans de jeunes cultures. De plus, les algorithmes de design de séquences des shRNA, bien qu'améliorées [203, 204], ne sont pas parfaits et seulement une fraction des constructions assureront une diminution significative du transcrit d'un gène cible (en moyenne 2-3shRNA sur 5 se sont avérés efficaces dans les cribles). Il faut aussi plusieurs constructions pour s'assurer que le phénotype observé ne résulte pas de l'effet potentiellement non-spécifique des shRNA (ou off-target effect), mais bien de la diminution des niveaux de transcrit du gène ciblé. L'utilisation de plusieurs shRNA dirigés contre un même gène cependant offre l'avantage de corréler l'intensité du phénotype avec les niveaux de diminution de transcrits. Les niveaux de transcrits sont toutefois rarement réduits à plus de 80% par rapport aux cellules contrôles (notre expérience), un niveau d'expression résiduelle qui demeure encore supérieure à une délétion complète d'un gène, nécessitant encore une approche par transgénèse.

5.3 Crible des HDM en RNAi

Les résultats du crible présenté au chapitre 4 suggèrent que l'activité des CSH est sen-

sible au dosage de diverses HDM de la famille JmjC, du moins pour Jarid1b, Phf8 et possiblement Fih (validation en cours, 1shRNA/3 confirmé). Devant l'importance de la méthylation des histones dans la configuration de la chromatine et l'identité cellulaire, et de par la nature réversible de cette modification, une contribution des HDM dans ce processus semble probable, et demeure une voie à explorer. Les données semblent s'arrimer avec des études récentes impliquant les HDM de la famille JmjC dans divers processus biologiques (section 1.3 de l'introduction).

5.3.1 Données du crible en regard de la littérature actuelle

Tel que discuté dans l'introduction (section 1.3), certaines HDM semblent impliquées dans l'hématopoïèse normale et leucémique, comme FBXL10 (JHDM1B, KDM2B) [182] et UTX (KDM6A) [189, 192]. Il faut bien mettre en perspective que le phénotype induit par des modulations des niveaux de transcrits de ces enzymes dépendra de la magnitude de la variation, et du contexte cellulaire. Concernant *Fbxl10*, une surexpression de ce gène dans le compartiment hématopoïétique semble conférer un avantage prolifératif et une moindre propension à la sénescence, sans nécessairement mener à une augmentation de l'AR des CSH en termes fonctionnels. Dans le crible par RNAi présenté dans cette thèse pour les HDM, au chapitre 4, cinq constructions distinctes ciblant *Jhdm1b* (*Fbxl10*) (Figure 4.2B) n'affecte pas la reconstitution sanguine des receveurs en-deçà du seuil inférieur de la normale, 16 semaines post-transplantation. Cette différence pourrait s'expliquer par des niveaux de diminution de transcrits n'ayant pas de répercussion sur l'activité des CSH. Alternativement, un phénotype pourrait devenir apparent à plus long-terme, plusieurs mois suivant la transplantation. Il faut aussi noter que l'expression forcé d'un gène à un niveau supra-physiologique peut modifier le destin cellulaire, sans nécessairement conduire à un contre-phénotype lors d'une diminution du niveau de transcrits. La surexpression de *Hoxb4* pourrait servir d'exemple en ce sens. En ce qui concerne la modulation du potentiel prolifératif des cellules leucémiques par FBXL10, il pourrait s'agir d'une dépendance spécifique à ce contexte.

Concernant UTX (H3K27me3/2 HDM), bien que les résultats d'une étude suggèrent qu'il soit un régulateur positif du potentiel prolifératif des cellules hématopoïétiques normales [189], son rôle en tant que suppresseur de tumeur émerge en parallèle [192]. Encore une fois, l'impact mesuré dépendra des niveaux de transcrits, et du contexte cellulaire spécifique. De façon intéressante, bien qu'*Utx* ne soit pas une cible de notre crible primaire, (Figure 4.2B), un sous-groupe de souris sacrifiées à très long-terme (1an) démontraient une augmentation de la reconstitution sanguine pas les cellules transduites avec un shRNA contre *Utx*. L'échantillon étant trop petit pour conclure, cette observation méritera une expérience de validation, afin étudier le potentiel de transformation à long-terme d'une diminution des niveaux d'*Utx* dans le système hématopoïétique.

5.3.2 JARID1B (KDM5B) et activité des CSH

Les efforts de validation du crible des HDM se sont concentrés sur *Jarid1b* (codant pour une H3K4me3/2 HDM), et l'augmentation de l'activité des CSH induite par des shRNA contre ce gène. Une diminution de *Jarid1b* s'accompagne d'un bloc de différentiation, et d'une augmentation de l'activité transcriptionnelle du cluster des gènes *Hoxa* en 5'. Les travaux futurs concernant ce gène devront comprendre l'identification des cibles directes de JARID1B, et les modifications épigénétiques correspondantes. La caractérisation des partenaires d'interaction de JARID1B, la nature du (ou des) complexe au sein duquel il agit sont également des questions d'intérêt. Notamment, il sera pertinent de déterminer si JARID1B oppose l'action d'un complexe méthyl-transférase, et si oui duquel. Un modèle de souris knockout conditionnel permettra aussi d'évaluer l'impact ponctuel d'une délétion complète de *Jarid1b* dans le système hématopoïétique, tel que discuté au chapitre 4. Toute la sphère des cibles potentiellement non-histone devra également être adressée. Il est à noter qu'un inhibiteur chimique de JARID1B a été récemment décrit [205], ce qui ouvre une autre voie expérimentale intéressante. Le potentiel de cette molécule à promouvoir l'expansion des CSH *in vitro* devra être évalué. Ce domaine de recherche est très actif de par son application thérapeutique potentielle, tel que récemment rapporté pour la molécule SR-1 (Self-Renewal 1), un inhibiteur du récepteur aryl-hydrocarbone pouvant soutenir l'expansion des CSH humaines en culture [206]. Encore plus intriguant sera de comprendre les différences fonctionnelles entre JARID1B et JARID1A, ces deux facteur arborant un haut niveau d'homologie, et se distinguant essentiellement à leur portion C-terminale, comprenant le 3ème domaine PHD (voir Fig1.15 de l'introduction).

5.3.3 PHF8 et reconstitution hématopoïétique

Contrairement à JARID1B, les résultats du crible des HDM suggèrent que PHF8 (H3K9me2/1, H4K20me1 HDM) est un régulateur positif de l'activité des CSH. Avec trois constructions distinctes, des populations cellulaires enrichies en CSH transduites avec des shRNA ciblant *Phf8* sont moins compétitives que les cellules contrôles dans des essais fonctionnels de transplantation. La caractérisation de ce phénotype devra être poursuivie, mais il est toutefois plus complexe de déterminer si un phénotype de perte-de-fonction est spécifique à la cellule souche. Il pourrait, par exemple, être secondaire à un défait global de prolifération des cellules hématopoïétiques. Cette HDM est encore peu étudiée, mais les données disponibles semblent suggérer que PHF8 soit un régulateur positif de la prolifération [207], et du cycle cellulaire, notamment de la progression de la phase G1/S [208]. Une interaction entre PHF8 et WDR5 du complexe méthyl-transférase MLL est décrite [209], ainsi que la capacité de PHF8 de lier la marque activatrice H3K4me3 par le biais de son domaine PHD. PFH8 est aussi rapporté comme un régulateur positif de la

transcription [210], régulant particulièrement l'expression de MSX1/MSXB, un facteur de transcription à homéodomaine [211]. Globalement, ces données pourraient s'arrimer avec le phénotype hématopoïétique et fournir des pistes d'exploration pour les études ultérieures concernant PHF8.

5.3.4 FIH; autre candidat potentiel du crible

Le crible présenté au chapitre 4 a permis d'identifier un second régulateur négatif de l'activité des CSH, soit l'inhibiteur de Hif1α (HIF1an), aussi nommé FIH (Factor Inhibiting Hif1α), dont la caractérisation fera partie d'études ultérieures. FIH est une enzyme JmjC dont l'activité catalytique modifie post-translationnellement le facteur de transcription HIF1α (Hypoxia-Inducible Factor 1α), de façon intéressante une cible non-histone. En présence de faibles tensions d'oxygène, le senseur métabolique HIF1α est actif, formant un hétérodimère avec HIF1β lui permettant de lier ses gènes cibles, et d'induire subséquemment leur transcription en interagissant aussi avec le co-activateur p300 [212]. Suite à une augmentation des concentrations en oxygène, HIF1α est soumis à l'activité d'hydroxylases, incluant HIF1an/FIH qui modifie un résidu asparagine essentiel à l'interaction entre HIF1α et p300. L'hydroxylation d'un résidu proline de HIF1α est médiée par une autre famille d'enzymes à domaine PHD, menant à la dégradation de la protéine par la voie du suppresseur de tumeur pVHL (Von Hippel–Lindau). Il existe donc une corrélation inverse entre les niveaux de HIF1α et de son inhibiteur, FIH. En théorie, une déstabilisation des transcrits de *Fih* par une approche en RNAi pourrait lever une force antagoniste exercée sur HIF1α, et freiner sa dégradation. Cet effet pourrait être particulièrement bénéfique pour des CSH en culture, un contexte de stress oxydatif élevé, qui favoriserait normalement la dégradation de HIF1α. L'influence positive de HIF1α sur l'activité des cellules souches normales et leucémiques est d'ailleurs rapporté [213]. De plus, les mutations de IDH1/2 décrites dans les leucémies aigues, tel que discuté dans l'introduction (section 1.3), résultent en une perturbation du métabolisme de l'α-kétoglutarate, générant un néo-métabolite (D-2-hydroxyglutarate) qui stabiliserait HIF1α, contribuant possiblement au maintien des CSL [194].

6. CONCLUSION

L'étude de différents facteurs nucléaires et la modulation de leur niveau a permis, en surexpression ou en RNAi, de mesurer leur impact sur le destin des cellules souches hématopoïétiques (CSH). Elle a notamment permis d'identifier parmis la famille des histones déméthylases, un régulateur positif (PHF8) et un régulateur négatif (JARID1B) de l'activité des CSH. Une meilleure compréhension des bases moléculaires de leur mécanisme d'action nécessitera des efforts ultérieurs en ce sens. Un des grands défis de l'avenir sera d'interroger la fonction de ces facteurs dans le contexte de cellules primaires humaines. Le progrès des diverses technologies de biologie moléculaire et cellulaire, dont le séquençage de nouvelle génération, la transfection des cellules humaines et les nouvelles stratégies de biobanking faciliteront la progression dans cette voie. Ultimement, il serait intéressant de pouvoir appliquer les résultats de ces études de façon translationnelle. L'optique étant d'élaborer de meilleures stratégies d'expansion des CSH pour des fins de transplantation, ou d'identifier des cibles thérapeutiques spécifiques pour le traitement des hémopathies malignes, en complément ou remplacement des agents de chimiothérapie conventionnels.

7. BIBLIOGRAPHIE

1. Cellot, S. and G. Sauvageau, *Zfx: at the crossroads of survival and self-renewal.* Cell, 2007. **129**(2): p. 239-41.

2. Cheshier, S.H., et al., In vivo proliferation and cell cycle kinetics of long-term self-renewing hematopoietic stem cells. Proc Natl Acad Sci U S A, 1999. **96**(6): p. 3120-5.

3. Kiel, M.J., et al., Haematopoietic stem cells do not asymmetrically segregate chromosomes or retain BrdU. Nature, 2007. **449**(7159): p. 238-42.

4. Catlin, S.N., et al., The replication rate of human hematopoietic stem cells in vivo. Blood, 2011. **117**(17): p. 4460-6.

5. Shepherd, B.E., et al., Estimating human hematopoietic stem cell kinetics using granulocyte telomere lengths. Exp Hematol, 2004. **32**(11): p. 1040-50.

6. Kamimura, T., et al., *Advances in therapies for acute promyelocytic leukemia.* Cancer Sci, 2011. **102**(11): p. 1929-37.

7. Cellot, S. and G. Sauvageau, *Gfi-1: another piece in the HSC puzzle.* Trends Immunol, 2005. **26**(2): p. 68-71.

8. Mikkola, H.K. and S.H. Orkin, *The journey of developing hematopoietic stem cells.* Development, 2006. **133**(19): p. 3733-44.

9. Bowie, M.B., et al., Identification of a new intrinsically timed developmental checkpoint that reprograms key hematopoietic stem cell properties. Proc Natl Acad Sci U S A, 2007. **104**(14): p. 5878-82.

10. Krause, D.S. and D.T. Scadden, *Deconstructing the complexity of a microenvironmental niche.* Cell, 2012. **149**(1): p. 16-7.

11. Martinez-Agosto, J.A., et al., *The hematopoietic stem cell and its niche: a comparative view.* Genes Dev, 2007. **21**(23): p. 3044-60.

12. Mercier, F.E., C. Ragu, and D.T. Scadden, *The bone marrow at the crossroads of blood and immunity.* Nat Rev Immunol, 2012. **12**(1): p. 49-60.

13. Sugiyama, T., et al., Maintenance of the hematopoietic stem cell pool by CXCL12-CXCR4 chemokine signaling in bone marrow stromal cell niches. Immunity, 2006. **25**(6): p. 977-88.

14. Argiropoulos, B. and R.K. Humphries, *Hox genes in hematopoiesis and leukemogenesis.* Oncogene, 2007. **26**(47): p. 6766-76.

15. Krivtsov, A.V. and S.A. Armstrong, *MLL translocations, histone modifications*

and leukaemia stem-cell development. Nat Rev Cancer, 2007. **7**(11): p. 823-33.

16. Kiel, M.J., et al., SLAM family receptors distinguish hematopoietic stem and progenitor cells and reveal endothelial niches for stem cells. Cell, 2005. **121**(7): p. 1109-21.

17. Osawa, M., et al., Long-term lymphohematopoietic reconstitution by a single CD34-low/negative hematopoietic stem cell. Science, 1996. **273**(5272): p. 242-5.

18. Spangrude, G.J., S. Heimfeld, and I.L. Weissman, *Purification and characterization of mouse hematopoietic stem cells.* Science, 1988. **241**(4861): p. 58-62.

19. Yilmaz, O.H., M.J. Kiel, and S.J. Morrison, SLAM family markers are conserved among hematopoietic stem cells from old and reconstituted mice and markedly increase their purity. Blood, 2006. **107**(3): p. 924-30.

20. Foudi, A., et al., Analysis of histone 2B-GFP retention reveals slowly cycling hematopoietic stem cells. Nat Biotechnol, 2009. **27**(1): p. 84-90.

21. Wagers, A.J. and I.L. Weissman, Differential expression of alpha2 integrin separates long-term and short-term reconstituting Lin-/loThy1.1(lo)c-kit+ Sca-1+ hematopoietic stem cells. Stem Cells, 2006. **24**(4): p. 1087-94.

22. Purton, L.E. and D.T. Scadden, *Limiting factors in murine hematopoietic stem cell assays.* Cell Stem Cell, 2007. **1**(3): p. 263-70.

23. Sauvageau, G., et al., Overexpression of HOXB4 in hematopoietic cells causes the selective expansion of more primitive populations in vitro and in vivo. Genes Dev, 1995. **9**(14): p. 1753-65.

24. Szilvassy, S.J., et al., Quantitative assay for totipotent reconstituting hematopoietic stem cells by a competitive repopulation strategy. Proc Natl Acad Sci U S A, 1990. **87**(22): p. 8736-40.

25. Hope, K.J., et al., An RNAi screen identifies Msi2 and Prox1 as having opposite roles in the regulation of hematopoietic stem cell activity. Cell Stem Cell, 2010. **7**(1): p. 101-13.

26. Cellot, S., et al., Sustained in vitro trigger of self-renewal divisions in Hoxb4hiPbx1(10) hematopoietic stem cells. Exp Hematol, 2007. **35**(5): p. 802-16.

27. Deneault, E., et al., A functional screen to identify novel effectors of hematopoietic stem cell activity. Cell, 2009. **137**(2): p. 369-79.

28. Huntly, B.J. and D.G. Gilliland, *Leukaemia stem cells and the evolution of cancer-stem-cell research.* Nat Rev Cancer, 2005. **5**(4): p. 311-21.

29. Warner, J.K., et al., *Concepts of human leukemic development.* Oncogene, 2004. **23**(43): p. 7164-77.

30. Fischer, A. and M. Cavazzana-Calvo, *Gene therapy of inherited diseases.* Lancet, 2008. **371**(9629): p. 2044-7.

31. Gratwohl, A., et al., Hematopoietic stem cell transplantation: a global perspective. JAMA, 2010. **303**(16): p. 1617-24.

32. Krumlauf, R., *Hox genes in vertebrate development.* Cell, 1994. **78**(2): p. 191-201.

33. Lewis, E.B., A gene complex controlling segmentation in Drosophila. Nature, 1978. **276**(5688): p. 565-70.

34. Schneuwly, S., A. Kuroiwa, and W.J. Gehring, *Molecular analysis of the dominant homeotic Antennapedia phenotype.* EMBO J, 1987. **6**(1): p. 201-6.

35. McGonigle, G.J., T.R. Lappin, and A. Thompson, *Grappling with the HOX network in hematopoiesis and leukemia.* Front Biosci, 2008. **13**: p. 4297-308.

36. Ekker, S.C., et al., The degree of variation in DNA sequence recognition among four Drosophila homeotic proteins. EMBO J, 1994. **13**(15): p. 3551-60.

37. Hoey, T. and M. Levine, Divergent homeo box proteins recognize similar DNA sequences in Drosophila. Nature, 1988. **332**(6167): p. 858-61.

38. Mann, R.S., *The specificity of homeotic gene function.* Bioessays, 1995. **17**(10): p. 855-63.

39. DiMartino, J.F., et al., The Hox cofactor and proto-oncogene Pbx1 is required for maintenance of definitive hematopoiesis in the fetal liver. Blood, 2001. **98**(3): p. 618-26.

40. Selleri, L., et al., Requirement for Pbx1 in skeletal patterning and programming chondrocyte proliferation and differentiation. Development, 2001. **128**(18): p. 3543-57.

41. Azcoitia, V., et al., The homeodomain protein Meis1 is essential for definitive hematopoiesis and vascular patterning in the mouse embryo. Dev Biol, 2005. **280**(2): p. 307-20.

42. Hisa, T., et al., Hematopoietic, angiogenic and eye defects in Meis1 mutant animals. EMBO J, 2004. **23**(2): p. 450-9.

43. Robertson, L.K., et al., An interactive network of zinc-finger proteins contributes to regionalization of the Drosophila embryo and establishes the domains of HOM-C protein function. Development, 2004. **131**(12): p. 2781-9.

44. Giampaolo, A., et al., HOXB gene expression and function in differentiating purified hematopoietic progenitors. Stem Cells, 1995. **13 Suppl 1**: p. 90-105.

45. Giampaolo, A., et al., Key functional role and lineage-specific expression of selected HOXB genes in purified hematopoietic progenitor differentiation. Blood, 1994. **84**(11): p. 3637-47.

46. Magli, M.C., et al., *Coordinate regulation of HOX genes in human hematopoietic cells.* Proc Natl Acad Sci U S A, 1991. **88**(14): p. 6348-52.

47. Pineault, N., et al., Differential expression of Hox, Meis1, and Pbx1 genes in primitive cells throughout murine hematopoietic ontogeny. Exp Hematol, 2002. **30**(1): p. 49-57.

48. Sauvageau, G., et al., Differential expression of homeobox genes in functionally distinct CD34+ subpopulations of human bone marrow cells. Proc Natl Acad Sci U S A, 1994. **91**(25): p. 12223-7.

49. Bijl, J., et al., Analysis of HSC activity and compensatory Hox gene expression profile in Hoxb cluster mutant fetal liver cells. Blood, 2006. **108**(1): p. 116-22.

50. Magli, M.C., C. Largman, and H.J. Lawrence, *Effects of HOX homeobox genes in blood cell differentiation.* J Cell Physiol, 1997. **173**(2): p. 168-77.

51. Zhang, X.B., et al., Differential effects of HOXB4 on nonhuman primate short- and long-term repopulating cells. PLoS Med, 2006. **3**(5): p. e173.

52. Krosl, J., et al., In vitro expansion of hematopoietic stem cells by recombinant TAT-HOXB4 protein. Nat Med, 2003. **9**(11): p. 1428-32.

53. Lebert-Ghali, C.E., et al., HoxA cluster is haploinsufficient for activity of hematopoietic stem and progenitor cells. Exp Hematol, 2010. **38**(11): p. 1074-1086 e1-5.

54. Di-Poi, N., et al., Additive and global functions of HoxA cluster genes in mesoderm derivatives. Dev Biol, 2010. **341**(2): p. 488-98.

55. Antonchuk, J., G. Sauvageau, and R.K. Humphries, *HOXB4-induced expansion of adult hematopoietic stem cells ex vivo.* Cell, 2002. **109**(1): p. 39-45.

56. Beslu, N., et al., Molecular interactions involved in HOXB4-induced activation of HSC self-renewal. Blood, 2004. **104**(8): p. 2307-14.

57. Ohta, H., et al., Near-maximal expansions of hematopoietic stem cells in culture using NUP98-HOX fusions. Exp Hematol, 2007. **35**(5): p. 817-30.

58. Kroon, E., et al., Hoxa9 transforms primary bone marrow cells through specific collaboration with Meis1a but not Pbx1b. EMBO J, 1998. **17**(13): p. 3714-25.

59. Bisaillon, R., et al., C-terminal domain of MEIS1 converts PKNOX1 (PREP1) into a HOXA9-collaborating oncoprotein. Blood, 2011. **118**(17): p. 4682-9.

60. Shah, N. and S. Sukumar, *The Hox genes and their roles in oncogenesis.* Nat Rev Cancer, 2010. **10**(5): p. 361-71.

61. Alcalay, M., et al., Acute myeloid leukemia bearing cytoplasmic nucleophosmin (NPMc+ AML) shows a distinct gene expression profile characterized by up-regulation of genes involved in stem-cell maintenance. Blood, 2005. **106**(3): p. 899-902.

62. Becker, H., et al., Favorable prognostic impact of NPM1 mutations in older patients with cytogenetically normal de novo acute myeloid leukemia and associated gene- and microRNA-expression signatures: a Cancer and Leukemia Group B study. J Clin

Oncol, 2010. **28**(4): p. 596-604.

63. van Zutven, L.J., et al., Identification of NUP98 abnormalities in acute leukemia: JARID1A (12p13) as a new partner gene. Genes Chromosomes Cancer, 2006. **45**(5): p. 437-46.

64. Wang, G.G., et al., Haematopoietic malignancies caused by dysregulation of a chromatin-binding PHD finger. Nature, 2009. **459**(7248): p. 847-51.

65. Cauwelier, B., et al., Clinical, cytogenetic and molecular characteristics of 14 T-ALL patients carrying the TCRbeta-HOXA rearrangement: a study of the Groupe Francophone de Cytogenetique Hematologique. Leukemia, 2007. **21**(1): p. 121-8.

66. Speleman, F., et al., A new recurrent inversion, inv(7)(p15q34), leads to transcriptional activation of HOXA10 and HOXA11 in a subset of T-cell acute lymphoblastic leukemias. Leukemia, 2005. **19**(3): p. 358-66.

67. Gough, S.M., C.I. Slape, and P.D. Aplan, NUP98 gene fusions and hematopoietic malignancies: common themes and new biologic insights. Blood, 2011. **118**(24): p. 6247-57.

68. Kroon, E., et al., NUP98-HOXA9 expression in hemopoietic stem cells induces chronic and acute myeloid leukemias in mice. EMBO J, 2001. **20**(3): p. 350-61.

69. Pineault, N., et al., Induction of acute myeloid leukemia in mice by the human leukemia-specific fusion gene NUP98-HOXD13 in concert with Meis1. Blood, 2003. **101**(11): p. 4529-38.

70. Iwasaki, M., et al., Identification of cooperative genes for NUP98-HOXA9 in myeloid leukemogenesis using a mouse model. Blood, 2005. **105**(2): p. 784-93.

71. Lin, Y.W., et al., NUP98-HOXD13 transgenic mice develop a highly penetrant, severe myelodysplastic syndrome that progresses to acute leukemia. Blood, 2005. **106**(1): p. 287-95.

72. Calvo, K.R., et al., Nup98-HoxA9 immortalizes myeloid progenitors, enforces expression of Hoxa9, Hoxa7 and Meis1, and alters cytokine-specific responses in a manner similar to that induced by retroviral co-expression of Hoxa9 and Meis1. Oncogene, 2002. **21**(27): p. 4247-56.

73. Alemdehy, M.F. and S.J. Erkeland, *MicroRNAs: key players of normal and malignant myelopoiesis.* Curr Opin Hematol, 2012.

74. Pasquinelli, A.E., MicroRNAs and their targets: recognition, regulation and an emerging reciprocal relationship. Nat Rev Genet, 2012. **13**(4): p. 271-82.

75. Lund, A.H., *miR-10 in development and cancer.* Cell Death Differ, 2010. **17**(2): p. 209-14.

76. Mansfield, J.H., et al., MicroRNA-responsive 'sensor' transgenes uncover Hox-

like and other developmentally regulated patterns of vertebrate microRNA expression. Nat Genet, 2004. **36**(10): p. 1079-83.

77. Yekta, S., I.H. Shih, and D.P. Bartel, *MicroRNA-directed cleavage of HOXB8 mRNA.* Science, 2004. **304**(5670): p. 594-6.

78. Rinn, J.L., et al., Functional demarcation of active and silent chromatin domains in human HOX loci by noncoding RNAs. Cell, 2007. **129**(7): p. 1311-23.

79. O'Neil, J. and A.T. Look, Mechanisms of transcription factor deregulation in lymphoid cell transformation. Oncogene, 2007. **26**(47): p. 6838-49.

80. Orkin, S.H. and L.I. Zon, *Hematopoiesis: an evolving paradigm for stem cell biology.* Cell, 2008. **132**(4): p. 631-44.

81. Tsai, F.Y., et al., An early haematopoietic defect in mice lacking the transcription factor GATA-2. Nature, 1994. **371**(6494): p. 221-6.

82. Tsai, F.Y. and S.H. Orkin, Transcription factor GATA-2 is required for proliferation/survival of early hematopoietic cells and mast cell formation, but not for erythroid and myeloid terminal differentiation. Blood, 1997. **89**(10): p. 3636-43.

83. Persons, D.A., et al., Enforced expression of the GATA-2 transcription factor blocks normal hematopoiesis. Blood, 1999. **93**(2): p. 488-99.

84. Hahn, C.N., et al., Heritable GATA2 mutations associated with familial myelodysplastic syndrome and acute myeloid leukemia. Nat Genet, 2011. **43**(10): p. 1012-7.

85. Fatemi, M., et al., Footprinting of mammalian promoters: use of a CpG DNA methyltransferase revealing nucleosome positions at a single molecule level. Nucleic Acids Res, 2005. **33**(20): p. e176.

86. He, Y.F., et al., Tet-mediated formation of 5-carboxylcytosine and its excision by TDG in mammalian DNA. Science, 2011. **333**(6047): p. 1303-7.

87. Ito, S., et al., Tet proteins can convert 5-methylcytosine to 5-formylcytosine and 5-carboxylcytosine. Science, 2011. **333**(6047): p. 1300-3.

88. Kouzarides, T., *Chromatin modifications and their function.* Cell, 2007. **128**(4): p. 693-705.

89. Jones, P.A. and S.B. Baylin, *The epigenomics of cancer.* Cell, 2007. **128**(4): p. 683-92.

90. Jaenisch, R. and A. Bird, Epigenetic regulation of gene expression: how the genome integrates intrinsic and environmental signals. Nat Genet, 2003. **33 Suppl**: p. 245-54.

91. Broske, A.M., et al., DNA methylation protects hematopoietic stem cell multipotency from myeloerythroid restriction. Nat Genet, 2009. **41**(11): p. 1207-15.

92. Trowbridge, J.J., et al., DNA methyltransferase 1 is essential for and uniquely regulates hematopoietic stem and progenitor cells. Cell Stem Cell, 2009. **5**(4): p. 442-9.

93. Trowbridge, J.J., et al., Haploinsufficiency of Dnmt1 impairs leukemia stem cell function through derepression of bivalent chromatin domains. Genes Dev, 2012. **26**(4): p. 344-9.

94. Ley, T.J., et al., *DNMT3A mutations in acute myeloid leukemia.* N Engl J Med, 2010. **363**(25): p. 2424-33.

95. Walter, M.J., et al., Recurrent DNMT3A mutations in patients with myelodysplastic syndromes. Leukemia, 2011. **25**(7): p. 1153-8.

96. Tadokoro, Y., et al., De novo DNA methyltransferase is essential for self-renewal, but not for differentiation, in hematopoietic stem cells. J Exp Med, 2007. **204**(4): p. 715-22.

97. Ko, M., et al., Impaired hydroxylation of 5-methylcytosine in myeloid cancers with mutant TET2. Nature, 2010. **468**(7325): p. 839-43.

98. Schuettengruber, B., et al., *Trithorax group proteins: switching genes on and keeping them active.* Nat Rev Mol Cell Biol, 2011. **12**(12): p. 799-814.

99. Ziemin-van der Poel, S., et al., Identification of a gene, MLL, that spans the breakpoint in 11q23 translocations associated with human leukemias. Proc Natl Acad Sci U S A, 1991. **88**(23): p. 10735-9.

100. Yu, B.D., et al., Altered Hox expression and segmental identity in Mll-mutant mice. Nature, 1995. **378**(6556): p. 505-8.

101. Jude, C.D., et al., Unique and independent roles for MLL in adult hematopoietic stem cells and progenitors. Cell Stem Cell, 2007. **1**(3): p. 324-37.

102. Ernst, P., et al., Definitive hematopoiesis requires the mixed-lineage leukemia gene. Dev Cell, 2004. **6**(3): p. 437-43.

103. McMahon, K.A., et al., Mll has a critical role in fetal and adult hematopoietic stem cell self-renewal. Cell Stem Cell, 2007. **1**(3): p. 338-45.

104. Terranova, R., et al., Histone and DNA methylation defects at Hox genes in mice expressing a SET domain-truncated form of Mll. Proc Natl Acad Sci U S A, 2006. **103**(17): p. 6629-34.

105. Dou, Y., et al., Physical association and coordinate function of the H3 K4 methyltransferase MLL1 and the H4 K16 acetyltransferase MOF. Cell, 2005. **121**(6): p. 873-85.

106. Steward, M.M., et al., Molecular regulation of H3K4 trimethylation by ASH2L, a shared subunit of MLL complexes. Nat Struct Mol Biol, 2006. **13**(9): p. 852-4.

107. Yokoyama, A., et al., Leukemia proto-oncoprotein MLL forms a SET1-like his-

tone methyltransferase complex with menin to regulate Hox gene expression. Mol Cell Biol, 2004. **24**(13): p. 5639-49.

108. Guenther, M.G., et al., *Global and Hox-specific roles for the MLL1 methyltransferase.* Proc Natl Acad Sci U S A, 2005. **102**(24): p. 8603-8.

109. Wang, P., et al., Global analysis of H3K4 methylation defines MLL family member targets and points to a role for MLL1-mediated H3K4 methylation in the regulation of transcriptional initiation by RNA polymerase II. Mol Cell Biol, 2009. **29**(22): p. 6074-85.

110. Milne, T.A., et al., MLL targets SET domain methyltransferase activity to Hox gene promoters. Mol Cell, 2002. **10**(5): p. 1107-17.

111. Li, Y., et al., The miR-17-92 cluster expands multipotent hematopoietic progenitors while imbalanced expression of its individual oncogenic miRNAs promotes leukemia in mice. Blood, 2012.

112. Mi, S., et al., Aberrant overexpression and function of the miR-17-92 cluster in MLL-rearranged acute leukemia. Proc Natl Acad Sci U S A, 2010. **107**(8): p. 3710-5.

113. Biondi, A., et al., *Biological and therapeutic aspects of infant leukemia.* Blood, 2000. **96**(1): p. 24-33.

114. Joannides, M. and D. Grimwade, *Molecular biology of therapy-related leukaemias.* Clin Transl Oncol, 2010. **12**(1): p. 8-14.

115. Balgobind, B.V., et al., Novel prognostic subgroups in childhood 11q23/MLL-rearranged acute myeloid leukemia: results of an international retrospective study. Blood, 2009. **114**(12): p. 2489-96.

116. Krivtsov, A.V., et al., Transformation from committed progenitor to leukaemia stem cell initiated by MLL-AF9. Nature, 2006. **442**(7104): p. 818-22.

117. Milne, T.A., et al., MLL associates specifically with a subset of transcriptionally active target genes. Proc Natl Acad Sci U S A, 2005. **102**(41): p. 14765-70.

118. Horton, S.J., et al., Continuous MLL-ENL expression is necessary to establish a "Hox Code" and maintain immortalization of hematopoietic progenitor cells. Cancer Res, 2005. **65**(20): p. 9245-52.

119. Milne, T.A., et al., Leukemogenic MLL fusion proteins bind across a broad region of the Hox a9 locus, promoting transcription and multiple histone modifications. Cancer Res, 2005. **65**(24): p. 11367-74.

120. Xia, Z.B., et al., The MLL fusion gene, MLL-AF4, regulates cyclin-dependent kinase inhibitor CDKN1B (p27kip1) expression. Proc Natl Acad Sci U S A, 2005. **102**(39): p. 14028-33.

121. Daigle, S.R., et al., Selective killing of mixed lineage leukemia cells by a potent

small-molecule DOT1L inhibitor. Cancer Cell, 2011. **20**(1): p. 53-65.

122. Nguyen, A.T. and Y. Zhang, *The diverse functions of Dot1 and H3K79 methylation.* Genes Dev, 2011. **25**(13): p. 1345-58.

123. Okada, Y., et al., *hDOT1L links histone methylation to leukemogenesis.* Cell, 2005. **121**(2): p. 167-78.

124. Caslini, C., et al., Interaction of MLL amino terminal sequences with menin is required for transformation. Cancer Res, 2007. **67**(15): p. 7275-83.

125. Yokoyama, A., et al., The menin tumor suppressor protein is an essential oncogenic cofactor for MLL-associated leukemogenesis. Cell, 2005. **123**(2): p. 207-18.

126. Caligiuri, M.A., et al., Rearrangement of ALL1 (MLL) in acute myeloid leukemia with normal cytogenetics. Cancer Res, 1998. **58**(1): p. 55-9.

127. Dorrance, A.M., et al., Mll partial tandem duplication induces aberrant Hox expression in vivo via specific epigenetic alterations. J Clin Invest, 2006. **116**(10): p. 2707-16.

128. Katsumoto, T., et al., *MOZ is essential for maintenance of hematopoietic stem cells.* Genes Dev, 2006. **20**(10): p. 1321-30.

129. Thomas, T., et al., Monocytic leukemia zinc finger protein is essential for the development of long-term reconstituting hematopoietic stem cells. Genes Dev, 2006. **20**(9): p. 1175-86.

130. Katsumoto, T., N. Yoshida, and I. Kitabayashi, Roles of the histone acetyltransferase monocytic leukemia zinc finger protein in normal and malignant hematopoiesis. Cancer Sci, 2008. **99**(8): p. 1523-7.

131. Borrow, J., et al., The translocation t(8;16)(p11;p13) of acute myeloid leukaemia fuses a putative acetyltransferase to the CREB-binding protein. Nat Genet, 1996. **14**(1): p. 33-41.

132. Kitabayashi, I., et al., Fusion of MOZ and p300 histone acetyltransferases in acute monocytic leukemia with a t(8;22)(p11;q13) chromosome translocation. Leukemia, 2001. **15**(1): p. 89-94.

133. Liang, J., et al., Acute mixed lineage leukemia with an inv(8)(p11q13) resulting in fusion of the genes for MOZ and TIF2. Blood, 1998. **92**(6): p. 2118-22.

134. Huntly, B.J., et al., MOZ-TIF2, but not BCR-ABL, confers properties of leukemic stem cells to committed murine hematopoietic progenitors. Cancer Cell, 2004. **6**(6): p. 587-96.

135. Rowley, J.D., Letter: A new consistent chromosomal abnormality in chronic myelogenous leukaemia identified by quinacrine fluorescence and Giemsa staining. Nature, 1973. **243**(5405): p. 290-3.

136. Camos, M., et al., Gene expression profiling of acute myeloid leukemia with translocation t(8;16)(p11;p13) and MYST3-CREBBP rearrangement reveals a distinctive signature with a specific pattern of HOX gene expression. Cancer Res, 2006. **66**(14): p. 6947-54.

137. Stark, B., et al., A distinct subtype of M4/M5 acute myeloblastic leukemia (AML) associated with t(8:16)(p11:p13), in a patient with the variant t(8:19)(p11:q13)--case report and review of the literature. Leuk Res, 1995. **19**(6): p. 367-79.

138. Imamura, T., et al., Rearrangement of the MOZ gene in pediatric therapy-related myelodysplastic syndrome with a novel chromosomal translocation t(2;8)(p23;p11). Genes Chromosomes Cancer, 2003. **36**(4): p. 413-9.

139. Ripperger, T., et al., Constitutional trisomy 8p11.21-q11.21 mosaicism: a germline alteration predisposing to myeloid leukaemia. Br J Haematol, 2011. **155**(2): p. 209-17.

140. Mills, A.A., Throwing the cancer switch: reciprocal roles of polycomb and trithorax proteins. Nat Rev Cancer, 2010. **10**(10): p. 669-82.

141. Cloos, P.A., et al., Erasing the methyl mark: histone demethylases at the center of cellular differentiation and disease. Genes Dev, 2008. **22**(9): p. 1115-40.

142. Shi, Y., et al., Histone demethylation mediated by the nuclear amine oxidase homolog LSD1. Cell, 2004. **119**(7): p. 941-53.

143. Chang, B., et al., *JMJD6 is a histone arginine demethylase.* Science, 2007. **318**(5849): p. 444-7.

144. Huang, J., et al., *p53 is regulated by the lysine demethylase LSD1.* Nature, 2007. **449**(7158): p. 105-8.

145. Allis, C.D., et al., *New nomenclature for chromatin-modifying enzymes.* Cell, 2007. **131**(4): p. 633-6.

146. Kooistra, S.M. and K. Helin, *Molecular mechanisms and potential functions of histone demethylases.* Nat Rev Mol Cell Biol, 2012. **13**(5): p. 297-311.

147. Shi, Y.J., et al., Regulation of LSD1 histone demethylase activity by its associated factors. Mol Cell, 2005. **19**(6): p. 857-64.

148. Metzger, E., et al., LSD1 demethylates repressive histone marks to promote androgen-receptor-dependent transcription. Nature, 2005. **437**(7057): p. 436-9.

149. Agger, K., et al., UTX and JMJD3 are histone H3K27 demethylases involved in HOX gene regulation and development. Nature, 2007. **449**(7163): p. 731-4.

150. De Santa, F., et al., The histone H3 lysine-27 demethylase Jmjd3 links inflammation to inhibition of polycomb-mediated gene silencing. Cell, 2007. **130**(6): p. 1083-94.

151. Lederer, D., et al., Deletion of KDM6A, a histone demethylase interacting with MLL2, in three patients with Kabuki syndrome. Am J Hum Genet, 2012. **90**(1): p. 119-

24.

152. Lee, M.G., et al., Demethylation of H3K27 regulates polycomb recruitment and H2A ubiquitination. Science, 2007. **318**(5849): p. 447-50.

153. Pasini, D., et al., JARID2 regulates binding of the Polycomb repressive complex 2 to target genes in ES cells. Nature, 2010. **464**(7286): p. 306-10.

154. Pasini, D., et al., Coordinated regulation of transcriptional repression by the RBP2 H3K4 demethylase and Polycomb-Repressive Complex 2. Genes Dev, 2008. **22**(10): p. 1345-55.

155. Peng, J.C., et al., Jarid2/Jumonji coordinates control of PRC2 enzymatic activity and target gene occupancy in pluripotent cells. Cell, 2009. **139**(7): p. 1290-302.

156. Shen, X., et al., Jumonji modulates polycomb activity and self-renewal versus differentiation of stem cells. Cell, 2009. **139**(7): p. 1303-14.

157. DiTacchio, L., et al., Histone lysine demethylase JARID1a activates CLOCK-BMAL1 and influences the circadian clock. Science, 2011. **333**(6051): p. 1881-5.

158. Takeuchi, T., et al., Gene trap capture of a novel mouse gene, jumonji, required for neural tube formation. Genes Dev, 1995. **9**(10): p. 1211-22.

159. Li, M.O., et al., Phosphatidylserine receptor is required for clearance of apoptotic cells. Science, 2003. **302**(5650): p. 1560-3.

160. Schneider, J.E., et al., Identification of cardiac malformations in mice lacking Ptdsr using a novel high-throughput magnetic resonance imaging technique. BMC Dev Biol, 2004. **4**: p. 16.

161. Tsukada, Y., et al., Histone demethylation by a family of JmjC domain-containing proteins. Nature, 2006. **439**(7078): p. 811-6.

162. Loh, Y.H., et al., Jmjd1a and Jmjd2c histone H3 Lys 9 demethylases regulate self-renewal in embryonic stem cells. Genes Dev, 2007. **21**(20): p. 2545-57.

163. Agger, K., et al., The H3K27me3 demethylase JMJD3 contributes to the activation of the INK4A-ARF locus in response to oncogene- and stress-induced senescence. Genes Dev, 2009. **23**(10): p. 1171-6.

164. Hayami, S., et al., Overexpression of the JmjC histone demethylase KDM5B in human carcinogenesis: involvement in the proliferation of cancer cells through the E2F/RB pathway. Mol Cancer, 2010. **9**: p. 59.

165. Jepsen, K., et al., SMRT-mediated repression of an H3K27 demethylase in progression from neural stem cell to neuron. Nature, 2007. **450**(7168): p. 415-9.

166. Pospisil, V., et al., Epigenetic silencing of the oncogenic miR-17-92 cluster during PU.1-directed macrophage differentiation. EMBO J, 2011. **30**(21): p. 4450-64.

167. Sen, G.L., et al., Control of differentiation in a self-renewing mammalian tissue by the histone demethylase JMJD3. Genes Dev, 2008. **22**(14): p. 1865-70.

168. Strobl-Mazzulla, P.H., T. Sauka-Spengler, and M. Bronner-Fraser, *Histone demethylase JmjD2A regulates neural crest specification.* Dev Cell, 2010. **19**(3): p. 460-8.

169. He, J., A.T. Nguyen, and Y. Zhang, KDM2b/JHDM1b, an H3K36me2-specific demethylase, is required for initiation and maintenance of acute myeloid leukemia. Blood, 2011. **117**(14): p. 3869-80.

170. Liu, G., et al., Genomic amplification and oncogenic properties of the GASC1 histone demethylase gene in breast cancer. Oncogene, 2009. **28**(50): p. 4491-500.

171. Xiang, Y., et al., *JARID1B is a histone H3 lysine 4 demethylase up-regulated in prostate cancer.* Proc Natl Acad Sci U S A, 2007. **104**(49): p. 19226-31.

172. Orkin, S.H., et al., *The transcriptional network controlling pluripotency in ES cells.* Cold Spring Harb Symp Quant Biol, 2008. **73**: p. 195-202.

173. Benevolenskaya, E.V., et al., Binding of pRB to the PHD protein RBP2 promotes cellular differentiation. Mol Cell, 2005. **18**(6): p. 623-35.

174. Christensen, J., et al., RBP2 belongs to a family of demethylases, specific for tri- and dimethylated lysine 4 on histone 3. Cell, 2007. **128**(6): p. 1063-76.

175. Lopez-Bigas, N., et al., Genome-wide analysis of the H3K4 histone demethylase RBP2 reveals a transcriptional program controlling differentiation. Mol Cell, 2008. **31**(4): p. 520-30.

176. Schmitz, S.U., et al., Jarid1b targets genes regulating development and is involved in neural differentiation. EMBO J, 2011. **30**(22): p. 4586-600.

177. Dey, B.K., et al., The histone demethylase KDM5b/JARID1b plays a role in cell fate decisions by blocking terminal differentiation. Mol Cell Biol, 2008. **28**(17): p. 5312-27.

178. Gildea, J.J., R. Lopez, and A. Shearn, A screen for new trithorax group genes identified little imaginal discs, the Drosophila melanogaster homologue of human retinoblastoma binding protein 2. Genetics, 2000. **156**(2): p. 645-63.

179. Secombe, J., et al., The Trithorax group protein Lid is a trimethyl histone H3K4 demethylase required for dMyc-induced cell growth. Genes Dev, 2007. **21**(5): p. 537-51.

180. Secombe, J. and R.N. Eisenman, The function and regulation of the JARID1 family of histone H3 lysine 4 demethylases: the Myc connection. Cell Cycle, 2007. **6**(11): p. 1324-8.

181. Saleque, S., et al., Epigenetic regulation of hematopoietic differentiation by Gfi-1 and Gfi-1b is mediated by the cofactors CoREST and LSD1. Mol Cell, 2007. **27**(4): p.

562-72.

182. Konuma, T., et al., Forced expression of the histone demethylase Fbxl10 maintains self-renewing hematopoietic stem cells. Exp Hematol, 2011. **39**(6): p. 697-709 e5.

183. Frescas, D., et al., JHDM1B/FBXL10 is a nucleolar protein that represses transcription of ribosomal RNA genes. Nature, 2007. **450**(7167): p. 309-13.

184. He, J., et al., The H3K36 demethylase Jhdm1b/Kdm2b regulates cell proliferation and senescence through p15(Ink4b). Nat Struct Mol Biol, 2008. **15**(11): p. 1169-75.

185. Issaeva, I., et al., Knockdown of ALR (MLL2) reveals ALR target genes and leads to alterations in cell adhesion and growth. Mol Cell Biol, 2007. **27**(5): p. 1889-903.

186. Cox, B.J., et al., *Phenotypic annotation of the mouse X chromosome.* Genome Res, 2010. **20**(8): p. 1154-64.

187. Lee, S., J.W. Lee, and S.K. Lee, UTX, a histone H3-lysine 27 demethylase, acts as a critical switch to activate the cardiac developmental program. Dev Cell, 2012. **22**(1): p. 25-37.

188. Lan, F., et al., A histone H3 lysine 27 demethylase regulates animal posterior development. Nature, 2007. **449**(7163): p. 689-94.

189. Liu, J., et al., A functional role for the histone demethylase UTX in normal and malignant hematopoietic cells. Exp Hematol, 2012.

190. Rui, L., et al., *Cooperative epigenetic modulation by cancer amplicon genes.* Cancer Cell, 2010. **18**(6): p. 590-605.

191. Vinatzer, U., et al., Mucosa-associated lymphoid tissue lymphoma: novel translocations including rearrangements of ODZ2, JMJD2C, and CNN3. Clin Cancer Res, 2008. **14**(20): p. 6426-31.

192. van Haaften, G., et al., Somatic mutations of the histone H3K27 demethylase gene UTX in human cancer. Nat Genet, 2009. **41**(5): p. 521-3.

193. Hu, Z., et al., A novel nuclear protein, 5qNCA (LOC51780) is a candidate for the myeloid leukemia tumor suppressor gene on chromosome 5 band q31. Oncogene, 2001. **20**(47): p. 6946-54.

194. Borodovsky, A., M.J. Seltzer, and G.J. Riggins, *Altered cancer cell metabolism in gliomas with mutant IDH1 or IDH2.* Curr Opin Oncol, 2012. **24**(1): p. 83-9.

195. Prensner, J.R. and A.M. Chinnaiyan, *Metabolism unhinged: IDH mutations in cancer.* Nat Med, 2011. **17**(3): p. 291-3.

196. Yan, H., et al., *IDH1 and IDH2 mutations in gliomas.* N Engl J Med, 2009. **360**(8): p. 765-73.

197. Mardis, E.R., et al., Recurring mutations found by sequencing an acute myeloid

leukemia genome. N Engl J Med, 2009. **361**(11): p. 1058-66.

198. Hsieh, A.C., et al., The translational landscape of mTOR signalling steers cancer initiation and metastasis. Nature, 2012.

199. Harris, W.J., et al., The Histone Demethylase KDM1A Sustains the Oncogenic Potential of MLL-AF9 Leukemia Stem Cells. Cancer Cell, 2012. **21**(4): p. 473-87.

200. Schenk, T., et al., Inhibition of the LSD1 (KDM1A) demethylase reactivates the all-trans-retinoic acid differentiation pathway in acute myeloid leukemia. Nat Med, 2012. **18**(4): p. 605-11.

201. Campisi, J. and F. d'Adda di Fagagna, *Cellular senescence: when bad things happen to good cells.* Nat Rev Mol Cell Biol, 2007. **8**(9): p. 729-40.

202. Rana, T.M., Illuminating the silence: understanding the structure and function of small RNAs. Nat Rev Mol Cell Biol, 2007. **8**(1): p. 23-36.

203. Dow, L.E., et al., *A pipeline for the generation of shRNA transgenic mice.* Nat Protoc, 2012. **7**(2): p. 374-93.

204. Hannon, G.J. and J.J. Rossi, *Unlocking the potential of the human genome with RNA interference.* Nature, 2004. **431**(7006): p. 371-8.

205. Kristensen, L.H., et al., Studies of H3K4me3 demethylation by KDM5B/Jarid1B/PLU1 reveals strong substrate recognition in vitro and identifies 2,4-pyridine-dicarboxylic acid as an in vitro and in cell inhibitor. FEBS J, 2012.

206. Boitano, A.E., et al., Aryl hydrocarbon receptor antagonists promote the expansion of human hematopoietic stem cells. Science, 2010. **329**(5997): p. 1345-8.

207. Bjorkman, M., et al., Systematic knockdown of epigenetic enzymes identifies a novel histone demethylase PHF8 overexpressed in prostate cancer with an impact on cell proliferation, migration and invasion. Oncogene, 2011.

208. Liu, W., et al., PHF8 mediates histone H4 lysine 20 demethylation events involved in cell cycle progression. Nature, 2010. **466**(7305): p. 508-12.

209. Feng, W., et al., PHF8 activates transcription of rRNA genes through H3K4me3 binding and H3K9me1/2 demethylation. Nat Struct Mol Biol, 2010. **17**(4): p. 445-50.

210. Fortschegger, K., et al., PHF8 targets histone methylation and RNA polymerase II to activate transcription. Mol Cell Biol, 2010. **30**(13): p. 3286-98.

211. Qi, H.H., et al., Histone H4K20/H3K9 demethylase PHF8 regulates zebrafish brain and craniofacial development. Nature, 2010. **466**(7305): p. 503-7.

212. Schofield, C.J. and P.J. Ratcliffe, *Oxygen sensing by HIF hydroxylases.* Nat Rev Mol Cell Biol, 2004. **5**(5): p. 343-54.

213. Takubo, K., et al., Regulation of the HIF-1alpha level is essential for hematopoi-

etic stem cells. Cell Stem Cell, 2010. **7**(3): p. 391-402.

ANNEXES 1

In vitro stem cell expansion: stepping closer towards self-renewal.

Cellot S, Sauvageau G., Gene Therapy (2006)

NEWS AND COMMENTARY

Gene Therapy (2006) 13, 1617–1618

www.nature.com/gt

In vitro stem cell expansion

Stepping closer towards self-renewal

S Cellot and G Sauvageau

Gene Therapy (2006) **13,** 1617–1618. doi:10.1038/sj.gt.3302804;
published online 1 June 2006

A recently published study by Zhang *et al.*[1] in *Nature Medicine* brings forward a new class of molecules serving as *ex vivo* expansion factors for hematopoietic stem cells (HSCs).

The continuous replenishment of mature blood cells relies on pluripotent HSCs, which can either self-renew and give rise to identical daughter stem cells or engage in differentiation and proliferation pathways involved in specific lineage formation. So far, mechanisms underlying cell fate decisions are not well characterized.

A symmetrical HSC self-renewal division generates two primitive stem cells, termed self-renewal of expansion (SR-E) (Figure 1a), whereas an asymmetrical type of division will generate an HSC and a differentiated progeny, preserving stem cell numbers, and named self-renewal of maintenance (SR-M) (Figure 1b).[2] Clearly, stem cells must undergo SR-E type of divisions to increase their numbers *in vivo*, as would be the case during ontogeny in the fetal liver and shortly after birth,[3] or following myeloablative bone marrow (BM) transplantation, where a critical interplay exists between intrinsic and extrinsic (e.g., micro-environmental) factors.

Attempts to achieve similar levels of HSC self-renewal *in vitro*, with optimization of the culture media with growth factors and cytokine or by retroviral gene transfer to BM cells,[4] have so far been modest, with up to a 40-fold net increase in HSC numbers in a 14-day culture period with BM cells engineered to overexpress HOXB4.[5] Indeed, most *ex vivo* culture conditions lead to symmetrical HSC divisions of differentiation, promptly leading to their depletion (Figure 1c). Maintenance and even modest *ex vivo* expansion of human HSCs would thus have significant impact for gene therapy protocols or for stem cell enrichment of grafts deemed unsuitable for transplantation purposes owing to scarce HSC content, as is often the case with cord blood samples. Avoiding the potential deleterious effects of insertional mutagenesis in doing so would have obvious clinical relevance.[6]

The work by Zhang *et al.*[1] provides further insight into conditions that favor survival and expansion of HSCs outside of their physiological niche. They have identified angiopoietin-like molecules, namely Angptl2 and Angptl3, through DNA microarray analysis of proteins differentially expressed in fetal liver CD3+Ter119 cells, which can support *ex vivo* expansion of HSCs,[7] as potential modulators of SR-M and SR-E divisions in culture. These proteins share similar characteristics with the angiopoietins, for instance, the coiled-coil and fibrinogen-like structural domains, but unlike them, they do not display binding affinity for the Tie tyrosine kinase receptor family, and their signal-transduction pathways are yet undefined.

Using competitive repopulation assays, 20 sorted side population (SP+) Sca+ (CD45.2+) BM cells, enriched in HSC content, were exposed for 5 days *in vitro* to either stem cell factor (SCF) alone or in combination with the conditioned medium of 293T human embryonic kidney cells transfected with Flag-tagged human Angptl2, and then co-transplanted in primary recipients (CD45.1+) together with 10 helper (CD45.1+) HSCs. Analyses of peripheral blood (PB) long-term reconstitution confirmed the *in vitro* depletion of HSCs in the presence of SCF alone, with no contribution from the donor (CD45.2+) cells to blood mature components. However, 10–20% reconstitution levels were observed when donor HSCs were concomitantly exposed to the conditioned supernatant of Flag-Angptl2-transfected cells. The experimental procedure was repeated using the serum-free STIF (*S*CF, *t*hrombopoietin, *i*nsulin-growth factor 2 and *f*ibroblast-growth factor 1) media and prolonging the culture period to 10 days, with or without Angptl2. Of note, the same group of investigators had previously reported eightfold *in vitro* increase in HSC numbers using this combination of growth factors alone.[8] Interestingly, cells exposed to both STIF media and Angptl2-containing supernatant for 10 days contributed more significantly to PB reconstitution (60–70%) at 9 months post-transplantation, than those exposed to STIF media alone (20–30%). These cultured cells retained terminal lymphomyeloid differentiation potential *in vivo* in primary and secondary recipients, with no evidence for malignant transformation.

To further strengthen the causal relationship between specific angiopoietin-like protein exposure and true stem cell expansion, the proteins were purified through affinity chromatography columns, and HSC frequency specifically calculated at

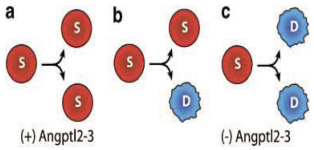

Figure 1 Symmetrical versus asymmetrical SR divisions. (**a**) HSCs can divide symmetrically with one parental cell giving rise to two identical daughter stem cells, hence increasing HSC numbers, a division termed SR-E, as occurs *in vivo* during ontogeny in the fetal liver, shortly following myeloablative BM transplantation, or *ex vivo* when HSCs are cultured in the presence of angiopoietin-like 2 or 3. (**b**) HSCs can also divide asymmetrically and generate both a primitive stem cell and a progeny committed to differentiation, thus preserving HSC numbers. This is termed SR of maintenance or SR-M, mainly the type of division believed to occur in the adult BM. (**c**) A stem cell can also divide symmetrically and give rise to two daughter cells committed to differentiation, a situation leading to HSC depletion, as is usually the case *in vitro* or *in vivo* in certain pathological conditions. Angptl2: angiopoietin-like 2; Angptl3: angiopoietin-like 3; D: differentiated cell; S: stem cell.

initiation and termination of culture, using transplantation at limiting dilution principles, thus enabling net HSC numbers increase to be calculated. At day 0 of culture, the HSC frequency, as evaluated by PB reconstitution at 6 months, was 1/39 for SP Sca+ freshly sorted cells. Upon exposure to Angptl2 and STIF for 10 days, this frequency rose to 1/1.6 cells, representing a net 24-fold *in vitro* expansion, or three times more than single use of STIF,[8] demonstrating the additive effect of this protein on HSC expansion. Considering the relatively modest and additive effect of Angpl2 (~3×) on HSC expansion compared to STIF media alone (~8×), the cellular mechanism (e.g., apoptosis, homing, cell division or self-renewal) affected by this orphan ligand cannot be ascertained until further experiments are performed.

Nonetheless, the authors provide compelling evidence regarding the pluripotency and the long-term repopulation potential of the expanded cells, confirming their stem cell nature. Comparable results, in terms of magnitude of HSC expansion, were obtained with purified Angptl3. The authors also underscore the importance of post-translational modifications present on human Angptl2, presumably glycosylation, and of the coiled-coil domain in carrying the reported effect on HSCs. Additional angiopoietin-like molecules, namely mouse Angptl3, human Angptl5, human Angptl7 and human microfibril-associated glycoprotein 4, also conferred an *in vivo* competitive repopulating advantage on *in vitro* exposed SP Sca1+ cells.

In conclusion, these studies provide an additional tool towards expanding HSCs, keeping in mind that the optimal setting or factor(s) that persistently trigger HSC self-renewal *in vitro* remain to be identified. ■

S Cellot is at the IRIC, Université de Montréal, PO Box 6128, Station Centre-Ville, Montreal, Quebec, Canada H3C 3J7.
E-mail: [redacted]
Published online 1 June 2006

1 Zhang CC, Kaba M, Ge G, Xie K, Tong W, Hug C, Lodish HF. Angiopoietin-like proteins stimulate *ex vivo* expansion of hematopoietic stem cells. *Nat Med* 2006; **12**: 240–245.
2 Lessard J, Faubert A, Sauvageau G. Genetic programs regulating HSC specification, maintenance and expansion. *Oncogene* 2004; **23**: 7199–7209.
3 Mikkola HK, Gekas C, Orkin SH, Dieterlen-Lievre F. Placenta as a site for hematopoietic stem cell development. *Exp Hematol* 2005; **33**: 1048–1054.
4 Sorrentino BP. Clinical strategies for expansion of haematopoietic stem cells. *Nat Rev Immunol* 2004; **4**: 878–888.
5 Antonchuk J, Sauvageau G, Humphries RK. HOXB4-induced expansion of adult hematopoietic stem cells *ex vivo*. *Cell* 2002; **109**: 39–45.
6 Hacein-Bey-Abina S, Von Kalle C, Schmidt M, McCormack MP, Wulffraat N, Leboulch P *et al*. LMO2-associated clonal T cell proliferation in two patients after gene therapy for SCID-X1. *Science* 2003; **302**: 415–419.
7 Zhang CC, Lodish HF. Insulin-like growth factor 2 expressed in a novel fetal liver cell population is a growth factor for hematopoietic stem cells. *Blood* 2004; **103**: 2513–2521.
8 Zhang CC, Lodish HF. Murine hematopoietic stem cells change their surface phenotype during *ex vivo* expansion. *Blood* 2005; **105**: 4314–4320.

ANNEXES 2

Zfx: at the crossroads of survival and self-renewal.

Cellot S, Sauvageau G. Cell 2007

Cell

REFERENCES

Arendt, D., and Nübler-Jung, K. (1994). Nature *380*, 37–40.

Denes, A.S., Jékely, G., Steinmetz, P.R.H., Raible, F., Snyman, H., Prud'homme, B., Ferrier, D.E.K., Balavoine, G., and Arendt, D. (2007). Cell, this issue.

De Robertis, E.M., and Sasai, Y. (1996). Nature *380*, 37–40.

Dohrn, A. (1875). Der Ursprung der Wirbelthiere und das princip des Functionswechsels (Leipzig: Verlag von Wilhelm Engelmann).

Lowe, C.J., Wu, M., Salic, A., Evans, L., Lander, E., Stange-Thomann, N., Gruber, C.E., Gerhar, T.J., and Kirschner, M. (2003). Cell *113*, 853–865.

Lowe, C.J., Terasaki, M., Wu, M., Freeman, R.M., Jr., Runft, L., Kwan, L., Haigo, S., Aronowicz, J., Lander, E., Gruber, C.E., et al. (2006). PLoS Biol. *4*, 1603–1619. 10.1371/journal.pbio.0040291.

Matus, D.Q., Pang, K., Marlow, H., Dunn, C.W., Thomsen, G.H., and Martindale, M.Q. (2006). Proc. Natl. Acad. Sci. USA *103*, 11195–11200.

Zfx: At the Crossroads of Survival and Self-Renewal

Sonia Cellot[1] **and Guy Sauvageau**[1,2,*]
[1]Laboratory of Molecular Genetics of Stem Cells, Institute for Research in Immunology and Cancer (IRIC), C.P. 6128 succursale Centre-Ville, Montréal, Québec H3C 3J7, Canada
[2]Department of Medicine and Division of Hematology and Leukemia Cell Bank of Quebec, Maisonneuve-Rosemont Hospital, Montréal, Québec H3C 3J7, Canada
*Correspondence: [redacted]
DOI 10.1016/j.cell.2007.04.002

As the molecular mechanisms that govern stem cell fate are beginning to be unraveled, Galan-Caridad et al. (2007) report in this issue of *Cell* a common role for the transcription factor Zfx in the self-renewal/maintenance of both embryonic stem cells and hematopoietic stem cells. Their work suggests that a regulator of self-renewal can be shared between two different cell types.

A key defining feature of stem cells is their ability to self-renew, that is, to preserve the identity of a parental cell through cell division in at least one of the two daughter cells. In general, the requirements for self-renewal include inhibition of differentiation with concomitant suppression of apoptosis and senescence pathways (Figure 1). Only under these circumstances does self-renewal occur, irrespective of stem cell type or the master fate regulators involved.

In this issue of *Cell*, Galan-Caridad et al. (2007) examined the self-renewal potential of murine embryonic stem cells (ESC) and tissue hematopoietic stem cells (HSC), two distinct types of stem cells that differ in several respects. First, ESC are derived from the inner cell mass of the early mammalian embryo and although only transient in vivo, they can be maintained in vitro as cell lines by the addition of serum (as a source of bone morphogenetic proteins) and leukemia inhibitory factor to the culture medium. HSC are specified in the aorta-gonad-mesonephros/yolk sac and then migrate to the fetal liver where they undergo expansion (from embryonic day 11.5–16.5). They ultimately migrate to the bone marrow niche (from embryonic day 17.5 onward) where they persist throughout adulthood, mostly in the G_0 phase of the cell cycle (Figure 1). Attempts to maintain or expand HSC outside of their in vivo niche remain modest, and HSC cell lines are not available currently. Second, ESC are pluripotent, that is, they can differentiate into all cell types of an adult animal; in contrast, HSC are multipotent, only giving rise to blood cell lineages. Third, quiescence and senescence are observed in HSC but not in ESC. Finally, ESC undergo symmetrical self-renewal divisions, with one stem cell giving rise to two daughter stem cells, resulting in an expansion in stem cell numbers. In contrast, adult HSC predominantly undergo asymmetrical self-renewal divisions, generating one stem cell and one more committed cell, thus preserving stem cell numbers while enabling blood cell regeneration in vivo. HSC undergo symmetrical self-renewal divisions only in specific and temporally restricted developmental contexts. Although key master regulators of HSC cell fate are still poorly defined, the molecular basis of ESC self-renewal are more rapidly unfolding, with recent evidence suggesting the involvement of two distinct groups of genes, *Nanog*/*Oct4*/*Sox2* and *Tbx3*/*Tcl1*/*Esrrb*/*Dppa4* (Ivanova et al., 2006), in the regulation of two separate pathways. Given the differences between ESC and HSC,

the question arises whether there are commonalities in the molecular mechanisms governing their self-renewal.

In this issue, Galan-Caridad et al. (2007) now describe a role for the zinc finger transcription factor Zfx in sustaining self-renewal divisions in both ESC and HSC. Given that *Zfx* knockout mice die at the neonatal stage, the authors generated a conditional *Zfx* allele in ESC to enable deletion of this gene in ESC and HSC at specific time points. Loss of Zfx in ESC resulted in near depletion of these cells in culture after only two to three passages, pointing to a proliferation defect with an accompanying increase in apoptosis that became very pronounced in serum-free conditions. Despite their rapid exhaustion in vitro, they still harbored markers of undifferentiated cells. Interestingly, Zfx-deficient ESC contributed to the majority of tissues in chimeric animals, excluding hematopoietic tissues, and could form teratomas upon subcutaneous injection into mice. These data suggest that Zfx normally suppresses apoptosis in ESC maintained in culture conditions that favor their self-renewal, but seems dispensable for their differentiation.

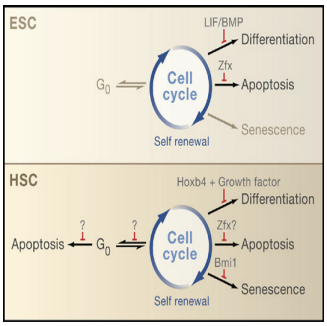

Figure 1. Self-Renewal and Survival in ESC and HSC

(Top) In culture conditions that maintain embryonic stem cells (ESC) in an undifferentiated state, leukemia inhibitory factor (LIF) and bone morphogenetic protein 4 (BMP4) are necessary to repress the onset of lineage commitment programs in ESC. To promote self-renewal, apoptotic pathways must also be inhibited, for example, through upregulation of *Tbx3* by the transcription factor Zfx (Galan-Caridad et al., 2007). Quiescence (G_0) and senescence have not been described in ESC.

(Bottom) To ensure efficient self-renewal, hematopoietic stem cells (HSC) in adult mammals also need to stave off differentiation (for example, with Hoxb4 and growth factors) and apoptosis (possibly through Zfx). A connection has been reported between induction of senescence in HSC lacking the Polycomb protein Bmi1 and decreased self-renewal capacity. Similarly, a factor that would drive HSC into apoptosis from G_0 would lead to their depletion. Question marks with inhibitory arrows refer to potential activities of Zfx.

In the hematopoietic system, adult mice lacking Zfx exhibited a steep decline in phenotypically defined HSC as early as 2–5 weeks postexcision of the allele, but their progeny transiently sustained blood cell formation. Clearly, self-renewal and maintenance of the long-term repopulating HSC is compromised in this setting, as explained by a moderate increase in apoptosis. Loss of the *Zfx* gene in the hematopoietic system of early embryos resulted in a more modest decrease in phenotypically defined fetal liver HSC, suggesting that Zfx is not required for this stage of development. In competitive adoptive HSC transfer experiments, Zfx-deficient stem cells displayed multilineage differentiation prior to depletion, but contribution of Zfx null cells to recipient peripheral blood reconstitution gradually declined over a 2–6 month period. The authors demonstrated that stem cell homing to the bone marrow was not affected, and seeding of the Zfx-deficient HSC into another niche, such as the spleen, was not found.

This study depicts fascinating aspects of HSC biology. To begin, it underscores the importance of following HSC behavior over time, to detect the onset of phenotypic aberrations, and thus attempt to decipher the underlying molecular dysfunction. Indeed, apoptosis may be maximal at the precise time point when HSC numbers begin to decline, and the reported difference in death rates between normal and Zfx null HSC could have been missed if cells were analyzed at a later time point. In addition, it provides an incentive to analyze data in light of cell-cycle phase distributions. For example, defects that would force HSC into apoptosis from G_0 may not directly involve self-renewal determinants, because by definition, self-renewal implies cell-cycle entry (Figure 1). Moreover, it must be remembered that some HSC properties, such as their ability to engraft, vary according to cell-cycle phase. In the future, it would also be interesting to determine if Zfx regulates HSC senescence. Moreover, it is tempting to draw a parallel between Zfx and other transcription factors that regulate HSC self-renewal such as Gfi1, Bmi1, Etv6, and FoxO (Hock et al., 2004a, 2004b; Lessard and Sauvageau, 2003; Park et al., 2003; Tothova et al., 2007).

After establishing that Zfx is important for the self-renewal of ESC and HSC, Galan-Caridad et al. (2007) investigated the underlying molecular circuits of Zfx in these two stem cell populations. Analysis of gene expression using microarrays revealed a common set of five downregulated and 20 upregulated Zfx target genes in ESC and HSC. Chromatin immunoprecipitation (ChIP) studies suggested that three of the downregulated genes are direct targets of Zfx and that their mRNA levels increased upon Zfx reintroduction. The authors examined additional candidate genes in Zfx-deficient ESC and observed that the master regulators of ESC pluripotency *Nanog*/*Oct4*/*Sox2* were only minimally affected by the removal of Zfx, whereas other ESC-specific genes such as *Ceacam1*, *Dub*, *Tbx3*, and *Tcl1* were all downregulated. ChIP assays further demonstrated that *Tbx3* and *Tcl1* are direct targets of Zfx. Interestingly, Tbx3 has been previously described to suppress apoptosis (Carlson et al., 2002), and downregulation of Tbx3 in Zfx null stem cells could provide an explanation for their increased cell death. Of note, a recent report suggests that Nanog does not regulate self-renewal in HSC (Tanaka et al., 2007).

The new work by Galan-Caridad et al. (2007) sheds light on the dual dependence of both pluripotent and multipotent stem cells on the transcription factor Zfx for their mainte-

Cell

nance. It also brings us to the intersecting paths of self-renewal and cell survival. Indeed, the direct comparison of ESC and HSC self-renewal and survival programs will require a more complete characterization of their respective components.

REFERENCES

Carlson, H., Ota, S., Song, Y., Chen, Y., and Hurlin, P.J. (2002). Oncogene *21*, 3827–3835.

Galan-Caridad, J.M., Harel, S., Arenzana, T.L., Hou, Z.E., Doetsch, F.K., Mirny, L.A., and Reizis, B. (2007). Cell, this issue.

Hock, H., Hamblen, M.J., Rooke, H.M., Schindler, J.W., Saleque, S., Fujiwara, Y., and Orkin, S.H. (2004a). Nature *431*, 1002–1007.

Hock, H., Meade, E., Medeiros, S., Schindler, J.W., Valk, P.J., Fujiwara, Y., and Orkin, S.H. (2004b). Genes Dev. *18*, 2336–2341.

Ivanova, N., Dobrin, R., Lu, R., Kotenko, I., Levorse, J., DeCoste, C., Schafer, X., Lun, Y., and Lemischka, I.R. (2006). Nature *442*, 533–538.

Lessard, J., and Sauvageau, G. (2003). Nature *423*, 255–260.

Park, I.K., Qian, D., Kiel, M., Becker, M.W., Pihalja, M., Weissman, I.L., Morrison, S.J., and Clarke, M.F. (2003). Nature *423*, 302–305.

Tanaka, Y., Era, T., Nishikawa, S.I., and Kawamata, S. (2007). Blood, in press. Published online March 14, 2007. 10.1182/blood.2006.08.039628.

Tothova, Z., Kollipara, R., Huntly, B.J., Lee, B.H., Castrillon, D.H., Cullen, D.E., McDowell, E.P., Lazo-Kallanian, S., Williams, I.R., Sears, C., et al. (2007). Cell *128*, 325–339.

Ephs and Ephrins Keep Pancreatic β Cells Connected

Rohit N. Kulkarni[1,*] and C. Ronald Kahn[2]
[1]Division of Cell and Molecular Physiology
[2]Division of Obesity and Hormone Action
Joslin Diabetes Center, Department of Medicine, Harvard Medical School, Boston MA 02215, USA
*Correspondence: [redacted]
DOI 10.1016/j.cell.2007.04.006

How insulin-secreting β cells of the pancreas communicate with each other is largely unknown. In this issue of *Cell*, Konstantinova et al. (2007) show that the signaling proteins EphA and ephrin-A modulate insulin secretion, providing fresh insights into the functional significance of the clustering of β cells, which occurs in islets.

The regulation of metabolic processes requires that cells communicate with their neighbors to ensure an appropriate response to the changing environment. The pancreas is a classic example of a tissue that depends on intercellular communication among the same (autocrine) and/or different (paracrine) cell types. The human pancreas is composed of over a million islets, each islet comprising several thousand cells including primarily insulin-secreting β cells but also glucagon-secreting α cells, somatostatin-secreting δ cells, pancreatic polypeptide-secreting (PP) cells, and ghrelin-producing ε cells. Within each islet, the different endocrine cells are thought to communicate with each other, either extracellularly via secreted products or directly through cell junctions. A role for paracrine and autocrine communication in the regulation of islet secretory function was proposed decades ago (Halban et al., 1982). For instance, insulin release from β cells can act on α cells to influence glucagon secretion, and somatostatin from δ cells acts as a paracrine inhibitor of neighboring α and β cells (Bonner-Weir and Orci, 1982; Samols and Stagner, 1990). Although intercellular exchange between β cells through membrane channels was confirmed by electrophysiologic and metabolic coupling experiments, the proteins and signaling mechanisms that underlie the communication between these insulin-secreting cells remain unclear. In this issue, Konstantinova et al. (2007) reveal that signaling via an ephrin ligand and its Eph receptor mediate communication between β cells.

Receptor tyrosine kinases (RTKs) play an important role in communicating crucial information from the environment to the inside of the cell to modulate fundamental cellular processes. The Eph receptors constitute the largest family of RTKs, and, together with their plasma membrane-bound ephrin ligands, have multiple functions during development and adulthood. Ephrins are divided into two subclasses: the A-subclass ligands (ephrin-A1 through ephrin-A5) are tethered to the cell membrane by a glycosylphosphatidylinositol anchor, whereas the B-subclass ligands (ephrin-B1 through ephrin-B3) have a transmembrane domain followed by a short cytoplasmic region (Kullander and Klein, 2002).

In contrast with most RTKs, the Eph family possesses a unique fea-

ANNEXES 3

Gfi-1: another piece in the HSC puzzle.

Cellot S, Sauvageau G. Trends Immunol 2005

References

1 Grubman, M.J. and Baxt, B. (2004) Foot-and-mouth disease. *Clin. Microbiol. Rev.* 17, 465–493
2 Rueckert, R.R. (1996) Picornaviridae: the viruses and their replication. In *Field's Virology* (Fields, B.N. *et al*., eds), pp. 609–654, Lippincott-Raven, Philadelphia and New York
3 Moraes, M.P. *et al*. (2002) Early protection against homologous challenge after a single dose of replication-defective human adenovirus type 5 expressing capsid proteins of foot-and-mouth disease virus (FMDV) strain A24. *Vaccine* 20, 1631–1639
4 Chen, W. *et al*. (2004) RNA interference targeting VP1 inhibits foot-and-mouth disease virus replication in BHK-21 cells and suckling mice. *J. Virol.* 78, 6900–6907
5 Denli, A.M. and Hannon, G.J. (2003) RNAi: an ever-growing puzzle. *Trends Biochem. Sci.* 28, 196–201
6 Fire, A. *et al*. (1998) Potent and specific genetic interference by double-stranded RNA in *Caenorhabditis elegans*. *Nature* 391, 806–811
7 McManus, M.T. and Sharp, P.A. (2002) Gene silencing in mammals by small interfering RNAs. *Nat. Rev. Genet.* 3, 737–747
8 Elbashir, S.M. *et al*. (2001) Duplexes of 21-nucleotide RNAs mediate interference in cultured mammalian cells. *Nature* 411, 494–498
9 Lecellier, C-H. and Voinnet, O. (2004) RNA silencing: no mercy for viruses? *Immunol. Rev.* 198, 285–303
10 Gitlin, L. and Andino, R. (2003) Nucleic-acid based immune system: the antiviral potential of mammalian RNA silencing. *J. Virol.* 77, 7159–7165
11 Li, H. *et al*. (2002) Induction and suppression of RNA silencing by an animal virus. *Science* 296, 1319–1321
12 Haasnoot, P.C.J. *et al*. (2003) Inhibition of virus replication by RNA interference. *J. Biomed. Sci.* 10, 607–616
13 Gitlin, L. *et al*. (2002) Short interfering RNA confers intracellular antiviral immunity in human cells. *Nature* 418, 430–434
14 Saleh, M-C. *et al*. (2004) RNA silencing in viral infections: insights from poliovirus. *Virus Res.* 102, 11–17
15 Song, E. *et al*. (2003) RNA interference targeting Fas protects mice from fulminant hepatitis. *Nat. Med.* 9, 347–351
16 McCaffrey, A.P. *et al*. (2003) Inhibition of hepatitis B virus in mice by RNA interference. *Nat. Biotechnol.* 21, 639–644
17 Xia, H. *et al*. (2002) siRNA-mediated gene silencing *in vitro* and *in vivo*. *Nat. Biotechnol.* 20, 1006–1010
18 Tiscornia, G. *et al*. (2003) A general method for gene knockdown in mice by using lentiviral vectors expressing small interfering RNA. *Proc. Natl. Acad. Sci. U. S. A.* 100, 1844–1848
19 Winston, W.M. *et al*. (2002) Systemic RNAi in *C. elegans* requires putative transmembrane protein SID-1. *Science* 295, 2456–2459
20 Baulcombe, D. (2002) Viral suppression of systemic silencing. *Trends Microbiol.* 10, 306–308
21 Li, H. *et al*. (2004) Interferon antagonist proteins of influenza and vaccinia viruses are suppressors of RNA silencing. *Proc. Natl. Acad. Sci. U. S. A.* 101, 1350–1355
22 Jackson, A.L. *et al*. (2003) Expression profiling reveals off-target gene regulation by RNAi. *Nat. Biotechnol.* 21, 635–637
23 Sledz, C.A. *et al*. (2003) Activation of the interferon system by short-interfering RNAs. *Nat. Cell Biol.* 5, 834–839
24 Chinsangaram, J. *et al*. (2003) A novel viral disease control strategy: adenovirus expressing interferon α rapidly protects swine from foot-and-mouth disease. *J. Virol.* 77, 1621–1625
25 Moraes, M.P. *et al*. (2003) Immediate protection of swine from foot-and-mouth disease: a combination of adenoviruses expressing interferon α and a foot-and-mouth disease virus subunit vaccine. *Vaccine* 22, 268–279
26 Wu, Q. *et al*. (2003) Adenovirus-mediated type I interferon expression delays and reduces disease signs in cattle challenged with foot-and-mouth disease virus. *J. Interferon Cytokine Res.* 23, 359–368
27 Rosas, M.F. *et al*. (2003) Stable expression of antisense RNAs targeted to the 5′ non-coding region confers heterotypic inhibition to foot-and-mouth disease virus infection. *J. Gen. Virol.* 84, 393–402

1471-4906/$ - see front matter
doi:10.1016/j.it.2004.12.002

Gfi-1: another piece in the HSC puzzle

Sonia Cellot and Guy Sauvageau

Institute of Research in Immunology and Cancer/Université de Montréal, C.P. 6128, Succ. Centre-Ville, Montréal, Québec, H3C 3J7, Canada

Recent work addresses the complex issue of stem cell regulation mechanisms. Both groups involved have studied the role of Gfi-1 in preserving the functional integrity of the adult hematopoietic stem cell (HSC) pool through a series of experiments, including phenotypic analysis of the primitive hematopoietic compartment, transplantation assays and cell cycle analyses. The results suggest that Gfi-1 deficiency leads to an exhaustion of HSCs in the adult mouse bone marrow, presumably through unrestricted cycling of these cells.

Introduction

Recent work on Gfi-1 (growth factor-independent-1), performed by Zeng *et al.* [1] and by Hock *et al.* [2], might shed some light into the utterly complex enigma of hematopoietic stem cell (HSC) regulation. Gfi-1, a transcriptional repressor harboring a Snail/Gfi-1 (SNAG) domain and six zinc-finger motifs, is expressed in several compartments of the hematopoietic system and is a member of the same oncogenic complementation group as the polycomb group gene Bmi-1 [3–9]. Evidence suggests that a dominant negative mutation of *Gfi-1* causes the human congenital neutropenia syndrome and leads to an increase in the elastase (ELA2) gene expression, linking these two genes in a common myeloid differentiation pathway [10].

The hematopoietic system relies on tissue-specific stem cells to consistently replenish its short-lived cellular components. Attributes of 'stemness' confer to this rare multipotent cell the capacity to proliferate and give rise to a more differentiated progeny, responsible for sustaining

Corresponding author: Sauvageau, G.[redacted]
Available online 7 January 2005

both myeloid and lymphoid lineages, and the ability to self-renew. Despite widespread interest, the molecular mechanisms regulating HSC self-renewal remain elusive. The concept of a long-lived precursor cell was perhaps first alluded to in ancient Greek mythology, when a furious Zeus condemned Prometheus to eternal punishment by attaching him to a rock at the summit of mount Caucasus, where an eagle would devour his liver during the day, while the torn hepatic tissue would regenerate itself during the night, only for repeated torture at dawn. Ideas and thoughts cross millenniums, and now the question becomes, how are stem cells generated and maintained?

Role of Gfi-1 in embryogenesis

Results on the function of Gfi-1 in HSCs are summarized in Figure 1 and Table 1 in parallel to the role of Bmi-1 in these same cells [11,12]. The absence of Gfi-1 during embryonic development does not seem to alter the specification mechanisms of HSCs because recipients of a high dose of *Gfi-1*$^{-/-}$ bone marrow (BM) cells are able to sustain donor-derived hematopoiesis for >3 months post-transplantation, as assessed by the distribution of the CD45.2 marker (donor origin) against the myeloid and lymphoid lineage differentiation markers in the host [1,2]. Indeed, only a multipotent stem cell present in the donor *Gfi-1*$^{-/-}$ mice BM compartment can functionally demonstrate this sustained reconstitution potential, with 100% of the mature elements of the blood still being derived from a *Gfi-1*$^{-/-}$ precursor cell, 12 weeks after the transplantation procedure.

This is in sharp contrast to the essential role of the stem cell leukemia (SCL)/tal-1 transcription factor in specifying HSC differentiation during early embryogenesis but whose expression is somewhat dispensable for later steps in HSC development, as previously reported by Mikkola *et al.* [13]. Reinforcing this point, phenotypic analysis of the KLS (c-kit^{+}, lineage^{-}, Sca^{+}) fraction of BM cells of *Gfi-1*$^{-/-}$ mice, known to contain true long-term repopulating HSCs at a frequency of ~1 in 30 cells, unveils slightly increased [2] or decreased [1] frequencies of this primitive compartment with respect to normal control mice, and the authors report normal total BM cellularity of the mutant mice [1,2], implying that they are potentially born with a close to normal HSC pool size.

Role of Gfi-1 in adult haematopoiesis

Phenotypically, *Gfi1*$^{-/-}$ mice display evidence of both myeloid and lymphoid lineage development at birth, however, maturation of these cells is defective. T and B cells are produced in reduced numbers with impaired functionality, the granulo–monocytic lineage cannot sustain the production of mature granulocytes, with accumulation of immature myeloid precursors in the blood and marked monocytosis, whereas red blood cell and platelet numbers seem initially adequate [6,14–16].

Zeng *et al.* [1] also report an altered clonogenic progenitor distribution, with profoundly decreased

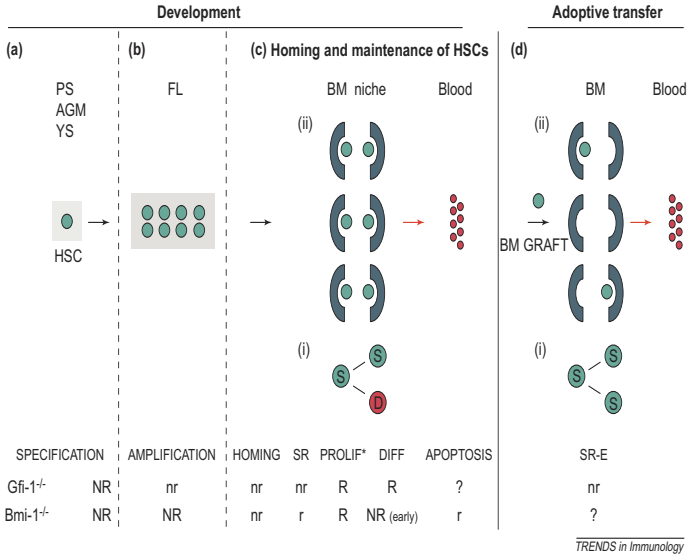

Figure 1. Milestones in hematopoietic stem cell (HSC) development and adoptive transfer, with stage specific requirements for Gfi-1 or Bmi-1 genes. **(a)** Embryonic developmental programs specify the generation of HSCs, in the extra-embryonic yolk sac (YS) and/or in the embryo *per se*, in the para-aortic splancho–pleura (PS) or aortic–gonadal–mesonephros (AGM) regions, followed by an expansion **(b)** of these primitive cells in the fetal liver (FL) [17]. This ensures a critical mass of HSCs that can then migrate and home **(c)** to the bone marrow (BM), where commitment to a more differentiated progeny occurs, followed by a transient and self-contained state of rapid proliferation that subsides and culminates in the emergence of the various mature blood cell types [18]. To preserve the stem cell pool, an asymmetrical type of cell division is believed to take place in the BM (c, i) [19], where a HSC gives rise to a biologically identical daughter cell and to a committed cell. In the early phase following BM transplantation [adoptive transfer, **(d)**], a given fraction of HSCs undergo a symmetrical type of cell division, leading to their net expansion (d, i). This phenomenon is referred to as self-renewal of expansion [SR-E, (d, i)]. Of note, the total HSC pool size of transplant recipients never reaches the normal physiological levels of untreated animals [compare (d, ii) with (c, ii)]. Requirements for Bmi-1 and Gfi-1 in HSC biology are summarized in the lower part of the figure. Abbreviations: D, differentiated cell; DIFF, differentiation; lowercase, inferred; NR, not required; PROLIF, proliferation (* see further details in Table 1); R, required; S, stem cell; uppercase, directly assessed.

Table 1. Proliferative defects in Gfi-1 vs Bmi-1 mutant HSCs[a,b]

Description	*Gfi-1*$^{-/-}$, young[c]	*Gfi-1*$^{-/-}$, old or 2ry[c]	*Bmi-1*$^{-/-}$, young[c]	*Bmi-1*$^{-/-}$ old or 2ry[c]
Cycling	↑ % in S phase	↑ % in S phase	?	↓ % in S phase
Proliferative potential	Probably normal	?	Reduced	Very reduced to absent
Self-renewal early post BMT (SR-E)	Probably normal	Probably normal	?	?
Self-renewal in adult BM	Probably normal	Probably normal	Probably abnormal	Probably very abnormal

[a]Abbreviations: BMT, bone marrow transplantation; Gfi-1, growth factor-independent-1; HSCs, hematopoietic stem cells; SR-E, self-renewal of expansion.
[b]Refs: for Gfi-1 [1,2], for Bmi-1 [11,12].
[c]Young, <3 weeks; old, >2 months; 2ry, secondary transplant recipient.

common lymphoid progenitor (CLP) and short-term repopulating HSC frequencies, a milder reduction in common myeloid progenitor (CMP) numbers and significant increase in granulo–monocytic progenitors (GMPs). Interestingly, by generating chimeric mice whose cells would either harbor heterozygous (+/−) or homozygous (−/−) disruption of *Gfi-1*, Hock *et al.* elegantly demonstrated by Southern blot analysis of DNA extracted from several cell types, including BM, spleen and thymus, that although both the *Gfi-1*$^{-/-}$ and *Gfi-1*$^{+/-}$ cells contributed to the hematopoietic tissues of young (<3 weeks) mice, the genetic fingerprint of *Gfi-1*$^{-/-}$ cells was no longer detectable in older mice (>2 months), except in tissues unrelated to the blood system. Similarly, hemoglobin isoform studies revealed a fading away of the *Gfi-1*$^{-/-}$ contribution to red blood cells, suggesting that *Gfi-1*$^{-/-}$ cells can initiate but not sustain hematopoiesis.

These age-related changes might explain the discrepancy between a slight increase in the KLS cell population documented in young (4 weeks) *Gfi1*$^{-/-}$ mice by Hock *et al.* [2], and a respective decrease (2- to fourfold) observed by Zeng *et al.* [1] in 4 to 8 week-old mice, in agreement with a stem cell depletion theory. Indeed, this discrepancy could also be attributed to differences in strain background of mice or gating procedures used by the two laboratories. One can also question the magnitude of the stem cell content generated in these animals at the completion of ontogeny programs. As inferred in their letter to *Nature*, Hock *et al.* report that a certain level of embryonic HSC expansion must have taken place to account for the level of hematopoiesis observed in young *Gfi-1*$^{-/-}$ mice, which is absolutely conceivable. Also, by transplanting day 14.5 fetal liver cells (FLCs) from *Gfi-1*$^{-/-}$ embryos into congenic hosts, at limiting dilution, one can estimate the stem cell frequency in this tissue, as was performed with *Gfi-1b*$^{-/-}$ (a closely related gene to *Gfi-1*) FLCs [2]. By analogy, using this approach, the HSC frequency in *Bmi-1*$^{-/-}$ day 14.5 fetal liver is estimated to be within normal limits, indicating that *Bmi-1* is not essential for the embryogenesis of HSCs but is absolutely required for their maintenance.

Functional assessment of *Gfi-1*$^{-/-}$ BM grafts

Experimental techniques available today only enable the retrospective assessment of stem cell properties, relying on the presence of a mature progeny (the legacy of a HSC) to draw conclusions on its characteristics, such as in transplantation assays. The low frequency of HSCs in the BM (estimated to be at ~1 in 100 000 cells) prevents direct and timely orchestrated analysis of stem cell regulatory mechanisms, including self-renewal. Nonetheless, these assays still provide extremely valuable information.

Both research papers, through serial transplantation experiments, clearly unravel the incapacity of *Gfi-1*$^{-/-}$ cells to survive adoptive transfer (perhaps secondary to a failure to symmetrically divide and expand), defined as self-renewal of expansion [SR-E, Figure 1d(i)], which is initially expected of HSCs present in a BM graft to ensure long-term lympho–myeloid reconstitution of the host. These cells perform poorly in a competitive transplantation setting, contributing to a slim but detectable host reconstitution only when present in large excess with respect to the control cells. Again, a lower stem cell frequency on the BM-cell population or a suboptimal SR-E mechanism might account for this behavior, however, this also raises an intriguing question: can the presence of a normal cell population partially revert the stem cell exhaustion phenotype of *Gfi-1*$^{-/-}$ cells? That is, is the defect inherent to the stem cell itself or is it a response to abnormal signaling loops emanating from multiple differentiation defects of the mature lineages? Certainly, the problem lies within the blood system, for *Gfi-1*$^{-/-}$ cells transplanted into a normal myeloablated host recreate the same mutant phenotype, whereas normal cells transplanted into a *Gfi-1*-null background can rescue hematopoiesis [1].

Along the same line of thought, the stem cell proliferation defect merits further discussion and can be arbitrarily subdivided into early or late (Table 1), corresponding to young (<3 weeks) and older (>2 months) mice, respectively. As stated earlier, *Bmi-1*$^{-/-}$ mice can generate a near normal HSC pool size during embryonic life but fail to maintain it in adult life, which is not quite the same scenario as in the absence of Gfi-1. As demonstrated through BrdU incorporation assays and cell cycle phase studies, the primitive *Gfi-1*$^{-/-}$ KLS cell population undergoes enhanced proliferation with respect to normal control cells, a phenomenon that is amplified with the additional stress of BM transplantation (BMT) [2]. Rightly so, Hock *et al.* evoke a possible role for Gfi-1 in restraining overt proliferation of HSCs, thus preventing their premature decline. The reported decrease in expression of the G1 checkpoint inhibitor p21 associated with the absence of Gfi-1, although a potential candidate pathway mediating increased cycling might not represent the sole mechanism involved in explaining stem cell fate, as inferred by the authors themselves.

Likewise, *Bmi-1* assumes functions in leukemic stem cells (LSCs) other than its repression of cyclin-dependent kinase inhibitors (CKIs) because weakly leukaemogenic but highly proliferative Bmi-1$^{-/-}$ clones, with impaired

expression of p19ARF and p16INK4a, can have their tumorigenic potential rescued by re-introduction of the *Bmi-1* gene [11]. Remarkably, when 500 sorted *Gfi-1*$^{-/-}$ KLS cells are transplanted along with a dose of helper cells, these give rise to a lessened, yet robust, lympho–myeloid reconstitution in the myeloablated recipient [1,2]. One might once more argue against a cell autonomous defect, and in favor of aberrant HSC proliferative signals sent by a dysfunctional progeny, which might be alleviated when the mutant stem cells are introduced into an organism in conjunction with normally committed cells. This is an ongoing debate and one way to address the question might be to perform a BrdU incorporation assay, in a post-transplantation setting, this time including both *Gfi-1*$^{-/-}$ and helper cells in the graft, hoping to somewhat normalize feedback loops and to quantify any decrease in the proliferative defect.

Concluding remarks

It is still to be shown that Gfi-1 regulates HSC homing or apoptosis, despite the interesting and thought provoking data presented by these two highlighted groups. However, these studies do demonstrate that the absence of Gfi-1 disrupts the functional integrity of BM HSCs, and might reveal an unsuspected cellular determinant for regulating HSC cycling.

Acknowledgements

We would like to thank Louise Leblanc, Jana Krosl, Jalila Chagraoui and Amélie Faubert for their assistance with the manuscript. S.C. is a Research Fellow of The Terry Fox Foundation through an award from the National Cancer Institute of Canada. G.S. holds a Canada Research Chair in Molecular Genetics of Stem Cell and is a Scholar of the Leukemia and Lymphoma Society.

References

1 Zeng, H. *et al.* (2004) Transcription factor Gfi1 regulates self-renewal and engraftment of hematopoietic stem cells. *EMBO J.* 23, 4116–4125
2 Hock, H. *et al.* (2004) Gfi-1 restricts proliferation and preserves functional integrity of haematopoietic stem cells. *Nature* 431, 1002–1007
3 Duan, Z. and Horwitz, M. (2003) Targets of the transcriptional repressor oncoprotein Gfi-1. *Proc. Natl. Acad. Sci. U. S. A.* 100, 5932–5937
4 Gilks, C.B. *et al.* (1993) Progression of interleukin-2 (IL-2)-dependent rat T cell lymphoma lines to IL-2-independent growth following activation of a gene (Gfi-1) encoding a novel zinc finger protein. *Mol. Cell. Biol.* 13, 1759–1768
5 Jafar-Nejad, H. and Bellen, H.J. (2004) Gfi/Pag-3/senseless zinc finger proteins: a unifying theme? *Mol. Cell. Biol.* 24, 8803–8812
6 Karsunky, H. *et al.* (2002) Inflammatory reactions and severe neutropenia in mice lacking the transcriptional repressor Gfi1. *Nat. Genet.* 30, 295–300
7 Scheijen, B. *et al.* (1997) Characterization of pal-1, a common proviral insertion site in murine leukemia virus-induced lymphomas of c-myc and Pim-1 transgenic mice. *J. Virol.* 71, 9–16
8 Schmidt, T. *et al.* (1996) MoMuLV proviral integrations identified by Sup-F selection in tumors from infected myc/pim bitransgenic mice correlate with activation of the gfi-1 gene. *Nucleic Acids Res.* 24, 2528–2534
9 Zhu, J. *et al.* (2002) Growth factor independent-1 induced by IL-4 regulates Th2 cell proliferation. *Immunity* 16, 733–744
10 Person, R.E. *et al.* (2003) Mutations in proto-oncogene GFI1 cause human neutropenia and target ELA2. *Nat. Genet.* 34, 308–312
11 Lessard, J. and Sauvageau, G. (2003) Bmi-1 determines the proliferative capacity of normal and leukaemic stem cells. *Nature* 423, 255–260
12 Park, I.K. *et al.* (2003) Bmi-1 is required for maintenance of adult self-renewing haematopoietic stem cells. *Nature* 423, 302–305
13 Mikkola, H.K. *et al.* (2003) Haematopoietic stem cells retain long-term repopulating activity and multipotency in the absence of stem-cell leukaemia SCL/tal-1 gene. *Nature* 421, 547–551
14 Hock, H. *et al.* (2003) Intrinsic requirement for zinc finger transcription factor Gfi-1 in neutrophil differentiation. *Immunity* 18, 109–120
15 Yucel, R. *et al.* (2003) The transcriptional repressor Gfi1 affects development of early, uncommitted c-Kit^{+} T cell progenitors and CD4/CD8 lineage decision in the thymus. *J. Exp. Med.* 197, 831–844
16 Saleque, S. *et al.* (2002) The zinc-finger proto-oncogene Gfi-1b is essential for development of the erythroid and megakaryocytic lineages. *Genes Dev.* 16, 301–306
17 Yoder, M.C. (2004) Generation of HSCs in the embryo and assays to detect them. *Oncogene* 23, 7161–7163
18 Lessard, J. *et al.* (2004) Genetic programs regulating HSC specification, maintenance and expansion. *Oncogene* 23, 7199–7209
19 Faubert, A. *et al.* (2004) Are genetic determinants of asymmetric stem cell division active in hematopoietic stem cells? *Oncogene* 23, 7247–7255

doi:10.1016/j.it.2004.12.005

ANNEXES 4

A functional screen to identify novel effectors of hematopoietic stem cell activity.

Deneault E, Cellot S, Faubert A, Laverdure JP, Fréchette M, Chagraoui J, Mayotte N, Sauvageau M, Ting SB, Sauvageau G., Cell 2009.

Cell

Resource

A Functional Screen to Identify Novel Effectors of Hematopoietic Stem Cell Activity

Eric Deneault,[1] Sonia Cellot,[1] Amélie Faubert,[1] Jean-Philippe Laverdure,[1] Mélanie Fréchette,[1] Jalila Chagraoui,[1] Nadine Mayotte,[1] Martin Sauvageau,[1] Stephen B. Ting,[1] and Guy Sauvageau[1,2,*]

[1]Molecular Genetics of Stem Cells Laboratory, Institute of Research in Immunology and Cancer (IRIC), University of Montreal, Montreal, Quebec H3C 3J7, Canada

[2]Division of Hematology and Leukemia Cell Bank of Quebec (BCLQ), Maisonneuve-Rosemont Hospital, Montreal, Quebec H1T 2M4, Canada

*Correspondence [redacted]

DOI 10.1016/j.cell.2009.03.026

SUMMARY

Despite tremendous progress made toward the identification of the molecular circuitry that governs cell fate in embryonic stem cells, genes controlling this process in the adult hematopoietic stem cell have proven to be more difficult to unmask. We now report the results of a novel gain-of-function screening approach, which identified a series of 18 nuclear factors that affect hematopoietic stem cell activity. Overexpression of ten of these factors resulted in an increased repopulating activity compared to unmanipulated cells. Interestingly, at least four of the 18 factors, *Fos, Tcfec, Hmgb1*, and *Sfpi1*, show non-cell-autonomous functions. The utilization of this screening method together with the creation of a database enriched for potential determinants of hematopoietic stem cell self-renewal will serve as a resource to uncover regulatory networks in these cells.

INTRODUCTION

The mature cell contingent of adult hematopoietic tissue is continuously replenished during the life span of an animal by the periodic supplies from hematopoietic stem cells (HSCs) that reside in a niche. To maintain blood homeostasis, these primitive cells rely on two critical properties, namely multipotency and self-renewal. The former enables differentiation into multiple lineages, while the latter ensures preservation of HSC fate upon cellular division. By definition, a self-renewal division implies that an HSC is permissive to cell cycle entry, while restrained from engaging in differentiation, apoptosis or senescence pathways. The transcriptional regulatory network of HSC self-renewal still remains largely undefined, an observation that contrasts with that of embryonic stem cells (ESCs), for which self-renewal is increasingly dissected molecularly (reviewed in Jaenisch and Young, 2008). Only a few nuclear factors have been documented as promoters of HSC expansion (reviewed in Hai-Jiang et al., 2008). Of these factors, *Hoxb4* and its derivatives (*Hoxa9*, *NA10HD*) are among the most potent and best documented (Ohta et al., 2007; Thorsteinsdottir et al., 2002).

The differential pace of progress propelling the fields of ESC and HSC research reflects, at least in part, seminal discoveries that rendered ESCs more amenable to large-scale experiments. First, although only observable as a transient state in vivo, ESCs derived from the inner cell mass can be maintained in vitro as cell lines by the addition of serum (as a source of bone morphogenic protein [BMP]) and leukemia inhibitory factor (LIF). Attempts to maintain or expand HSCs ex vivo as homogenous populations have been modest, and successful development of cell lines have not been reported, hampering harvest of large numbers of HSCs. Second, a stringent surrogate marker to follow the HSC multipotent state, comparable to the pluripotency tags of Oct4, Nanog, AP, or SSEA1 for ESCs, is still lacking. Albeit yielding small numbers, current cell sorting strategies allow isolation of HSC populations to near purity (Kiel et al., 2005). However, shortly upon facing the selective pressures of in vitro culture conditions, changes in cell phenotype are observed (Uchida et al., 2004), impeding HSC tracking in this context. The gold standard to confirm HSC activity for cells kept in culture remains the in vivo competitive repopulation assay. Importantly, generation of retroviral vectors provides highly efficient tools to infect and thereby modulate gene expression in both ESCs and HSCs (Root et al., 2006).

The demonstration that in mouse fibroblasts a given nucleocytoplasmic configuration, or state, can be reverted to a stem cell phenotype by the enforced overexpression of four defined nuclear factors, i.e., Oct4, Sox2, c-Myc, and Klf4, stands as a conceptual breakthrough (Takahashi and Yamanaka, 2006). Indeed, the ability to create induced pluripotent stem cells, or iPS cells, suggests that a putative role for as yet unidentified nuclear factors in orchestrating HSC fate is probable. With this mindset, interrogation of stem cell expression profile databases was undertaken. From this data set, a listing and ranking of nuclear factors whose transcripts were abundant in stem cell-enriched subpopulations was generated. Over 100 of the highest-scoring candidates were then functionally tested in HSCs, using a high-throughput overexpression in vitro to in vivo assay tailored to circumvent current limitations imposed by the biology of HSCs. As detailed below, these studies serve as a further step

Cell

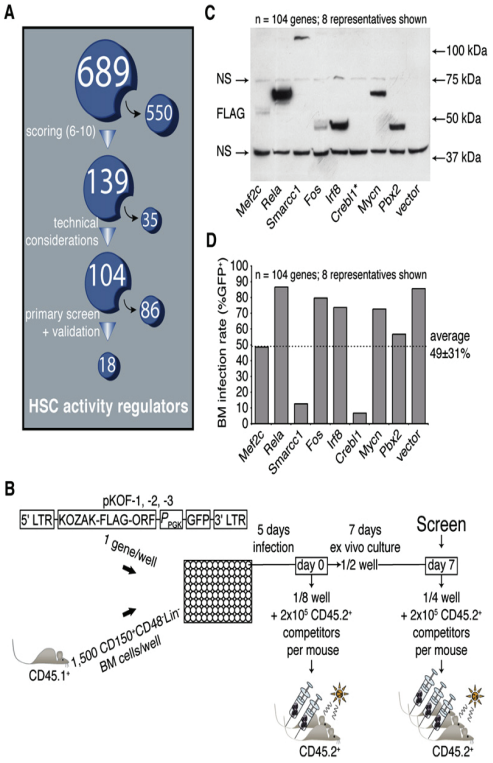

Figure 1. Experimental Design of Nuclear Factors Screening Strategy

(A) A list of candidate genes (see Table S1 for the complete list) was generated as described in the Results. The 689 nuclear factors were subsequently ranked on the basis of an algorithm that stratifies them according to properties predictive of self-renewal regulation. The highest scoring candidates (n = 139) were further selected for functional assessment with a retroviral overexpression approach. Of these, 104 were tested (see "*" in Table S1), and the remaining 35 genes were excluded for technical reasons.

(B) The coding sequence of each tested candidate was subcloned into one out of three modified MSCV vectors, each containing a different reading frame (pKOF-1, -2 and -3). Respective retroviral producers were seeded in a single well of a 96-well plate and cocultured for 5 days with 1500 $CD150^+CD48^-Lin^-$ freshly sorted bone marrow $CD45.1^+$ cells. Immediately upon infection (day 0), one-eighth of each well was transplanted into two congenic recipient mice along with 2×10^5 total BM cells ($CD45.2^+$). A similar assay, this time with three recipient mice, was performed after an additional week of ex vivo culture (day 7), on which the screen was performed.

(C) Expression of candidate proteins in retroviral-producing cells was tested by western immunoblotting and revealed with an anti-FLAG antibody. A list of predicted and observed molecular weights for most proteins tested in this screen is available in Table S2. NS, nonspecific signal; *, example of a protein that could not be detected by western blot analysis (see also Table S2).

(D) Range of retroviral gene transfer efficiencies of sampled candidate genes on the basis of EGFP expression assessed at day 4 of HSC culture (only eight representatives shown; dashed line represents average on all 104 genes).

forward into the exploration of the molecular circuitry that governs HSC self-renewal.

RESULTS

Selection and Ranking of Candidate Genes

As a corollary of ESC studies, it can be proposed that HSC fate is also controlled by a series of master regulators analogous to Oct4 and several subordinate effectors, providing sound basis for the generation of a stem cell nuclear factors database. Toward this end, we created a database consisting of 689 nuclear factors (Figure 1A; Table S1 available online; see also http://www.bioinfo.iric.ca/self-renewal/) considered as candidate regulators of HSC activity. This list was predominantly derived from microarray gene expression profiling of normal and leukemia stem cells, including our recently generated FLA2 leukemia (1 in 1.5 cells is a leukemia stem cell, A.F. and G.S., unpublished data). Genes obtained after a review of the literature on stem cell self-renewal were also added to the list (see legend of Table S1 for references). Genes in this database were then ranked from 1 (lowest priority) to 10 (highest priority) on the basis of three factors: differential expression between primitive and more mature cell fractions (e.g., HSC-enriched), expression level (high levels were given highest priority), and the consistency of findings between data sets. Genes with a score of 6 and above (n = 139) were selected for functional studies, of which 104 were tested (Figure 1A; see also asterisks in Table S1). Interestingly, the list of selected candidates is highly enriched for bona fide regulators of hematopoiesis, namely *Egr1*, *Gata2*, *Sfpi1* (PU.1), *Foxo1*, *Meis1*, *Myb*, *Hoxa9*, and *Runx1* (Min et al., 2008; reviewed in Lessard et al., 2004). However, the majority of the other candidates have no reported function in primitive hematopoietic cells.

Design and Principle of the Screen

The screening protocol is outlined in Figure 1B. In brief, high-titer retroviruses were produced in 96-well plates seeded with viral producer cells using an optimized procedure. Protein extracts derived from producer cells in each of the 104 wells were analyzed by western blotting, which confirmed the presence of a FLAG protein in 89% of the cases (Figure 1C provides eight representative candidates; details for all 104 genes are listed in Table S2, sixth column), with 92% of these proteins showing the expected molecular size (Table S2, compare the fifth and sixth columns). $CD150^+CD48^-Lin^-$ mouse bone marrow (BM) cells were infected during 5 days and transplanted at two different time points (i.e., day 0 and day 7 in Figure 1B). Under these conditions, the average gene transfer to the cultured $CD150^+CD48^-Lin^-$ cells was at 49% ± 31% (Figure 1D provides eight representative candidates; details for all 104 genes are

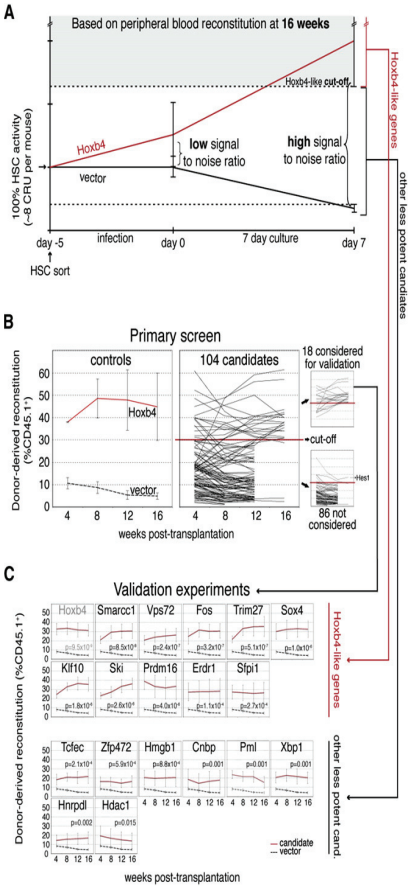

Figure 2. Identification of Positive Candidates with *Hoxb4*-like Activity

(A) Estimation of HSC activity during viral transduction and culture. Lines show estimation of HSC activity in recipients of day −5, day 0, or day 7 bone marrow (BM) cells transduced with *Hoxb4* (red) or control vector (black). Two independent experiments were performed with purified and whole bone marrow cells for *Hoxb4*, and three with purified BM cells for controls. Extrapolation of HSC numbers in recipients (y axis) was based on relative reconstitution levels observed in the CRU assay performed with our starting HSC subpopulation in Figures S2B–S2C. In all experiments, each mouse received eight equivalent day −5 HSCs (representing 100% HSC activity and evaluated by CRU assay) and 20 equivalent fresh competitor HSCs (see legend of Figure S2 for details). Cutoff for identification of *Hoxb4*-like candidates used in the primary screen/validation experiments (shaded area) is set on the basis of the standard deviation/error of the mean reconstitution level observed in multiple recipients of *Hoxb4*-transduced HSCs. Cutoff for other less potent candidates (area between dotted lines) is used only in validation experiments and is based on statistical difference between candidates and vector control.

(B) Graft-derived hematopoiesis was evaluated at 4 week intervals in recipients of cultured HSCs during the primary screen. As a set of reference values, the left panel indicates peripheral blood reconstitution levels from mice transplanted with cells from cultures initiated with a positive regulator of self-renewal (*Hoxb4*) in relation to values observed with control vectors (mean of pKOF-1, -2 and -3), all after 7 days of culture. Mean reconstitution level values listed in Table S3, second column). Harvested cells from each well were transplanted into irradiated recipients together with 2×10^5 congenic BM cells. Donor-derived peripheral white blood cell reconstitution was assessed after short (4 and 8 weeks) and long (12 and 16 weeks) periods of time after transplantation.

Previous results obtained from several in vivo transplantation experiments, using freshly transduced $CD150^+CD48^-Lin^-$ cells, revealed marked interrecipient heterogeneity in hematopoietic tissue reconstitution for a given candidate gene, thereby raising the critical issue of signal-to-noise discrimination. Optimization of this parameter was crucial for increasing the specificity of the screen while limiting to a minimum the number of mice that would be required. Toward this goal, we confirmed previous findings (Antonchuk et al., 2002) showing that the activity of *Hoxb4*-overexpressing HSCs is enhanced during short-term cultures (see red line in Figure 2A). For control (i.e., vector-transduced) HSCs, we also confirmed a noticeable decline in their activity during the 7 day culture (black line in Figure 2A). Interestingly, this HSC activity was preserved during the infection period (Figure 2A). Importantly, we found that recipients of these cultured control $CD150^+CD48^-Lin^-$ cells showed much less variation in blood cell reconstitution levels than those transplanted with "day 0" cells (compare error bars at day 0 versus day 7 on the black line in Figure 2A). In search for additional genes with *Hoxb4*-like activity, it appears that the signal-to-noise ratio is thus substantially enhanced by keeping cells in such cultures (Figure 2A). For this reason, the primary screen was performed with cells harvested at day 7 of the culture (see "Screen" in Figure 1B).

Primary Screen and Validation

The minimal cutoff level for selection of positive candidates in the primary screen was set on the basis of the standard deviation of the mean reconstitution level observed in multiple recipients of *Hoxb4*-transduced $CD150^+CD48^-Lin^-$ cells (Figure 2B, see also shaded area in Figure 2A). We therefore expected the newly identified candidates to be equivalent to, or more potent than, for each of the 104 tested candidates (at day 7) are compiled and presented in the middle panel, with the established cutoff level for a gain-of-function readout. Candidates clustering above the cutoff level for identification of *Hoxb4*-like genes (shaded area in Figure 2A), corresponding to 30% $CD45.1^+$ donor-derived cells in the primary screen, were selected for the validation experiments (upper-right panel), while those below were disregarded (lower-right panel). One candidate (*Hes1*) was eliminated on the basis of the marked reduction in repopulation noted between early and late time points (upper line in lower-right panel). Values are presented as mean ±SEM of independent experiments (n) for the left panel (n = 2 for *Hoxb4* and n = 3 for control vector; mean of three mice per experiment) and as mean ±SD for the middle and right panels (n = 3 mice for each candidate cDNA). Note that several mice were eliminated at 12 or 16 weeks after transplantation because they did not meet our criteria for hit selection (see also Table S3, ninth and tenth columns).

(C) Validation experiments confirming ten *Hoxb4*-like genes and eight other less potent candidates. p values were established at the 16 weeks after transplantation time point. Values are shown as mean ±SEM. The number of independent experiments (n) per candidate gene equals four, except for control vectors (n = 8); *Sox4*, *Zfp472*, *Xbp1*, and *Hnrpdl* (n = 5); and *Hoxb4*, *Cnbp*, *Ski*, and *Prdm16* (n = 3). For each experiment, a mean of three mice per gene was evaluated. cand., candidates.

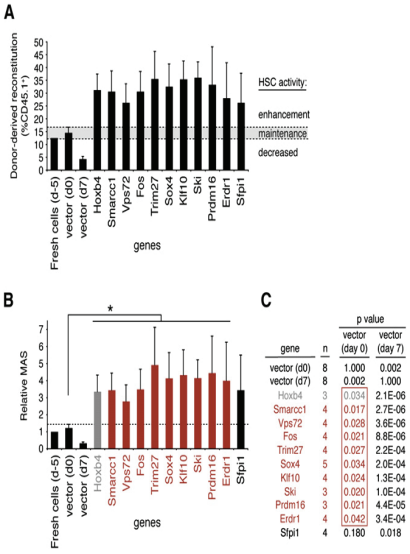

Figure 3. HSC Activity Is Enhanced by Overexpression of the Newly Identified *Hoxb4*-like Genes

(A) Percentages of donor-derived blood cells at 16 weeks after transplantation in primary mice recipients of day 7 culture cells (experiments in Figure 2C) for the ten identified hits. Bars at the far left show values for freshly purified $CD150^+CD48^-Lin^-$ cells, day 0 control cells (empty vector), and day 7 control and *Hoxb4*-transduced cells, as references. The shaded area represents mean reconstitution levels observed in mice transplanted with day 0 control-transduced HSCs, ±1 SEM. Reconstitution values falling within this range are considered to reflect HSC activity derived from an injected dose of HSCs equivalent to culture input numbers, i.e., 8 competitive repopulation units (CRUs) (see Figure S2C). d-5, day −5; d0, day 0; d7, day 7. Note that two different cDNA were tested for *Trim27* (see Figure S5).

(B) The mean activity of stem cells (MAS) was calculated from the data obtained in (A). As previously established, the MAS is equivalent to repopulation units (RUs) divided by CRUs (Ema and Nakauchi, 2000), where RU represents the donor-derived reconstitution level divided by the competitor-derived reconstitution level. MAS index was normalized to 1 for freshly sorted cells and excluded the gene transfer efficiency in its estimation for the candidate genes. In cases where gene transfer is low, this could lead to underestimated values. Grafts overexpressing genes shown in red and marked by an asterisk give rise to a MAS significantly higher than day 0 control grafts ($p \leq 0.05$). Note that values are presented as the MAS relative to that of fresh cells (d −5), which was set at a value of 1. d-5, day −5; d0, day 0; d7, day 7.

(C) p values derived from MAS values presented in (B) comparing data obtained from control vectors (day 0 or 7) and validated genes. Day 0 p values framed in red (penultimate column) mirror the order and color code of candidate genes presented in (B) and are ≤0.05. In comparison, day 7 p values are listed in the adjacent column.; n, number of independent experiments; d0, day 0; d7, day 7.

Hoxb4 in inducing enhanced HSC activity. With this criterion, a total of 18 hits were identified for a frequency of 17% (18/104; Figure 2B, upper-right panel; see also Table S3, tenth column). These 18 hits included *Cnbp*, *Erdr1*, *Fos*, *Hdac1*, *Hmgb1*, *Hnrpdl*, *Klf10*, *Pml*, *Prdm16*, *Sfpi1* (PU.1), *Ski*, *Smarcc1* (Baf155), *Sox4*, *Tcfec*, *Trim27*, *Vps72*, *Xbp1*, and *Zfp472*.

To validate the primary screen, we repeated the procedure described in Figure 1B in several independent experiments and confirmed ten primary hits (upper panels in Figure 2C; details in Table S3). From left to right and top to bottom, genes are presented on the basis of the level of statistical significance reached in these experiments, in comparison to control vector: *Hoxb4* (positive control, gray in Figure 2C), *Smarcc1*, *Vps72*, *Fos*, *Trim27*, *Sox4*, *Klf10*, *Ski*, *Prdm16*, *Erdr1*, and *Sfpi1*, for a positive predictive value (PPV) of 56%. Although the other eight candidates failed to demonstrate *Hoxb4*-like activity (i.e., shaded area in Figure 2A), it is noteworthy that they all significantly enhanced HSC activity to level above that detected with vector-transduced cells (see "other less potent candidates" in Figures 2A and 2C).

We then explored whether the ten newly identified *Hoxb4*-like genes are endogenously expressed in populations highly enriched in HSCs. To test this, we sorted cells from hematopoietic tissues isolated from unmanipulated mice sacrificed at three different developmental stages including E14.5 fetal liver (HSC-enriched subset number 1) and postnatal bone marrow, where a switch between cycling (3 weeks, subset number 2) and quiescent (4 weeks, subset number 3) HSCs has been described (Bowie et al., 2006). In line with the selection of these factors in our database, all ten genes are highly expressed in HSC-enriched populations with endogenous levels exceeding those of TATA binding protein (TBP), used as endogenous control (see relative threshold cycle [Ct] values for all HSC-enriched subsets in Figure S1A). Interestingly, most of these genes are expressed at higher levels in HSC-enriched populations than in total tissues (total bone marrow or fetal liver, Figure S1B). This observation is most prominent in the fetal liver-derived HSC-enriched subset (upper panel Figure S1B). We next verified the level of overexpression achieved for each of these genes after retroviral infection in sorted $CD150^+CD48^-Lin^-cKit^+Sca1^+$ BM cells and documented relative increases in mRNA levels that could be as low as 3-fold (e.g., *Smarcc1*) to as high as 1000-fold and above (e.g., *Fos*; Figure S1C).

Most Genes Identified Confer Enhancement in HSC Activity

One important question is whether the newly identified genes enhance or simply maintain input stem cell activity. To address this point, we compared the reconstitution levels by donor cells isolated (at day 7) from test cultures to that observed in recipients which received an equivalent number of freshly purified $CD150^+CD48^-Lin^-$ cells. As shown in Figure 3A, baseline long-term HSC (LT-HSC) activity (Sauvageau et al., 2004), measured at ~12%–16% reconstitution level (see left black bars in Figure 3A), was essentially preserved during the 5 day infection period and set the baseline values for maintenance of input HSC activity (shaded area in Figure 3A). From this, we could determine that all validated hits conferred a net increase in HSC reconstitution activity above that determined for fresh cells (Figure 3A).

In order to further quantitate the impact of our validated genes on HSC activity, we used the mean activity of stem cell (MAS) index as reported by Ema and Nakauchi (2000). This value, which provides a measure of the proliferative output per LT-HSC, is easily applicable to our culture condition since they were all

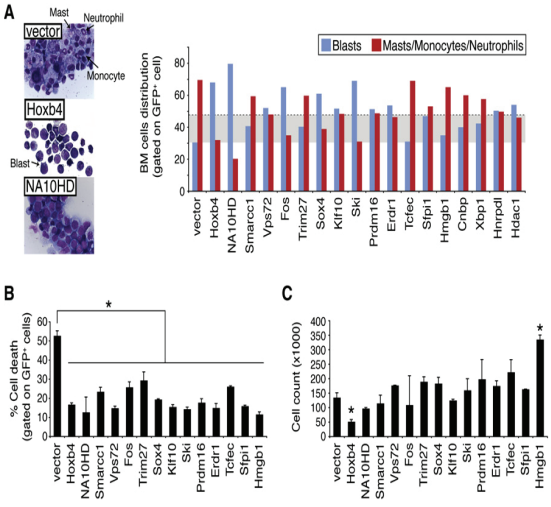

Figure 4. In Vitro Differentiation, Survival, and Proliferation Profiles of Cultured Cells

(A) Morphological analysis of cytological preparations of the starting HSC fraction overexpressing most of identified primary hits at day 7 of culture. Proportions of immature (blasts: black arrow in middle-left insert) versus terminally differentiated cells (neutrophils, monocytes and masts cells: black arrows in upper-left insert) for respective cultures are depicted in the right panel. A field comprising 100 cells was examined per independent experiment (n), and values are presented as mean; n = 3, except for vector (n = 6) and *Hoxb4*, *Ski*, *Tcfec*, *Sfpi1*, and *Hmgb1* (n = 1). The shaded area represents the mean of vector plus two standard deviations. Note that a vast majority of the less significant hits described in Figure 2C are included in this study (i.e., *Tcfec*, *Hmgb1*, *Cnbp*, *Xbp1*, *Hnrpdl*, and *Hdac1*). BM, bone marrow.

(B) Annexin V and PI stains were used to determine the fraction of cell death in cultures initiated with our validated hits and the less potent gene candidates (*Tcfec* and *Hmgb1*) as well as empty vector, *Hoxb4*, or *NA10HD*, serving as controls. Assessment was performed at the day 4 time point of culture. Values are presented as mean ±SD of two independent experiments (n), where n represents the analysis of 30,000 cells. * $p \leq 0.05$.

(C) Cell proliferation was assessed by flow cytometry-based cell counts (y axis) at day 4 of cultures. Analyses were performed for the same gene candidates as in (B). Values are presented as mean ±SD of two independent experiments. * $p \leq 0.05$.

initiated with a constant number of input LT-HSC measured at ~62 competitive repopulating units (CRU) per well (see Figures S2B–S2C for CRU assessment). The MAS was 3-fold higher for *Hoxb4*-transduced cells than for controls (Figure 3B). Similarly, the MAS varied between 2.8 (*Vps72*) and 4.9 (*Trim27*) for all ten hits identified in our screen (Figure 3B). Except for *Sfpi1* ($p = 0.18$), all values reached statistical significance (see p values in red in Figure 3C).

Impact of Candidate Genes on Cell Proliferation, Death, and Differentiation In Vitro

There is growing evidence to suggest that HSC self-renewal involves the active repression of a differentiation program, which is coupled to cell division (Cellot and Sauvageau, 2007). In support of this, we recently found that *Hoxb4*- or *NA10HD*-transduced cells, which actively undergo in vitro self-renewal divisions, show evidence of differentiation arrest (Figure 4A, left panels) (Cellot et al., 2007). We investigated whether our newly identified hits behave similarly. To achieve this, we first analyzed the cytological characteristics of transduced and sorted $CD150^+CD48^-Lin^-$ cells after a 7 day in vitro culture period (prior to their transplantation). In this context, cultures initiated with control vector-transduced cells contained 70% ± 8% of differentiated cells. These included neutrophils, monocytes, and mast cells (Figure 4A, arrows in upper-left panel with summary of results in right panel). Conversely, cellular differentiation was reduced in cultures initiated with HSCs transduced with most of the candidates (Figure 4A, right panel). The increase in the proportion of undifferentiated to differentiated cells was most important for *Vps72*, *Fos*, *Sox4*, *Klf10*, *Ski*, *Prdm16*, *Erdr1*, and *Sfpi1* when compared to cultures initiated with control vector-transduced HSCs (see blue bars exceeding shaded area, representing mean of vector plus two standard deviations). Note that while some of these genes are as potent as *Hoxb4* in this assay, none exceeds *NA10HD* in keeping cells undifferentiated.

We also monitored transduced $CD150^+CD48^-Lin^-$ cells for cell death and proliferation. Figure 4B shows that all factors analyzed conferred a significant reduction in the proportion of dead cells harvested at day 4 of culture. Surprisingly, besides *Hmgb1*, there were no significant increases in total cell numbers in these cultures (Figure 4C). In fact, some genes such as *Hoxb4*, and possibly *NA10HD*, were associated with a reduction in total cell counts (Figure 4C).

Transduced HSCs Differentiate In Vivo

The in vitro differentiation arrest displayed by *Hoxb4*- or *NA10HD*-transduced HSCs is eventually reverted after their transplantation in vivo (Cellot et al., 2007; Ohta et al., 2007). Thus, depending on the environment, these two genes can either interfere with (e.g., in vitro in the presence of high levels of growth factors) or not affect (e.g., in vivo under steady state conditions) HSC differentiation. To determine whether the newly identified regulators of HSC activity are similarly permissive to HSC differentiation in vivo, we used four different approaches. First, we evaluated the general health, spleen size, and bone phenotype (white versus red) of each recipient. Except for the recipients of *Prdm16*-transduced cells, which eventually developed splenomegaly and myeloproliferation with white femurs at 20 weeks after transplantation (data not shown), none of the mice transplanted with cells expressing our nine other genes ever presented this or any other hematological phenotype. Second, we performed cytological evaluation of bone marrow and spleen derived from representative mice for each gene. Results from these analyses were normal for all groups, except for the

Cell

Prdm16 cohort, which showed an excess of poorly differentiated myeloid cells in their bone marrow, as previously determined by others (Shing et al., 2007), and the *Ski* cohort, in which the number of lymphocytes in the bone marrow was reduced (data not shown). Besides recipients of *Prdm16*-transduced cells, spleens were never infiltrated with myeloid cells, nor did they include enhanced numbers of erythroblasts. To confirm this, we devised a third approach consisting of flow cytometry analysis on donor-derived ($CD45.1^+$) cells. The results, presented in Figure 5A for the peripheral blood, bone marrow, and thymus of a representative mouse (*Trim27*) and summarized in Figure 5B for all groups, largely confirmed our cytological evaluation. Indeed, except for recipients of *Ski*-transduced cells, which showed a marked reduction in B lymphocytes in their peripheral blood and marrow with a compensatory increase in other cell types, most groups of mice either showed normal distributions of various cell types or presented some minor variations. We further extended this analysis by gating only on $CD45.1^+$/GFP^+ cells for genes in which this was possible and ended with the same conclusions, with the exception that B cell differentiation was not observed in *Klf10*-transduced cells (Figure S3A). Finally, clonal analyses of recipients that were reconstituted with retrovirally marked cells were performed on bone marrow (less than 5% T cells) and thymus (less than 5% non-T cells). A representative result is presented in Figure 5C for *Trim27*, showing that identical clones contributed to the reconstitution of these two tissues, thus reinforcing the finding that these transduced HSCs remain competent in T cell differentiation although they displayed enhanced reconstitution activity. This finding can be extended to all other genes except for *Ski, Prdm16*, and *Erdr1*, for which we cannot be certain that the same clone contributed to thymic and bone marrow reconstitution (Figure S3B).

We also used quantitative RT-PCR assays to monitor overexpression levels of the different transgenes in $CD150^+CD48^-Lin^-$, $CD150^+CD48^+Lin^-$, B, and myeloid cells isolated from bone marrow to verify whether the in vivo reversal of the differentiation arrest noted in vitro (as shown in Figure 4A) was associated with loss of transgene expression. Results presented in Figure 5D suggest that overexpression of *Vps72*, *Fos*, *Sox4*, *Klf10*, *Ski*, *Erdr1*, and *Sfpi1* does not interfere with in vivo differentiation as several types of immature/differentiated cells still express the transgene. However, in vivo extinction of the transgene may have occurred for the three following genes: *Smarcc1*, *Trim27*, and *Prdm16*.

Together, these results confirm that the majority of the *Hoxb4*-like genes identified in our screen conferred enhanced HSC activity without causing hematological diseases or profoundly altering cell differentiation, while still overexpressing the transgenes at least until 20 weeks after transplantation. *Prdm16* was a notable exception.

Evidence of Self-Renewal Divisions by Transduced HSCs

We next verified whether HSCs transduced with each of the confirmed hits remained capable of symmetrical self-renewal divisions in vitro. To address this, we performed clonal analysis (i.e., proviral integration pattern) of hematopoietic tissues derived from selected recipients that were highly reconstituted (17%–83% $CD45.1^+$ cells) at 20 weeks after transplantation, a time point deemed sufficient for inferring that reconstitution is solely derived from the LT-HSC. For eight of the ten newly identified *Hoxb4*-like genes, namely *Smarcc1*, *Vps72*, *Trim27*, *Sox4*, *Klf10*, *Ski*, *Prdm16*, and *Erdr1*, we observed proviral DNA in the vast majority of mice that were analyzed (i.e., 43/49; Figure 6, two upper panels). Several different clones with long-term reconstitution ability contributed to hematopoiesis among different recipients from a given experiment, and from subsequent validation experiments. In several instances, we could identify the same proviral integrations in the DNA from two different mice reconstituted by cells derived from the same culture, demonstrating that LT-HSC self-renewal has indeed occurred in these cultures (see "a"–"g" in Figure 6). We also performed this analysis with the less potent candidates and found evidence for HSC self-renewal for *Cnbp* and *Xbp1* (see clones "h" and "i" in Figure 6). Together, these data indicate that a significant proportion of HSCs engineered to overexpress our validated hits remained capable of symmetrical self-renewal divisions in vitro.

Evidence of a Non-Cell-Autonomous Activity for Selected Genes

Surprisingly, we could not reveal any integrated provirus in the majority of recipients transplanted with cells transduced with the *Hoxb4*-like genes *Fos* and *Sfpi1* (Figure 6, bottom panels). This suggests that untransduced HSCs in these cultures have favorably responded to some extrinsic factors. A detailed evaluation of recipients from which these observations are derived is provided in Table S4. Consistent with the presence of a non-cell-autonomous effect, we observed that upon exposure to *Fos* or *Sfpi1* viral producer cells, HSC contribution to long-term repopulation increased from 5%–6% after 5 days of infection (i.e., day 0) to 26%–31% with 7 additional days of culture (Table S4, compare %CD45.1 at day 0 [seventh column] to that at day 7 [eighth column]). The absence of *Fos* and *Sfpi1* proviruses in the hematopoietic system of long-term recipients is surprising considering the high level of gene transfer to transplanted cells (Table S4, third column). This possibly indicates that these genes also intrinsically interfere with HSC repopulation when overexpressed, leading to depletion of transduced HSCs. Similar observations were found with *Tcfec* and *Hmgb1*, members of the less potent category (data not shown).

To provide more-direct evidence of non-cell-autonomous activities for *Fos*, *Sfpi1*, *Tcfec*, and *Hmgb1*, we transduced non-viral-producing NIH 3T3 cells with each of these constructs and used them as feeder cells replacing the viral producers described in Figure 1B. Overexpression of each of these four factors in NIH 3T3 cells was verified by quantitative RT-PCR, with a relative fold difference above baseline values ranging from 3-fold (*Hmgb1*) to 18,000-fold (*Tcfec*) (data not shown). As per our experimental protocol, 1500 $CD150^+CD48^-Lin^-$ cells were seeded on non-viral-producing cells and maintained for 7 days prior to their transplantation into irradiated hosts. Strikingly, we found that three of the four genes, namely *Fos*, *Tcfec*, and *Hmgb1*, conferred a similar impact on HSC activity whether viral-producing or non-viral-producing cells were present in the cultures (see Table 1). Interestingly, background-level

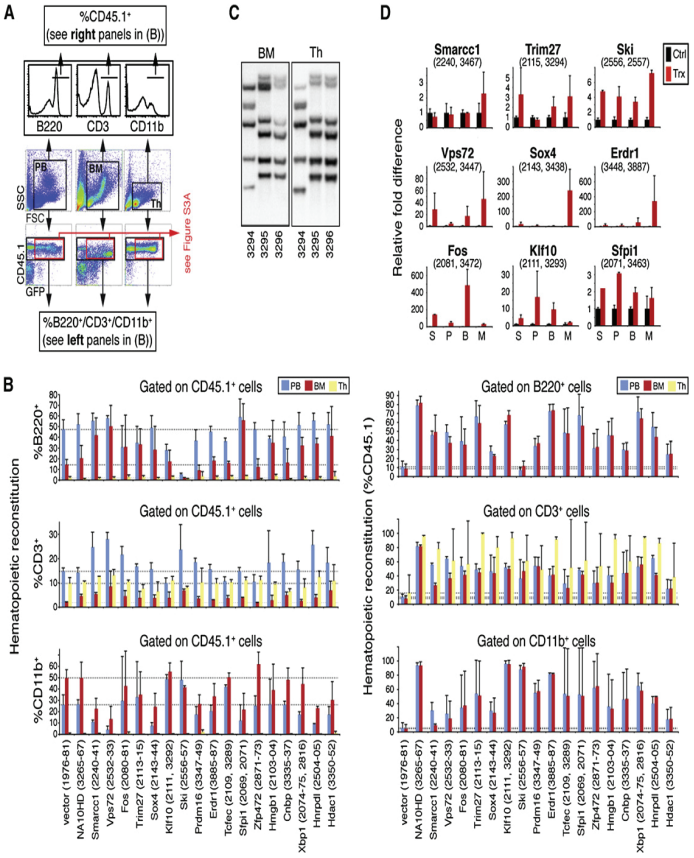

Figure 5. In Vivo Differentiation Potential of HSCs Overexpressing Validated Hits

(A) In vivo differentiation potential along the lymphomyeloid lineages was assessed in long-term recipients (20 weeks after transplantation) of HSCs transduced with *Trim27*, used as an example. Immunophenotypic analysis by flow cytometry was performed with specific antibodies against B, T, and myeloid cell surface markers (B220, CD3, and CD11b, respectively) on the CD45.1$^+$ population of cells derived from the peripheral blood, bone marrow (BM), and thymus of these mice (and on CD45.1$^+$/GFP$^+$ cells in Figure S3A).

(B) Compilation of B-/T-lymphoid and myeloid cell percentages within the CD45.1$^+$ population (left panels) and of CD45.1$^+$ cell proportions in the B-lymphoid, T-lymphoid, or myeloid populations (right panels) of blood, thymus, and BM tissues, as gathered in (A), for most of the primary hits. Values are presented as mean ±SD. Mouse identification numbers are presented between brackets. Dashed lines indicate values obtained with control mice (vector) for the different hematopoietic tissues. Note that multilineage reconstitution was observed in all of mice analyzed except for those transplanted with cells transduced with *Ski*, which showed a block in B-lymphoid differentiation. The proportion of CD45.1$^+$ cells within the B-lymphoid or myeloid populations in the thymus was not calculated in the right panels because these populations represent less than 5% of total cells in this tissue. Since weak donor-derived reconstitution levels were observed in mice transplanted with control vector cells at day 7 of culture (i.e., 4% in Figure 3A), we used mice transplanted with control vector cells at day 0 of culture in this case. Values pertaining to less statistically significant hits are also presented (*Tcfec*, *Zfp472*, *Hmgb1*, *Cnbp*, *Xbp1*, *Hnrpdl*, and *Hdac1*).

(C) Proviral integration pattern studies by Southern blot analysis performed on genomic DNA extracted from bone marrow (left panel) and thymus (right panel) of three long-term recipients of *Trim27*-overexpressing HSCs. Each lane represents a specific mouse (ID number below). For a given animal, identical integrations are found in both tissues, indicating a common precursor cell origin. Identical clones are also observed in two distinct recipients, retrospective molecular evidence for a self-renewal division in vitro. Multipotentiality (BM and thymus) analyses in reconstituted tissues harvested from primary recipients of culture cells overexpressing the various validated hits are shown in Figure S3B.

(D) Quantitative RT-PCR analysis of mRNA expression levels of nine of the ten newly identified *Hoxb4*-like gene transcripts. For technical reasons, *Prdm16* was excluded from the analysis. RNA was extracted from distinct bone marrow cell fractions isolated from long-term, highly reconstituted recipients of day 7 culture cells (S, CD150$^+$CD48$^-$Lin$^-$; P, CD150$^+$CD48$^+$Lin$^-$; B, B220$^+$; M, Mac$^+$). Average ΔCt values (representative of expression levels) were determined with β-actin serving as an endogenous control to normalize levels of target gene expression. Relative fold differences were determined using control cells as a reference calibrator for each candidate gene. Reactions were done in triplicate; black bars represent mean endogenous expression levels ±SEM of three independent wild-type mice (Ctrl); red bars represent mean overexpression levels ±SEM of two transplanted mice (Trx) from two independent experiments. The identification numbers of mice used in this assay are presented between brackets. Note that control black bars on each panel are set at a relative fold difference value of 1.

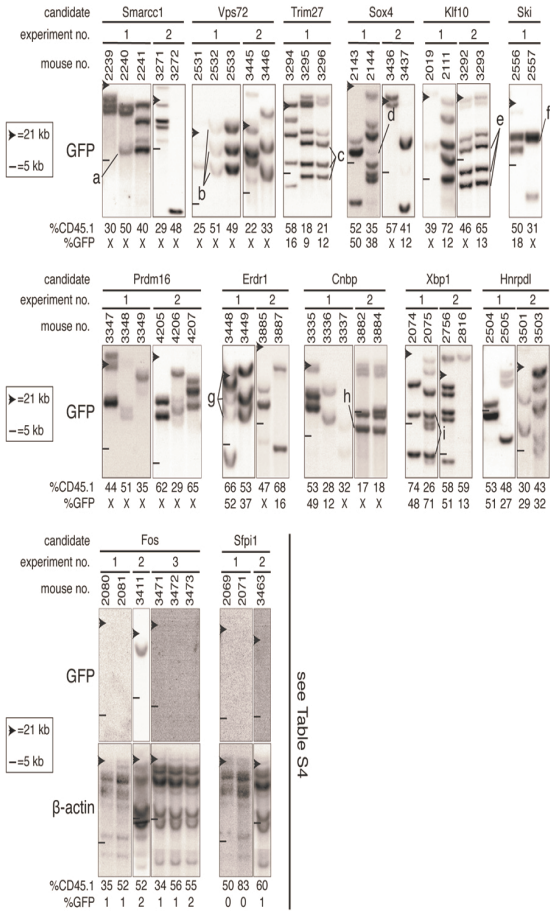

Figure 6. Clonal Analysis to Track HSC Self-Renewal Divisions

Southern blot analyses of genomic DNA extracted from the bone marrow (BM) of selected long-term recipients (20 weeks after transplantation) of day 7 culture cells. Each blot was hybridized with a GFP-specific probe and systematically exposed for the same period of time. Each well was equally loaded, taking into consideration donor-derived peripheral blood reconstitution level of recipients as measured 16 weeks after transplantation (i.e., 17%–83% CD45.1$^+$ cells). Top and bottom panels show gene sets for which proviral DNA was either detected or absent in the majority of recipients analyzed, respectively. For most bottom panels, the brightness and contrast was enhanced using Photoshop to further verify the absence of integrated proviral DNA, and a β-actin probe was also used to confirm the presence of genomic DNA. Clones that self-renewed during the 7 day culture, prior to transplantation, are labeled "a" to "i" and identified in more than one recipient. "X" indicates that GFP expression was not detectable for these constructs/clones. Note that panel 5, representing the *Trim27* gene, is also included in Figure 5C (left panel).

reconstitution was found in recipients of cells kept on *Sfpi1*-transduced NIH 3T3 cells, possibly indicating a more complex cellular network involved with this gene.

DISCUSSION

In this study, we combined the power of expression profiling and functional studies to uncover candidate factors that impact on HSC activity. Our experimental procedure included an efficient production of high-titer retroviruses, a sharp and discriminating HSC gain-of-function signal optimized by an ex vivo culture step together with a robust and reliable in vivo assay (see importance of culture step for signal-to-noise discrimination in Figure S4). Using this strategy, we individually tested 104 preselected candidates revealing 18 genes that conferred a clear repopulation advantage to HSCs. Of these, ten displayed a *Hoxb4*-like effect, thereby greatly extending the repertoire of potential regulators of HSC activity. These factors, which are highly and in some case preferentially expressed in HSCs, are implicated in a diversity of processes, such as chromatin modification (e.g., *Smarcc1* and *Vps72*), stress response (e.g., *Fos*), and gene transcription (e.g., *Trim27* and *Klf10*) (see Table S4 and legend for more details on these *Hoxb4*-like factors). With this significant cohort of genes impacting HSC activity, it was possible to discern a subset of four factors (i.e., *Fos, Tcfec, Sfpi1* and *Hmgb1*) that exerted their influence on stem cell function through a non-cell-autonomous phenomenon. Importantly, the non-cell-autonomous activity of three of these four factors was confirmed in gene transfer-free conditions.

Identified Hits Display *Hoxb4*-like HSC Activity

Similar to our previous results with *Hoxb4*-overexpressing HSCs, nine of the ten hits identified in this screen also significantly conferred increased HSC activity to levels above those observed with input cells (genes in red in Figures 3B–3C). Considering the ~50% average gene transfer level, not taken into consideration in the evaluation of the mean activity of stem cells (MAS) reported in Figure 3B, the impact of some of our confirmed hits was likely underestimated. Interestingly, our newly identified candidates also induced a maturation block in vitro, which was reversed in vivo. Moreover, and similar to *Hoxb4*, the majority of these genes failed to enhance cellular proliferation in vitro.

The increase in HSC repopulation potential (i.e., activity) observed with *Hoxb4* overexpression involves a net expansion (self-renewal) of these cells (Antonchuk et al., 2002). Although

Table 1. HSC Activity Is Enhanced Extrinsically

	GP+E86 (virus)		NIH 3T3 (no virus)[a]	
	%GFP	%CD45.1	%GFP	%CD45.1
vector	62 ± 26	4 ± 1	0 ± 0	5 ± 2
Fos	71 ± 9	31 ± 8	0 ± 0	35 ± 14
Sfpi1	37 ± 17	26 ± 12	0 ± 0	2 ± 1
Tcfec	48 ± 21	22 ± 8	0 ± 0	13 ± 5
Hmgb1	22 ± 14	20 ± 10	0 ± 0	14 ± 5

Donor-derived reconstitution levels (%CD45.1$^+$) observed 16 weeks after transplantation in mice transplanted with cells cocultured either with virus-producing cells (GP+E-86) or similar cells not producing virus (NIH 3T3), both overexpressing selected genes. Values are presented as mean ±SEM of independent experiments (n) per candidate gene, where n = 4, except for control vector, where n = 8. For each independent experiment, a mean of three mice per gene was evaluated.

[a] Mice were analyzed at 16 (experiments 1 and 2) and 8 (experiments 3 and 4) weeks after transplantation; %GFP, gene transfer assessed by flow cytometry.

our validated candidates show *Hoxb4*-like effects and we could document self-renewal divisions in vitro for several HSCs engineered to express these genes (Figure 6), it is important to stress that the formal proof for HSC expansion (enhancement in self-renewal divisions) as the driving force behind these effects will require intensive investigations that combine serial determinations of HSC numbers at consecutive time points (e.g., ΔCRU assay) with large-scale clonal analyses as previously reported for the *Hoxb4* gene (Antonchuk et al., 2002; Cellot et al., 2007). Indeed, among several possibilities, enhancement in proliferative potential combined with in vitro HSC maintenance could explain the *Hoxb4*-like effects observed with our validated hits. Secondary transplantation assays performed with selected candidates (*Vps72*, *Klf10*, *Erdr1*, and *Fos*, Table S5) argue against, but do not refute, such a possibility.

The eventual identification of shared target genes between these factors would further strengthen this argumentation. Of interest, attempts to build transcriptional networks, or hubs, among the hit genes have currently proven inconclusive, when most of the respective mRNA expression levels were assessed in HSCs freshly transduced with each of the candidate genes (see http://www.bioinfo.iric.ca/self-renewal/Network/).

Non-Cell-Autonomous Enhancement in HSC Activity

The non-cell-autonomous influence exerted by *Fos*, *Tcfec*, and *Hmgb1* was confirmed in cultures with NIH 3T3 support, confirming that gene transfer to sorted HSCs was not required for these three genes. In line with these findings, the proportion of GFP-positive cells was 0% in recipients of cells kept for 7 days in NIH 3T3-containing cultures (see column four in Table 1). It is also important to stress that these so-called "non-cell-autonomous" factors were identified in a context of overexpression, which in some cases (i.e., *Fos*) was outstanding (e.g., 38,000-fold above endogenous levels in some experiments, data not shown), potentially resulting in toxicities to transduced HSCs. It is therefore likely that several of these factors normally perform cell-autonomous activity in steady-state hematopoiesis. *Sfpi1* is a notable example for this (Rosenbauer et al., 2006).

The results obtained with *Sfpi1* during the screen and several additional experiments could not be confirmed in viral-free cultures. Reasons for this remain unclear. Several possibilities exist, including the presence of non-cell-autonomous contribution by some differentiated hematopoietic cells found in our culture or by essential cofactors unique to GP+E-86 viral producer cells.

These results thus raise critical questions about a possible, and even essential, contribution by the feeder cells (in this case NIH 3T3) to the observed effects on HSC activity. While this level of characterization is beyond the scope of our paper, this set of experiments exposes a complexity, often underestimated, when packaging (feeder) cell lines are used for cocultures in gene transfer studies. Awareness of this potentially confounding factor must therefore be taken into consideration in future experiments.

Although the demonstration of the non-cell-autonomous activity is relatively straightforward (e.g., three of the four factors described above), the proof for cell-autonomous function (e.g., the other newly identified factors) is more difficult to obtain within the scope of our experimental design. Thus, it is possible that some of the eight other *Hoxb4*-like genes (*Smarcc1*, *Vps72*, *Trim27*, *Sox4*, *Klf10*, *Ski*, *Prdm16*, and *Erdr1*) also or only display non-cell-autonomous activity.

Future of the Resource

Entries pertaining to candidate nuclear factors implicated in stem cell activity are stored in an open-access database (http://www.bioinfo.iric.ca/self-renewal/), as part of a building block in creating an interactive resource for the scientific community. Information thus far includes mRNA expression profiles, together with specific probe and primer sets, blood reconstitution patterns over time with possibilities of data reanalysis, and the complete nuclear factor list with ranking criteria. This database will eventually include similar data emerging from ongoing gain- and loss-of-function screens from different laboratories that will exploit this resource.

Thus far, nuclear factor candidates clustering in the uppermost levels (eight to ten) of our classification harbor a 23% primary hit rate, compared to 12% for those scoring lower (six to seven). This suggests that while positive HSC regulators tend to segregate in the top ranks, other downstream genes listed in our database (scores 1–5, n = 585 candidates) also include potential determinants of HSC self-renewal, with putative derivation of cross-regulation nodes as mentioned.

Our understanding of HSC self-renewal will mirror advancements in the rapidly evolving field of cellular therapy. As pioneered with *Hoxb4* (Krosl et al., 2003a), recombinant TAT-fusion proteins could be envisioned and therapeutically tested on human cells. Moreover, findings from this work will potentially pave the way to identify the mediator(s) that link these non-cell-autonomous candidates to enhanced HSC activity, thereby bypassing the requirement for retroviral vectors in the goal of expanding HSCs for clinical purposes.

EXPERIMENTAL PROCEDURES

Retroviral Vectors

MSCV-*Hoxb4*-IRES-*GFP* and MSCV-*NUP98*-HOXA10HD-IRES-*GFP* (*NA10HD*) were previously described (Antonchuk et al., 2001; Ohta et al., 2007). For all

Cell

candidate genes, single open reading frames (ORFs) were amplified by PCR (see Table S2 and the Supplemental Experimental Procedures for details).

Animals

(C57Bl/6J-CD45.2 x C3H/HeJ) F1 recipient mice and (C57Bl/6J-CD45.1-Pep3b x C3H/HeJ) F1 congenic donor mice were bred at a specific pathogen-free (SPF) animal facility at IRIC in Montreal.

CRU Assay on HSC-Enriched Populations

CRU assay and calculation were performed as described originally (Szilvassy et al., 1990) with modifications as in Sauvageau et al. (1995). Recipients were considered reconstituted (i.e., positive) when $\geq$1% of their peripheral blood leukocytes were of donor ($CD45.1^+$) origin at 18–20 weeks after transplantation. Two CRU assays were performed with $CD150^+CD48^-Lin^-$ cells and one CRU assay for the $CD150^+CD48^-Lin^-cKit^+Sca1^+$ subpopulation.

Bone Marrow Cell Culture, Retroviral Infection, and Transplantation

Generation of retrovirus-producing GP+E-86 cells, or gene-overexpressing NIH 3T3, were performed as previously described (Krosl et al., 2003b) and seeded in a 96-well plate format, enabling production of a single ecotropic pseudotyped retrovirus per well (for GP+E-86). See the Supplemental Experimental Procedures for details.

Flow Cytometry Assessment of Donor-Derived Hematopoiesis

The contribution of donor cells to peripheral blood reconstitution was determined at regular intervals after transplantation in individual recipients. See the Supplemental Experimental Procedures for details.

Analysis of Proliferation and Cell Death

Transduced cells harvested at day 4 of culture with trypsinization were counted with BD Trucount™ Tubes (BD Biosciences, San Jose, CA) according to manufacturer's guidelines, or stained with Alexa350-annexin V (Invitrogen Molecular Probes, Eugene, OR) and propidium iodide (50 μg/ml) in accordance with the manufacturer's instructions. Individual well contents were analyzed by flow cytometry. Gates were set to exclude GP+E86 retroviral producers by forward- and side-scatter criteria.

Resource Database and Web Application

The open-source postgreSQL relational database engine was used to store the accumulated data, and the web application was built with the open-source Webware application server framework. The application is designed to house results from other ongoing screens from our lab as well as screens performed elsewhere. As such, a sections-based authentication system has been implemented in order to restrict access to sensitive or nonpublished results. We expect this website to become an open-access resource for teams working on deciphering the molecular basis for stem cell self-renewal.

Statistical Analysis

The significance of differences was determined by a two-tailed Student's t test.

SUPPLEMENTAL DATA

Supplemental Data include Supplemental Experimental Procedures, five figures, and six tables and can be found with this article online at http://www.cell.com/supplemental/S0092-8674(09)00325-0.

ACKNOWLEDGMENTS

The authors thank J. Krosl, R. Bisaillon and B.T. Wilhelm for technical help, C. Charbonneau from IRIC imagery platform, D. Gagné from IRIC flow cytometry platform, and P. Chagnon and R. Lambert from IRIC genomic platform for their expertise with quantitative RT-PCR. We also want to acknowledge C. Perreault, M. Therrien, K.J. Hope, and R.K. Humphries for discussions and critical comments about the manuscript. This work was supported by the Canadian Institute of Health Research (CIHR) Team Grant in Hematopoietic Stem Cell Self-Renewal: From Genes to Bedside (Grant number 154290, 2006-2011). G.S. holds a Canada Research Chair on molecular genetics of stem cells; E.D. and S.C. are recipients of a CIHR studentship and Clinician Scientist award, respectively; J.C. holds an American Society of Hematology fellowship; M.S. holds a National Canadian Institute of Cancer studentship; and S.B.T. is the recipient of National Health Medical Research Council and a Royal Australian College of Physicians fellowships. IRIC is supported in part by the Canadian Center of Excellence in Commercialization and Research (CECR), the Canada Foundation for Innovation (CFI), and the Fonds de Recherche en Santé du Québec (FRSQ).

Received: September 9, 2008
Revised: January 19, 2009
Accepted: March 16, 2009
Published: April 16, 2009

REFERENCES

Antonchuk, J., Sauvageau, G., and Humphries, R.K. (2001). HOXB4 overexpression mediates very rapid stem cell regeneration and competitive hematopoietic repopulation. Exp. Hematol. *29*, 1125–1134.

Antonchuk, J., Sauvageau, G., and Humphries, R.K. (2002). HOXB4-induced expansion of adult hematopoietic stem cells ex vivo. Cell *109*, 39–45.

Bowie, M.B., McKnight, K.D., Kent, D.G., McCaffrey, L., Hoodless, P.A., and Eaves, C.J. (2006). Hematopoietic stem cells proliferate until after birth and show a reversible phase-specific engraftment defect. J. Clin. Invest. *116*, 2808–2816.

Cellot, S., and Sauvageau, G. (2007). Zfx: at the crossroads of survival and self-renewal. Cell *129*, 239–241.

Cellot, S., Krosl, J., Chagraoui, J., Meloche, S., Humphries, R.K., and Sauvageau, G. (2007). Sustained in vitro trigger of self-renewal divisions in Hoxb4hiPbx1(10) hematopoietic stem cells. Exp. Hematol. *35*, 802–816.

Ema, H., and Nakauchi, H. (2000). Expansion of hematopoietic stem cells in the developing liver of a mouse embryo. Blood *95*, 2284–2288.

Hai-Jiang, W., Xin-Na, D., and Hui-Jun, D. (2008). Expansion of hematopoietic stem/progenitor cells. Am. J. Hematol. *83*, 922–926.

Jaenisch, R., and Young, R. (2008). Stem cells, the molecular circuitry of pluripotency and nuclear reprogramming. Cell *132*, 567–582.

Kiel, M.J., Yilmaz, O.H., Iwashita, T., Terhorst, C., and Morrison, S.J. (2005). SLAM family receptors distinguish hematopoietic stem and progenitor cells and reveal endothelial niches for stem cells. Cell *121*, 1109–1121.

Krosl, J., Austin, P., Beslu, N., Kroon, E., Humphries, R.K., and Sauvageau, G. (2003a). In vitro expansion of hematopoietic stem cells by recombinant TAT-HOXB4 protein. Nat. Med. *9*, 1428–1432.

Krosl, J., Beslu, N., Mayotte, N., Humphries, R.K., and Sauvageau, G. (2003b). The competitive nature of HOXB4-transduced HSC is limited by PBX1: the generation of ultra-competitive stem cells retaining full differentiation potential. Immunity *18*, 561–571.

Lessard, J., Faubert, A., and Sauvageau, G. (2004). Genetic programs regulating HSC specification, maintenance and expansion. Oncogene *23*, 7199–7209.

Min, I.M., Pietramaggiori, G., Kim, F.S., Passegue, E., Stevenson, K.E., and Wagers, A.J. (2008). The transcription factor EGR1 controls both the proliferation and localization of hematopoietic stem cells. Cell Stem Cell *2*, 380–391.

Ohta, H., Sekulovic, S., Bakovic, S., Eaves, C.J., Pineault, N., Gasparetto, M., Smith, C., Sauvageau, G., and Humphries, R.K. (2007). Near-maximal expansions of hematopoietic stem cells in culture using NUP98-HOX fusions. Exp. Hematol. *35*, 817–830.

Root, D.E., Hacohen, N., Hahn, W.C., Lander, E.S., and Sabatini, D.M. (2006). Genome-scale loss-of-function screening with a lentiviral RNAi library. Nat. Methods *3*, 715–719.

Rosenbauer, F., Owens, B.M., Yu, L., Tumang, J.R., Steidl, U., Kutok, J.L., Clayton, L.K., Wagner, K., Scheller, M., Iwasaki, H., et al. (2006). Lymphoid

cell growth and transformation are suppressed by a key regulatory element of the gene encoding PU.1. Nat. Genet. *38*, 27–37.

Sauvageau, G., Thorsteinsdottir, U., Eaves, C.J., Lawrence, H.J., Largman, C., Lansdorp, P.M., and Humphries, R.K. (1995). Overexpression of HOXB4 in hematopoietic cells causes the selective expansion of more primitive populations in vitro and in vivo. Genes Dev. *9*, 1753–1765.

Sauvageau, G., Iscove, N.N., and Humphries, R.K. (2004). In vitro and in vivo expansion of hematopoietic stem cells. Oncogene *23*, 7223–7232.

Shing, D.C., Trubia, M., Marchesi, F., Radaelli, E., Belloni, E., Tapinassi, C., Scanziani, E., Mecucci, C., Crescenzi, B., Lahortiga, I., et al. (2007). Overexpression of sPRDM16 coupled with loss of p53 induces myeloid leukemias in mice. J. Clin. Invest. *117*, 3696–3707.

Szilvassy, S.J., Humphries, R.K., Lansdorp, P.M., Eaves, A.C., and Eaves, C.J. (1990). Quantitative assay for totipotent reconstituting hematopoietic stem cells by a competitive repopulation strategy. Proc. Natl. Acad. Sci. USA *87*, 8736–8740.

Takahashi, K., and Yamanaka, S. (2006). Induction of pluripotent stem cells from mouse embryonic and adult fibroblast cultures by defined factors. Cell *126*, 663–676.

Thorsteinsdottir, U., Mamo, A., Kroon, E., Jerome, L., Bijl, J., Lawrence, H.J., Humphries, K., and Sauvageau, G. (2002). Overexpression of the myeloid leukemia-associated Hoxa9 gene in bone marrow cells induces stem cell expansion. Blood *99*, 121–129.

Uchida, N., Dykstra, B., Lyons, K., Leung, F., Kristiansen, M., and Eaves, C. (2004). ABC transporter activities of murine hematopoietic stem cells vary according to their developmental and activation status. Blood *103*, 4487–4495.